THE IMPORTANCE OF EXTENSIONAL STRAINS IN THE ANALYSIS OF REINFORCED CONCRETE STRUCTURES

A.C. LIEBENBERG

RE-SUBMITTED APRIL 1965.

September, 1964

SUBMITTED TO THE UNIVERSITY OF CAPE TOWN FOR THE DEGREE Ph.D.

THE IMPORTANCE OF EXTENSIONAL STRAINS IN THE ANALYSIS OF REINFORCED CONCRETE STRUCTURES

with particular reference to :

I. The stiffness and strength of slab-type stairs.

II. A stress-strain function for concrete.

III. Arch action in reinforced concrete floor slabs.

IV. The extension of the columns of stiff-frames in tall buildings subjected to horizontal forces.

C O N T E N T S

SUMMARY : AN ANALYSIS OF THE CONTRIBUTION TO KNOWLEDGE OF THE THESIS : "THE IMPORTANCE OF EXTENSIONAL STRAINS IN THE ANALYSIS OF REINFORCED CONCRETE STRUCTURES"

GENERAL

The subject matter of the above-mentioned thesis has been sub-divided into four books, each of which represents a distinct contribution to knowledge although they together form a whole. The common theme of Books I, III and IV is the importance of extensional stresses and strains which are usually considered to be of secondary magnitude but which under certain conditions become of primary importance in the correct analysis of building structures. Book II is included as it formed the basis of the development of the theory in Book III. The order of arrangement corresponds approximately with the chronological development.

BOOK I.

The subject-matter of Book I on stairways was original and new when developed by the author in 1952. Although other research workers were at that time thinking along similar lines for stairs supported at the edges, the author developed the theory independently. He was probably the first to use the concept of the space-interaction of plates in an interpretation of the results of full scale and model tests and to carry out photo-elastic analysis of stairway models. When his theory was published it was the only comprehensive work on the subject which included an analysis of the interaction of extensional forces at the intersection of the intermediate landing and the flights of free stairs.

The theory was subsequently extended by the author to obtain compatibility of deflections in the case of free stairs and had been applied in practice by him prior to the publication of the paper by Siev in which the latter extended the author's theory in a similar manner except that the basic equations were not quite correct as pointed out by the author in a contribution to the discussion of Siev's paper. The author's application of the analogy of a finite beam on an elastic foundation to

/account for ...

account for the stress concentration at the intersection of the flights and the intermediate landing as revealed by the photo-elastic analysis is original and has not yet been published.

Although the economic benefits of the above-mentioned theory are not great, it has enabled architects to achieve aesthetic effects that were previously not possible. A large number of stairs throughout the world have recently been designed using these principles, with one notable example in Cape Town.

BOOK II.

The stress-strain function developed in Book II is an attempt to establish a simple function of which the mathematical form corresponds with the physical behaviour pattern of concrete prisms under uniaxial stress. By comparison with the complex functions developed by others it is quite simple yet agrees well with accurate experimental work for a large range of concrete strengths. The shape of the theoretical stress-strain curve agrees well with experimental values for the full loading cycle, including the descending portion of the curve which is peculiar to concrete. The same principles underlying this function were used to develop the arching stress function which is the basis of the empirical theory developed in Book III. The conclusions arrived at by the author regarding the existence of micro-cracks caused by shrinkage and the influence thereof on the initial modulus of elasticity of concrete were subsequently confirmed by electron-microscope work by others in America.

BOOK III.

This book forms the major part of the thesis and is based on experimental work carried out over a period of several years. The tests on the Old Alliance House carried out in 1957 were at that stage unique in that they constituted the first systematic investigation of arch action in slabs by full scale tests to destruction. This work was carried out in co-operation with Prof. Robertson and a member of his staff so that the

/author cannot ...

author cannot claim full credit in that respect. The author's major contribution has however been in the subsequent laboratory work and the development of the analytical elasto-plastic and empirical theories. The latter theory which is original in its entirety has produced useful results and is probably well advanced even at this stage beyond other attempts to develop feasible theories.

The author, in conjunction with Prof. Robertson, was one of the first to recognise arch action in normally reinforced concrete slabs as early as 1952 when analysing the results of the test to destruction on the lower flight of the stairs of the Old Dental Hospital building. This was the first test which produced conclusive evidence of the existence of arching forces in slabs and was directly instrumental in the recognition by Prof. Ockleston of the same phenomenon in the tests on the floor slabs of the same building.

The empirical theory developed by the author for one-way spanning slab elements from the results of laboratory tests was used as the basis of an empirical-phenomenological theory for two-way spanning slabs. The results of the analysis of the full scale tests carried out on slab panels of the Old Alliance House were used in conjunction with the above-mentioned theory to establish quantitative values for various parameters. On account of its empirical nature the theory is not complete but it may well serve as a useful tool for further research by others in order to obtain sufficient data for the development of a comprehensive theory.

BOOK IV.

This book deals with the importance of taking into account the extension of the columns of stiff frames acting in conjunction with shear walls in the analysis of tall buildings subjected to horizontal forces. The contribution to knowledge in this respect concerns the methods developed by the author of achieving rapid convergence in a relaxation

/method of ..

method of solution which is combined with standard iteration procedures. The method was developed by the author in 1961 when analysing the interaction of shear walls and stiff-frames for an 18 storey building recently completed. Although this analysis was novel at that stage various papers dealing with similar problems have recently been published. Most of these papers are however based on simplified assumptions and neglect column extension. The author is aware of only two published as recently as June, 1964, in which column extension is taken into account. For both simple and complex problems the method proposed by the author has definite advantages over both these methods.

---

*

FOOTNOTE TO LAST SENTENCE OF SECOND PARAGRAPH ON PAGE 10

Extensional forces constitute a system of forces acting in the mid-surface planes of those members which are thin plates, (or along the centroidal axes of those members which are columns or ties).

THE IMPORTANCE OF EXTENSIONAL STRAINS IN THE ANALYSIS OF REINFORCED CONCRETE STRUCTURES

GENERAL INTRODUCTION

The mathematical formulation and solution of all problems in the analysis of engineering structures, requires some degree of simplification or abstraction. These simplified basic assumptions concern the engineering properties of the materials, the configuration of the structure and the applied loads. It is usually possible to simplify the analysis by suitably arranging the configuration of the structure to eliminate or reduce the number of redundancies, but this may severely limit the scope of application. Accordingly engineers have resorted to making simplifying assumptions coupled with a commensurate factor of safety in order to be able to design structures which defy accurate analysis. This method has become so generalised that the tendency has developed for practising engineers to accept certain theories based on approximate assumptions without always questioning the accuracy and the range of applicability when extending theories or when developing new structures.

This work is concerned with an investigation of certain phenomena in reinforced concrete structures which have in the past been overlooked or incorrectly classified as secondary effects for the reason mentioned above. It has been confined to a study of extensional stresses and strains* and three cases only are considered.

Book I which is mainly composed of published work deals with slab-type stairs and the interaction of the flights and landings. The high load-carrying capacity and great stiffness of such stairs are accounted for by the extensional forces induced by this interaction. The first part describes full scale tests to destruction carried out in 1952 on the South stairs of the Old Dental Hospital building in Johannesburg and gives an analysis of the behaviour pattern. The theory of slab-type stairs is developed in the second part and extended in the third part to obtain compatibility of deflections in the case of free stairs.

/In the ..

✳

FOOTNOTE TO LAST PARAGRAPH ON PAGE 11

A distinction must be made between the extensional forces induced in floor slabs and those acting in stairways as described in Book I. In stairways which have members intersecting at large inclinations, extensional forces are fully effective from the initial stages of the loading. The extensional forces induced in plane slabs by arch action, on the other hand, are not of significance initially and they only become effective after crack formation and deflections of a considerable magnitude due to the formation of what is virtually a new structure not unlike an articulated arch or dome contained within the slab thickness.

In the fourth part deflection tests on a model of a free stairway are described and the results compared with the theory.

In the fifth part a study is made of the stress concentration at the intersection of the flights and the intermediate landing due to the relative flexibility of the latter. This work is based on a photo-elastic analysis of tests carried out on a model made of Araldite casting resin "B". The resultant stress distribution as revealed by these tests is successfully accounted for by a theoretical analysis based on the analogy of a finite beam on an elastic foundation. In the sixth part the application of the theory in practice is discussed and illustrated by a typical calculation.

Book II also consists of published material and describes the development of a stress-strain function for concrete subjected to uni-axial stress. The relevance of this part to the general subject stems from the fact that it forms the basis of the empirical-theory of arch action developed in Book III and also includes a description of the effect of shrinkage and the resultant micro-cracking on the modulus of elasticity of concrete. Although shrinkage effects in general have not been included in this work it may be appropriate to point out that stresses and strains induced by shrinkage are of primary importance in many structures although very often little attention is given to the resultant problems. Here again engineers tend to accept certain types of shrinkage cracks as inevitable whereas proper design and detailing can get close to eliminating them.

Book III is to be published shortly and deals with the so-called arch action due to extensional or membrane forces which are induced in floor slabs* with lateral restraint at the boundaries when subjected to transverse loading. This phenomenon is an outstanding example of a secondary force system which under certain conditions becomes a primary load-carrying system prior to ultimate failure. It forms the major part of this thesis and the subject is fairly comprehensively dealt with. It includes a description of the historical development and an exposition of the basic principles together with a

/discussion ....

discussion of the problems involved in the development of a theory. Various theories are compared and an elasto-plastic theory and an empirical-phenomenological theory are developed for one-way spanning slab elements. The latter theory is based on a large number of laboratory tests and is extended to apply in the case of two-way spanning panels. This is done by an analysis of full scale tests on the slab panels of a building carried out prior to demolition. The empirical theory is favoured for its relative simplicity and accuracy. In conclusion the most probable future developments and the application of the theory in practice are discussed and the economic implications briefly analysed.

Book IV deals with the importance of taking into account the extension of the columns of stiff frames acting in conjunction with shear walls in the analysis of tall buildings subjected to horizontal forces. A method is developed of obtaining rapid convergence in a solution based on relaxation combined with standard iteration procedures.

B O O K I

THE STIFFNESS AND STRENGTH OF SLAB TYPE STAIRS

P A R T 1

LOAD TESTS ON STAIRWAYS OF A REINFORCED CONCRETE BUILDING IN JOHANNESBURG

TESTS ON THE OLD DENTAL HOSPITAL, JOHANNESBURG

Paper No. 4

LOAD TESTS ON STAIRWAYS OF A REINFORCED CONCRETE BUILDING IN JOHANNESBURG.

by

A. C. LIEBENBERG

HE CONCRETE ASSOCIATION DECEMBER, 1956

LOAD TESTS ON STAIRWAYS OF A REINFORCED CONCRETE BUILDING IN JOHANNESBURG.

by

A.C. Liebenberg, B.Sc.(Eng.), A.M.I.C.E., A.M.I.Struct. E.

SYNOPSIS.

This paper is the fourth of a series dealing with full-scale loading tests which were carried out on the Old Dental Hospital in Johannesburg, a three storey reinforced concrete framed building, during the course of the demolition of the structure after it had been in service for approximately ten years.

The paper describes tests carried out on a reinforced concrete stairway of the slab type. The results obtained indicate that the behaviour of these stairs under load was basically different from that normally assumed, and that the method of design commonly used by engineers in practice is over-conservative for particular types of stairs.

The actual behaviour is analysed and a more rational method of design suggested.

LOAD TESTS ON STAIRWAYS OF A REINFORCED CONCRETE BUILDING IN JOHANNESBURG.

1.00 INTRODUCTION:

The stairs tested were part of the building housing the Oral and Dental Hospital of the University of the Witwatersrand, a reinforced concrete structure of normal construction, which had been completed in the latter part of 1942.

It was scheduled for demolition early in 1952 so as to make way for the new Johannesburg Railway Station. These tests were carried out during January and February 1952 immediately prior to the demolition and formed part of a greater scheme of tests [1 - 5] organized by a special committee formed for this purpose under the chairmanship of Dr. A.J. Ockleston, Professor of Structural Engineering at the University of the Witwatersrand.

2.00 DESCRIPTION OF STAIRS:

2.10 General.

The staircase was of the slab type, the flights spanning between floor landings and intermediate landings midway between floors. The total width of the stairs was about 4 ft. 9 in. with a horizontal clear span between landings of 11 feet. The external edges were built into the 4½ inch brick partition walls. The intermediate landings were slabs approximately 4 ft. 9 in. wide, the ends of which were supported on 4½ inch brick partition walls. The external edge which faced a large window was entirely free. The clear span between the supporting walls was 9 ft. 6 inches.

The average waist thickness of the slabs forming the flights was slightly in excess of 5 inches, and that of the intermediate landings $8\frac{3}{4}$ inches. On top of the structural concrete there was a screeding between 1 inch and 2 inches thick.

2.20 Original Design.

The original calculation sheets indicated that the stair flights had been designed as slabs spanning between landings and having some fixity at the junction with the landings. The effective span had been assumed to be 12 ft. 0 inches; the mid-span bending moment as $\frac{wl^2}{12}$; the dead load to be equivalent to 106 lb. per sq. ft. and the superimposed live load as 50 lb per sq. ft. This gave a mid-span bending moment of 23000 lb inches per ft. width of stairs.

The nominal concrete mix being 1:2:4 this necessitated approximately 0.35 square inches of mild steel reinforcement per ft. width calculated in accordance with the Local Building Bye-laws in force at that time. These Bye-laws were modelled on the 1933 Code of Practice for Reinforced concrete.

The intermediate landings had been designed as slabs simply supported on and spanning between the $4\frac{1}{2}$ inch partition walls with an effective span of 10 ft. 0 inches. The dead load had been taken as 105 lb per sq. ft. and the superimposed live load as 50 lb per sq. ft. The total load due to the flights spanning on the intermediate landings including the live load had been assumed as uniformly distributed over the full width and span of the landing. The total design load on the landings had thus been taken as 350 lb per sq. ft. which gave a midspan moment of approximately 53,000 lb inches per ft. width. This necessitated 0.425 sq. inches of mild steel reinforcement per

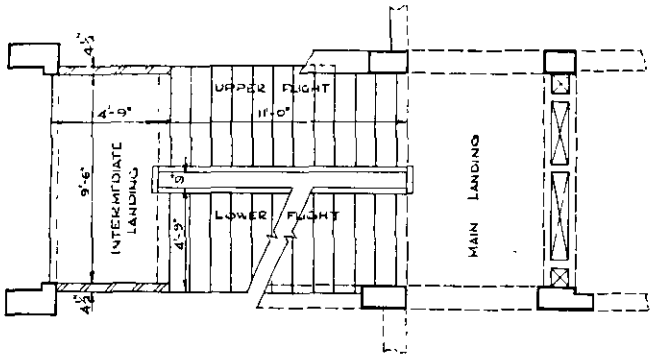

PLAN OF SOUTH STAIR FIG. 2.1 A

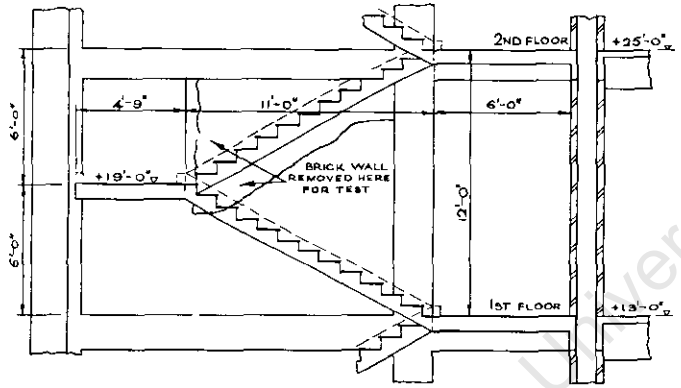

SECTIONAL ELEVATION OF SOUTH STAIR FIG. 2.1B

0 1 2 3 4 5 FEET
SCALE

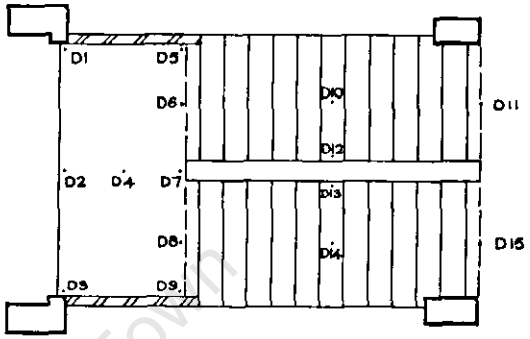

FIG. 3.2 A
POSITIONS OF DEFLECTOMETERS

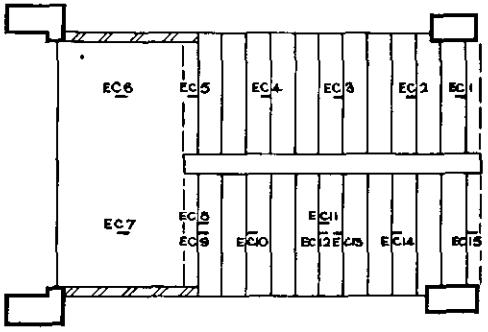

FIG. 3.2 B
POSITIONS OF ELECTRICAL STRAIN GAUGES ON UPPER SURFACE OF STRUCTURAL CONCRETE. (EC8 & EC11 ON SURFACE OF SCREEDING)

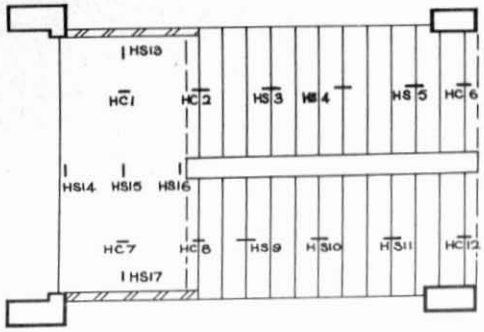

FIG. 3·2 C

POSITIONS OF HUGGENBERGER MECHANICAL STRAIN GAUGES ON LOWER SURFACE OF STRUCTURAL CONCRETE (HC) & ON STEEL BARS (HS)

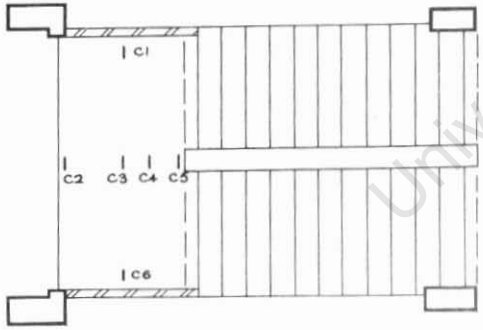

FIG. 3·2 D

POSITIONS OF GAUGE POINTS FOR THE HUGGENBERGER DEFORMETER ON UPPER SURFACE OF INTERMEDIATE LANDING. (C4 ON SCREEDING)

Figure 3.2*E* — RECORDING STRAIN AT POSITION C_4 BY HUGGENBERGER DEFORMETER. NOTE THE THICKNESS OF THE SCREEDING.

foot width in the bottom of the slab or a total of 2.0 sq. inches. The main landings had been considered as continuous slabs, the mid-span moment being $\frac{wl^2}{12}$.

2.30 Reinforcement

The main reinforcement in the stair flights consisted of 9 - $\frac{1}{2}$" dia. mild steel bars spaced at 6$\frac{1}{2}$" centres. (i.e. approximately 0.37 sq. inches per foot width). This reinforcement had been placed in the bottom of the slab only. No top reinforcement was provided at the junction of the flights with the landings. The stair reinforcement extended into the bottom and across almost the full width of the intermediate landing. The distribution reinforcement consisted of 5/16 inch diameter bars spaced at approximately 15 inch centres. The cover to the reinforcement varied from $\frac{1}{2}$ inch to practically nothing.

The landing reinforcement consisted of 2 - 5/8 inch dia. mild steel bars near the inner edge and 10 - $\frac{1}{2}$ inch dia. bars at approximately 5$\frac{1}{2}$ inch centres (Total cross-sectional area approximately 2.6 sq. inches). The distribution steel consisted of 10 - 5/16 inch dia. bars at approximately 10 inch centres.

3.00 DESCRIPTION OF TESTS

3.10 Preliminary

Several tests were carried out to determine the stiffness of the South stairway of the building. These tests were confined to the two flights and intermediate landing between the 1st and 2nd floors. Both uniform loads obtained by stacking rail chairs over the loaded area and concentrated

loads applied by hydraulic jacks were used.

Before commencing the actual tests the partition walls immediately above and below the external edges of the stair flights were removed. This was done so as to leave the flights spanning freely between landings, without any edge fixity, thereby approximating more closely to the actual design assumptions. Time did not permit of investigating the effects of such walls. The inverted kerbing to the internal edges, which was of similar material to the screeding was removed to the level of the top of the screeding on the steps and landing. The steel rails were cut free from the flights.

3.20 Preparation

The deflections were determined by suspended weight deflectometers connected by invar wires to hooks embedded at 15 selected positions on the underside of the stairs. The bases of the deflectometers were rigidly fixed to the stairs immediately below by means of plaster of Paris so that all deflections recorded for a particular point were relative to the corresponding point in the stairs immediately below. Where the wire deviated from the vertical for practical reasons the required correction $\frac{\delta}{\cos\theta}$ was applied. Strain gauges of the mechanical Huggenberger type were attached to the concrete and steel in 17 positions on the soffite.

15 Electrical strain gauges (type A.11) were fitted at various positions on the upper surface of the concrete. This arrangement was decided on for practical reasons as it was more convenient to protect the electric gauges against disturbance by operators during stacking of rail chairs and the application of loads by jack. These strains were recorded directly in ink on a circular paper chart by a Baldwin S.R.4

Scanner and Recorder. A Huggenberger deformeter was used for six positions on the upper surface of the intermediate landing.

3.21 For tests involving the application of loads in excess of estimated safe loads, cribs of railway sleepers were stacked up to within a few inches of the stairs to protect the instruments and operators against a possible sudden collapse.

3.30 Application of loads

Uniformly distributed loads were applied by means of stacking rail chairs, each weighing approximately 45 lb, over the loaded area.

3.31 Concentrated loads were applied by means of a 50 ton hydraulic jack. In addition to the gauge attached to the jack itself a pressure cell was used to determine the actual load applied. Both these gauges had been carefully calibrated. An 18" x 6" R.S.J. spanning across the stairs and supported up against the reinforced concrete beams forming part of the staircase frame at the level of the upper floor was used to provide the back thrust to the jack.

By distributing the jack load by means of a 14" x 6" R.S.J. onto sleepers laid across the width of the lower flight the effect of two equal line loads at third points of span was obtained.

3.40 Testing Procedure

3.41 Test 8A. Tests were carried out to determine the stiffness of the two stair flights and common intermediate landing by applying a uniformly distributed load in the form of rail chairs stacked on the loaded area. The load was applied in

increments of 56.5 lb. per sq. ft. of horizontal area up to an equivalent of approximately 226 lb per sq.ft. superimposed load, thus giving a maximum total load of about 332 lb per sq. ft. or 2.1 times the design load. Readings of deflection and strain were recorded during loading and unloading and the procedure repeated. The loading was applied as follows:-

(i) Uniformly distributed load applied to top flight only - repeated for lower flight.

(ii) Uniformly distributed load applied to both flights simultaneously.

(iii) Uniformly distributed load applied to landing only.

3.42 Test 8B. Concentrated point loads were applied on the intermediate landing at third points of the span and 3 ft. 9 inches from the free edge, so as to determine its stiffness with the stair flights intact. The load was applied in increments of approximately 4,500 lb to a maximum of about 22,000 lb.

3.43 Test 8C. In this test, line loads were applied to the lower stair flight at approximately third points of span. At first the load was applied in increments up to a maximum of 8,500 lb total load and then removed. Thereafter it was increased to 13,000 lb and again released. In the next test the first visible crack appeared on the upper surface in the waist of the stairs at the junction of the flight with the intermediate landing at an applied load just in excess of 13,000 lb, not including the weight of the equipment which amounted to approximately 800 lb.

This crack did not visibly extend right across the width of the flight and on removal of the load, closed up again. On reapplication of the load it again became visible, cracks

also appearing simultaneously at a load of 11,000 lb on the underside at the lower third point and on the upper surface in the second waist from the main landing at the lower end of the flight. The fact that this crack did not occur in the lowest waist was due to the stair flight being monolithic with the column at the lower end, thus reducing the effective span. At this load the initial crack extended the full width of the flight. A crack extending for about 12 inches along the supporting wall and thence for about 18 inches at approximately 45° to the wall was observed on the upper surface of the intermediate landing as indicated in the accompanying figure 3.4A.

Further increments of load caused the existing cracks to widen and also new cracks to appear on the underside directly below the waists at and between the load points. A crack also appeared on the upper surface in the lowest waist extending across the flight and along the edge adjoining the column. The crack at the second waist from the lower end partially closed up on the appearance of this crack. See fig. 3.4A.

The load was released at 30,000 lb and again re-applied to reach a maximum of 50,000 lb whereafter the gauge reading dropped considerably and showed no increase on being jacked.

3.44 Test 8D. The object of this test was an attempt to obtain the relationship between the actual bending moment in the stair flight at the junction with the landings and the measured strains.

The central portion of the upper flight was cut away using a pneumatic drill. The upper projecting part cantilevering from the main landing was cut free from the column and loaded with rail chairs and the corresponding strains recorded. This could unfortunately not be repeated on the

lower projection as due to insufficient propping a crack developed across it during drilling operations. The upper projection which had no top reinforcement failed through tensile failure of the concrete at a distributed load of 3,780 lb which caused a calculated bending moment at the section of failure of 89,700 lb. ins.

3.45 Test 8E. This test was performed on the intermediate landing after having cut away both flights. The object was to investigate the interaction of the flights and the landing by comparison with test 8B.

The loading procedure was equivalent to that described in test 8B. After several repetitions the load was increased to 67,000 lb at which failure occurred as a result of the reinforcement yielding. Seven cracks were observed on the underside. The crack spacing at the inner edge measured from the East Wall was 29", 8", 7", 6½", 15", 17", 7½", 24". The cracks were widest at the inside edge (nearest the loads) and extended almost to the opposite edge.

By the time the slab failed the 4½ inch walls supporting its ends had cracked, and the brickwork immediately below the slab showed signs of crushing failure.

4.00 PROPERTIES OF MATERIALS

4.10 Sampling and testing of materials

After completion of the tests, samples of steel and concrete were collected and railed to Cape Town for testing.

4.11 The concrete was cut into four six-inch cubes, one 24" x 6" x 6" prism, and two 30" x 4" x 4" prisms.

The cutting was done by emery wheel and the accuracy such that the greatest diversion from the above dimensions was less

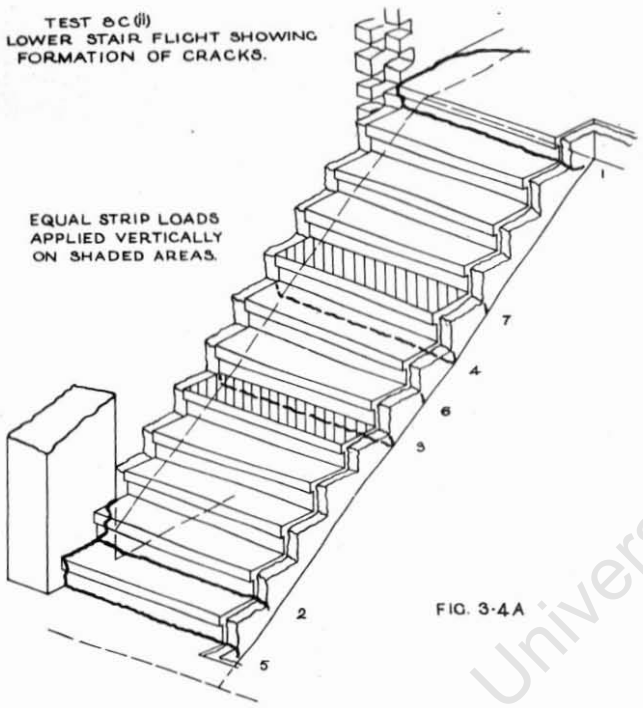

FIG. 3·4A

Figure 3.4*AA* — TEST 8A(i) IN PROGRESS.

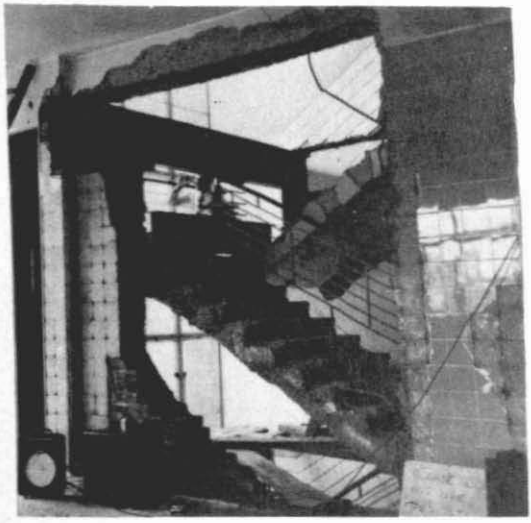

Figure 3.4*B* — TEST 8B IN PROGRESS.

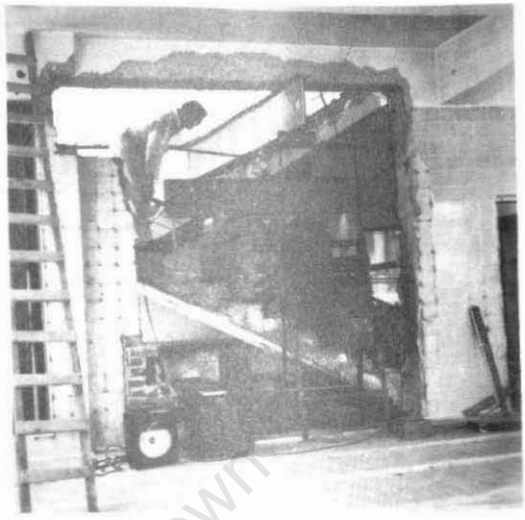

Figure 3.4*C* — TEST 8C IN PROGRESS.

Figure 3.4*D* — TEST 8D IN PROGRESS.

Figure 3.4*E* — TEST 8E IN PROGRESS.

than 0.2 inches.

4.12 The cubes were tested in a compression testing machine at the laboratories of the University of Cape Town. To reduce the effects of the irregularities the cubes were compressed between soft-boarding.

The failure loads were 96,000 lb; 156,000 lb; 130,000 lb; 137,000 lb., respectively giving equivalent failure stresses of 2670, 4340, 3620 and 3810 lb. per sq. inch respectively. The Schmidt concrete Sclerometer which had been used to estimate the strength of the concrete in situ gave results based on the maker's calibration curve considerably in excess of these averaging about 7,000 lb per sq. inch.

4.13 Marten gauges with 8" gauge lengths were attached to the 30" x 6" x 6" prism so as to obtain the stress strain relationship of the concrete in compression. The resulting stress-strain curve had the familiar shape giving a secant modulus of elasticity at 1000 lb per sq. inch of 3.0×10^6 lb per sq. inch. The prism failed at approximately 3500 lb per sq. inch.

4.14 The 30" x 4" x 4" prisms were used for obtaining the modulus of rupture. By first breaking the specimens at the centre and again re-using the two halves it was possible to get six results by the standard testing procedure viz. applying a mid-point load on the 4" x 4" specimen supported at 12" centres. The loads recorded were 2880 lb; 2000 lb; 2990 lb; on the first specimen and its two halves and 2370 and 2420 lb on the second. The average was thus 2432 lb giving an average modulus of rupture ($R = \frac{9}{32} W$) of 684 lb per sq. in.

4.15 For the purposes of this analysis the following properties of the concrete have been assumed:-

Compressive strength by cube test..... 4000 lb per sq. in.
Modulus of rupture ..... 680 lb per sq. in.
Modulus of elasticity.....3 x 10^6 lb per sq.in.

4.20 Steel samples

Ten $\frac{1}{2}$ inch diameter and two 5/8 inch diameter steel samples were tested using the Ewing extensometer to determine the stress-strain relationship.

The following are typical results representing an average specimen:-

Yield stress ..... = 45,000 lb. per sq. in.
Ultimate stress ..... = 66,000 lb. per sq. in.
Elongation on 8" gauge length .... = 29%
Youngs' modulus ..... = 29.0 x 10^6 lb. per sq. in.

The maximum deviations from these results were approximately 6.6%, 6.0%; 10% and 3.3% respectively.

The average strain at commencement of yield was 0.00155.

4.30 Brick walls.

Tests were carried out at the University of the Witwatersrand by Dr. A.J. Ockleston on various specimens of brickwork. As the intermediate landing was supported on $4\frac{1}{2}$ inch brickwalls forming one half of a cavity wall, the results of tests done on two brickwork specimens plastered one side only are of interest.

The one specimen, consisting of seven courses, was approximately 23 inches high x 27 inches long x 5 inches thick (including a plaster thickness of 0.8 inches). The elastic modulus determined by taking the mean result of at least 4 runs was 0.24 x 10^6 lb. per sq. inch and the crushing strength 330 lb per sq. inch.

The second specimen consisted of 4 courses and had

dimensions 13 inches x 27 inches x 4.6 inches with a plaster thickness of 0.4 inches. The elastic modulus was 0.29 x 10^6 lb per sq. inches and the crushing strength 460 lb per sq. inch.

5.00 ANALYSIS OF RESULTS.

In the following descriptions, internal forces have been sub-divided into:-

(a) Normal forces and shear forces which are analogous to the stresses occurring in slices and are together called extensional forces (also known as planar or membrane forces) because they produce extension (positive or negative) in the linear elements at the middle surface of the flight or landing slabs.

(b) Bending or torsional moments and transverse forces, which correspond closely to the stresses occurring in plates and are together termed bending forces.

This classification is similar to that used by Lundgren in his work on cylindrical shells.

5.10 Test 8A

The recorded deflections and strains produced during the initial stages of test 8A were small, so that it was decided to exceed the design load by a factor of 2.1. Some of the results recorded are graphically illustrated in fig.'s 5.1A to 5.1F. In this analysis more importance has been attached to deflection readings as the strains recorded were rather erratic.

No cracks were observed during this test and it appeared that the concrete was capable of resisting all the imposed stresses. The greatest recorded tensile strains were induced in the top of the stair flights by hogging bending moments

acting at the junction with the landings. No top reinforcement had been provided at these sections. The electrical strain gauges on the upper surface had been attached to the structural concrete surface as a rule, with two exceptions, which were attached to the surface of the screeding. Both these indicated that the screeding was effectively acting as an integral part of the structure. The bond between screeding and concrete was exceedingly good. Great difficulty was experienced in removing it cleanly from the concrete surface.

5.11 The stairs approximated to an elastic structure during this test, the permanent deflections produced at midspan of flights on release of the applied loads being about 10% of the deflections due to the maximum load applied. The recorded deformations of the intermediate landing slab were of much smaller magnitude but of a more permanent nature as illustrated in the accompanying diagrams. These deformations were however very small and bearing in mind the degree of accuracy of the instruments not necessarily of any real significance.

5.12 It appears from the results recorded that the behaviour of the stair flights was greatly influenced by the concrete columns and beams adjacent to the floor landings. The additional restraint produced at these points very effectively reduced the deflections and strains in the flights. In the case of the lower flight where the column was larger the effect was more marked as is illustrated by the deflection diagram 5.1D.

5.13 The relative deflections, bending and twist produced between sections could be deduced from the deflections recorded.

From Fig.5.1E which indicates the deflections recorded for a uniformly distributed load applied to the landing only, it is

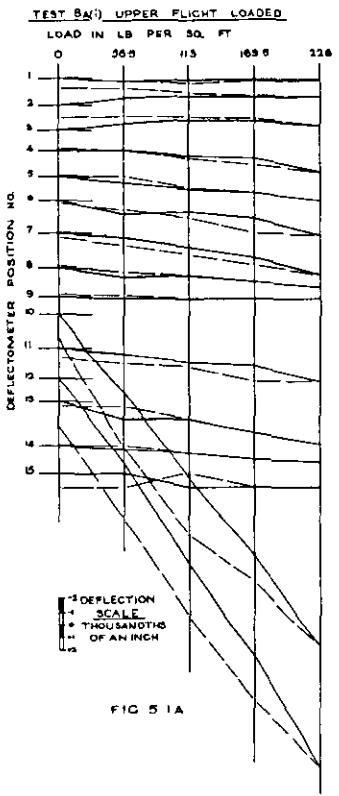

FIG 5 1A

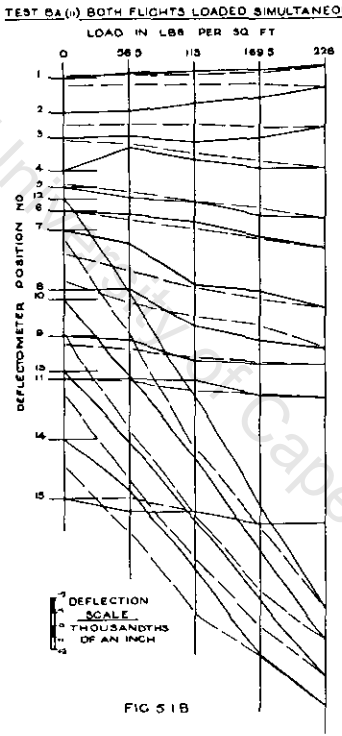

FIG 5 1B

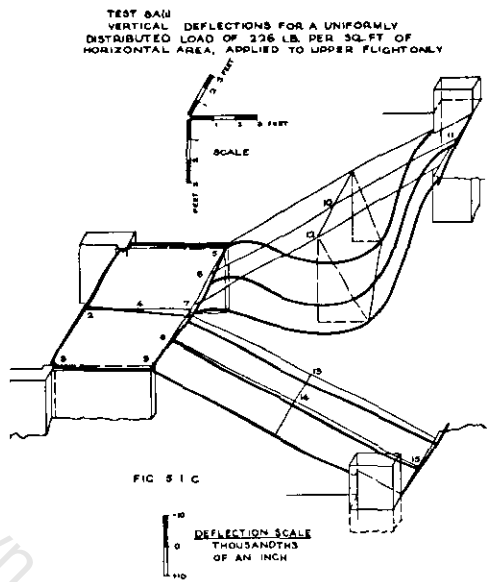

FIG 5 1C

by loading applied to an adjacent flight were comparatively small. This evidence together with the fact that the flights possessed insufficient bending stiffness, leads to the conclusion that the stiffening effect produced by the interaction of landing and flights was almost entirely due to extensional forces acting in the planes of the landing and flights (vide 5.00) and that in fact the stairs behaved in a way basically different from that assumed in the design.

5.15 Strain readings indicated that the flights acted as slabs spanning between the edges of the landings, the intersection of flights and landings being the effective "supports". These "supports" were not however rigid in the usual sense of the word as the edge deflections of the landing slightly exceeded the deformation of the wall supports thus producing a distortion of the "support". The distortion was however small compared with the deformation of the stair flights.

The additional restraint produced by the columns renders (vide 5.12) an analysis of the stair flights even more complex. Calculations based on the deflections recorded indicate that the maximum sagging bending moment at midspan of the upper flight occurred along the inner edge and approximated to $0.073\ wl^2$. (w being the superimposed load per sq.ft. of horizontal area and l equal to the horizontal clear span of 11 feet). In this calculation the screeding was considered to form part of the structure, the concrete was assumed to be uncracked and due account was taken of the varying section of the stairs. This indicates that the constraint produced by the landings and columns was considerable.

The strains recorded, although at times rather erratic confirmed the foregoing deductions. In the case of the lower flight the restraint provided by the columns was still greater,

The analysis of stairs is dealt with more comprehensively in Parts 2 and 3 but for clarity the procedure can be summarized as follows:-

The analysis may be performed in two stages:

(1) Assume the structure is supported at the intersections of members by immovable "supports", hinged for rotations only;

* (a) Find the extensional forces, moments and shears which may be termed the secondary force system;

(b) Find the reactions on the "supports".

(2) Apply the reversed reactions as the only loads on the structure;

** (a) Find the extensional forces, moments, shears and torsions due to this loading termed the primary force system;

(b) Add primary and secondary force systems 1(a) and 2(a) to give the final forces.

* Note: This is the analysis of a redundant structure on immovable supports.

** Note: This analysis must take account of the deflections.

The effect of deflections may be negligible when extensional forces alone are involved; and in any case the calculation is simplified as loads are applied only at ends of members. The effect of deflections is considered in Part 3.

the maximum moment approximating to $0.063\ wl^2$.

5.16 The torsional stiffness of the landing being relatively small and the opposite edge entirely free, the "support" bending moments induced by the flights were principally resisted by the components of moments acting obliquely in the landing slab and reacting in the supporting walls. This was confirmed by the mode of failure as described in 3.43. The crack pattern could probably be taken as an indication of the direction of the principle bending forces, which would be normal to the direction of the crack.

5.20 Analysis of behaviour*

It is clear from the foregoing that the generally accepted method of design as used in the case of these particular stairs (vide 2.20) and in which the action of extensional forces is neglected is an over simplification of the problem giving a very conservative result.

5.21 Stairs of this type can be classified with thin-walled prismatic structures which together with shell type structures have been extensively used in recent years. As the analysis of such structures is involved and beyond the scope of the average designer the application of the structural principles which make such structures feasible has generally been limited to schemes where it is economically justifiable.

5.22 Simplified methods have been suggested by various authors[6-8]. These methods are however approximate in that compatability of deflections is neglected and the assumption is made that the Bernouilli - Euler straight line theory of flexure applies to cases where the depth span ratio of members approaches or exceeds unity.

In the case of the stairs under consideration the flights would be assumed to span between the junctions with the landings. The intermediate landing would be treated as a slab supported on three sides the wall supports forming two sides and the junction with the flights the third. The bending moments in the flights and landings would be determined by the usual methods taking due account of continuity over the "supports".

This supporting action is the result of extensional forces produced in the slab elements by reaction against one another when under load. For these extensional forces to act it is however essential that there should be external members like slabs, walls, beams or columns with sufficient stiffness to provide balancing reactions. A free-standing staircase supported on slender columns only, could not act in this way. The applied loading would then be resisted by bending forces only produced by the stair elements spanning between beams and columns. These external supports determine the action of the extensional forces. The stairs under consideration differed from all the cases dealt with by the authors mentioned. An approximate solution of the forces that would act in stairs similar to those tested, is suggested below. Two cases will be considered:-

(a) A uniformly distributed loading applied to two adjacent flights only.

The exact distribution of the vertical reactions R_F due to bending forces caused by the above loading on the intersection line ZZ in fig. 5.2A(i) is not known. The same procedure can however be adopted as is done in practice for slabs spanning on beams by making a conservative estimate in the form of an equivalent uniform distribution as shown in Fig. 5.2A(iv). The value of R_F, the reaction per unit width of flight would be equal to $K_2 w_f L$ where K_2 depends on the conditions of continuity

*

The words "at any pair of these positions is equally divided" should be altered to read "the restraint at any one of the above points is taken as equal to the force applied to the joint there as described in (2) on page 37A. Therefore the forces applied to the flight along line ZZ form a couple, with vertical component $M = \frac{1}{2}b^2R_f$. The couple creates extensional forces in the flight whose distribution along ZZ has maximum values $\pm \frac{6M}{b^2}$, presuming a straight line variation of stress. The extensional force in the flight at section ZZ is tensile at point(2) and the vertical component of the extensional force per unit width is $3R_f$.

These are the forces described in 2(a) on page 37A."

of the stair flights, w_f is the uniformly distributed load applied to the stair flights per unit horizontal area, and L is the horizontal span.

The extensional forces are determined by considering the equilibrium of the various slab elements. The vertical reactions R_F are principally resisted by the vertical resultants R_V of the extensional forces E_F and E_L produced at the intersection ZZ in the flights and landing respectively. The distribution of these resultants R_V depends on the loading and the external restraints action on the slab elements. It is assumed that the stair flights in this particular case are fixed against deflection at positions 1 and 2; and 3 and 4 respectively, and that the restraint produced at any pair of * these positions is equally divided. Assuming furthermore that the straightline theory of flexure rigidly applies a distribution as indicated in fig. 5.2A (v) can be deduced. The unbalanced resultants of R_F and R_V are resisted by bending forces in the slab elements adjacent to intersection ZZ. The above assumptions are obviously only approximate. Although the horizontal components of deflections were not recorded there was evidence in one case (vide fig.5.4B) of some horizontal sway in a direction parallel to the landings. This would effect the distribution of the extensional forces.

It can be deduced from the above-mentioned assumptions and those mentioned in 5.22 that:-

$$R_V = 3R_F = 3K_2 w_f L$$

From figs. 5.2A(ii) and (iii)

$$E_F = \frac{R_V}{\sin \theta} = \frac{3K_2 w_f L}{\sin \theta}$$

$$E_L = \frac{R_V}{\tan \theta} = \frac{3K_2 w_f L}{\tan \theta}$$

From fig. 5.2A(i)

Considering the equilibrium of the stair flights

$$S_1 = \frac{E_F b^2 \cos \theta}{3L} = \frac{K_2 w_f b^2}{\tan \theta}$$

Considering the equilibrium of the intermediate landing

$$S_2 = \frac{2S_1 M}{B} + \frac{E_L b^2}{3B}$$

$$= \frac{K_2 w_f b^2}{B \tan \theta}(2M + L)$$

also $S_2 = S_1 \frac{(2M + L)}{B}$

As a result of more external restraints, the extensional forces produced in the main landing slab will be smaller.

(b) A uniformly distributed load applied to the intermediate landing only.

By similar argument as above, it can be shown that the distribution of the vertical resultants of the extensional forces is as indicated in fig. 5.2B(v) and that $R_V = R_L$ .... (vide fig. 5.2B(iv)) Where $R_L = K_3 w_1 \frac{BM}{b}$

w_1 = Uniformly districuted loading per unit area of landing

B, M and b are the dimensions indicated in fig.5.2B(i)

K_3 = is a factor depending on the support conditions of the landing slab and such that the above expression for R_L denotes the equivalent uniformly distributed reaction, due to bending forces, on the intersection line ZZ.

40A.

* The expression for S_1, on page 40 is not valid if the R_F values at the top and bottom of the flight differ.

Referring to Fig. 5.2.B for load on landing only, the restraint R_F at the foot of the flight will be reversed in direction. Using the same assumptions as on page 39A the maximum value of R_V at ZZ is equal to $3R_L$ exactly as for case (a). The forces described in 1(a) of page 37A (termed the "local direct forces" in Part 2 of the thesis) are to be added subsequently.

— analysis of

(a) the stresses due to bending forces produced by the applied load in the slab elements acting as described above.

and superimposed thereon

(b) the stresses produced by the resultant extensional forces and the balancing reactions.

The actual distribution of stress at the junction of flights and landings could differ considerably from that suggested as it would depend on the relative stiffnesses of external restraints and on the proportions of the slab elements.

In the case of the staircase tested the landing was restrained in a direction parallel to the forces S_1 (vide fig. 5.2A(i) by the two columns at the outer corners only. As previously mentioned there was evidence of some sidesway in this direction probably due to these columns being relatively less stiff than the other external restraints. The resultant effect of such sidesway would be to induce bending forces in

$$E_L = \frac{R_V}{\tan \theta} = \frac{3K_2 w_f L}{\tan \theta}$$

From fig. 5.2A(i)

Considering the equilibrium of the stair flights

$$S_1 = \frac{E_F b^2 \cos \theta}{3L} = \frac{K_2 w_f b^2}{\tan \theta}$$

Considering the equilibrium of the intermediate landing

$$S_2 = \frac{2S_1 M}{B} + \frac{E_L b^2}{3B}$$

$$= \frac{K_2 w_f b^2}{B \tan \theta}(2M + L)$$

also $S_2 = S_1 \frac{(2M + L)}{B}$

As a result of more external restraints, the extensional forces produced in the main landing slab will be smaller.

(b) A uniformly distributed load applied to the intermediate landing only.

By similar argument as above, it can be shown that the distribution of the vertical resultants of the extensional forces is as indicated in fig. 5.2B(v) and that $R_V = R_L$ .... (vide fig. 5.2B(iv)) Where $R_L = K_3 w_1 \frac{BM}{b}$

w_1 = Uniformly districuted loading per unit area of landing

B, M and b are the dimensions indicated in fig.5.2B(i)

K_3 = is a factor depending on the support conditions of the landing slab and such that the above expression for R_L denotes the equivalent uniformly distributed reaction, due to bending forces, on the intersection line ZZ.

* The expression for S_1 , on page 40 is not valid if the R_F values at the top and bottom of the flight differ.

Referring to Fig. 5.2.8 for load on landing only, the restraint R_F at the foot of the flight will be reversed in direction. Using the same assumptions as on page 39A the maximum value of R_V at ZZ is equal to $3R_L$ exactly as for case (a). The forces described in 1(a) of page 37A (termed the "local direct forces" in Part 2 of the thesis) are to be added subsequently.

41A.

* The expression for S_1 is not valid in terms of the assumptions made on page 40A.

The stresses referred to in paragraph (a) are due to the forces 1(a) of page 37A and those described in paragraph (b) are due to the forces 2(a) of page 37A.

From figs.5.2B(ii) and (iii)

$$E_{F1} = \frac{E_{F2}}{2} = \frac{R_V}{\sin\theta} = \frac{K_3 w_1 BM}{b \sin\theta}$$

$$E_{L1} = \frac{E_{L2}}{2} = \frac{R_V}{\tan\theta} = \frac{K_3 w_1 BM}{b \tan\theta}$$

From fig.5.2B(i)

Considering the equilibrium of the stair flights

$$* \quad S_1 = \frac{E_{F1} b^2 \cos\theta}{2L} = \frac{K_3 w_1 BMb}{2L \tan\theta}$$

Considering the equilibrium of the intermediate landing

$$S_2 = \frac{2S_1 M}{B} - \frac{E_{L1} bc}{2B}$$

5.23 The design of a staircase by this method would require an analysis of

(a) the stresses due to bending forces produced by the applied load in the slab elements acting as described above.

and superimposed thereon

(b) the stresses produced by the resultant extensional forces and the balancing reactions.

The actual distribution of stress at the junction of flights and landings could differ considerably from that suggested as it would depend on the relative stiffnesses of external restraints and on the proportions of the slab elements.

In the case of the staircase tested the landing was restrained in a direction parallel to the forces S_1 (vide fig. 5.2A(i) by the two columns at the outer corners only. As previously mentioned there was evidence of some sidesway in this direction probably due to these columns being relatively less stiff than the other external restraints. The resultant effect of such sidesway would be to induce bending forces in

the main landings so as to resist the unbalanced extensional forces causing the sway. A redistribution of extensional forces would also take place.

The stresses due to extensional forces as calculated by the above method were however small compared with the bending stresses so that even if a very conservative estimate were made the error in the calculated total stresses would not be excessive.

5.24 It is obvious that an analysis based on the above assumptions would give lower bending stresses than the conventional method. In the case of the landing slab the difference would be considerable.

5.25 The results of these tests seem to indicate that the actual behaviour of the stairs corresponded with the assumptions made in the above analysis. The deformation of the "supports" provided by the intersections of the slab elements was not much in excess of that of the wall supports and was small compared with the deflections caused by bending of the flights, as is clearly illustrated by the deflection diagrams. It would appear that neglecting compatability of deflections in the determination of bending forces in this type of stairs would be no more serious than in the design of slabs supported on beams and walls, as is done in common practice.

5.30 Tests 8B and 8E

The supporting action produced by the extensional forces as described in 5.22 was well borne out by comparison of the results obtained in subjecting the landing to precisely the same loading, firstly with the stair flights intact (test 8B) and at a later stage with the flights cut off (test 8E). The deflections recorded during these tests are diagramatically represented in figs 5.3A and 5.3B.

43A.

Fig. 5.2.8 is not valid in terms of the assumptions made on page 40A.

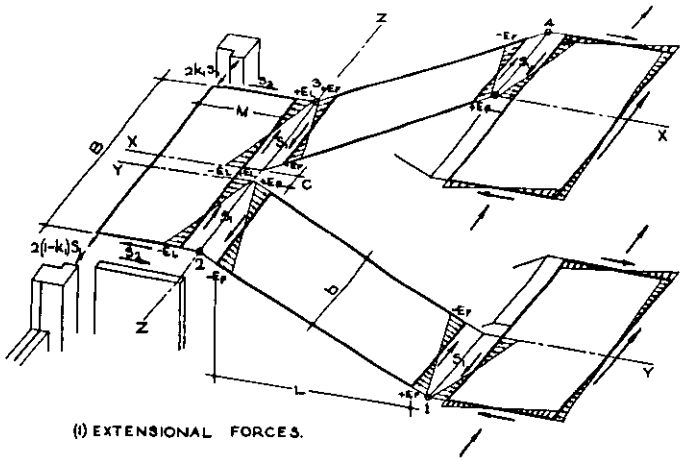

(i) EXTENSIONAL FORCES.

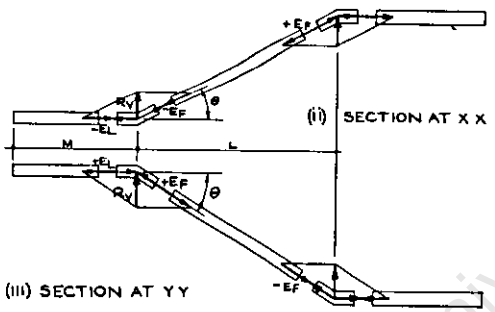

(ii) SECTION AT X X

(iii) SECTION AT YY

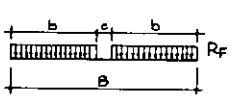

(iv) VERTICAL REACTION ALONG Z Z OF BENDING FORCES IN LB. PER UNIT LENGTH.

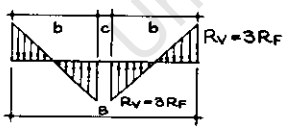

(V) VERTICAL REACTION ALONG ZZ OF EXTENSIONAL FORCES IN LB. PER UNIT LENGTH.

FIG 5·2A UNIFORMLY DISTRIBUTED LOAD APPLIED TO TWO ADJACENT FLIGHTS ONLY.

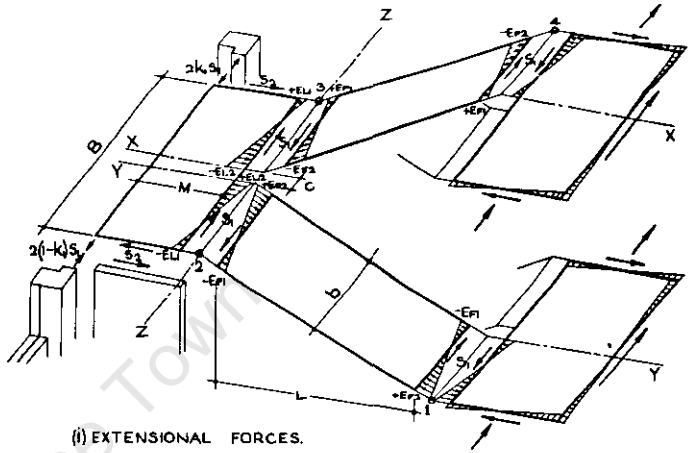

(i) EXTENSIONAL FORCES.

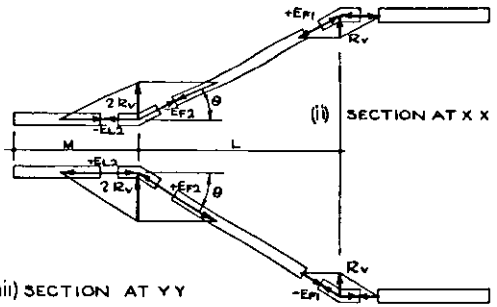

(ii) SECTION AT X X

(iii) SECTION AT YY

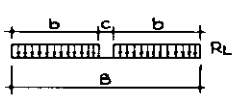

(iv) VERTICAL REACTION ALONG Z Z OF BENDING FORCES IN LB PER UNIT LENGTH.

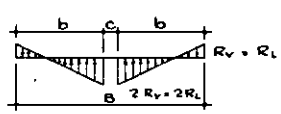

(V) VERTICAL REACTION ALONG Z Z OF EXTENSIONAL FORCES IN LB. PER UNIT LENGTH.

FIG 5·2 B UNIFORMLY DISTRIBUTED LOAD APPLIED TO INTERMEDIATE LANDING ONLY

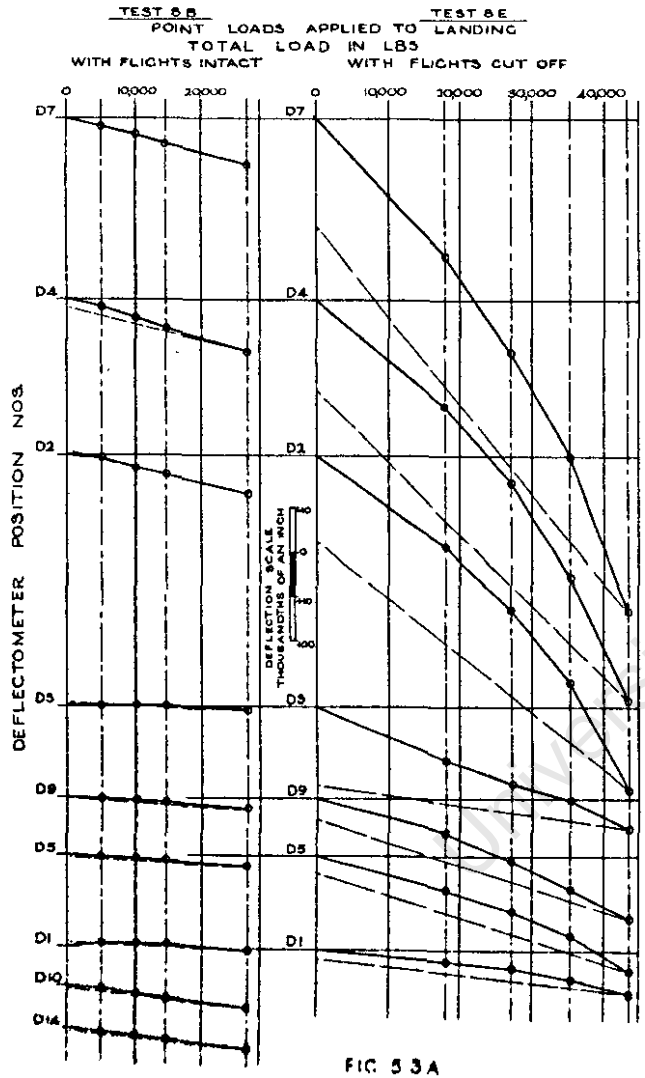

FIG 5.3A

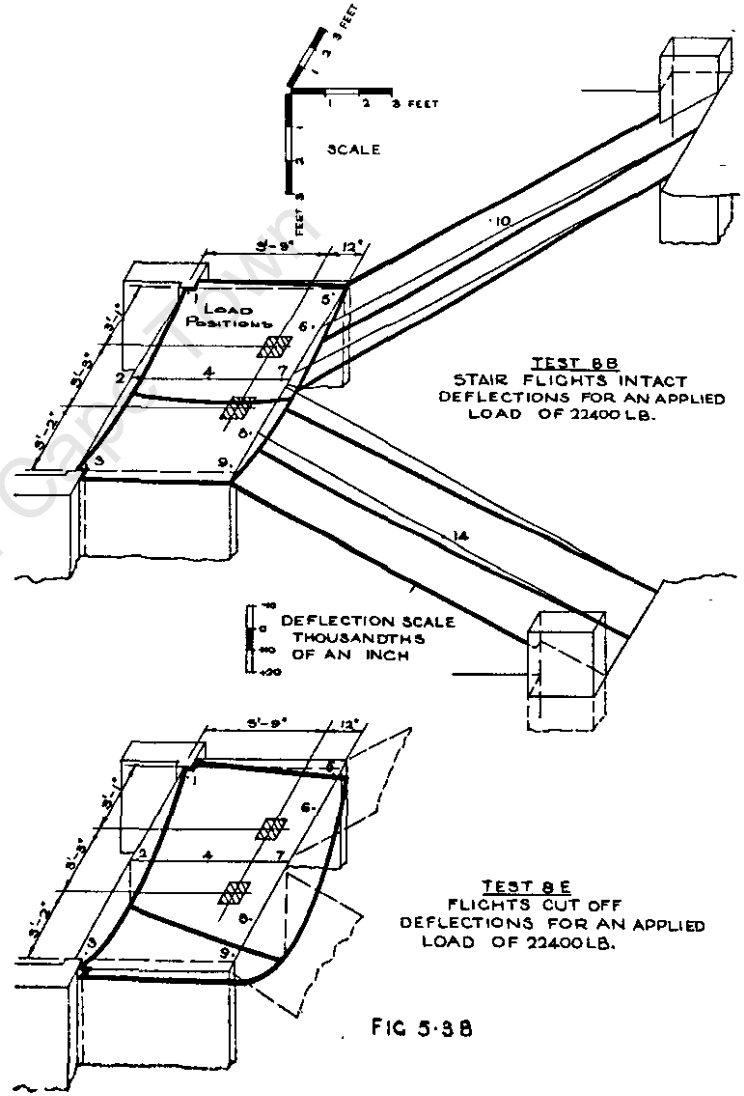

FIG 5.3B

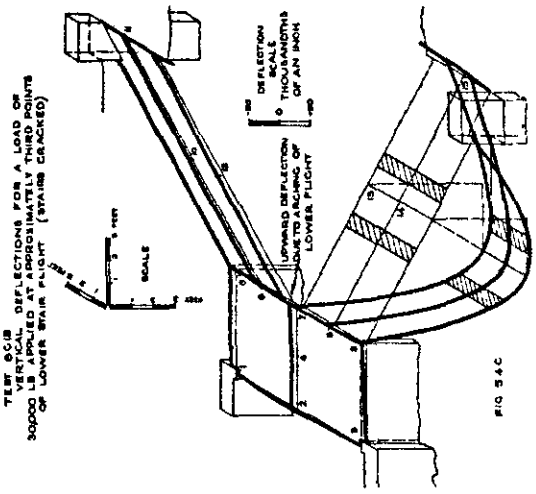

FIG 8.4C

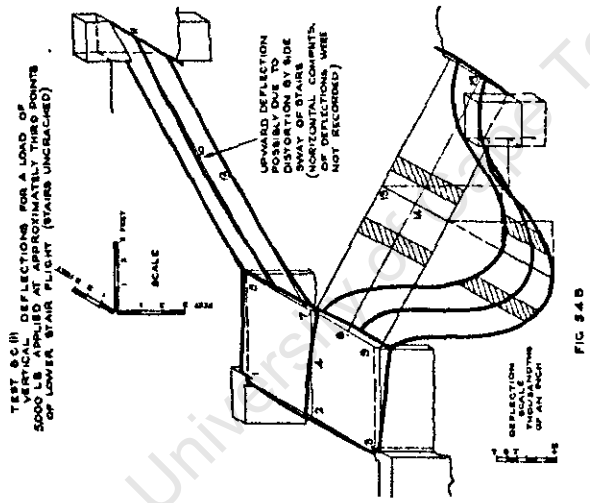

FIG 8.4B

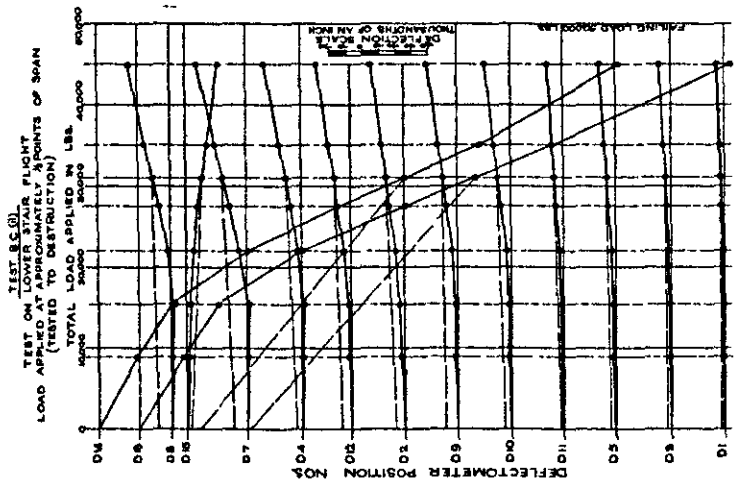

FIG. 8.4A

The strains recorded during test 8B were small, the greatest occurring transversely to the span direction of the landing at the junction with the flights. These strains were probably due to extensional forces superimposed on bending as the strain gauges on both faces indicated tension in the upper flight and compression in the lower flight.

For test 8E the landing had been reduced to a slab spanning in one direction only. The load at failure (67,000 lb) was somewhat in excess of the estimated ultimate load of approximately 50,000 lb calculated by using Whitney's formula with allowance for the eccentricity and assuming the slab to be simply supported. The discrepancy may well be accounted for by the fact that the slab was actually "built in" at the supports. The maximum stress on the brickwork due to the direct load plus the bending moment would have been in excess of 300 lb. per sq. inch. At this load the brickwork showed signs of crushing failure. This agrees well with the results obtained on samples (vide 4.30). The effect of the eccentricity of the applied loads was clearly borne out by the deflections and the mode of failure. The cracks initially appeared at the inner edge and gradually spread across the width of the landing. At failure they almost extended to the outer edge.

5.40 Test 8C

Test 8C confirmed the results obtained in 8A as regards the general behaviour of the stairs under load. In excess of a load of 9,000 lb the general behaviour however altered considerably. Up to this stage bending forces in the flight had apparently provided the major resistance as was evident from the strains recorded and the downward deflection of the edges of both landings. (We are here considering the flight as an element as distinct from the stairs as a whole which was

supported by extensional and bending forces). Beyond this stage it was clear that direct compressive forces, acting between the applied loads and the landings, which acted as horizontal girders resisting the thrust action, provided a considerable portion of the resistance. This was deduced from the fact that the intermediate landing began deflecting upwards as a result of the thrust action. Without this "arching" action it would be difficult to account for the exceedingly high ultimate load attained which exceeded the estimated ultimate load obtained by using Whitney's formula and taking the screeding into account, by a factor in excess of 3.0. The loads were not applied precisely at the third points of span and the total superimposed load of 50,000 lb, which was actually attained, induced a bending moment of 1,270,000 lb. ins. at the lower load. This is equivalent to the bending caused by a uniformly distributed load of approximately 1470 lb per sq. ft.

5.50 Test 8D

The object in view was not achieved by this test as a result of the stiffening effect produced during the previous tests by the column at the upper support. This rendered the problem very complex and although it was possible to deduce the exact moments acting at the gauge points EC1 and HC6 from the strains recorded during any test it did not give the desired solution of the span moments. When cutting away this stair it became clear why the restraint at the column adjacent to the upper flight had been considerably less than for the lower flight. A piece of sheet metal had been inserted between part of the stair and the column during construction. The stairs were probably cast after the columns, nevertheless where concrete adjoined concrete the bond was good judging by the restraints produced.

The maximum stress at failure calculated by the straight line theory and based on the assumption that concrete has the same elastic properties in tension as compression was equal to 240 lb per sq. inch taking the topping into account, and 350 lb per sq. inch if only the structural concrete is assumed to have resisted the load immediately prior to failure. This was somewhat lower than the modulus of rupture of the samples tested, which averaged 680 lb per sq. inch.

6.00 CONCLUSIONS

It would be unwise to generalize as regards any conclusions drawn from these tests as they were limited to one particular set of stairs. As regards the general behaviour of reinforced concrete these tests confirmed the conclusions drawn from the greater scheme of tests and described in work already published.

As regards the behaviour of the stairs as a structure very interesting results were recorded which very clearly illustrated the underlying structural principles. It was apparent that extensional forces (also known as planar or membrane forces) as distinct from bending forces, very effectively increased the stiffness of the stairs. In addition "arching" increased the ultimate resistance of the stair flight tested, by a factor in excess of 3.0.

Although a design incorporating these structural principles is highly complex and in many cases insoluble in the "exact" sense of the word, simplified methods may well be used to great advantage in practice, provided the limitations of such methods are clearly understood, as it can be shown by conservative estimates that the extensional stresses produced in stairs of the normal dimensions, dictated by practical considerations, are usually small. As in the case of the stairs tested

bending forces which can be calculated by similar methods as are used for ordinary slabs, would primarily determine the failing loads (vide 5.22). Where these stresses are not negligible the possibility of buckling failure due to extensional forces should however be borne in mind. It is also important to stress the necessity of sufficient external restraints to provide balancing reactions to the internal extensional forces. Additional external restraint would have been provided by the walls, along the stair edges, which were removed prior to the tests. The extensional stresses would have been reduced thereby as well as the bending stresses in the stairs flights, which would have been equivalent to slabs supported on three sides.

It would appear that neglecting compatability of deflections in the determination of bending forces for this type of stair would be no more serious than in the design of slabs supported on beams and walls as is done in common practice.

The analysis of stairs has not received much attention probably on account of the fact that the cost of the material involved is usually only a small fraction of the total cost of the building. It is however possible in some cases to greatly enhance the architecture by utilizing the structural principles as described in 5.2 whereby columns and beams may be eliminated. As an example, the external columns and beams of a fire escape stairs projecting from a building could be eliminated without the use of excessively thick concrete slabs.

In the case of the stairs tested, the dimensions of the stairs were apparently dictated by the architecture. Utilization of the above-mentioned principles would however have brought about a saving in reinforcement.

7.00 ACKNOWLEDGMENTS

This paper is published with the approval of the Management Committee which was responsible for the organization of the tests on the Old Dental Hospital, and thanks are expressed on behalf of the Committee to all those who by their support, co-operation and assistance contributed to the success of the tests.

The Author wishes to express his appreciation to Professor Ockleston, Chairman of the Management Committee, for his great assistance and for the loan of instruments from his department; to Prof. R.G. Robertson and the Council of the University of Cape Town whose grant from the Staff Research Fund made it possible for the Author to carry out this work; to the National Building Research Institute for the loan of valuable instruments; to the South African Railways for assistance in providing labour and equipment and to all those who in various ways assisted in carrying out these tests.

REFERENCES.

1. A.J. Ockleston: Loading Tests on the Floor Systems of a Reinforced Concrete Building,

Preliminary volume of proceedings of Conference on the Correlation between Calculated and Observed Stresses and Displacements in Structures, Institution of Civil Engineers, August 1955, p. 231, and

Transactions of the South African Institution of Civil Engineers, February 1956, p61.

2. A.J. Ockleston: Load Tests on a Three Storey Reinforced Concrete Building in Johannesburg,

The Structural Engineers, October 1955, p. 304.

3. A.J. Ockleston: General Report on Tests on the Old Dental Hospit

Concrete Association, Johannesburg, 1956.

4. A.J. Ockleston and I.R. Scott: The Determination of the Properti of Materials from the Old Dental Hospital,

Concrete Association, Johannesburg, 1956.

5. A.J. Ockleston: The Effect of Floors and Walls on the Behaviour of Reinforced Concrete Frameworks subject to Horizontal Loads,

Concrete Association, Johannesburg, 1956.

6. A.J. Ashdown: The Design of Prismatic Structures,

Concrete Publications Ltd., London, 1951

7. A. Krysztal: The Design of Staircases,

Concrete and Constructional Engineering, July, 1954 p. 230.

8. W. Fuchssteiner: Treppen,

Betonkalender 1955, p.183, Wilhelm Ernst & Sohn, Berlin, 1955.

PRINTED BY

THE CONCRETE ASSOCIATION

Head Office: 326 Libertas, 62 Marshall Street, P.O. Box 3899, Johannesburg.

Cape Regional Office: Atkinson House, Strand Street, Cape Town.

Rhodesian Regional Office: P.O. Box 2234, Bulawayo, Southern Rhodesia.

Transvaal Regional Office: P.O. Box 5021, Johannesburg.

PART 2

THE DESIGN OF SLAB-TYPE

REINFORCED CONCRETE STAIRWAYS

PART 2

THE DESIGN OF SLAB TYPE REINFORCED CONCRETE STAIRWAYS

GENERAL

There appear at present to be two definite schools of thought on the analysis of reinforced concrete slab-type stairs. The first, expounded by Fuchsteiner[1] and others, is based on the simplification of the stair structure into a space frame composed of linear bar elements. The second method, first developed by the author before 1956[2] [3] and subsequently extended independently by Siev[4] and the author[5], and since applied in practice by many engineers is based on the concept of space interaction of plates and the stiffness resulting from the induced extensional forces. In spite of the above publications and the successful application in practice of the theory many engineers apparently find difficulty in accepting the basic concepts of the second method. In a paper[6] published as recently as July 1964, the Fuchsteiner theory is extended for a type of free stair for which its accuracy can be questioned on the following grounds :

(a) For plate-like members with a small length to width ratio the assumption that the structural behaviour can be equated to that of a linear bar element with corresponding sectional properties is an over-simplification as it neglects the effects of extensional forces acting eccentrically in a section which, on account of its small depth, is relatively flexible about the planar axes. Due to the relatively small bending and torsional stiffness of the flights the extensional forces cannot always be equated to concentric forces acting in conjunction with planar couples as will be clear when studying the theory in the following section.

(b) The same kind of argument applies in the region near O in fig. 2.1. The linear bar analogy neglects the "interference" in this zone between the flights and intermediate landing.

/The additional ...

The additional stiffness due to this "interference" or interaction is considerable, especially if the clear horizontal distance between the flights is small.

It would appear from experience gained by the author in the design of stairs that :-

(a) the theory as proposed in this Part is adequate for stairs in which the clear horizontal distance c between parallel flights does not exceed about half the width b of the flights but that

(b) for stairs where the above dimension c exceeds half the width b of the flights, the extended theory as described in Part 3 should be applied. This ratio is only approximate as all the dimensions obviously affect the behaviour of the stairs.

Fuchsteiner's theory is probably only sufficiently accurate for $\frac{c}{b}$ ratios exceeding a value of the order of 1.5 whereas most stairways in practice have $\frac{c}{b}$ ratios of less than this. If c is small the distribution of bending moments about the X-axis (fig. 2.1) in the intermediate landing is not uniform as given by the Fuchsteiner theory, but is in fact concentrated at O as indicated. A model of this type of free stairway tested to destruction (See Part 4) failed due to bending at DL, the crack commencing at D.

The accuracy of Fuchsteiner's theory increases as the width of the flights becomes small compared with the linear dimensions and the stairway approximates more closely to a linear bar structure.

REFERENCES - PART 2 - GENERAL

(1) FUCHSTEINER, W., "Die freitragende Wendeltreppe" Beton-und Stahlbetonbau (Berlin), V.49, Nov. 1954, pp. 258 - 259.

(2) LIEBENBERG, A.C. "Load tests on stairways of a Reinforced Concrete Building in Johannesburg." The Concrete Association, Johannesburg, 1956.

(3) LIEBENBERG, A.C., "The Design of Slab Type Reinforced Concrete Stairways". The Structural Engineer. May, 1960. pp. 156 - 164.

(4) SIEV, A., "Analysis of Free Straight Multiflight Staircases." Proceedings A.S.C.E., V.88, No. ST3, Part I, June 1962, pp. 207 - 232.

(5) LIEBENBERG, A.C. "Contribution to discussion on paper reference (4)." Proceedings A.S.C.E., Vol. 88, No. ST6, December 1962. pp. 327 - 333.

(6) SAUTER, F., "Free-standing stairs". Journal of the A.C.I., July 1964. Proceedings V. 61. No. 7 p.p. 847 - 870.

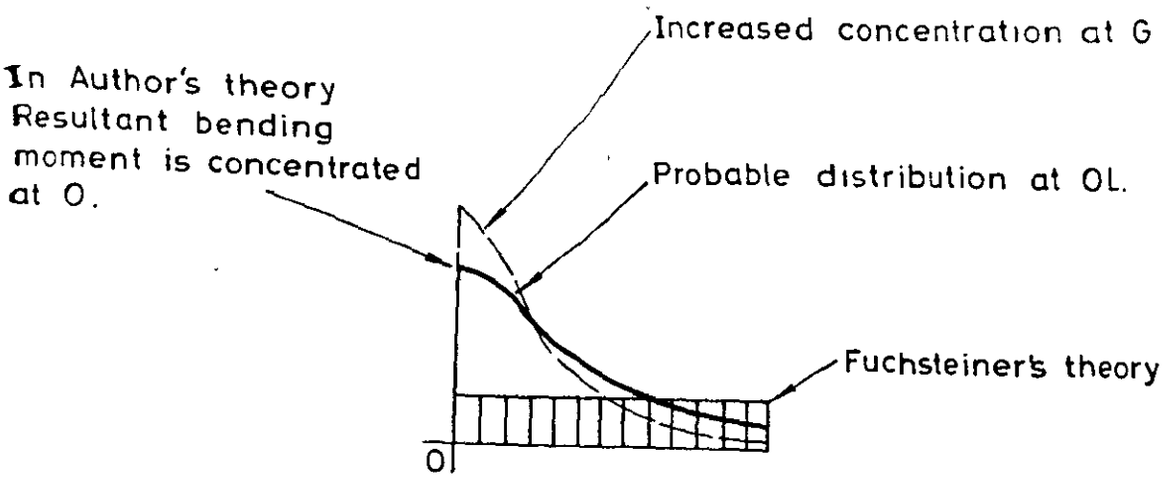

DISTRIBUTION OF BENDING MOMENTS ABOUT X-AXIS ALONG O-L FOR SYMMETRICAL LOADING

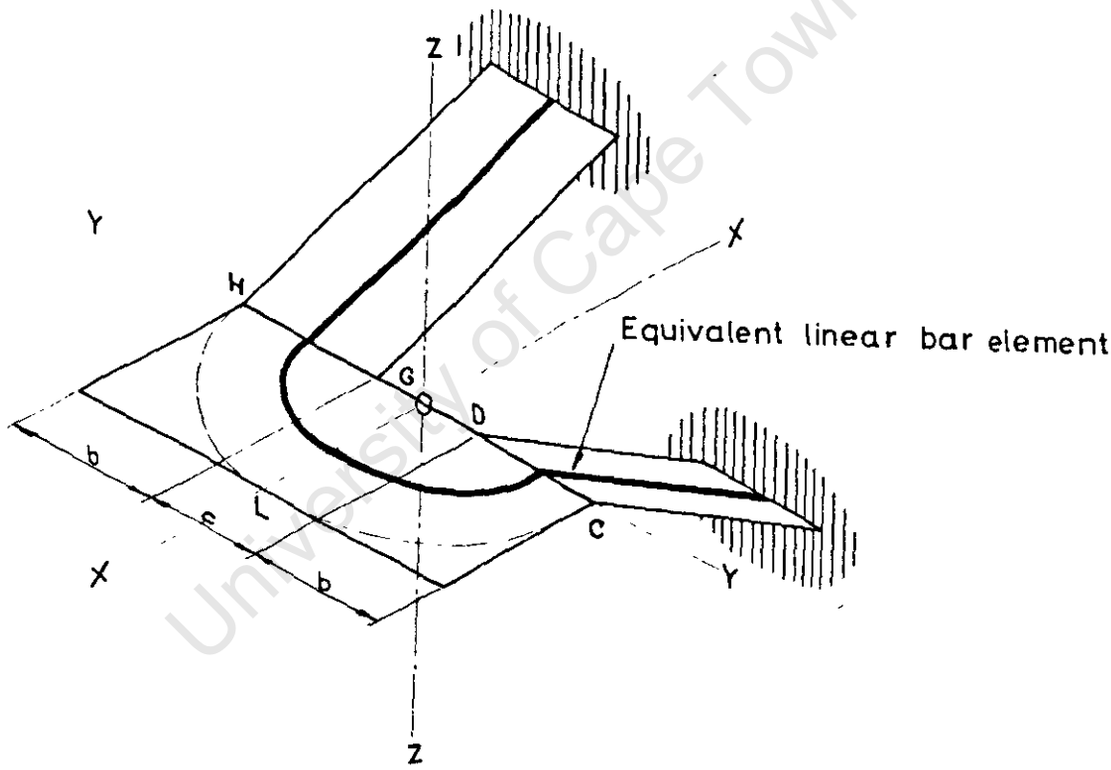

SUBSTITUTION OF SPACE STRUCTURE BY A SPACE FRAME COMPOSED OF LINEAR BAR ELEMENTS AS PROPOSED BY FUCHSTEINER.

FIG. 2·1.

REPRINT FROM

THE STRUCTURAL ENGINEER

THE JOURNAL OF THE
INSTITUTION OF STRUCTURAL ENGINEERS

The Design of Slab Type Reinforced Concrete Stairways

by A. C. Liebenberg (Associate-Member)

Reprinted from the May 1960 issue by permission of the Council of the Institution of Structural Engineers

The Design of Slab Type Reinforced Concrete Stairways

by A. C. Liebenberg, B.Sc.(Eng.), A.M.I.Struct.E., A.M.I.C.E.

Synopsis

The Author develops a method of design of slab type stairways, based on deductions made from full scale and scale model tests, which incorporates the extensional stiffness produced by the interaction of the stair flights and landings and which has been successfully applied in practice.

Although the very simple analytical procedure does not yield 'exact' solutions the inaccuracies involved appear to be small for most cases occurring in practice. Not only does the method lead to economy in design but the architecture can in many cases be enhanced by the elimination of beams and columns without the use of excessively thick sections, which would be required if the design procedures used in normal practice were employed.

Introduction

The normal practice in the design of slab type stairs, as typified by the recommendations of the "B.S. Code of Practice for Reinforced Concrete No. 114, 1957, Clauses 341 and 342," is to neglect the extensional stiffness provided by the interaction of the stair flights and landings and to consider the total resistance to the loading to be provided by bending forces only. Full scale load tests[1] carried out on a stairway of a reinforced concrete building in Johannesburg in 1952 demonstrated clearly that the normal method of analysis gives an incorrect picture of the load carrying mechanism in many types of stairs and leads to incorrect and unnecessarily conservative designs.

The conditions necessary for total or partial extensional stiffness to be produced exist in many types of stairways occurring in practice. As it would, however, be difficult to lay down general rules covering all the possible variations it is proposed to develop the analytical method for a few typical cases from which the general design procedure will be obvious. The Author has applied this method of analysis to the design of several types of stairs which have been constructed with complete success. Various Authors have in recent papers[2] described stairs designed along similar lines, but the basic approach to the problem as presented here is new.

Analysis

An 'exact' analysis of slab type stairs in accordance with the theory of elasticity is beyond the scope of existing rigorous mathematical methods. One of the more powerful numerical methods would have to be applied. Such an amount of work could not be justified in practice for a structure of this type. The method developed below is only an approximate method, but compares favourably with normal design procedures used in the design of reinforced concrete slab and beam systems in which compatibility of strains and deflections is mostly neglected and similar arbitrary assumptions as regards load and stress distribution are made. These and other so-called secondary effects which cannot be accurately determined on account of the many uncertainties inherent in reinforced concrete can usually be ignored because they are included in the factor of safety.

As the thickness of the slab elements of stairs is usually small compared with the planar dimensions the extensional stiffness may, under certain conditions greatly exceed the flexural stiffness. (The ratio is not equivalent to that of shell structures but is nevertheless significant). The *primary load carrying system* in such stairs is therefore produced by extensional (also known as membrane or planar) forces caused by the interaction of the stair flights, the landings and other external restraints such as walls, columns, beams and floor slabs. These 'points' or 'lines' of intersection of the slab elements become in effect 'supports' to the *secondary load carrying system* of bending forces in the slab elements, due to the fact that the resultant components of the extensional forces at these intersection points provide reactions which balance the shear forces in the slab elements.

The tests referred to above indicated that the deflections of the 'supports' at the intersection lines were small compared with the deflections due to bending of the stair flights and were of the same order of magnitude as the deformation of the brick wall supports. These 'supports' are therefore taken into account in the determination of the bending forces in the slab elements, the same assumptions being made as in normal design practice for the design of slab and beam systems.

The primary system may be *complete* in that it consists only of extensional forces or it may be an *incomplete* primary system which in order to have stability requires bending stiffness in certain members to supplement the incomplete extensional force system. It is essential to stress the necessity of such systems being completely stable for all possible modes of loading with sufficiently stiff external restraints to provide the reactions to the unbalanced internal extensional forces.

The sub-division of the analysis as described above is for convenience only. The relative importance of the two systems will depend on many factors including the type of stairs, the thickness of the slab elements in relation to the planar dimensions and the relative stiffnesses of the external restraints. It is seldom possible to make an accurate assessment of all these factors but as will be explained later, great accuracy is not required.

The analytical procedure can be summarised as follows :—

*

The component of the load in the plane of the slab is resisted by local direct forces which are extensional forces that are resisted by the imaginary "supports".

The resultant reactions on these imaginary "supports" as illustrated in fig. 1(e) and described in column 2 of page 59 are consequently composed of the shear forces (due to the secondary load carrying system) acting transversely to the slabs and the local direct forces acting in the plane of the slabs.

The effect of the deflection of these imaginary "supports" is negligible for this case.

The secondary load carrying system and local direct forces are as described in paragraph 1(a) on page 37A.

(a) Ascertain whether the conditions necessary for a primary system to function are present and determine the type of primary system and the effective 'supports' provided thereby to the secondary bending force system and any local direct forces that will result from any applied loading acting at an inclination to the axis of any member.

(b) Provide imaginary external restraints at the above-mentioned 'supports' so as to prevent displacement but allowing free rotation.

(c) Determine the magnitude of the secondary bending forces and local direct forces acting in the members due to the applied loading.

(d) Determine the resultant reactions on the imaginary 'supports'.

(e) Determine the magnitude of the forces in the primary system due to forces equal but opposite to these reactions. The actual stresses induced will be due to the combined effect of the forces acting in both systems.

Case I :—

Consider the stairs shown diagrammatically in Fig. 1(a). This is a simple case of a triangular arch and will serve well as an illustration of the method of analysis. The conditions necessary for a complete primary system to function are present. For the purposes of explanation an applied line loading acting as shown will be considered. Any other loading could be dealt with in a similar manner.

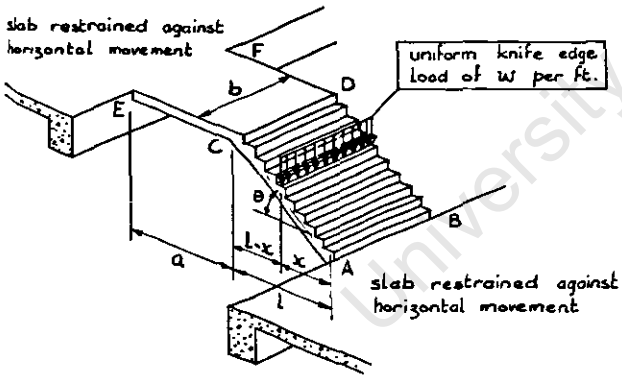

fig. 1(a) CASE 1

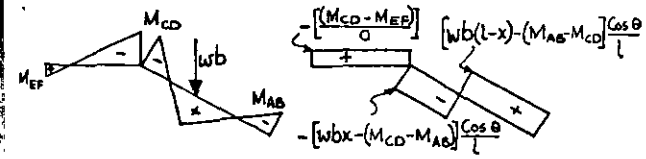

fig. 1(b) Bending Moments fig 1(c) Shear Forces

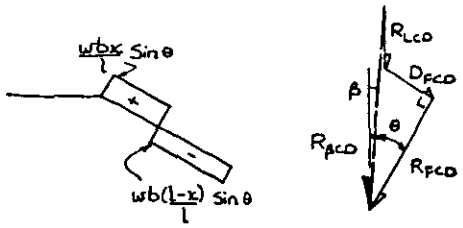

fig. 1(d) Local Direct Forces fig. 1(e) Force Diagram.

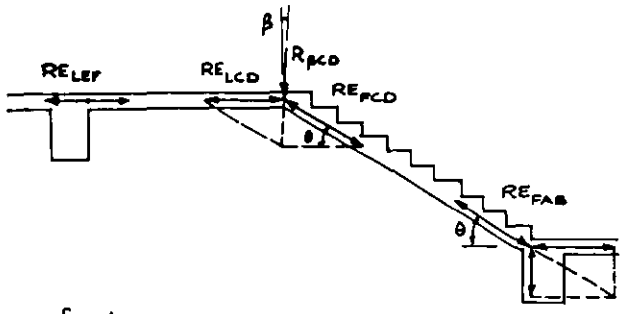

fig. 1(f) Resultant Extensional Forces

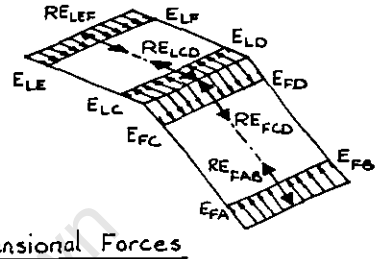

fig. 1(g) Extensional Forces

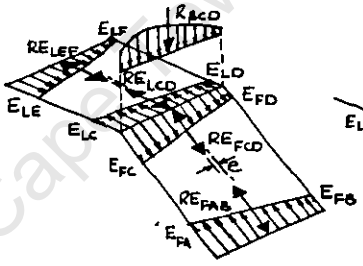

fig. 1(h).

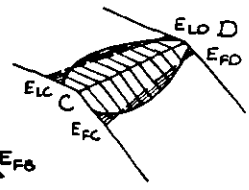

fig. 1(k).

In addition to the supports AB and EF the intersection line CD acts as a 'support' to the secondary bending force system. The actual bending forces will depend on the conditions of restraint at AB and EF and can be determined approximately by methods similar to those used in normal practice for the analysis of continuous slab systems.

For the bending forces and local direct forces shown in Figs. 1(b) to 1(d) the resultant reaction $R_{\beta CD}$ at CD acting at an angle β with the vertical will consist of three components as shown in Fig. 1(e), viz. :—

(i) $R_{FCD} = (wbx - [M_{CD} - M_{AB}]) \frac{\cos \theta}{l}$

due to the bending forces in the flight and acting at an angle θ with the vertical.

(ii) A vertical reaction $R_{LCD} = \frac{-[M_{CD} - M_{EF}]}{a}$

due to the bending forces in the landing and

(iii) a reaction $D_{FCD} = \frac{wbx}{l} \sin \theta$

due to the local direct force in the flight.

Consequently the extensional force in the landing

$RE_{LCD} = RE_{LEF}$ [see Fig. 1(f)].

$= -R_{\beta CD} (\sin \beta + \cos \beta \, . \, \cot \theta)$

(Tensile forces are assumed to be positive).

If $M_{CD} - M_{AB} = 0$ then $\beta = 0$ and the resultant reaction will act vertically and will be equal to

$$R_{\beta CD} = \frac{wbx}{l} - \frac{(M_{CD} - M_{EF})}{a} \quad \ldots \quad (\beta = 0)$$

The extensional forces in the flight (including the local direct forces) are :—

$$RE'_{FCD} = -R_{\beta CD} \cdot \frac{\cos\beta}{\sin\theta} + \frac{wbx}{l}\sin\theta$$

and

$$RE'_{FAB} = -R_{\beta CD}\frac{\cos\beta}{\sin\theta} - \frac{wb(l-x)}{l}\sin\theta$$

(See notation on page 163).

Neglecting edge effects the extensional forces per unit width or the stresses can be determined approximately. In this particular case the extensional forces will be uniformly distributed across the width as shown in Fig. 1(g).

For a non-uniform loading the distribution of the resultant reaction $R_{\beta CD}$ at CD may also be non-uniform and non-linear as shown in Fig. 1(h).

In such a case the shape of the extensional stress distribution in the landing slab and stair flight at the intersection line CD will actually approximate to that of the reaction $R_{\beta CD}$. It is, however, sufficiently accurate to assume that the Bernouilli-Euler straight line stress distribution is applicable. In comparison with the bending stresses, the extensional stresses are in most cases small so that a considerable error in the analysis may not affect the final value significantly. As a result of the above assumptions there may be unbalanced forces acting at the intersection line CD. Although the effect of these forces is usually negligible some allowance should be made in the case of heavy concentrated loads acting at or near the line CD.

Although a precise solution of this problem is not possible by simple methods, it can be dealt with as described below.

For a distribution of the resultant reactions due to bending forces at CD as shown in Fig. 1(k), the unbalanced forces will be as shown shaded. These unbalanced forces will be resisted by a combination of extensional and bending forces. For a case like this where the intersection line CD is continuous over the full width, the extensional forces will resist almost the total of the unbalanced forces and the secondary bending forces can be safely neglected. The unbalanced extensional forces therefore have to be 'dissipated' through a certain length of slab which procedure will give a distribution of stress approximating more closely to the actual.

This problem is not unlike that of the deep beam. An approximate solution can be found by assuming the dissipation of the unbalanced forces to occur over a length equal to b. The stress produced thereby can be determined by the approximate method suggested by Magnel[3] for end blocks in prestressed concrete beams wherein he assumed a 45° spread of direct forces and that the stress diagram due to the bending moment acting in the plane of the slabs is a parabola of the third degree, the stress being zero at a distance b from CD. It will very rarely be necessary in practice to make any allowance for this effect.

If the resultant $R_{\beta CD}$ acts at a distance 'e' off the centre line of the flight the extensional force in the landing at C, assuming tensile forces to be positive will be

$$E_{LC} = +\frac{RE_{LCD}}{b}\left(1+\frac{6e}{b}\right)$$

$$= -\frac{R_{\beta CD}}{b}(\sin\beta + \cos\beta.\cot\theta)\left(1+\frac{6e}{b}\right)$$

and at D will be

$$E_{LD} = +\frac{RE_{LCD}}{b}\left(1-\frac{6e}{b}\right).$$

$$= -\frac{R_{\beta CD}}{b}(\sin\beta + \cos\beta.\cot\theta)\left(1-\frac{6e}{b}\right)$$

and similarly for the other forces.

Any movement of the supports AB and EF will cause CD to deflect and will therefore affect the magnitudes of the bending forces which in turn will determine the magnitude of the extensional forces. Provided the characteristics of the supports are known the resultant internal forces could be calculated but this would involve more work than is justified for such a small structure. A conservative estimate could however be made by covering a range of possible solutions. The problem is not unlike that of normal plane slabs supported on beams walls and columns where a considerable relative deflection of supports may occur—an everyday problem for the practising designer. Bearing in mind the latest developments of the plastic and ultimate load or loadfactor methods of design any errors involved in the above procedure cannot be serious.

Any type of loading on the stairs e.g. partially distributed loading, point and line loads such as a balustrade wall along the outer edges, could be treated in a similar manner, the only complication being the calculation of the bending forces which is in no way different to the problems arising in the design of slabs supported on walls or beams.

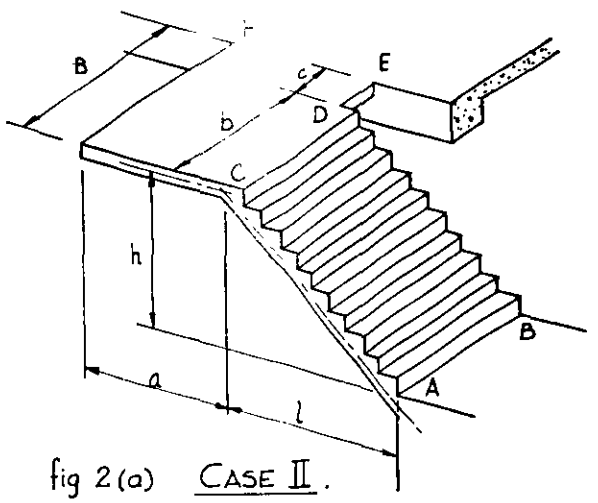

fig 2(a) CASE II.

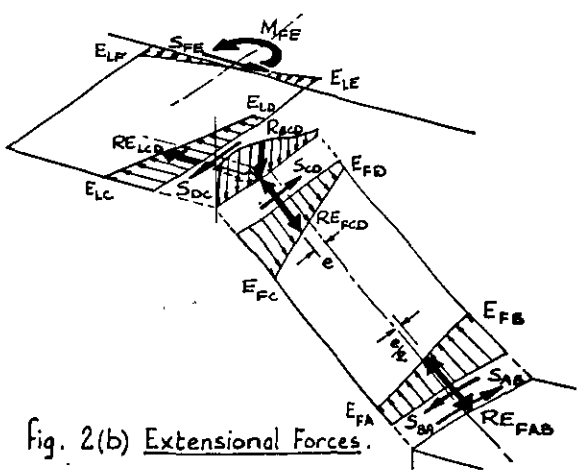

Fig. 2(b) Extensional Forces.

In determining the internal forces the stairs can be considered to be of a homogenous isotropic material, as is common practice in the design of shell roofs and similar structures, and the steel reinforcement thereafter positioned so as to resist all tensile forces in accordance with normal reinforced concrete design practice.

Case II :—

The stairs shown diagrammatically in Fig. 2(a) and consisting of a cantilever landing slab and a single flight rigidly supported at the lower end also complies with the conditions necessary for a complete primary system to act. The primary system which is shown in Fig. 2(b) provides full support to the bending forces at the intersection line CD. The bending forces and local extensional forces are consequently calculated by the normal procedures considering the slab elements to be continuous and to be supported at AB, CD and EF.

As in Case I the resultant reaction $R\beta_{CD}$ at CD will consist of various components depending on the loading and may act at an angle β with the vertical and at an eccentricity 'e' off the centre line of the flight.

If D_{FCD} is the local extensional force in the flight due to the loading on the flight calculated as in Case I then the resultant extensional force in the flight at CD

$$RE'_{FCD} = RE_{FCD} + D_{FCD}$$

where

$$RE_{FCD} = -\,R_{\beta CD}\frac{\cos\beta}{\sin\theta}$$

and the resultant extensional force in the landing at CD

$$RE_{LCD} = -\,R_{\beta CD}\,(\sin\beta + \cos\beta.\cot\theta)$$

As for Case I the force distribution can be assumed to be linear.

Consequently :—

$$E_{FC} = -\left[R_{\beta CD}\frac{\cos\beta}{b\sin\theta}\left(1+\frac{6e}{b}\right)\right] \quad \text{per unit width}$$

and

$$E'_{FC} = -\left[R_{\beta CD}\frac{\cos\beta}{b\sin\theta}\left(1+\frac{6e}{b}\right)\right] + \left[\frac{D_{FCD}}{b}\left(\frac{1+6e'}{b}\right)\right] \quad \text{per unit width}$$

where e' is the eccentricity of D_{FCD}

$$E_{FD} = -\left[R_{\beta CD}\frac{\cos\beta}{b\sin\theta}\left(1-\frac{6e}{b}\right)\right] \quad \text{per unit width}$$

$$E'_{FD} = -\left[R_{\beta CD}\frac{\cos\beta}{b\sin\theta}\left(1-\frac{6e}{b}\right)\right] + \left[\frac{D_{FCD}}{b}\left(1-\frac{6e'}{b}\right)\right] \quad \text{per unit width}$$

$$E_{LC} = +\frac{RE_{LCD}}{b}\left[1+\frac{6e}{b}\right] \quad \text{per unit width}$$

$$E_{LD} = +\frac{RE_{LCD}}{b}\left[1-\frac{6e}{b}\right] \quad \text{per unit width}$$

Considering the equilibrium of the flight

$$RE_{FAB} = RE_{FCD} = -\,R_{\beta CD}\frac{\cos\beta}{\sin\theta}$$

$$RE'_{FAB} = RE'_{FCD} - W_F\sin\theta = -\,R_{\beta CD}\frac{\cos\beta}{\sin\theta} + D_{FCD} - W_F\sin\theta$$

(where W_F is the total load on the flight).

$$S_{AB} = S_{CD} = \frac{1}{\sqrt{h^2+l^2}}\left[-\,RE_{FCD}.\frac{3}{2}e\right] = \frac{1}{\sqrt{h^2+l^2}}\left[R_{\beta CD}\frac{\cos\beta}{\sin\theta}\frac{3}{2}e\right]$$

$$S'_{AB} = S'_{CD} = \frac{1}{\sqrt{h^2+l^2}}\left[R_{\beta CD}\frac{\cos\beta}{\sin\theta}.\frac{3}{2}.e - D_{FCD}.e^{1} + W_F\sin\theta.e'' + D_{FAB}.e'''\right]$$

where e'' is the eccentricity of the resultant of W_F and e''' is the eccentricity of the local direct force D_{FAB}

$$E_{FA} = +\frac{RE_{FAB}}{b}\left(1-\frac{3e}{b}\right) \quad \text{per unit width}$$

$$E'_{FA} = E_{FA} + \frac{D_{FAB}}{b}\left(1-\frac{6e'''}{b}\right) \quad \text{per unit width}$$

$$E_{FB} = +\frac{RE_{FAB}}{b}\left(1+\frac{3e}{b}\right) \quad \text{per unit width}$$

$$E'_{FB} = E_{FB} + \frac{D_{FAB}}{b}\left(1+\frac{6e'''}{b}\right) \quad \text{per unit width}$$

Considering the equilibrium of the landing :—

$$S_{FE} = -\,RE_{LCD}$$

$$E_{LF} = \frac{S_{CD}}{a} - \frac{6}{a^2}\left[-\,RE_{LCD}\left(\frac{b}{2}+e+c\right) + S_{CD}.\frac{a}{2}\right] \quad \text{per unit width}$$

$$E_{LE} = \frac{S_{CD}}{a} + \frac{6}{a^2}\left[-\,RE_{LCD}\left(\frac{b}{2}+e+c\right) + S_{CD}.\frac{a}{2}\right] \quad \text{per unit width}$$

Case II (b) :—

If the one edge of the flight (BD) were to be built into a wall an additional resistance in the form of a shear force S_{BD} would act along the edge of the flight. Due to the additional support along the edge, the flight could be considered as a slab supported on three edges when determining the bending forces.

Considering the equilibrium of the flight for this case :—

$$RE'_{FAB} = RE'_{FCD} - W_F\sin\theta + S'_{BD}$$

i.e.

$$S'_{BD} - RE'_{FAB} = -\,RE'_{FCD} + W_F.\sin\theta$$

i.e.

$$S'_{BD} = K_S\,(-\,RE'_{FCD} + W_F\sin\theta)$$

and

$$-\,RE'_{FAB} = (1-K_S)\,(-\,RE'_{FCD} + W_F\sin\theta)$$

where K_S cannot be determined by simple methods. A conservative estimate can however be made.

Case III :—

The staircase shown in Fig. 3(a) is of the 'scissors' type being supported at the main landings only. The primary system for this case can never be complete and is statically indeterminate.

The easiest approach in solving this case is to commence by determining the resultants at the intersection lines of the slab elements due to the bending forces and then to draw imaginary straight lines (within the planes of the slab elements) from these resultants to the most rigid supports. The resultant extensional forces will always tend to flow directly towards the most rigid supports. If a set of such direct extensional forces is in complete equilibrium, the primary system may be said to be complete. If, however, equilibrium does not exist, certain types may attain full equilibrium with the assistance of bending forces set up by deformation of

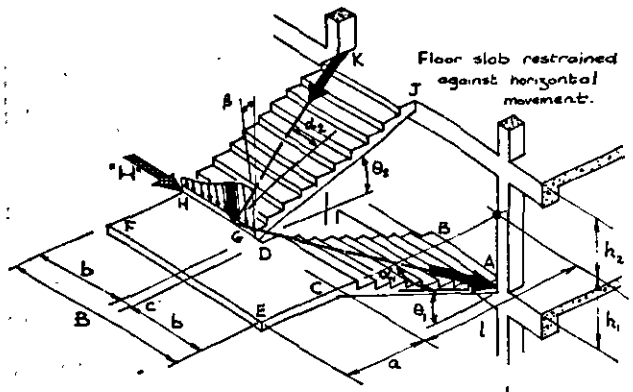

fig. 3(a) CASE III.

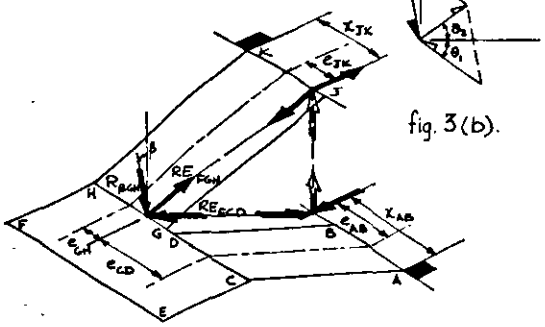

fig. 3(c)

fig. 3(b).

the slab elements. The primary system may then be said to be *incomplete*. The deformation of the structure due to extensional forces is small compared to such bending deformation and may be neglected.

The case under consideration is clearly not in equilibrium under the primary system assumed and would require an additional force 'H' acting as shown and equal to

$$'H' = RE''_{FGH} \sin\alpha_2 - RE''_{FCD} \sin\alpha_1$$

also :—

$$-(RE''_{FGH} \cos\alpha_2 \cos\theta_2) - (RE''_{FCD} \cos\alpha_1 \cos\theta_1) = R_{\beta GH} \sin\beta$$

$$(RE''_{FGH} \cos\alpha_2 \sin\theta_2) - (RE''_{FCD} \cos\alpha_1 \sin\theta_1) = R_{\beta GH} \cos\beta$$

(See Fig. 3(b)).

from which 'H' can be determined.

As 'H' is an imaginary force the final solution can now be obtained by applying a force equal in magnitude to 'H' but acting in the opposite direction. This will cause the stairs to undergo a sidesway. This will be resisted by extensional and bending forces in the slab elements causing a displacement of the resultant extensional forces until full equilibrium is attained.

This can only occur when the resultant extensional forces in the two flights act in the same vertical plane so as to have no resultant component in the direction of 'H'. The resultant at A will move towards B and the resultant at K will move towards J thus causing bending in the main landings. Assuming that the deformations due to extensional forces are negligible in comparison with those due to bending of the main landings, the displacement of these resultants X_{AB} and X_{JK} (Fig. 3(c)) will depend primarily on the stiffness of the edges of the main landings in a direction coinciding with the planes of the flights.

If, for example, the upper landing has negligible stiffness compared with the lower landing $X_{JK} = 0$ and $X_{AB} = B$.

If the landings and flights are identical

$$X_{JK} = X_{AB} = \frac{B}{2}$$

and the resultant forces will act at midspan of the main landings. For intermediate cases a precise calculation would be complex but here again an estimate can be made.

The extensional stresses in the flights and landings can now be calculated by a similar procedure as for Case II.

Bending forces will be caused by the loads spanning between the 'supports' as well as by the unbalanced components of the extensional forces and bending shear forces acting at the main landings and along the intersection line CH of the intermediate landing.

Consider the line CH. The unbalanced forces acting on the intermediate landing edge will be as shown in Fig. 3(d).

The unbalanced vertical forces indicated are as a result of the assumption made that the straight line stress distribution applies. The effect hereof is usually negligible but in extreme cases could be dealt with as described previously. The unbalanced forces acting in the plane of the lower flight will be resisted primarily by extensional forces in the intermediate landing and the flights along CD and GH but between D and G considerable bending forces will be induced. The shear forces and bending moments acting in the plane of the lower flight are shown in Figs. 3(e) and 3(f). Bending forces will be induced along the edge DG of the intermediate landing by the vertical components of these forces, whereas the horizontal components will induce extensional forces. In a case such as this where the primary system is incomplete care should be taken as the straight line stress distribution may be erroneous by a considerable amount. As the bending stiffness of the landing is relatively small the force components resisted by bending forces cannot be distributed for the

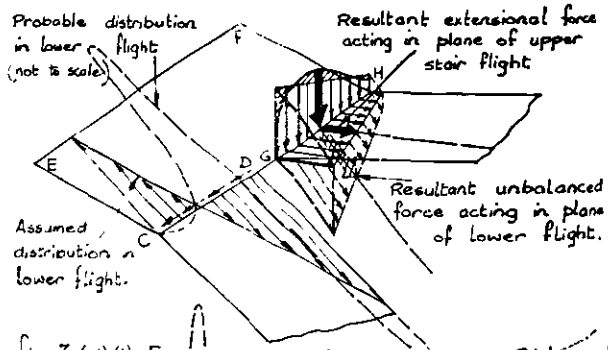

fig 3(d)(i) EXTENSIONAL FORCES AT CH.

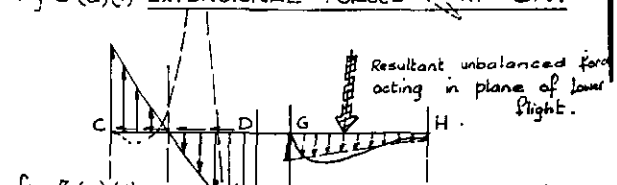

fig. 3(d)(ii) EXT FORCES IN PLANE OF L. FLGHT

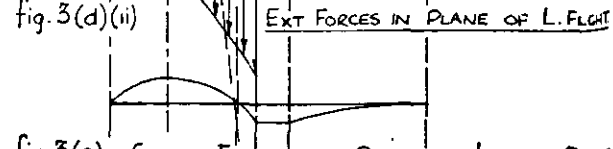

fig. 3(e). SHEAR FORCES IN PLANE OF LOWER FLGHT

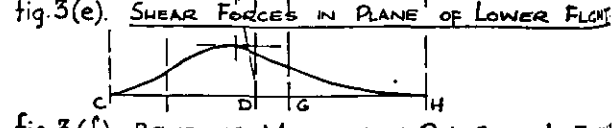

fig. 3(f). BENDING MOMENTS IN PLANE OF L. FLGHT

Instead of using an imaginary horizontal force to provide equilibrium in the initial stages of the argument a more direct approach could be adopted by simply commencing with the obvious fact that "if torsion in the flights is neglected then to be in equilibrium the reactions of the extensional forces must lie in one plane with the resultant of the applied load".

*

FOOTNOTE TO COL. 2 ON PAGE 62

The unbalanced vertical forces referred to here are indicated by shading in fig. 3(d)(i) and are identical to the unbalanced forces described on page 60 which result from the fact that the reaction of the secondary bending forces and local direct forces on the imaginary "support" CH is not linearly distributed, whereas the distribution of the vertical resultant of the extensional forces in the flight and intermediate landing is by assumption linear.

*

"The resultant extensional force in the stair flights, Fig. 3h, produced by the loading (2) of page 37A must act in a plane on the centre line of the stairs; see page 61A also.

The vertical component of the extensional force in the lower flight, together with the loading along CD, form a couple, acting on CD, which is balanced by a similar couple on GH produced by the upper flight. The couples have magnitude $\frac{1}{2}mb(b + c)$ where m is the vertical component of the reaction on CD. These couples apply a bending moment to the landing, and torsion to the flights.

Neglecting torsion, it is seen that the moment caused at the centre of the landing is hogging, of magnitude $\frac{1}{2}mb(b + c)$

full width of the lower flight and consequently a concentration of stress at the inner edge will result. Some allowance should be made for this effect. In most cases in practice the stresses as calculated can be more than doubled without greatly influencing the design. In the case of opposite loading where tensile forces are involved the reinforcement can be concentrated at the inner edge of the upper flight.

Torsional stiffness apart from resisting local forces is not essential for the stability of this type of stairs. In stairs having considerable torsional stiffness a different force distribution will result. Torsion in slab elements has been fully dealt with by various Authors[4]. In stairs of normal dimensions the torsional stiffness of the slab elements is relatively small and can be neglected for the sake of simplicity.

Any loading on the stairs can be treated in a similar manner. For a symmetrical stairs with a uniformly distributed loading the resultant extensional forces (or primary system) will act in a plane on the centre line of the stairs. The unbalanced resultant forces acting at the midspans of the main landings will be resisted by bending forces in combination with secondary extensional forces. Although the stair flights and intermediate landing slab can be relatively thin the main landings will have to be capable of supporting in effect the total weight of the stairs at midspan.

The extensional forces acting at the lines of intersection of the slab elements in a stairway of this type with a uniformly applied distributed load is shown in Fig. 3 (g) (i).

β_1 and β_2 will in most cases be small and the reactions at the intersection lines can for simplicity be considered to act vertically.

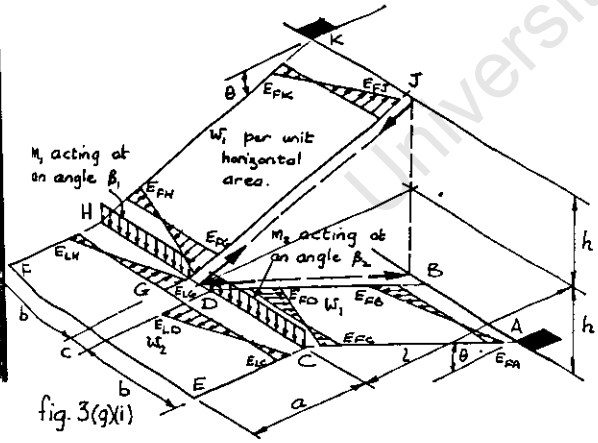

fig. 3(g)(i)

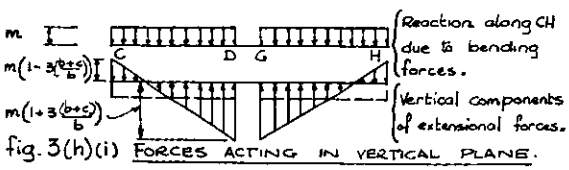

fig. 3(h)(i) FORCES ACTING IN VERTICAL PLANE.

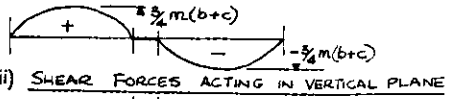

fig. 3(h)(ii) SHEAR FORCES ACTING IN VERTICAL PLANE

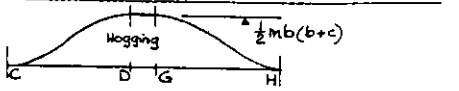

fig. 3(h)(iii) BENDING FORCES ACTING IN VERT PLANE.

$$m_1 = m_2 = \left[k_1 w_1 lb + k_2 w_2 a\left(b + \frac{c}{2}\right)\right]\frac{1}{b} = m$$

$$RE_{FCD} = -RE_{FGH} = -\frac{mb}{\sin\theta}$$

$$RE^1_{FCD} = -RE^1_{FGH} = -\frac{mb}{\sin\theta} + \frac{w_1 lb \sin\theta}{2}$$

The magnitudes of the extensional forces are as follows :—

$$E_{FA} = +\frac{RE_{FCD}}{b}\left[1 - \frac{3(b+c)}{b}\right] = -\frac{m}{\sin\theta}\left[1 - \frac{3(b+c)}{b}\right] \quad \text{per unit width}$$

$$E'_{FA} = +E_{FA} - w_1 l\frac{\sin\theta}{2} \quad \text{per unit width}$$

$$E_{FB} = +\frac{RE_{FCD}}{b}\left[1 + \frac{3(b+c)}{b}\right] = -\frac{m}{\sin\theta}\left[1 + \frac{3(b+c)}{b}\right] \quad \text{per unit width}$$

$$E'_{FB} = +E_{FB} - w_1 l\frac{\sin\theta}{2} \quad \text{per unit width}$$

$$E_{FC} = E_{FA} \text{ and } E'_{FC} = E_{FC} + \frac{w_1 l \sin\theta}{2} \quad \text{per unit width}$$

$$E_{FD} = E_{FB} \text{ and } E'_{FD} = E_{FD} + \frac{w_1 l \sin\theta}{2} \quad \text{per unit width}$$

$$E_{LC} = -\frac{m}{\tan\theta}\left[1 - \frac{3(b+c)}{b}\right] \quad \text{per unit width}$$

$$E_{LD} = -\frac{m}{\tan\theta}\left[1 + \frac{3(b+c)}{b}\right] \quad \text{per unit width}$$

$$E_{LG} = -E_{LD} \text{ and } E_{LH} = -E_{LC} \quad \text{per unit width}$$

$$E_{FG} = -E_{FD} \text{ and } E_{FH} = -E_{FC} \quad \text{per unit width}$$

$$E'_{FG} = E_{FG} - \frac{w_1 l \sin\theta}{2} \text{ and } E'_{FH} = E_{FH} - \frac{w_1 l \sin\theta}{2} \quad \text{per unit width}$$

$$E_{FJ} = -E_{FB} \text{ and } E'_{FK} = -E_{FA} \quad \text{per unit width}$$

$$E'_{FJ} = E_{FJ} + \frac{w_1 l \sin\theta}{2} \text{ and } E_{FK} = E'_{FK} + \frac{w_1 l \sin\theta}{2} \quad \text{per unit width}$$

The unbalanced resultants of the primary extensional forces along CH act in this case in a vertical plane and are shown in Fig. 3 (h) (i).

The shear forces and bending moments due to these forces are shown in Fig. 3 (h) (ii) and (iii).

By similar methods the bending and extensional forces at any section can be determined.

Note that the assumption has been made that the vertical reaction of the bending shear forces at CH is uniformly distributed. This is a conservative assumption as the load concentration will actually be higher towards D and G, thereby causing smaller bending moments on CH.

Case IV :—

The staircase shown in Fig. 4 is similar to Case III with the exception that the end of the intermediate landing is restrained horizontally and vertically as shown. The extensional forces for any loading can be determined by a similar procedure. If the wall supporting the landing is relatively ' rigid ' in comparison with the vertical bending stiffness of the main landings the moments caused by sidesway will be resisted within the flights and intermediate landing by extensional

and bending forces, the result being a 'shift' of the resultant extensional forces as shown.

$R_{\beta CD}$ is determined from the bending forces.

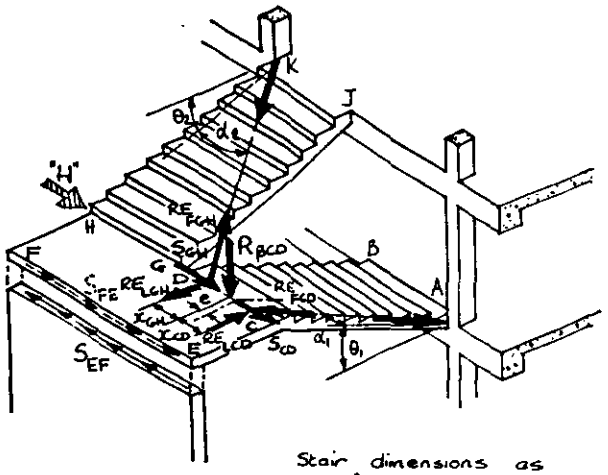

Stair dimensions as for fig. 3(a).

Fig. 4

Considering the equilibrium of the intermediate landing :—

$$R_{\beta CD}.\cos\beta = -RE_{FCD}.\cos\alpha_1 \sin\theta_1 + RE_{FGH}.\cos\alpha_2.\sin\theta_2 \quad . \quad . \quad (1)$$

$$RE_{LGH} + R_{\beta CD}.\sin\beta = -RE_{LCD} \quad . \quad . \quad . \quad (2)$$

where

$$RE_{LGH} = RE_{FGH}.\cos\alpha_2.\cos\theta_2 \quad . \quad . \quad . \quad . \quad (3)$$

$$RE_{LCD} = RE_{FCD}.\cos\alpha_1.\cos\theta_1 \quad . \quad . \quad . \quad . \quad (4)$$

$$S_{FE} = S_{GH} + S_{CD} \quad . \quad . \quad . \quad . \quad . \quad . \quad . \quad (5)$$

where

$$S_{GH} = RE_{FGH}.\sin\alpha_2 \quad . \quad . \quad . \quad . \quad . \quad . \quad (6)$$

$$S_{CD} = -RE_{FCD}.\sin\alpha_1 \quad . \quad . \quad . \quad . \quad . \quad . \quad (7)$$

$$RE_{LGH}.X_{GH} - RE_{LCD}.X_{CD} = S_{FE}.a \quad . \quad . \quad (8)$$

$$RE_{FGH}\cos\alpha_2.\sin\theta_2.X_{GH} + RE_{FCD}.\cos\alpha_1 \sin\theta_1.X_{CD} = 0 \quad . \quad . \quad . \quad . \quad . \quad (9)$$

$$\frac{3}{2}b + c - e - X_{GH} = \frac{l}{\cos\theta_2}.\tan\alpha_2 \quad . \quad . \quad . \quad (10)$$

$$\frac{b}{2} + e - X_{CD} = \frac{l}{\cos\theta_1}.\tan\alpha_1. \quad . \quad . \quad . \quad . \quad (11)$$

The internal extensional forces can consequently be determined.

The secondary extensional and bending forces can be determined as before.

If the wall supporting the intermediate landing is not 'rigid' the solution will be somewhere between that of Cases III and IV.

Case V :—

If the intermediate landing is also restrained at the two sides CE and FH as shown in Fig. 5, complete equilibrium can be attained by the set of extensional forces shown which can be determined as before by simple equilibrium equations.

If the wall restraints are not 'rigid' the solution will be somewhere between that of Cases III and V, depending on the relative stiffnesses.

Note that loads applied to the main landings will also be supported by the extensional force system in this particular case as the points C and H are restrained against deflection by the wall supports.

Complex Privary ystems :—

In stairs l ne or more redundant restraints two or more p systems may operate conjointly. It is usually p to make a reasonable estimate of the distributio he load between such systems based on the estima tive stiffnesses. As the stresses are usually small not necessary to achieve great accuracy ther s furthermore suggested that the following prop s may be an additional justification for this ch to the problem.

1. *If any slab stairs or similar structure in which the slab thickness ll compared with the overall dimensions is subjected applied load or set of loads any stable primary or set of systems, as defined previously, may be and provided that the sum of the stresses induced component parts by the primary forces and the sc bending forces for such a system are not in exces ultimate stresses or do not cause instability, then s a primary system or some other primary system, to sustain an equal or greater loading, will oper fectively before failure occurs.*

This proposit analogous to the load factor method used in t sign of beams and frames. It is based on the a ion that if for any particular loading the actu sses at a point in the structure exceed that given the analysis based on the assumed system, then bef the ultimate load resistance is attained the syste alter so as to accommodate the forces acting, in the same way that moment redistribution occ frames.

2. *The correct on is that system or set of systems for which the total nal strain energy is a minimum. The total strain energy will be a minimum when the strain energy due to nding forces is a minimum or in other words the cor solution is that which, provided that stability is achie , causes a minimum of bending in the slab elements.*

This proposition is precisely true only for a structure in which the thickness of the slab elements is very small compared with the planar dimensions. It will, however, be approximately true for most cases occurring in practice.

The application of the Method in practice :— It must be emphasized that this method of analysis cannot be applied indiscriminately to all types of structures as the errors inherent in the assumptions made may be significant in certain cases. For stairs of the normal dimensions dictated by practical considerations the extensional stresses are, however, small compared with the bending stresses, so that even if a considerable error

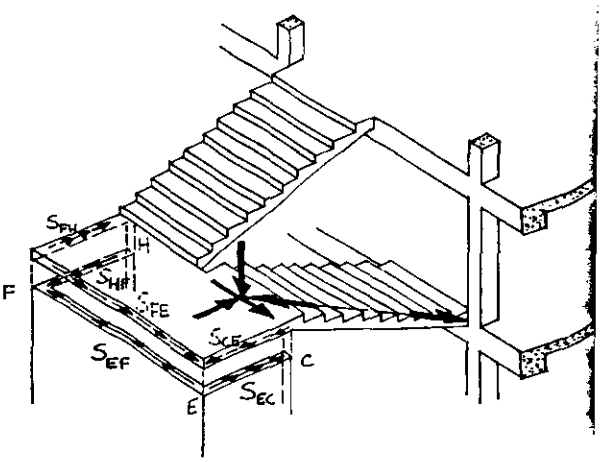

Fig. 5

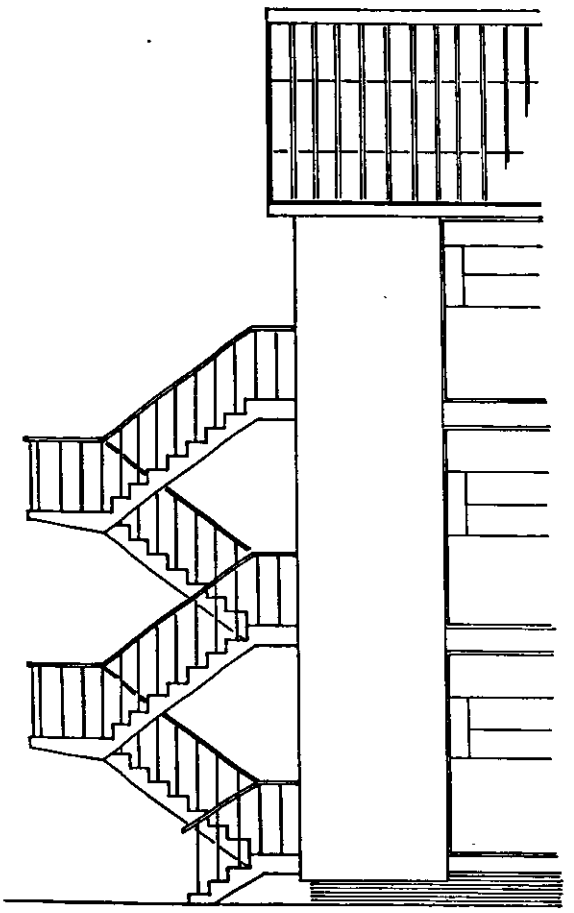

Fig. 6

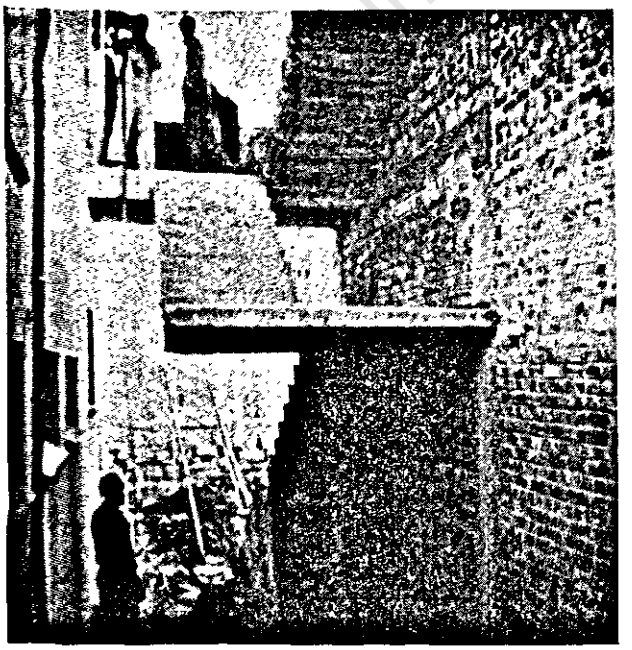

Fig. 7

is made it will not necessarily affect the value of the total stresses by very much. The analysis of the extensional stresses within the slab elements after the determination of the stresses or forces at the boundaries (intersection lines or supports) can be based on the same assumptions.

In actual fact the problem is not unlike the deep girder problem, the solution of which is difficult. In certain obvious cases much can be accomplished by intuitive 'scientific guessing' based on known results.

It is essential that the external supports to the internal extensional forces should be sufficiently rigid as a small horizontal displacement may cause considerable vertical deflection of the 'Supports' at the lines of intersection of the slab elements depending on the proportions of the stairs.

Where the external supports are relatively rigid (i.e. floor slabs with many restraints) the deflection of the 'supports' are, however, negligible. In some cases where the external restraints are not rigid or where doubt as to the efficacy of these restraints may exist, it may be possible to make an estimate of the forces acting and an approximate determination of the resultant deflections. The effect of the deflection of the 'supports' provided by the primary system may then be allowed for in the determination of the bending forces. In this determination great accuracy is not required if we bear in mind the latest developments of the plastic and ultimate-load or load-factor methods of design in which a considerable re-distribution of bending moments is allowed. It is no less difficult to make an accurate determination of actual bending moments in floor slabs supported on beams especially where the beams are relatively light and subject to considerable deflection.

Although tests have indicated that the restraint provided by brickwork can be considerable, it is to a large extent an unknown factor bearing in mind the possibility of a shrinkage 'gap' between concrete and brickwork and the variable properties of brickwork. Precautions should be taken to ensure positive support where brickwork is used to provide external restraint. Where the extensional forces are small in magnitude frictional forces may, however, provide sufficient resistance.

The fire escape stairs illustrated in Fig. 6 have been designed for a block of flats to be constructed near Cape Town and the photograph (Fig. 7) shows another type in a building in Oudtshoorn, which is typical of several stairways constructed with complete success. The brick wall to the right is a boundary wall and the intermediate landing is not cantilevered from it, but is supported by the flights.

Notation

$R\beta_{CD}$ —is the resultant reaction due to the secondary bending force system and local direct forces acting at the intersection line CD at an angle β with the vertical.

R_{FCD} —is the reaction at CD due to the bending forces in the flight acting at right angles to the flight.

R_{LCD} —is the reaction at CD due to the bending forces in the landing acting at right angles to the landing.

D_{FCD} —is the reaction at CD due to the local direct forces in the flight acting in the plane of the flight.

RE_{FCD} —is the resultant extensional force in the flight at CD due to the reaction $R\beta_{CD}$ but not including the effect of the local direct forces in the flight.

RE'_{FCD} —is the resultant extensional force in the flight at CD due to the reaction $R\beta_{CD}$ and including the effect of the local direct forces in the flight.

RE_{LCD} —is the resultant extensional force in the landing at CD.

E_{FC} —is the extensional force per unit length in the flight at C not including the local direct force.

E'_{FC} —is the extensional force per unit length in the flight at C including the local direct force.

E_{LC} —is the extensional force per unit length in the landing at C.

S_{CD} —is the shear force acting along the intersection line CD due to the primary force system but not including the effect of local direct forces.

S'_{CD} —is the shear force acting along the intersection line CD due to the primary force system and including the effect of local direct forces.

References

1. Lieberl[illegible], A. C., Load tests on Stairways of a Reinforced Concre[illegible]g in Johannesburg. *The Concrete Association* Johan[illegible], 1956.
2. Anon[illegible], An unusual staircase. *Concrete and Constructional Engi[illegible]*, April, 1957.
   Andre[illegible], The Filliot Secondary School, Putney. *The Struct[illegible]neer*, Nov., 1956.
3. Magnel, [illegible]estressed Concrete. *Concrete Publications Limited.*
4. Gerstle, [illegible]and Clough R. W., The Torsional Rigidity of Rectangular Slabs. *American Concrete Institute*, Nov., 1953.

Discussion

The Coun[illegible]d be glad to consider the publication of corresp[illegible]n connection with the above paper Commun[illegible]on this subject intended for publication should be [illegible]ded to reach the Institution by 30th July 1960.

Book Reviews

Handbook of Heavy Construction, edited by F. W. Stubbs. (New York and London : McGraw-Hill, 1959). 9 in. × 6 in., 1040 pp., £7 3s. 6d.

This American handbook gives the methods, data and working information required in all branches of heavy construction. The contributing authors are specialists in their respective fields, each with considerable experience, and collectively they represent active contractors, manufacturers, distributors and consulting engineers.

The book is divided into nine sections, the first dealing with excavation and transportation of earth and rock, and including a section on dewatering. The second section on concrete has chapters on selection of materials and mix proportions, aggregates, concrete batching, mixing, placing and curing, pneumatically applied concrete, instrusion grouting, precast and prestressed concrete, reinforcing steel and formwork.

Section 3, dealing with steel, has chapters on steel erection, electric arc-welding and flame cutting and welding, and the following three sections are on heavy timber construction, bituminous pavements and cross country pipelines. Section 7 on foundations deals with piles and pile driving, cofferdams and caissons, and the following section on miscellaneous equipment and operations, includes floating equipment and river diversion. The volume concludes with chapters on contractor's organization and planning, the work of a resident engineer, construction contracts, and planning for safety.

In addition to being a comprehensive work of reference for contractors, this handbook will also be of value to consulting engineers, designers, architects and to students wishing to obtain information on the subjects covered. The volume is well produced and contains more than six hundred illustrations.

Analysis of Continuous Beam Bridges, Vol. 1, Carry Over Procedure, by J. J. Tuma, S. E. French and T. I. Lassley (Oklahoma State University School of Civil Engineering Research Publication No. 3, 1959). 11 in. × 8½ in.

This report, which is the first publication in a series entitled " Analysis of Continuous Beam Bridges " deals with the application of the numerical carry-over moment method to the analysis of continuous beam bridges subjected to stationary or moving loads, applied couples, displacements of supports or changes in temperature. The method is a numerical successive approximation, which may be carried out to a desired degree of accuracy. The study is restricted to coplanar systems and the customary assumptions of beam analysis are introduced.

The publication is divided into six parts. The derivation of the general three moment equation for beams of variable section and the definitions of the beam constants are given in the first chapter. The geometry and the integral functions of beams with parabolic haunches are discussed in the second chapter. The algebraic formulae of beam constants such as angular flexibilities, carry-over values and load functions for beams mentioned before are derived in the third and fourth chapters. The numerical evaluation of these algebraic formulae is made by means of a high speed computer and the results recorded in tabular form in the fifth chapter. The application of the numerical carry-over procedure in connection with the tables of beam constants is illustrated by two examples in the last chapter.

PART 3

THE EXTENSION OF THE THEORY OF DESIGN OF SLAB-TYPE STAIRS TO OBTAIN COMPATIBILITY OF DEFLECTIONS IN FREE STAIRWAYS

INTRODUCTION

The theory of design of slab-type stairs as developed in Part 2 is adequate for the design of most cases occurring in practice. However in 1960 the author was requested by a firm of architects to design a free stairway similar to that of Case III in Part 2, but in which the dimension c, the clear distance between the adjoining flights, was equal to 0.72 times the width of the flights. The primary extensional force system would therefore be incomplete to a high degree and the consequential bending deformation of the intermediate landing and torsional stresses in the flights would not be negligible. It was felt that an extension of the approximate theory previously developed was called for. Although still in no sense "exact", the theory developed below is sufficiently accurate for this scale of structure and agrees well with the results of model tests as described in Part 4.

THE NATURE OF THE PROBLEM

Due to bending deformation of the intermediate landing of free stairways in which the flights are widely spaced, considerable torsional and bending forces may be induced in the flights in addition to the primary extensional and secondary bending forces referred to in the analysis developed in Part 2. In order to determine the order of magnitude of these forces an equation of compatibility expressed in terms of the deformation of the line of intersection of the intermediate landing and the flights is required.

ASSUMPTIONS MADE

(1) The assumptions made in Part 2 apply with the exception that bending and torsional deformations are taken into account by approximate methods.

/(2) The edge ...

* It will be clear from figure 9(e) that the intermediate landing will be subjected to a bending moment M_{xo} about the OX-axis and by a couple M_h about an axis parallel to OZ. Due to its great stiffness in its own plane the deformation due to bending moments about the OZ axes will be small but it may undergo considerable deformation due to bending about the OX axes. If the torsional stiffness of the flights is negligible the moments acting at the intersection line GH with the upper flight can be resolved as shown in fig. 9(f). If however the torsional rigidity and bending stiffness of the stair flights is comparable with that of the bending stiffness of the intermediate landing, the bending moment about an axis parallel to the OX axis is reduced to M'_{xo} as shown in fig. 9(g). Fig. 9(b) represents this reduction in bending moment and is equivalent to the shaded triangle of moments in fig. 9(g) which explains the derivation of the third term of equation 3.1 on page 68.

(2) The edge beams or slabs supporting the stairs at the floor levels are assumed to be infinitely rigid.

(3) The stiffness of the intermediate landing is assumed to be infinite in its own plane so that the points C, D, G and H in figure 8 remain approximately co-linear in plan.

(4) Bending deformation of the landing about the X-axis is assumed to be confined to the neighbourhood of the interval DG. This assumption is made on the grounds that the flexibility of the free edge of the landing in this interval must be relatively great compared to the intervals CD and GH where interaction with the flights would result in great bending stiffness. As the dimension c increases relative to b, the accuracy of this assumption will increase. The compatibility calculation as given below, is essential only for cases in which c is large which provides further justification for the assumption.

THE COMPATIBILITY EQUATION

Due to extensional strains in the flights, displacement of the ends CD and GH must take place. These displacements must however be compatible with the deformation and displacement of the adjoining edge CDGH of the intermediate landing. The relative displacements can best be expressed in terms of a Williott diagram.

For a uniformly distributed loading ω per unit horizontal area over the whole stairway and with reference to fig. 10 the extension of lines CD and GH meet at O because of the requirements of symmetry and the assumption that the landing is infinitely stiff in its own plane. The following equations express the conditions of equilibrium of forces and compatibility of deformations at the intersection line CH.

Using the notation of Part 2 and with reference to figs. 8 and 9,* bending equilibrium at O about the X-axis is expressed by

$$M_{x,o} = \frac{m'b(b+c)}{2} - \frac{M_t}{\cos\theta} \qquad \ldots (3.1)$$

/where ...

where m' = vertical component of the reaction per unit length along CD and GH caused by the secondary bending force system and resisted by the primary extensional force system.

M_t = the torsional moment acting in each flight.

Bending deformation of edge CH of the intermediate landing is expressed by

$$\frac{\lambda}{b} = \frac{M_{x,o}\, c}{2EI_{DG}} \qquad \text{.... (3.2)}$$

where λ is the vertical deflection of C and H relative to D and G respectively.

EI_{DG} is the effective modulus of rigidity of the edge DG if subjected to bending moments acting along DG about axes parallel to the X-axis.

With reference to fig. 10, the total torsional twist of a flight (about its own longitudinal axis) at the intersection line (say CD) is equal to

$$\frac{\mathcal{T}}{b} = \frac{\lambda}{b} \cdot \frac{\sin(\theta+\phi)}{\sin\phi} \qquad \text{.... (3.3)}$$

where $\mathcal{T}$ is the deflection of C relative to D measured at right angles to the plane of the flight.

Therefore

$$\lambda = M_t \frac{b\, l \sin\phi}{GC.\cos\theta.\sin(\theta+\phi)} \qquad \text{.... (3.4)}$$

where GC is the torsional rigidity of the flights.

From the geometry of fig. 10 and with reference to fig. 9(d)

$$\frac{\varepsilon_{FC} - \varepsilon_{FD}}{\lambda} = \frac{\cos(\theta+\phi)}{\sin\phi} \qquad \text{.... (3.5)}$$

where ε_{FC} = extension of the flight at C

$$= \left(\frac{E'_{FC}}{Ed} - \frac{6\,M_t \tan\theta}{Edb^2}\right)\frac{l}{\cos\theta} - \frac{\omega' l^2 \sin\theta}{2Ed\cos\theta}$$

$$= \left(-\frac{m'}{Ed\sin\theta}\left[1 - \frac{3(b+c)}{b}\right] + \frac{\omega' l \sin\theta}{2Ed} - \frac{6\,M_t \tan\theta}{Edb^2}\right)\frac{l}{\cos\theta} - \frac{\omega' l^2 \sin\theta}{2Ed\cos\theta} \qquad \text{.... (3.6)}$$

where ω' is the portion of the load resisted by extensional forces.

/Also ...

Also $\varepsilon_{FD} = \left(\frac{E'_{FD}}{E.d} + \frac{6M_t \tan\theta}{E.d.b^2}\right)\frac{l}{\cos\theta} - \frac{\omega' l^2 \sin\theta}{2Ed\cos\theta}$

$$= \left(-\frac{m'}{Ed.\sin\theta}\left[1 + \frac{3(b+c)}{b}\right] + \frac{\omega' l \sin\theta}{2Ed} + \frac{6M_t \tan\theta}{Edb^2}\right)\frac{l}{\cos\theta} - \frac{\omega' l^2 \sin\theta}{2Ed\cos\theta} \quad \text{... (3.7)}$$

Therefore $\left(\frac{m'}{\lambda Ed\sin\theta}\left[6\frac{(b+c)}{b}\right] - \frac{12M_t \tan\theta}{\lambda Edb^2}\right)\frac{l}{\cos\theta}$

$$= \frac{\cos\theta.\cos\phi - \sin\theta.\sin\phi}{\sin\phi} \quad \text{... (3.8)}$$

and $\cot\phi = \frac{6m'l(b+c)}{\lambda Edb\sin\theta.\cos^2\theta} - \frac{12M_t l.\tan\theta}{\lambda Edb^2\cos^2\theta} + \tan\theta$ ... (3.9)

By equating $M_t = m'b^2e$

where eb is the effective reduction due to the torsional moment M_t of the lever arm of the reaction $m'b$ causing bending of the intermediate landing about O, and substituting equation 3.2 in equation 3.1,

$$\frac{2EI_b}{bc}\lambda = m'\left[\frac{b(b+c)}{2} - \frac{b^2e}{\cos\theta}\right]$$

$$\therefore \frac{\lambda}{m'} = \left[\frac{b^2c(b+c)}{4EI_{bc}} - \frac{b^3ce}{2EI_{bc}\cos\theta}\right] \quad \text{... (3.10)}$$

Now $\frac{\sin(\theta+\phi)}{\sin\phi} = \sin\theta.\cot\phi + \cos\theta$

Substituting for $\cot\phi$ from equation 3.9

$$\frac{\sin(\theta+\phi)}{\sin\phi} = \frac{6m'l(b+c)}{\lambda Edb\cos^2\theta} - \frac{12M_t l\tan^2\theta}{\lambda Ed b^2\cos\theta} + \sin\theta.\tan\theta + \cos\theta$$

By substitution in equation 3.4

$$\frac{\lambda}{m'} = \frac{b^3el}{GC\cos\theta}\cdot\frac{\sin\phi}{\sin(\theta+\phi)}$$

$$= \frac{b^3el}{GC\cos\theta\left\{\frac{m'}{\lambda}\left[\frac{6l(b+c)}{Edb\cos^2\theta} - \frac{12el\tan^2\theta}{Ed\cos\theta}\right] + \sin\theta.\tan\theta + \cos\theta\right\}}$$

$$\therefore \frac{b^3 e l}{GC\cos\theta} = \left[\frac{6l(b+c)}{Edb\cos^2\theta} - \frac{12el\tan^2\theta}{Ed\cos\theta}\right] + \frac{\lambda}{m'}\left[\sin\theta.\tan\theta + \cos\theta\right]$$

Substituting for $\frac{\lambda}{m'}$ from equation 3.10,

$$e\left[\frac{b^3 l}{GC\cos\theta} + \frac{12l\tan^2\theta}{Ed\cos\theta} + \frac{b^3 c(\sin\theta.\tan\theta + \cos\theta)}{2EI_{DG}\cos\theta}\right]$$

$$= \frac{6l(b+c)}{Edb\cos^2\theta} + \frac{b^2 c(b+c)(\sin\theta.\tan\theta + \cos\theta)}{4EI_{DG}}$$

$$\therefore e = \frac{\left[\frac{6l(b+c)}{Edb\cos^2\theta} + \frac{b^2 c(b+c)(\sin\theta.\tan\theta + \cos\theta)}{4EI_{DG}}\right]}{\left[\frac{b^3 l}{GC\cos\theta} + \frac{12l\tan^2\theta}{Ed\cos\theta} + \frac{b^3 c(\sin\theta.\tan\theta + \cos\theta)}{2EI_{DG}\cos\theta}\right]}$$

... (3.11)

and $$\cot\phi = \frac{24 l I_{DG}\left[\frac{b+c}{\sin\theta} - 2bc.\tan\theta\right]}{d b^3 c\cos\theta\left[(b+c)\cos\theta - 2bc\right]} + \tan\theta$$

... (3.12)

Equations 3.11 and 3.12 can be evaluated by direct substitution of known parameters and are thus independent of the magnitude of loading. They are, however, dependent on the type of loading. Using these values, the unknowns M_t, λ and $M_{x,o}$, can be determined in terms of m'. Now if m is the equivalent total reaction at CH due to ω the total load then $m = m' + m''$

... (3.13)

where m'' is the additional load supported by bending forces.

With reference to fig. 10, the vertical deflection at the midpoint of CD is equal to

$$\delta_o + \lambda\left(\frac{l}{2} + \frac{c}{2b}\right) = \frac{4m''l^3}{Ed^3\cos\theta}$$

... (3.14)

/in which ...

in which

$$\delta_o = \frac{\varepsilon_{u,o}}{\sin\theta} = \frac{m'l}{Ed\sin^2\theta.\cos\theta}\left[1+3\left(\frac{b+c}{b}\right)^2\right] - \frac{6M_t l\tan\theta}{Ed.b^2\sin\theta.\cos\theta}.\frac{(b+c)}{b}$$

... (3.15)

Accordingly a solution of all the unknowns can be obtained to give compatibility of deformation at the intersection line C-H in terms of the assumptions made.

If s is measured in the plane of any flight from the intersection line CH then the sideway Δ_{CH} of the stairs at line CH if AB and JK are fixed is equal to

$$\Delta_{CH} = \frac{12}{Edb^3}\int_0^{\frac{l}{\cos\theta}}\left[\frac{m'b}{\sin\theta}.\frac{b+c}{2} - M_t\tan\theta\right]s.ds$$

$$= \frac{6}{Edb^3}\left[\frac{m'b(b+c)}{2\sin\theta} - M_t\tan\theta\right]\frac{l^2}{\cos^2\theta}$$

... (3.16)

With reference to fig. 10 the rotation of the intermediate landing about the Z-axis $\rho = \frac{\varepsilon_{FC}-\varepsilon_{FD}}{b.\cos\theta} + \frac{\lambda\tan\theta}{b}$ ... (3.17)

UNSYMMETRICAL LOADING

The solution for unsymmetrical loading can be obtained quite simply by combining symmetrical and assymetrical loading.

In the latter case no rotation of the intermediate landing can take place due to the corresponding asymmetry of the stairs and the Williott diagram can be readily constructed and the necessary equations formulated.

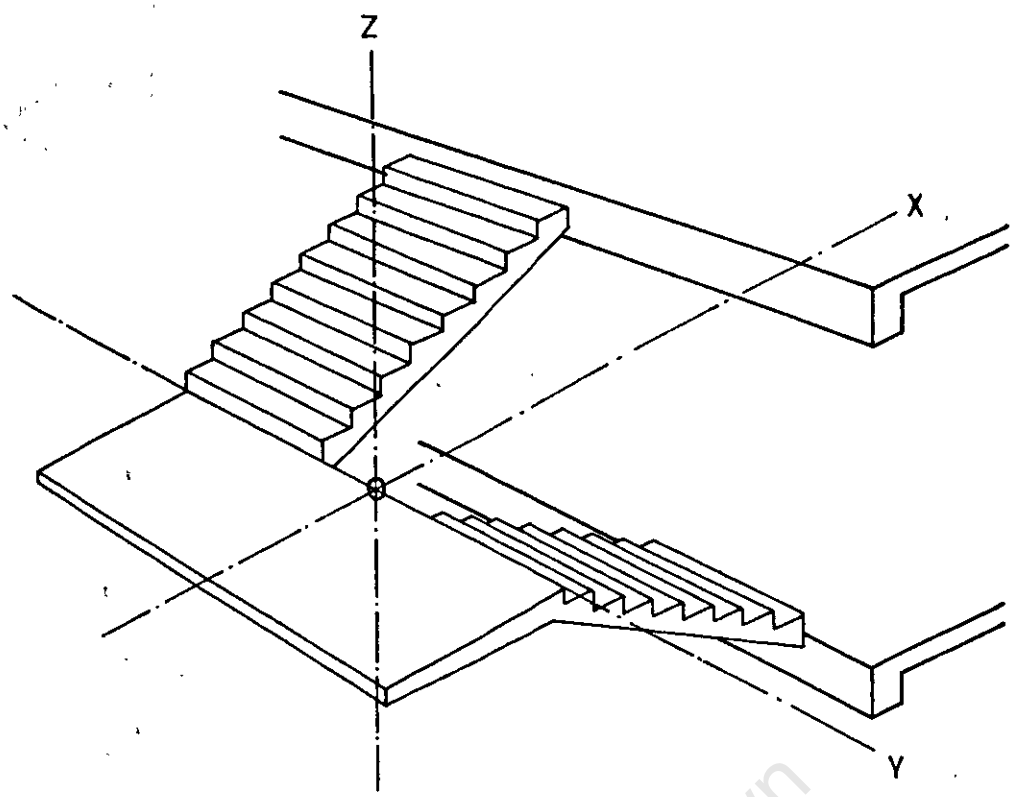

FREE STAIRWAY

FIG.8 (a)

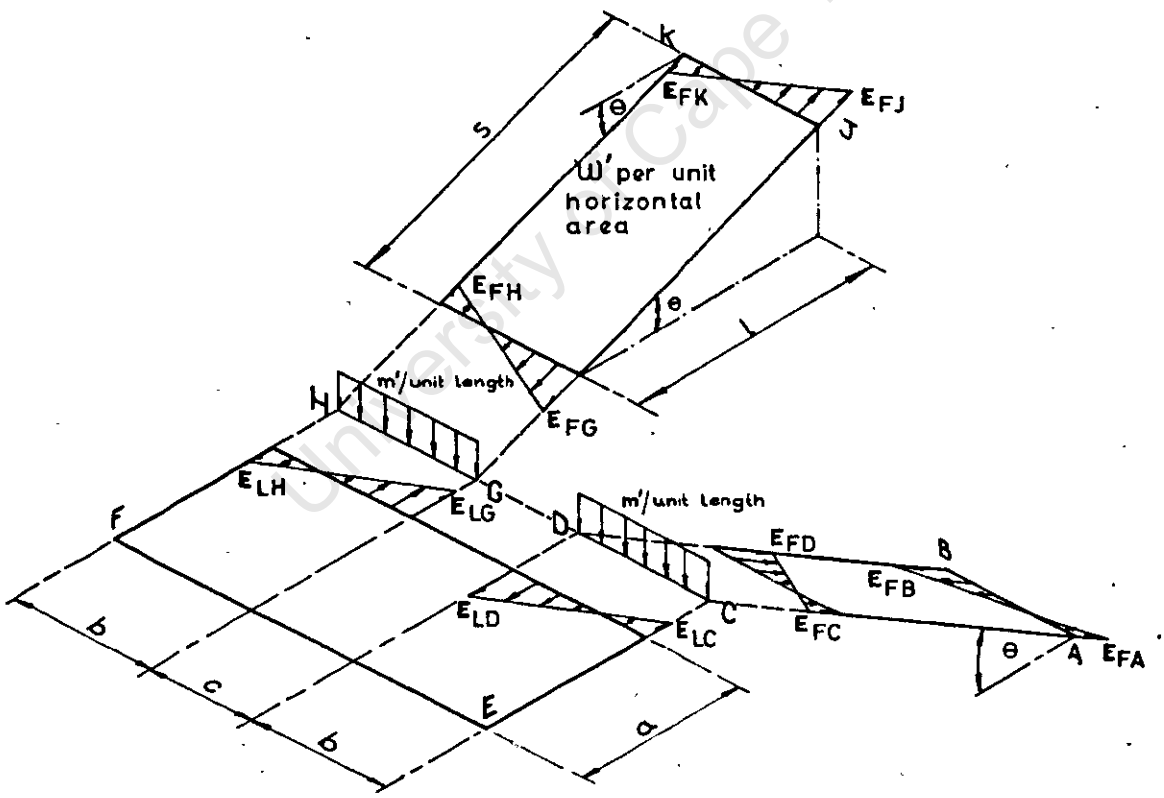

EXPLODED DIAGRAM SHOWING EXTENSIONAL FORCES AT INTERSECTION LINES.

FIG.8 (b)

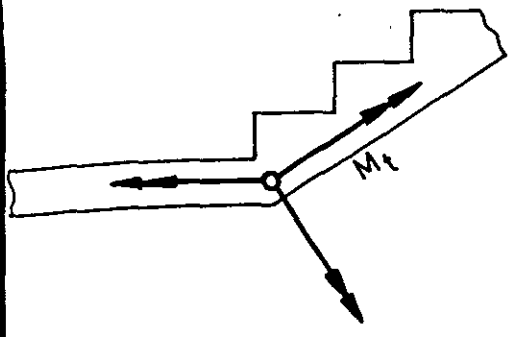

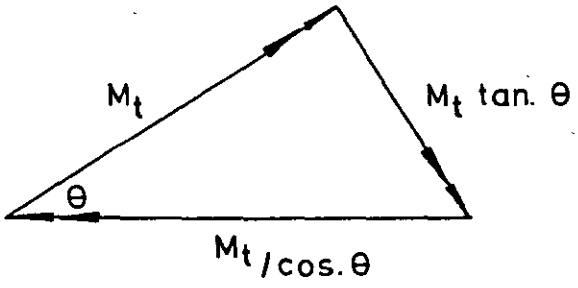

RESOLUTION OF TORSIONAL AND BENDING MOMENTS AT INTERSECTION

FIG.9(a)

FIG.9(b)

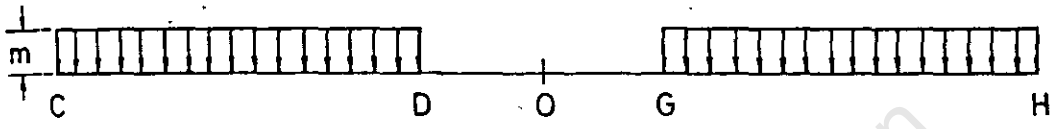

Reaction along C–H due to bending forces

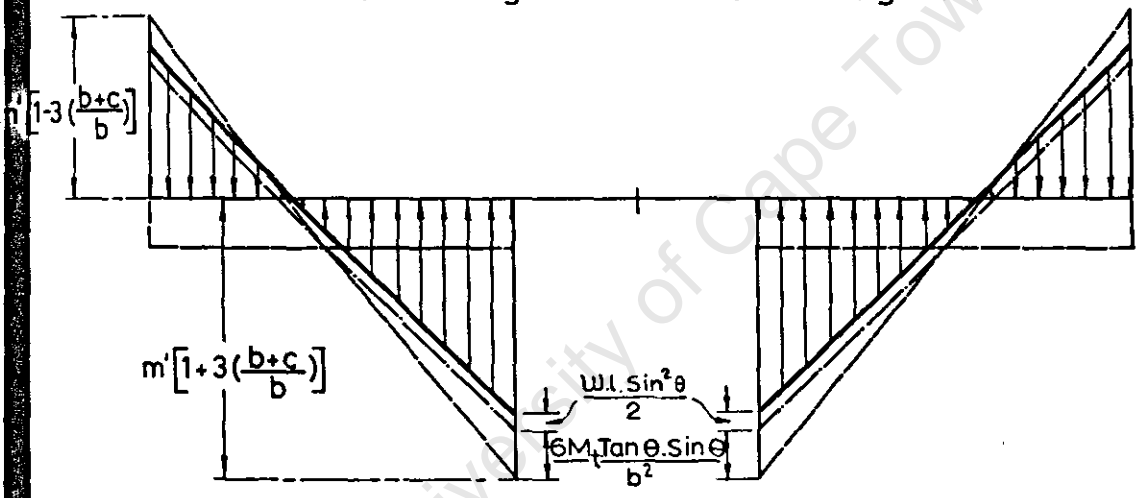

Vertical components of extensional forces due to reaction 'm', torsional moment M_t and local direct forces in flights.

FIG.9(c)

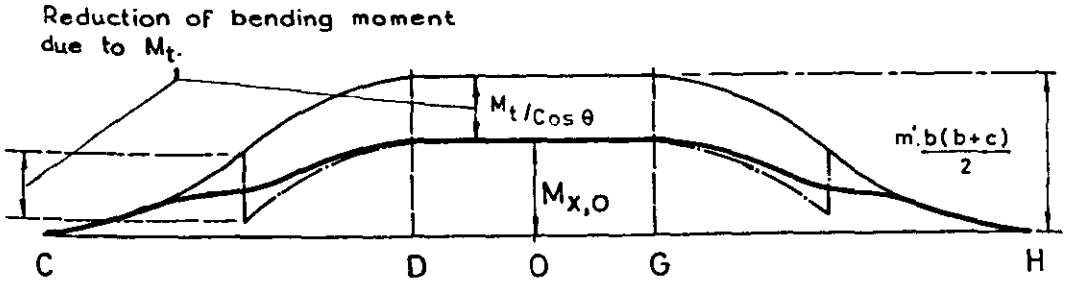

Bending moments about X-axis along intersection line CDGH

FIG.9(d)

*

Fig. 10 gives the displacements in the OX and OZ directions (see fig. 8_a) of the points C, D, O, G and H on the line of intersection CH if viewed from H towards C (fig. 8b). The dimensions ξ give the extensions (positive or negative) due to extensional stresses in the flights of the particular points indicated by the suffices. The broken lines indicate the deflections at right angles to the planes of the flights which terminate in the profile C'D'O'G'H' on account of the requirements of compatibility at the intersection line CH. Due to the symmetry of the deformations and the assumed infinite stiffness of the intermediate landing, C'D' and H'G' must have equal but opposite slopes and must lie in a straight line if viewed in plan. The extensions of these lines must therefore meet at O". The profile C'D'O'G'H' gives the projection of the deformed intersection line CH on the plane XOZ. The landing also sways in the direction CH and rotates about the axis OZ (see figs. 8a. & 8b).

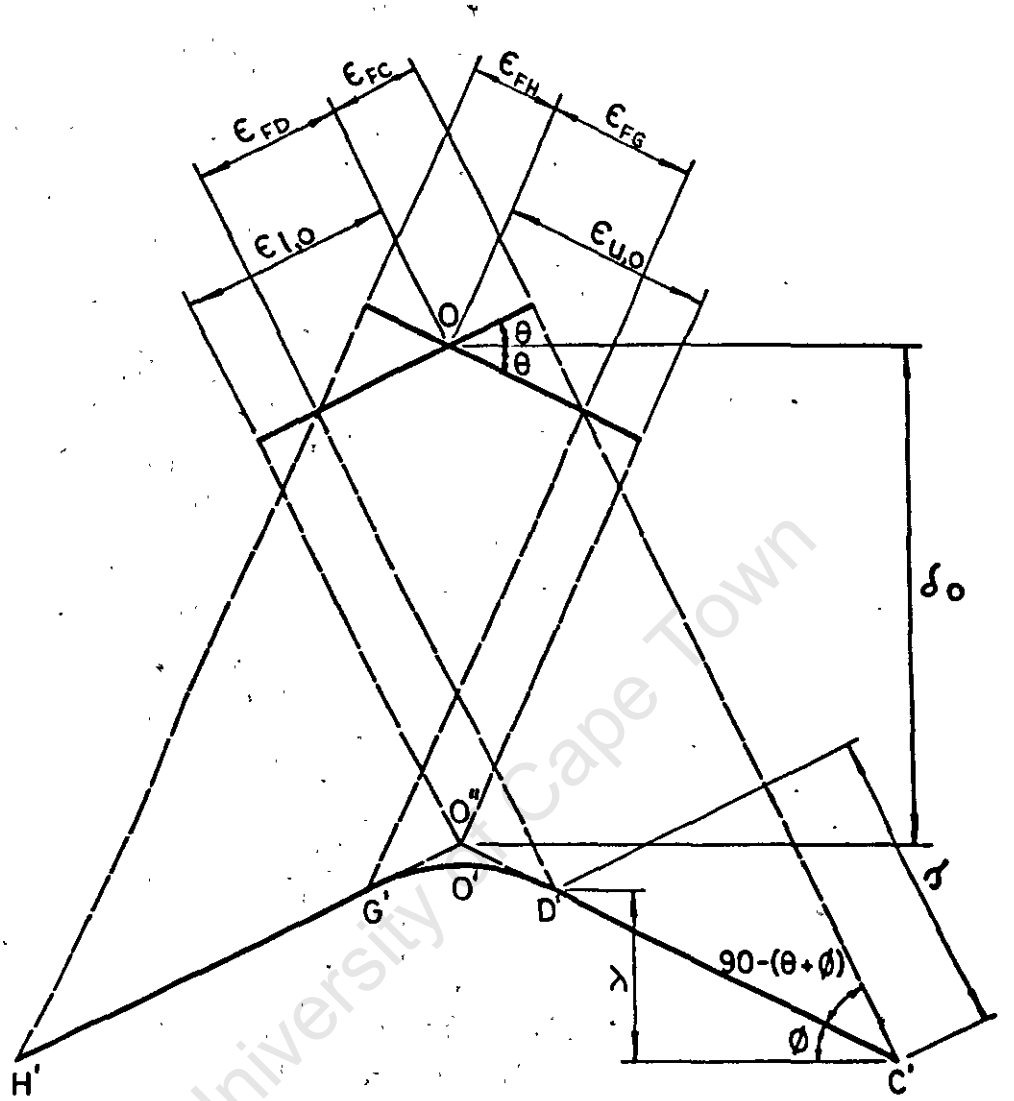

WILLIOT DIAGRAM OF DISPLACEMENTS* DUE TO STRAIN IN FLIGHTS FOR SYMMETRICAL LOADING

FIG. 10.

PART 4

DEFLECTION TESTS ON A MODEL OF A FREE STAIRWAY

INTRODUCTION

In Part 5, Section 1, of this Book a description is given of a photo-elastic analysis of a model of a free stairway made of Araldite casting resin "B". Although the model was built to a small scale it was nevertheless considered that tests in which various deflections were recorded might yield useful results for the verification of the foregoing theory. For a description of the model and testing jig, reference should be made to the above-mentioned section.

BRIEF DESCRIPTION OF TESTS

The arrangement for the deflection test is illustrated in fig. 11. The vice was rigidly bolted to the table and application of load by the spring loaded jack described in Section 1 of Part 5 caused no measurable deflections of the jig. The dial gauges were so arranged that the deflection could be recorded at three positions along the line of intersection of the landing and the flights as well as the rotation and translation of the intermediate landing in its own plane. Several runs of loading and unloading were carried out.

ANALYSIS OF TEST RESULTS

The results of a single run of loading are illustrated in fig. 12, together with the theoretical values as calculated by the theory developed in Part 3. The larger experimental values can probably be accounted for in two ways. Firstly, the stress concentration at the line of intersection of the flights and landing, as revealed by the photo-elastic analysis described in Part 5, together with a similar concentration at the bolts, would increase the deflection. The large stresses at these two extremities do not extend very far along the length of the flight but on account of their intensity must nevertheless have a marked influence on the magnitude of the deflections. Secondly, slippage occurring at one or more of

/the bolts ...

the bolts due to lack of perfect fit would further increase the deflection. If slippage were to occur at the bolts nearest the flights then it could be reversible, which would explain the irregularities in the experimental curves.

When the apparatus was designed the tests described here were not envisaged. Slippage of this order of magnitude had negligible effect on the photo-elastic analysis.

TEST TO DESTRUCTION

After completion of the photo-elastic work described in Part 5, a test to destruction with eccentric loading applied at position A (see figs. 13 and 16), but with a different loading device, was carried out by increasing the load in small increments.

Calculations indicated that the maximum tensile stress would occur due to bending of the intermediate landing at the junction of the inner edges of the landing and the lower flight. As the elastic theory is not applicable in the ultimate range precise calculations were not possible. Neglecting the effects of torsion and bending of the upper flight the bending moment referred to above would be equal to $\frac{W}{2} \times 2.5''$ $= 1.25W$ lb. ins. Using the fully plastic (rectangular stress-block theory) the ultimate bending moment of resistance of the landing per inch width would be $f_u \times \left(\frac{0.25}{2}\right)^2 = 10{,}000 \times \left(\frac{0.25}{2}\right)^2$ $= 156$ lb.ins./in. width.

The landing actually failed at a load of 136 lb. Calculations indicate that it is unlikely that the flights resisted more than 30 lb. in bending and torsion, so that at least 106 lbs. was resisted by extensional forces, which would have resulted in a bending moment of 1.25 x 106 = 136 lb. ins.

The effective width of landing required to resist this moment would therefore have been approximately $\frac{136 \text{ lb. ins.}}{156 \text{ lb.ins./in. width.}}$ = 0.87 inches, which is reasonable.

The plane of fracture across the landing is clearly visible in fig. 13. Note the conchoidal shape at the inner edge.

/Conclusions ...

CONCLUSIONS

Bearing in mind the scale of the model and the discrepancies discussed above, the results of these tests are in good agreement with the deflections predicted by the theory. It appears that some allowance must be made for the effects of stress-concentration. The precise nature of the concentration of stress round the bolt-holes is not known but an approximate analysis based on assumed stresses that were estimated from the results of the photo-elastic work gave corrected deflection values in very close agreement with the experimental values.

The mode of failure as revealed by the test to destruction confirmed the predictions of the theory, viz. that the bending moment at the inner edge of the intermediate landing would initiate failure.

FIG. 11.

ARRANGEMENT FOR DEFLECTION TEST
ON MODEL OF
FREE STAIRWAY

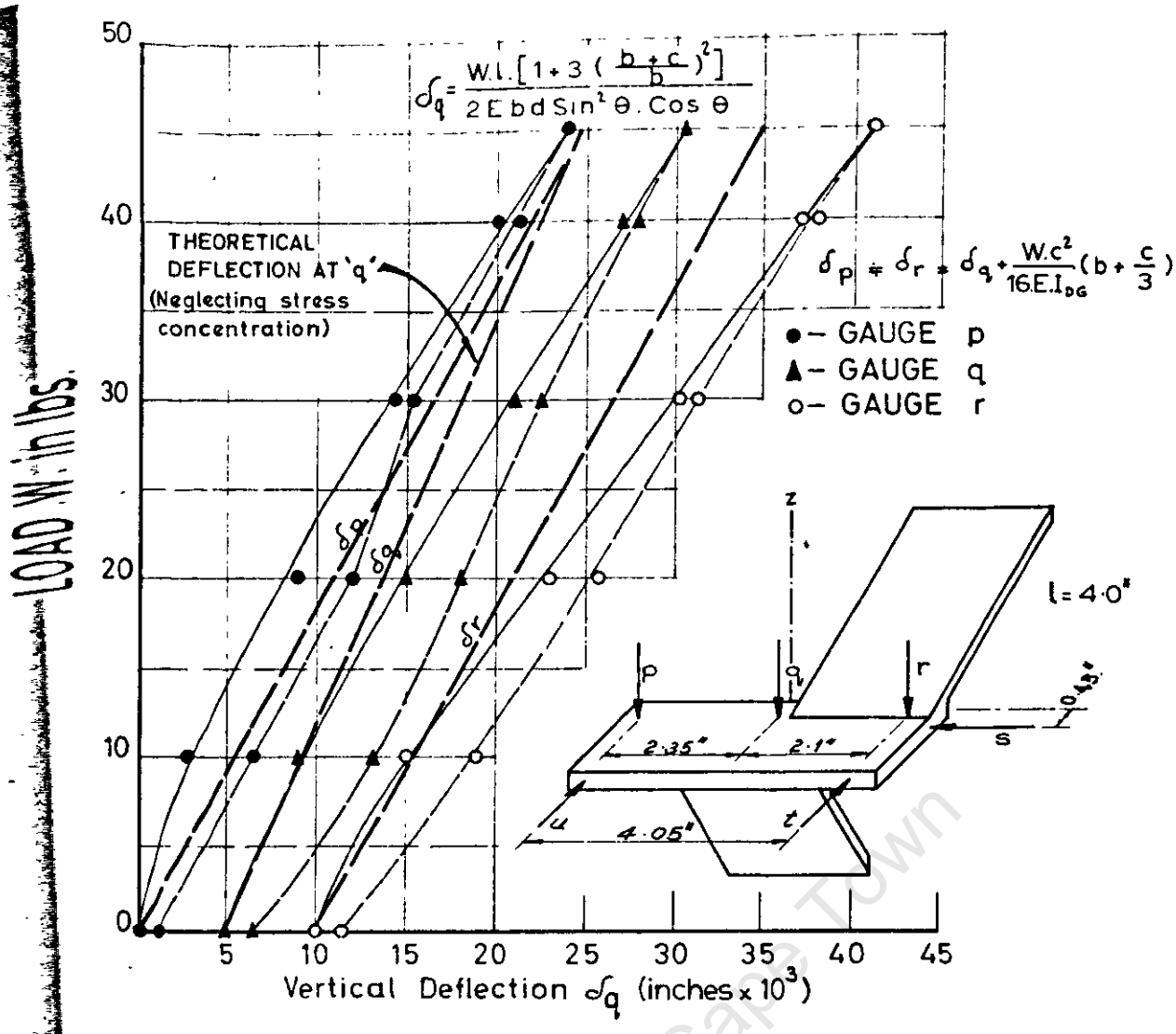

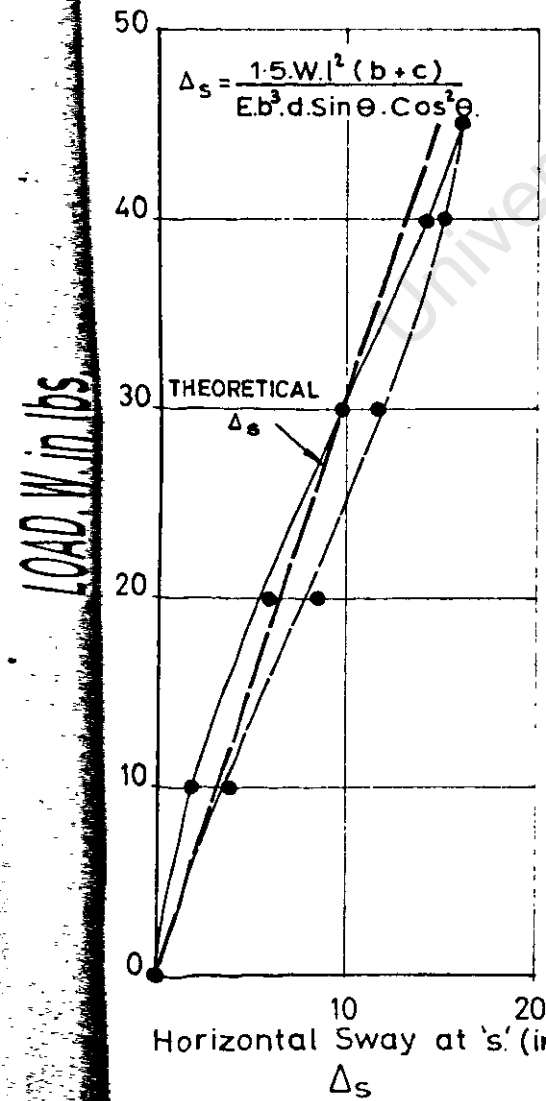

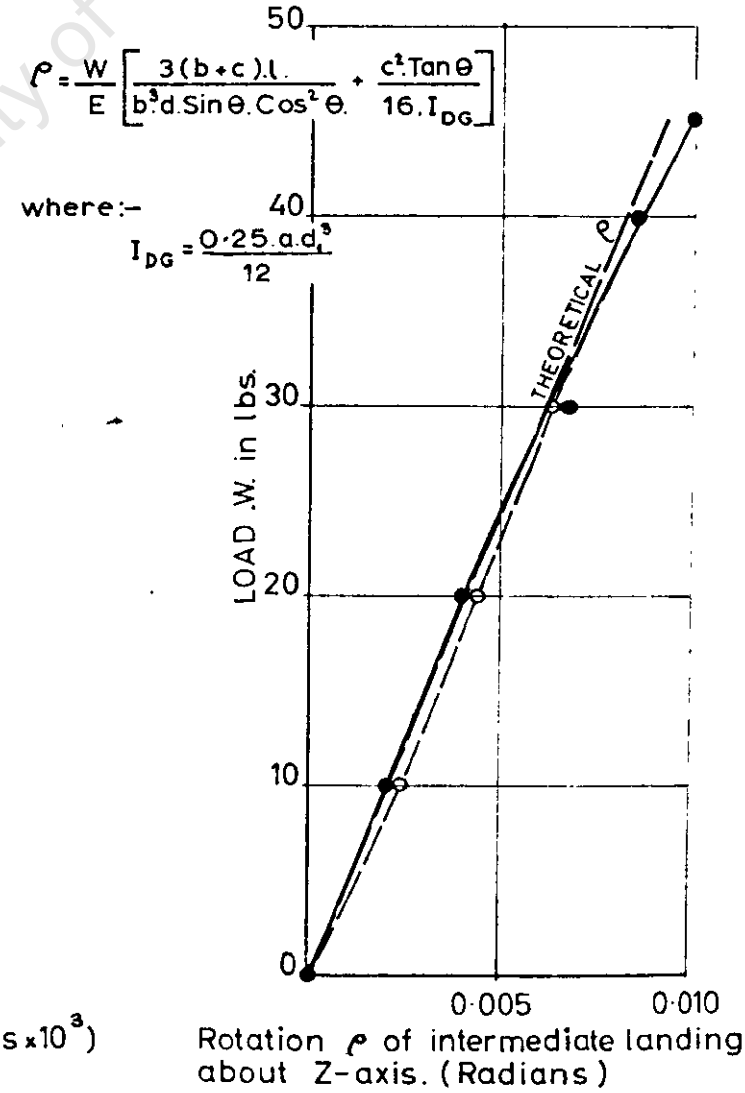

FIG. 12.

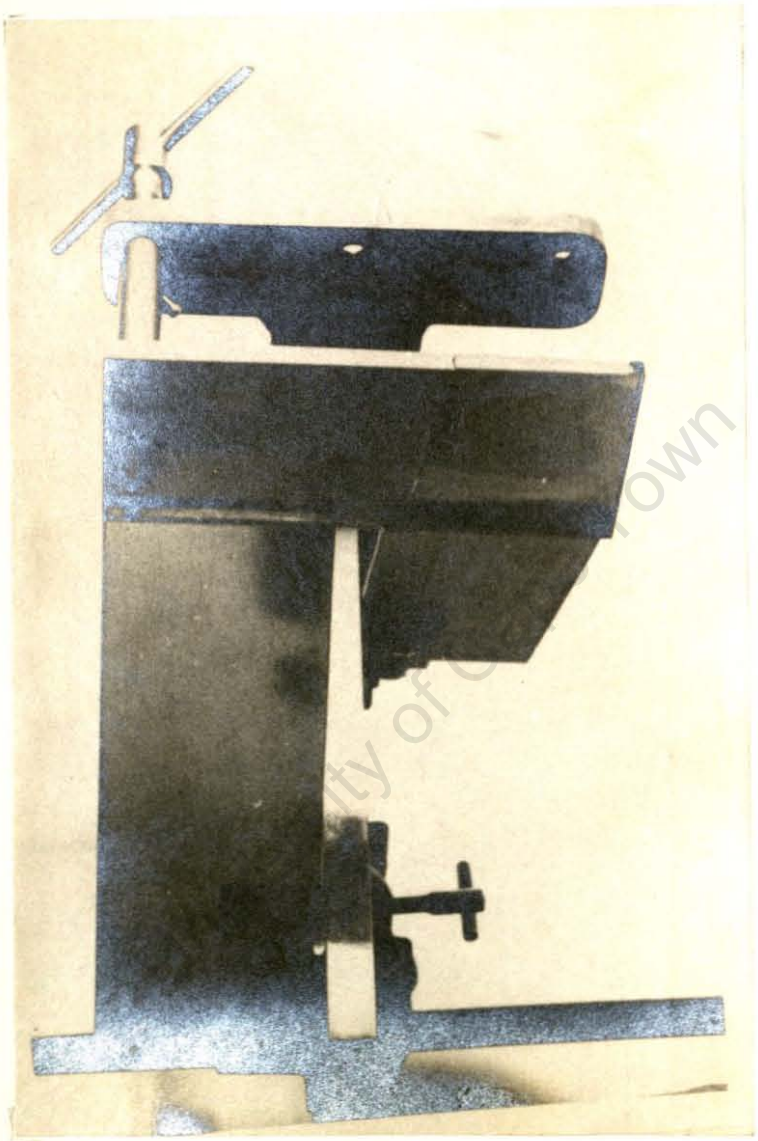

FIG. 13.

VIEW OF ARALDITE MODEL OF FREE STAIRWAY WITH ECCENTRIC LOADING SHOWING MODE OF FAILURE OF INTERMEDIATE LANDING

PART 5.

AN ANALYSIS OF THE STRESS-CONCENTRATION AT THE INTERSECTION OF THE FLIGHTS AND THE INTERMEDIATE LANDING OF A FREE STAIRWAY

GENERAL

In the paper which forms the main content of Part 2 of this Book mention is made of the suspected concentration of stress at the intersection of the flights and the intermediate landing of a free stairway. This was deduced from the fact that the bending stiffness of the landing was relatively small compared with the extensional stiffness of the flights.

As explained in Parts 2 and 3, bending moments are induced along this intersection line as a result of the vertical components of the extensional forces in the flights. The straight-line distribution assumed in this approximate analysis could only be correct for very stiff landings. As this is invariably not the case the extensional forces resisted by bending moments cannot be effectively distributed along the full width of the flights at the intersection line. This results in the above-mentioned concentration of stress at the inner edges of the flights. As stated in the original paper it is necessary in the design of stairs to make some allowance for this effect. It was tentatively suggested that the stress as calculated by the straight-line theory should be doubled and the probable stress distribution was indicated.

It was however felt that the matter should not be left there. In order to make a more accurate assessment of the nature of this stress concentration the author devised a procedure for carrying out a photo-elastic analysis of a model of a free stairway made of Araldite casting resin "B". A description of this work is given in Section 1 below. In order to account for the stress distribution as revealed by the above-mentioned analysis he subsequently succeeded in developing a theoretical method of analysis based on the analogy of a finite flexible beam on an elastic foundation. This theory, which has produced very good results, is described in Section 2 below.

PART 5

SECTION 1

PHOTO-ELASTIC ANALYSIS OF A MODEL OF A FREE STAIRWAY

ACKNOWLEDGEMENTS

The work described below was made possible by the assistance given to the author by the staff of the Department of Mechanical Engineering at the University of Cape Town. The author is greatly indebted to Mr. K.E. Machin for his assistance in making the model and jig and in carrying out the tests and the photography.

DESCRIPTION OF MODEL AND LOADING JIG

The stairway model is illustrated in fig. 14 and the dimensions are given in fig. 15. The material used was Araldite Casting resin "B" which is a hot setting resin used with Hardener 901. The stairway was made up from three slabs which were cast to approximate dimensions and thereafter accurately machined. Any residual stressed were relieved by placing the slabs in the moulds in the oven at 140°C for 2 to 3 hours and allowing to cool slowly. Thereafter the slabs were bonded together with the same material. Annealing of the completed model was done in a special mould. At room temperature Young's modulus of Araldite "B" is 4.5×10^5 lb. per in^2 and its ultimate tensile strength 10,160 lb. per in^2. Its fringe value is 60.5 lbs. per inch per fringe.

The loading jig which was of welded steel construction was specially designed so that the model could be handled when under load. The jig is illustrated in figs. 14 and the dimensions are given in fig. 16. It was so proportioned that both flights and the intermediate landing were visible if placed at right angles to the axis of the polariscope. The stair flights were clamped to flat cleats by double bolting. Although this did not provide an absolutely rigid end connection it was sufficient for the purposes of this analysis. The author is aware of the fact that cleats extending for the full width of the flights would probably have produced more realistic

conditions of fixity. The jig was so designed that loading could be applied at the three positions A, B and C indicated in fig. 16 by means of a spring loaded jack specially designed for this purpose. Two projecting pins, one of which was fixed to the jack itself and the other to the piston at the other extremity of the spring as illustrated in fig. 16, served as the gauge for determining the applied load. The jack was calibrated in terms of the clear distance between these pins as measured with vernier calipers. The load-compression relationship of the jack was perfectly linear up to the capacity of the spring which was just in excess of 70 lbs.

BRIEF DESCRIPTION OF PROCEDURE ADOPTED IN CARRYING OUT THE PHOTO-ELASTIC ANALYSIS

It is not the intention to define the terms used or to elaborate on the theory of photo-elasticity or to describe the procedure of stress measurement in detail as these are described in many text-books on the subject and only the end result is of interest for the purpose of this work. Only a brief description and various relevent comments will be made.

The arrangement of the circular polariscope used for this work is illustrated in fig. 17 with the stairway model shown in position. Photographs were taken with a monochromatic light source with two filters (Wratten 58 and Wratten 77) at a speed of ½ second and an aperture of f4 on a Linagraph Ortho film. Typical photographs of the flights under stress are illustrated in figs. 18A, 18B and 19A to 19D.

ANALYSIS OF RESULTS

In order to simulate the behaviour of a reinforced concrete prototype as nearly as possible the dimensions of the model stair were given corresponding proportions with the exception that the steps were omitted. The model could accordingly not be classified in the strict sense of the word as a structure composed of membrane elements. These elements of necessity become plates with three dimensional properties. Distortion of these plates relative to their initial planes would accordingly result in strain differentials through the

thickness, so that in terms of photo-elastic theory a state of plane stress would not exist. A precise interpretation of the fringe pattern is accordingly not feasible as the optical effect is an integral involving the stress at all points along the ray as it passes through the thickness of the plate. We are however primarily interested in the stress pattern due to the extensional force resultants which are assumed to act in the middle plane. Great accuracy is therefore not claimed for this method and the results must be interpreted in the light of the foregoing.

It was however apparent that the distortion of the flights for the load applied at position B were not large and had very small effect on the results. The clarity of the isotropic region (see figs. 18A and 18B) and the fact that it remained stationary was probably an indication that distortion of the flights was not serious. The landing however suffered serious distortion and did not produce useful results. For eccentric loading at positions A and C (See fig. 19A to 19D) the flights also suffered distortion as can be deduced from the photographs. As the load increased the isotropic region faded and eventually disappeared, whereafter the first fringe also began to fade. In order to ensure that the correct fringe values were recorded the fringes were counted as, with increasing load, they passed through particular points in the face of the model.

The stress-distribution curve (fig. 18c) gives the difference between the principal stresses acting at points along the sections shown. At the inner and outer edges of the flight only one principal stress parallel to the particular edge exists. This value, which is also the peak value at the inner edge, is accordingly a true stress (except for bending distortion); but the values in the section, although qualitatively of great interest, are unlikely to be precise stress values. It would nevertheless appear that the minor principal stress is of a small order. The determination of the true stresses was not considered of sufficient importance to warrant the

additional work required, especially as the accuracy was affected by distortion. The stress distribution curve was plotted, using both the results of the dark field and light field, the latter giving half order fringes.

For plotting the curve illustrated in fig. 19E the isotropic point was taken from a photograph at low load, the assumption being made that after disappearance due to distortion the effective position remained unchanged. The lower order fringe values are also not reliable as can be seen from fig. 19E.

CONCLUSIONS

Although the method described above has many shortcomings it would appear to give a good indication of the stress distribution at various sections along the flights, confirming the suspected concentration of stress. Even quantitatively it appears to be of value as the force resultant determined by integration of the experimental stress curves is in good agreement with the theoretical extensional force component acting in the flights.

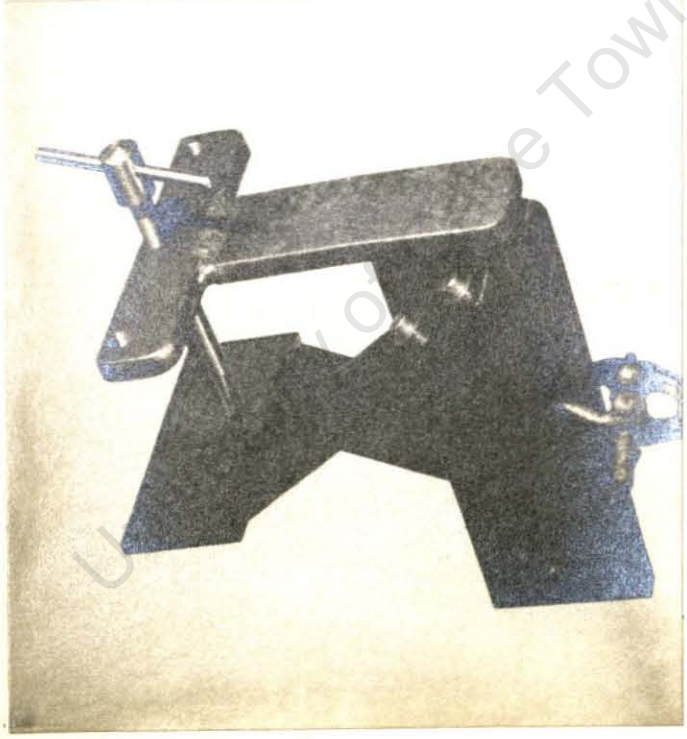

FIG. 14.

VIEW SHOWING ARALDITE MODEL OF FREE STAIRS BOLTED TO TESTING JIG

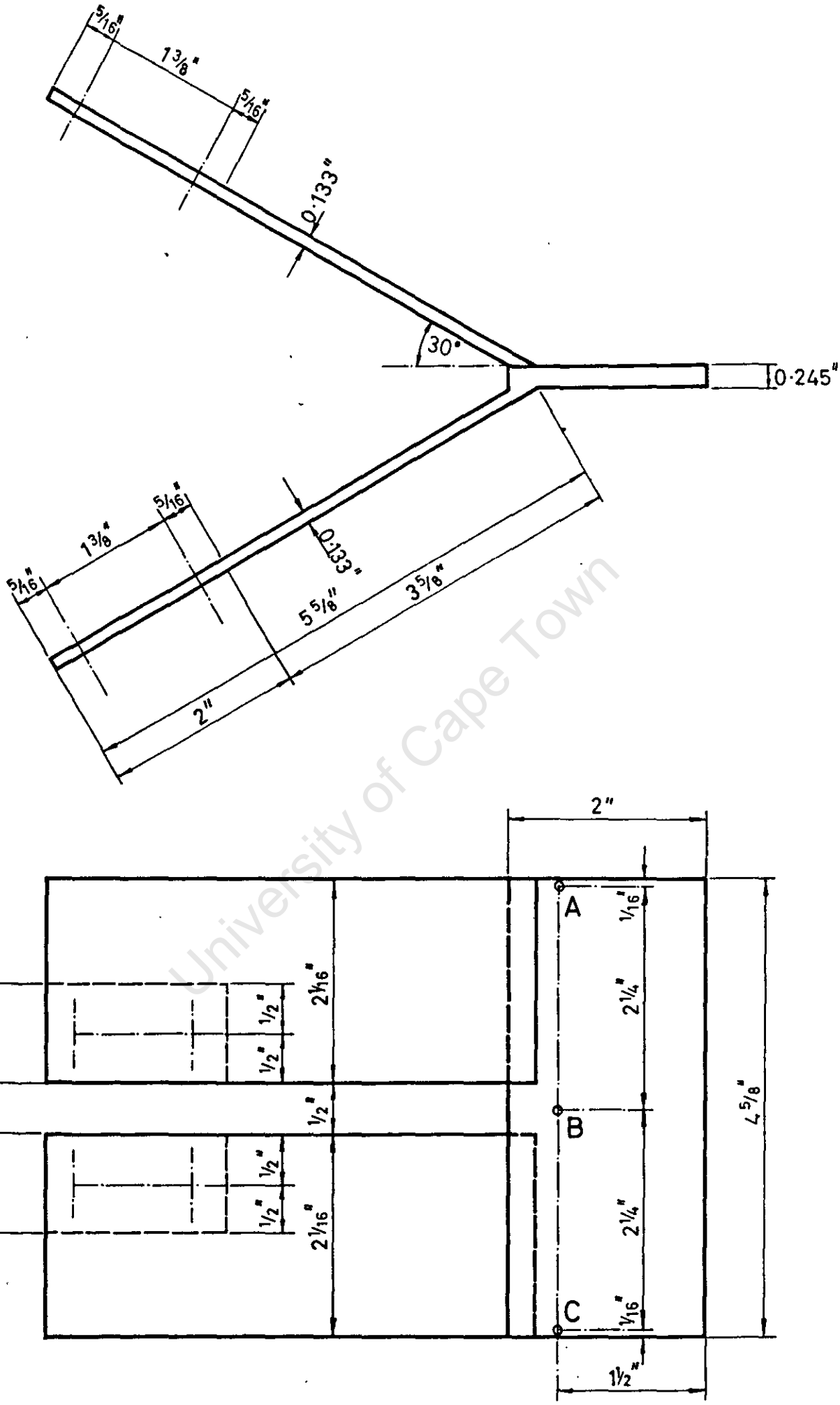

FIG. 15.

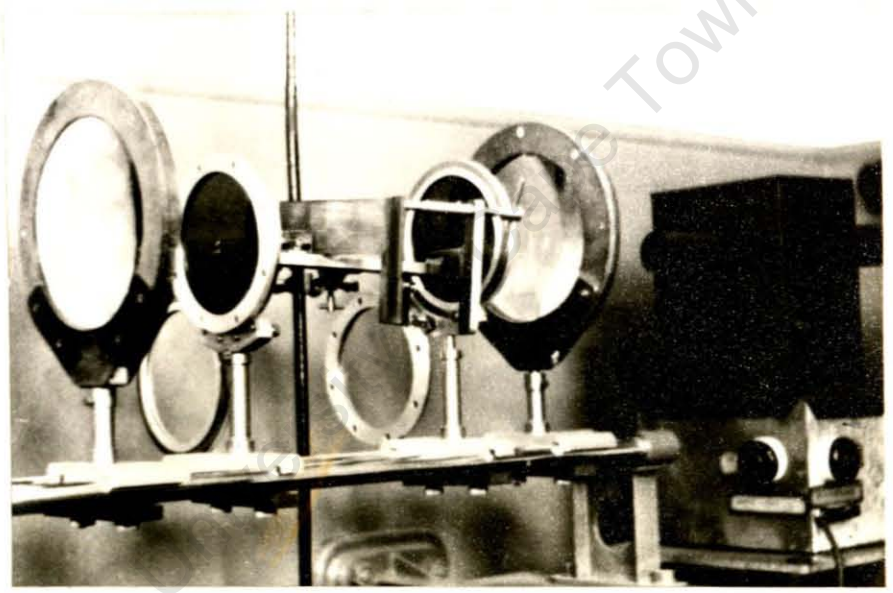

FIG. 17.

GENERAL ARRANGEMENT OF CIRCULAR POLARISCOPE
SHOWING METHOD OF POSITIONING MODEL

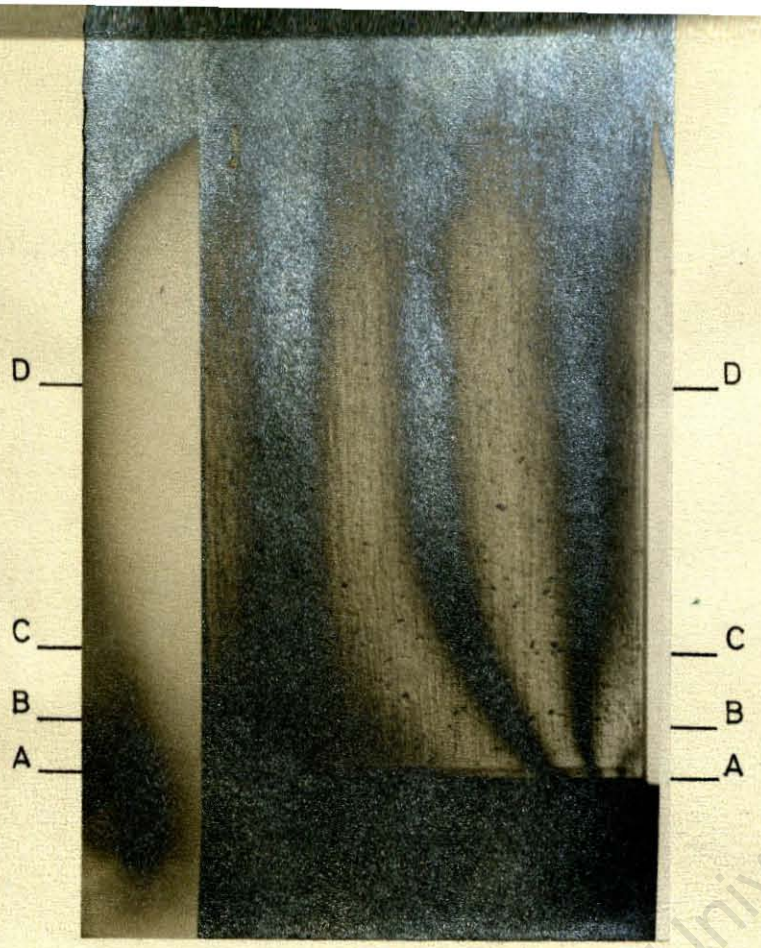

FIG. 18A.

STRESS PATTERN IN LOWER FLIGHT (LIGHT FIELD) FOR 50½ LB. LOAD AT POSITION B.

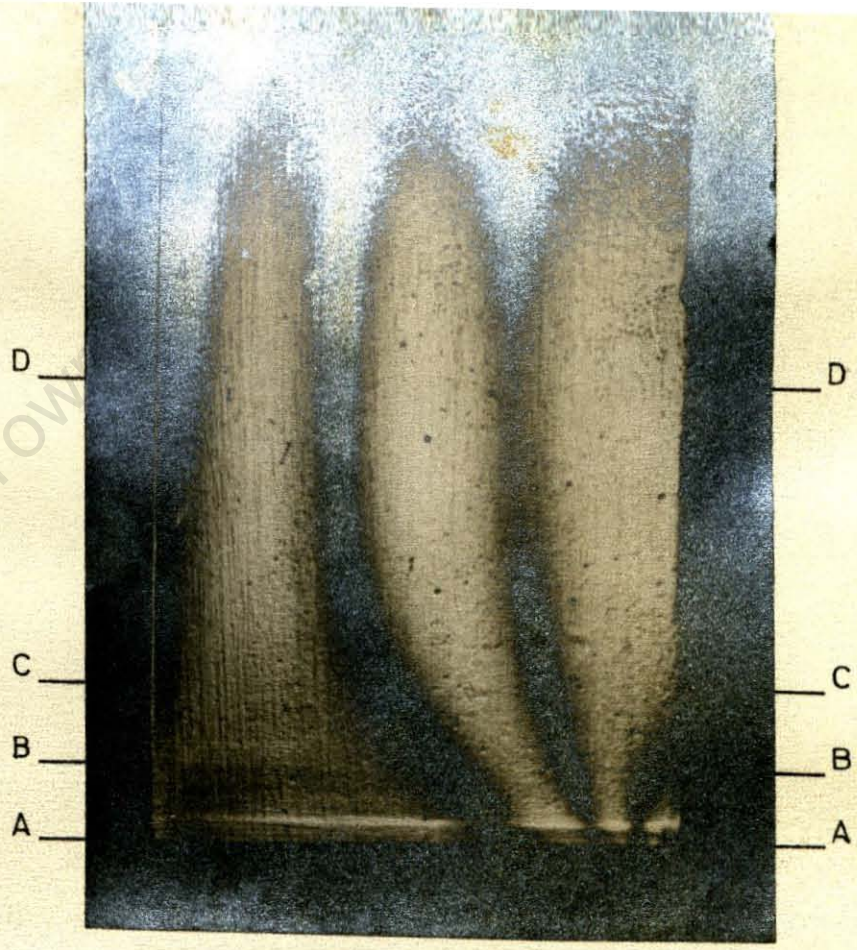

FIG. 18B.

STRESS PATTERN IN LOWER FLIGHT (DARK FIELD) FOR 50½ LB. LOAD AT POSITION B.

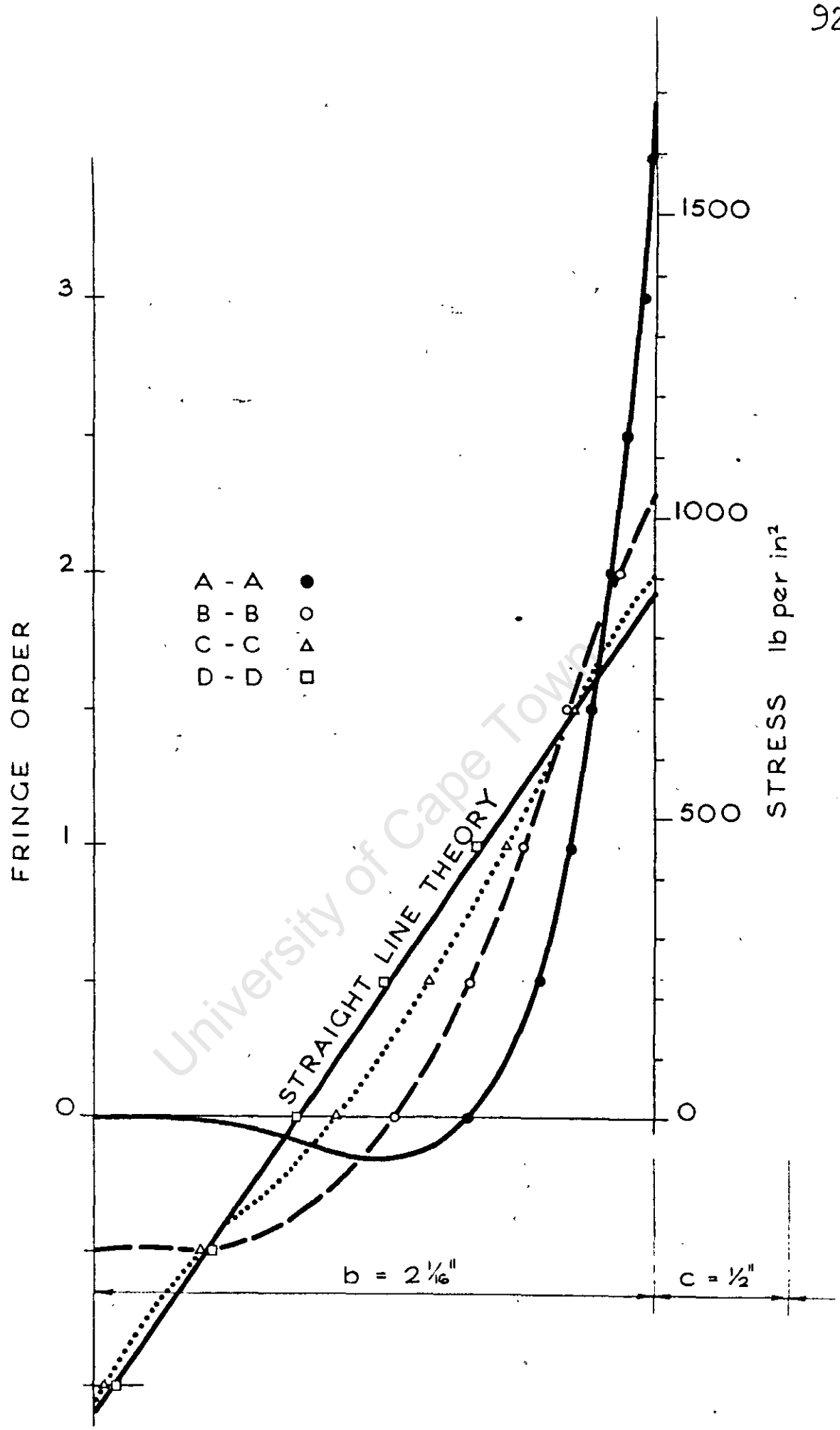

Fig 18c Stress distribution at various sections of lower flight showing concentration at intersection with landing for 50½ lb loading at B.

FIG. 19A.

STRESS PATTERN IN
LOWER FLIGHT (DARK FIELD)
FOR 15 LB. LOAD AT A.

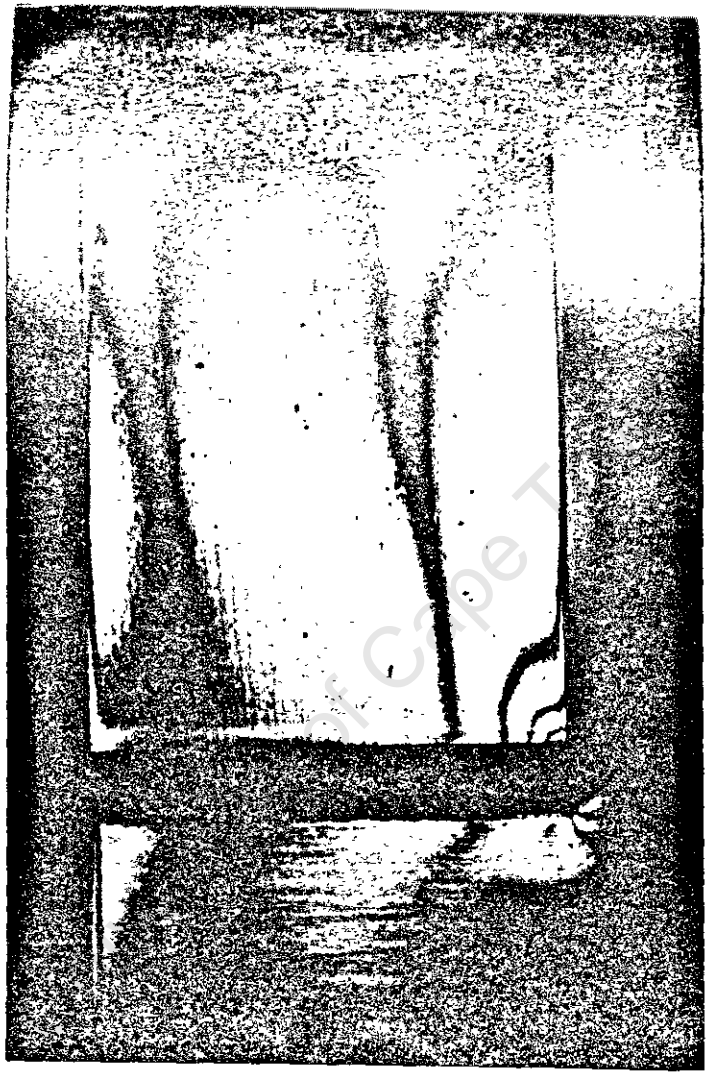

FIG. 19B.

STRESS PATTERN IN
LOWER FLIGHT (DARK FIELD)
FOR 23 LB. LOAD AT A.

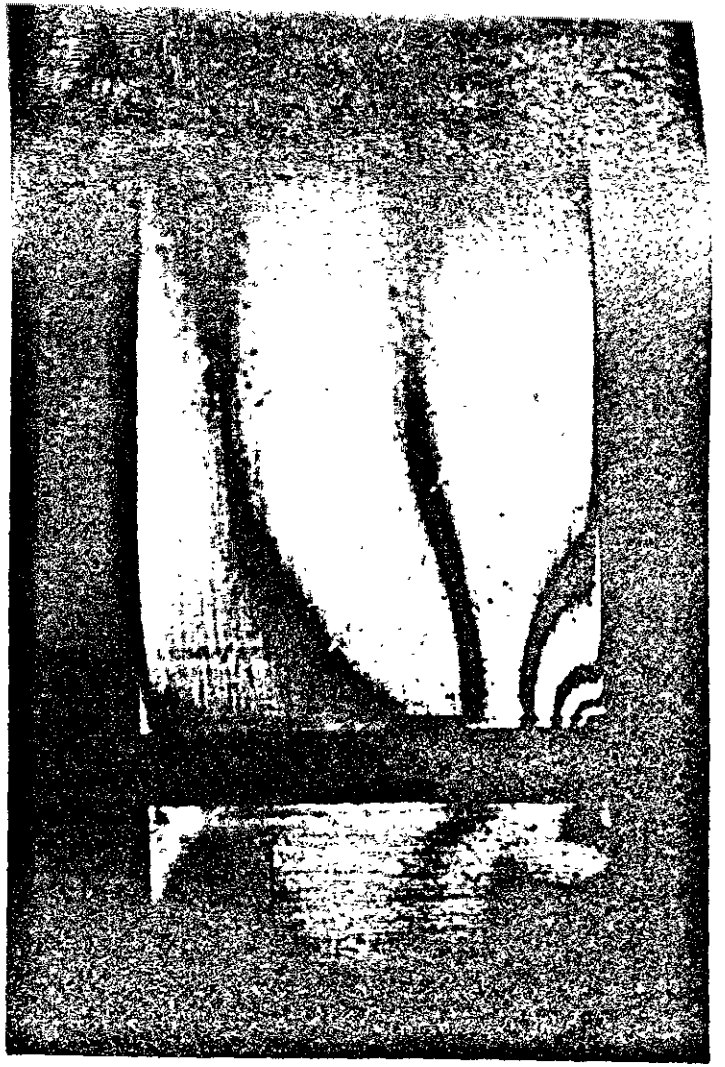

FIG. 19C.

STRESS PATTERN IN
LOWER FLIGHT (DARK FIELD)
FOR 31 LB. LOAD AT A.

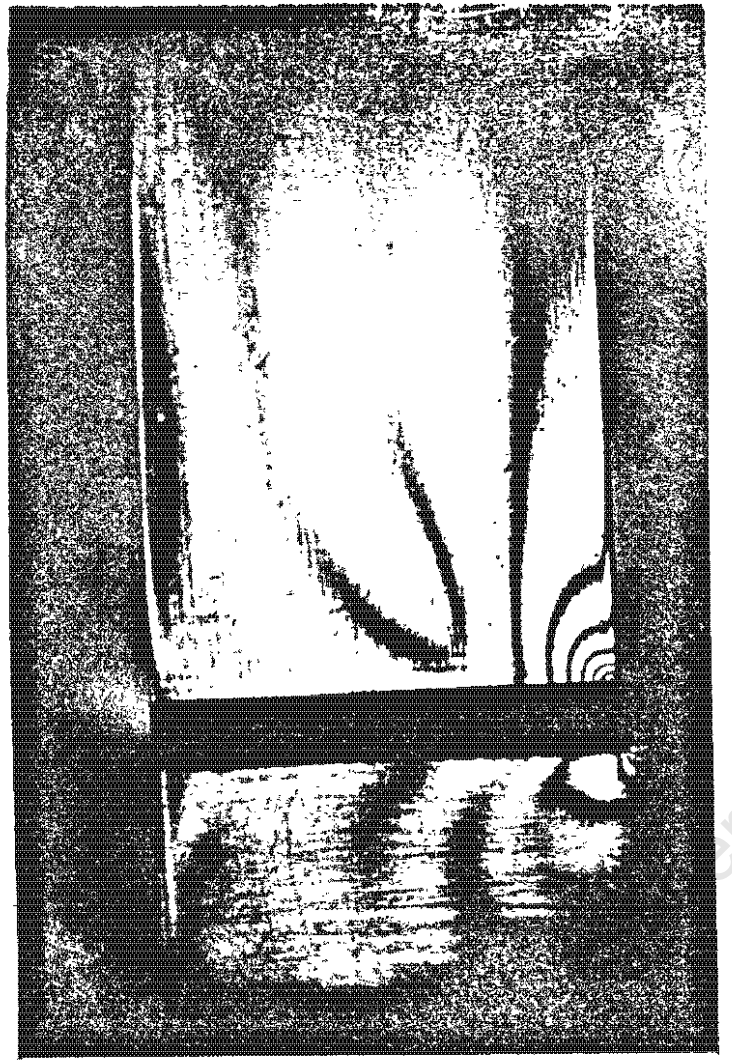

FIG. 19D.

STRESS PATTERN IN
LOWER FLIGHT (DARK FIELD)
FOR 38 LB. LOAD AT A.

FIG. 19E.

STRESS PATTERN IN
LOWER FLIGHT (DARK FIELD)
FOR 48½ LB. LOAD AT A.

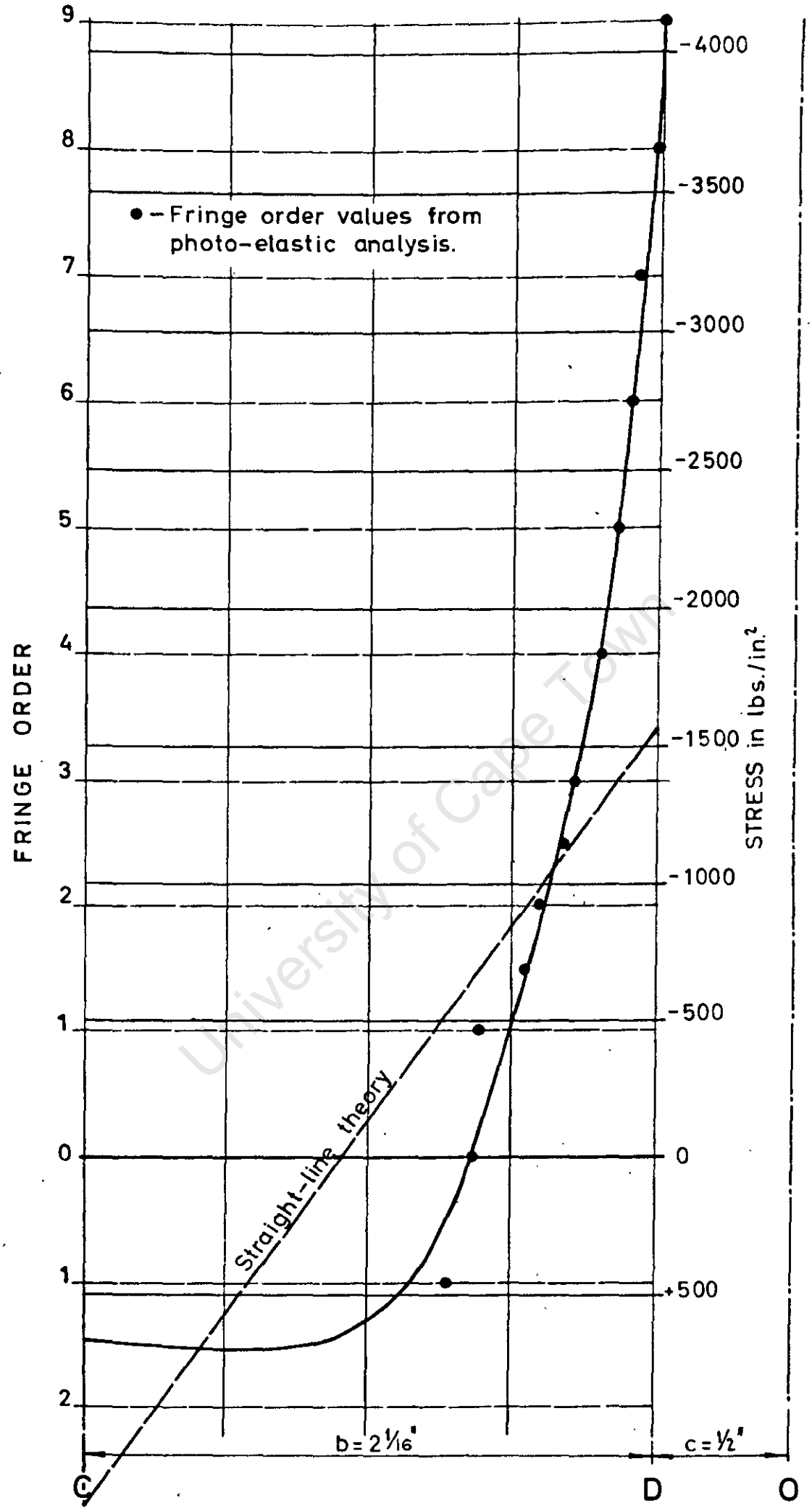

STRESS DISTRIBUTION AT INTERSECTION LINE CD WITH 38 lb. LOAD AT A.

FIG. 19 F.

97A.

(M. Hetenyi in his book "Beams on Elastic Foundation", published by The University of Michigan Press, Ann Arbor, has dealt with this case in more concise form, pages 52, 53).

an elastic foundation is as follows :

$$y = e^{\beta x}(A\cos\beta x + B\sin\beta x) + e^{-\beta x}(C\cos\beta x + D\sin\beta x)$$

where $\beta = \sqrt[4]{\frac{k}{4EI}}$, k = the modulus of the foundation

E = Young's modulus

I = moment of inertia of the beam

A, B, C, D are constants depending on the particular circumstances.

To find the solution for a finite beam the unknown constants can be determined in terms of the known forces at the extremities as shown at the end of this section*.

In order to apply the solution derived in this way to any particular case it is necessary to establish the values of the various parameters. The most difficult to establish are values of k the effective modulus of the flights and I_x the effective moment of inertia of the landing. As the bending moments act at the edge of the landing it follows that the full width cannot be effective.

In order to compare the theoretical analysis with the results of the photo-elastic work the following assumptions have been made.

(a) $M_o = P_o \times \frac{c}{4}$ (assuming some torsion in the flights.)

(b) $I_x = \frac{0{\cdot}25\, a d_1^3}{12}$

where a is the width of the landing and

d_1 is the thickness of the landing.

$k = k_1 \frac{E d \sin^2\theta}{s}$ lb/in/in.

where θ is the inclination of the flights as in Part 2

d is the thickness of the flights

s is the length of the flights measured along the slope.

E is Young's modulus of the material.

k_1 is a parameter such that $\frac{s}{k_1}$ is the effective length of the flights.

Having determined the function y by substitution of the values determined from the above relationships it is possible to calculate the stress distribution in the stair flights from the relation

that at $x = x_1$ the stress in the flight is equal to $\frac{k y_1}{d \sin\theta}$

where y_1 , corresponds with x_1 .

Stress curves plotted for various values of k_1 are shown in fig. 21. It will be noted that the curve for $k_1 = 3.0$ corresponds almost precisely with the experimental values, so that the effective length of the flight is $\frac{s}{3}$, where s was assumed to be 4" for the model.

It does not of course follow that the initial assumption (b) that the effective width of the landing is 0.25 times the actual width is correct as different values with corresponding values k_1 could give equally good results. It is very probable however that the assumed value is approximately correct as the effective length of $\frac{s}{3}$ corresponds closely to the position (indicated by the photo-elastic analysis), where the stress distribution in the flight becomes linear. If the flight were fixed at this section by a rigid support the effect of linear stress distribution and the corresponding strains could be simulated by a rotation of the rigid support about an axis at right angles to the plane of the flight. This would not affect the analogy as sway and deflection of the flights is essential to attain the compatibility of the forces and deformations previously assumed.

The various ratios assumed above would vary for different cases and cannot be accurately assessed. The analogy however does simplify the explanation of the nature of the stress concentration.

2.

e.

$$0 = \beta^2 e^{\beta b}\left[2B\cos\beta b - 2A\sin\beta b\right] + \beta^2 e^{-\beta b}\left[-2D\cos\beta b + 2C\sin\beta b\right]$$

---------(b)

At $x = 0$ S.F. $= P_0$

e. $$-\frac{P_0}{EI_x} = 2\beta^3\left[(B-A) + (D+C)\right]$$ -------(c)

At $x = b$ S.F. $= 0$

e. $$0 = 2\beta^3 e^{\beta b}\left[(B-A)\cos\beta b - (B+A)\sin\beta b\right] + 2\beta^3 e^{-\beta b}\left[(D+C)\cos\beta b + (D-C)\sin\beta b\right]$$

$$= 2\beta^3 e^{\beta b}\left[B(\cos\beta b - \sin\beta b) - A(\cos\beta b + \sin\beta b)\right] + 2\beta^3 e^{-\beta b}\left[D(\cos\beta b + \sin\beta b) + C(\cos\beta b - \sin\beta b)\right]$$

---------(d).

From (a)

$$B = D - \frac{M_0}{2\beta^2 EI_x}$$ ---------(e).

Substituting B in (c)

$$-\frac{P_0}{2\beta^3 EI_x} = D - \frac{M_0}{2\beta^2 EI_x} - A + D + C$$

$$\therefore A = \left(\frac{P_0 - \beta M_0}{2\beta^3 EI_x}\right) + 2D + C$$ ---------(f)

Substituting for B and A in (b)

$$0 = \beta^2 e^{\beta b}\left[\left(2D - \frac{M_0}{\beta^2 EI_x}\right)\cos\beta b - \left(\frac{P_0 - \beta M_0}{\beta^3 EI_x} + 4D + 2C\right)\sin\beta x\right] + \beta^2 e^{-\beta b}\left[-2D\cos\beta b + 2C\sin\beta b\right]$$

$$0 = e^{\beta b}\left[-\frac{M_0}{EI_x}\cos\beta b - \left(\frac{P_0 - \beta M_0}{\beta EI_x}\right)\sin\beta b\right] + 2\beta^2 e^{\beta b}\left[D\cos\beta b - (2D+C)\sin\beta b\right] + 2\beta^2 e^{-\beta b}\left[C\sin\beta b - D\cos\beta b\right]$$

i.e.

$$0 = \beta^2 e^{\beta b}\left[2B\cos\beta b - 2A\sin\beta b\right] + \beta^2 e^{-\beta b}\left[-2D\cos\beta b + 2C\sin\beta b\right]$$

--------(b)

At $x = 0$ S.F. $= P_0$

i.e. $$-\frac{P_0}{EI_x} = 2\beta^3\left[(B-A) + (D+C)\right]$$ --------(c)

At $x = b$ S.F. $= 0$

i.e. $$0 = 2\beta^3 e^{\beta b}\left[(B-A)\cos\beta b - (B+A)\sin\beta b\right] + 2\beta^3 e^{-\beta b}\left[(D+C)\cos\beta b + (D-C)\sin\beta b\right]$$

$$= 2\beta^3 e^{\beta b}\left[B(\cos\beta b - \sin\beta b) - A(\cos\beta b + \sin\beta b)\right] + 2\beta^3 e^{-\beta b}\left[D(\cos\beta b + \sin\beta b) + C(\cos\beta b - \sin\beta b)\right]$$

---------(d).

From (a)

$$B = D - \frac{M_0}{2\beta^2 EI_x}$$ ---------(e).

Substituting B in (c)

$$-\frac{P_0}{2\beta^3 EI_x} = D - \frac{M_0}{2\beta^2 EI_x} - A + D + C$$

$$\therefore A = \left(\frac{P_0 - \beta M_0}{2\beta^3 EI_x}\right) + 2D + C$$ --------(f)

Substituting for B and A in (b)

$$0 = \beta^2 e^{\beta b}\left[\left(2D - \frac{M_0}{\beta^2 EI_x}\right)\cos\beta b - \left(\frac{P_0 - \beta M_0}{\beta^3 EI_x} + 4D + 2C\right)\sin\beta x\right] + \beta^2 e^{-\beta b}\left[-2D\cos\beta b + 2C\sin\beta b\right]$$

$$0 = e^{\beta b}\left[-\frac{M_0}{EI_x}\cos\beta b - \left(\frac{P_0 - \beta M_0}{\beta EI_x}\right)\sin\beta b\right] + 2\beta^2 e^{\beta b}\left[D\cos\beta b - (2D+C)\sin\beta b\right] + 2\beta^2 e^{-\beta b}\left[C\sin\beta b - D\cos\beta b\right]$$

$$\therefore C\left[2\beta^2\left(e^{\beta b}\sin\beta b - e^{-\beta b}\sin\beta b\right)\right]$$

$$= e^{\beta b}\left[-\frac{M_o}{EI_x}\cos\beta b - \frac{P_o-\beta M_o}{\beta EI_x}\sin\beta b\right]$$

$$+ D\left[2\beta^2 e^{\beta b}(\cos\beta b - 2\sin\beta b) - 2\beta^2 e^{-\beta b}\cos\beta b\right]$$

$$C\left[4\beta^2\sin\beta b.\sinh\beta b\right] = e^{\beta b}\left[-\frac{M_o}{EI_x}\cos\beta b - \frac{P_o-\beta M_o}{\beta EI_x}\sin\beta b\right.$$

$$+ D\left[4\beta^2(\cos\beta b\sinh\beta b - e^{\beta b}\sin\beta b\right.$$

$$\therefore C = \frac{e^{\beta b}\left[-\frac{M_o}{EI_x}\cos\beta b - \frac{P_o-\beta M_o}{\beta EI_x}\sin\beta b\right.}{4\beta^2\sin\beta b.\sinh\beta b} + D\left[\frac{\cos\beta b}{\sin\beta b} - \frac{e^{\beta b}}{\sinh\beta b}\right.$$

$$= X_1 + D X_2 \qquad \text{---------- (d)}$$

Substituting in (d).

$$0 = 2\beta^3 e^{\beta b}\left\{\left(D - \frac{M_o}{2\beta^2 EI_x}\right)(\cos\beta b - \sin\beta b)\right.$$

$$\left. -\left(\frac{P_o-\beta M_o}{2\beta^3 EI_x} + 2D + X_1 + DX_2\right)(\cos\beta b + \sin\beta b)\right]$$

$$+ 2\beta^3 e^{-\beta b}\left\{D(\cos\beta b + \sin\beta b) + (X_1 + DX_2)(\cos\beta b - \sin\beta b)\right\}$$

$$\therefore D = \left\{\begin{array}{l} e^{\beta b}\left[-\frac{M_o}{2\beta^2 EI_x}(\cos\beta b - \sin\beta b) - \left(\frac{P_o-\beta M_o}{2\beta^3 EI_x} + X_1\right)(\cos\beta b + \sin\beta b)\right] \\ \quad + e^{-\beta b}\left[X_1(\cos\beta b - \sin\beta b)\right] \\ \hline e^{\beta b}\left[(\sin\beta b - \cos\beta b) + (2 + X_2)(\cos\beta b + \sin\beta b)\right] \\ \quad - e^{-\beta b}\left[(\cos\beta b + \sin\beta b) + X_2(\cos\beta b - \sin\beta b)\right] \end{array}\right.$$

---------- (f)

For the model used in the photo-elastic analysis :—

$$I_x = \frac{0.25}{12} a d_1^3 = \frac{0.25 \times 2 \times (0.245)^3}{12}$$

$$= 0.000,612 \quad in.^4$$

E for Araldite casting resin 'B' = 4.46×10^5 lb/in.²

$b = 2.063''$

$$\beta = \sqrt[4]{\frac{k}{4EI_x}}$$

$$k = k_1 \frac{E d \sin^2\theta}{s} = k_1 \frac{4.46 \times 10^5 \times 0.133 \times (0.5)^2}{4}$$

$$= 3710\, k_1 \quad lb/in/in.$$

for $2P_0 = 50.50$ lb (See fig. 20.)

$$P_0 = 25.25 \text{ lb}$$

$$M_0 = P_0 \times \frac{c}{4} = 25.25 \times 0.125''$$

$$= 3.16 \text{ lb.in.}$$

Substituting the above values in equations (e), (f), (g) and (h) the solution of

$$y = e^{\beta x}(A \cos\beta x + B \sin\beta x) + e^{\beta x}(C \cos\beta x + D \sin\beta x)$$

can be found for any value of x from $x = 0$ to $x = b$.

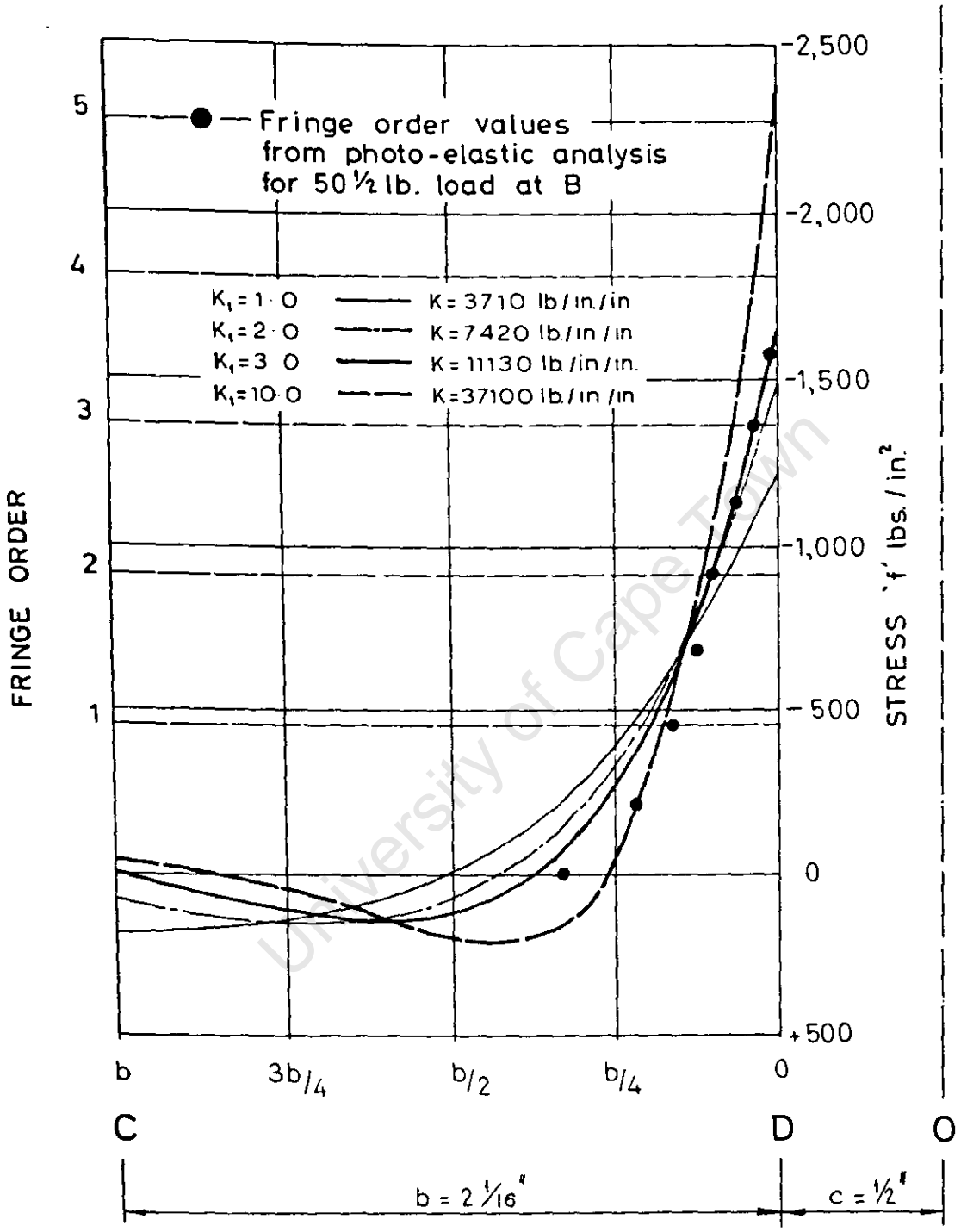

FIG. 21.

Comparison of theoretical and experimental stress distribution at intersection line C D.

PART 6

THE APPLICATION IN PRACTICE OF THE THEORY OF DESIGN OF STAIRWAYS

All the theoretical work developed in the foregoing parts have been based on the assumption that the material of the stairways is homogeneous. In the application of the theory to reinforced concrete stairways the assumption is made that the theoretical distribution of stresses due to extensional forces is maintained in spite of hair cracks. This is common practice in the design of many types of structures, including shell roofs and prismatic structures. All extensional tensile forces are assumed to be taken by steel reinforcement which, after taking into account the effects of bending and torsional moments, is distributed in such a manner as to give a resultant force corresponding with the analysis. The stress concentration in the flights and intermediate landing presents no problem as the reinforcement is simply concentrated at the relevant positions.

Details of a typical stairway are given in fig. 22. Another stairway which considerably enhances the architecture of a building in Cape Town now nearing completion is shown in figs. 23A and 23B with details in fig. 23C. Load deflection tests were carried out on this stair and at an applied load of 100 lb. per ft.^{2} the deflection at the mid-point of the line of intersection of the flights and intermediate landing was only 0.004 ins. As will be noted this agrees well with the theoretical value calculated in Appendix I-1.

PART 6

THE APPLICATION IN PRACTICE OF THE THEORY OF DESIGN OF STAIRWAYS

All the theoretical work developed in the foregoing parts have been based on the assumption that the material of the stairways is homogeneous. In the application of the theory to reinforced concrete stairways the assumption is made that the theoretical distribution of stresses due to extensional forces is maintained in spite of hair cracks. This is common practice in the design of many types of structures, including shell roofs and prismatic structures. All extensional tensile forces are assumed to be taken by steel reinforcement which, after taking into account the effects of bending and torsional moments, is distributed in such a manner as to give a resultant force corresponding with the analysis. The stress concentration in the flights and intermediate landing presents no problem as the reinforcement is simply concentrated at the relevant positions.

Details of a typical stairway are given in fig. 22. Another stairway which considerably enhances the architecture of a building in Cape Town now nearing completion is shown in figs. 23A and 23B with details in fig. 23C. Load deflection tests were carried out on this stair and at an applied load of 100 lb. per ft.^{2} the deflection at the mid-point of the line of intersection of the flights and intermediate landing was only 0.004 ins. As will be noted this agrees well with the theoretical value calculated in Appendix I-1.

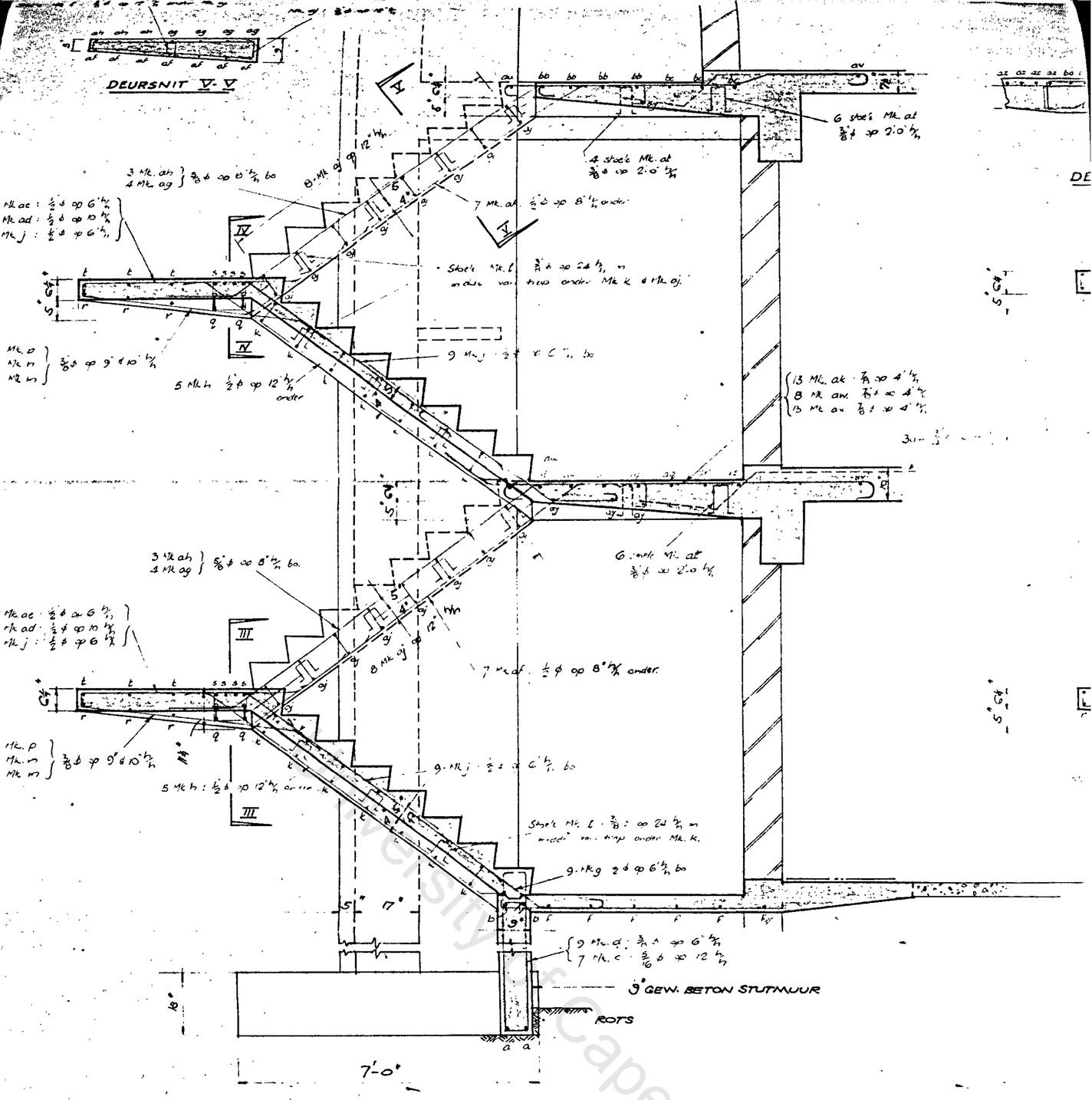

DEURSNIT : II–II ; SKAAL : ½" = 1'-0"

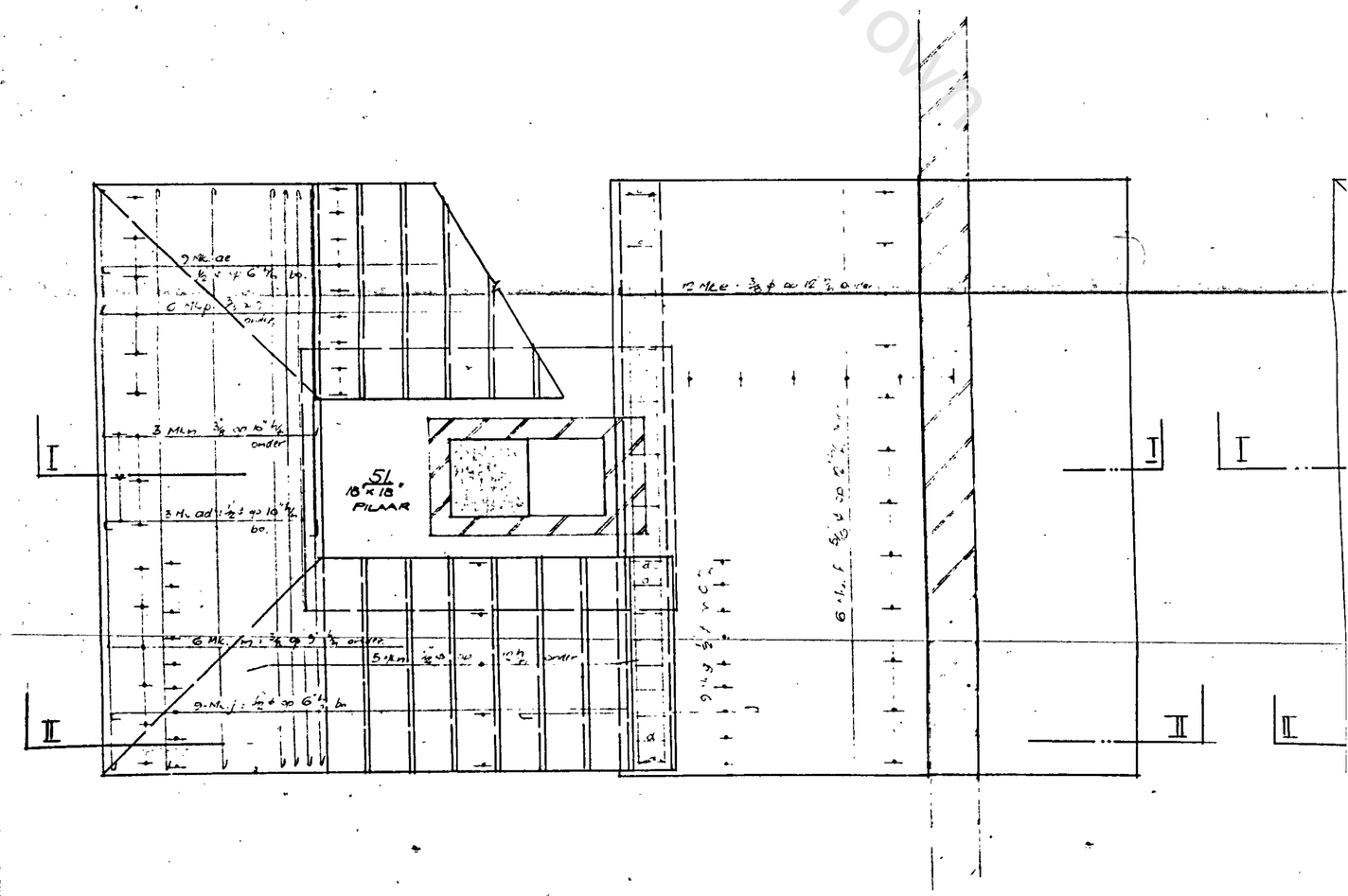

PLAN VAN TRAP VANAF 1985.90 VLAK TOT 1STE BORDES ; SKAAL : ½" = 1'-0"

fig. 22.

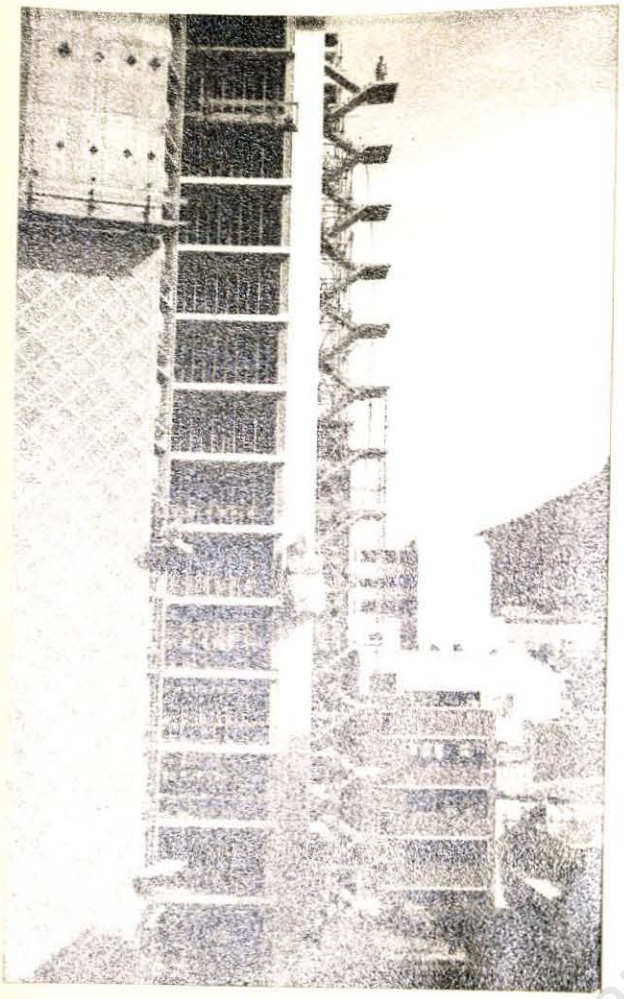

TWO VIEWS OF A FIRE ESCAPE STAIRWAY RECENTLY COMPLETED IN CAPE TOWN.

FIG. 23A.

FIG. 23B.

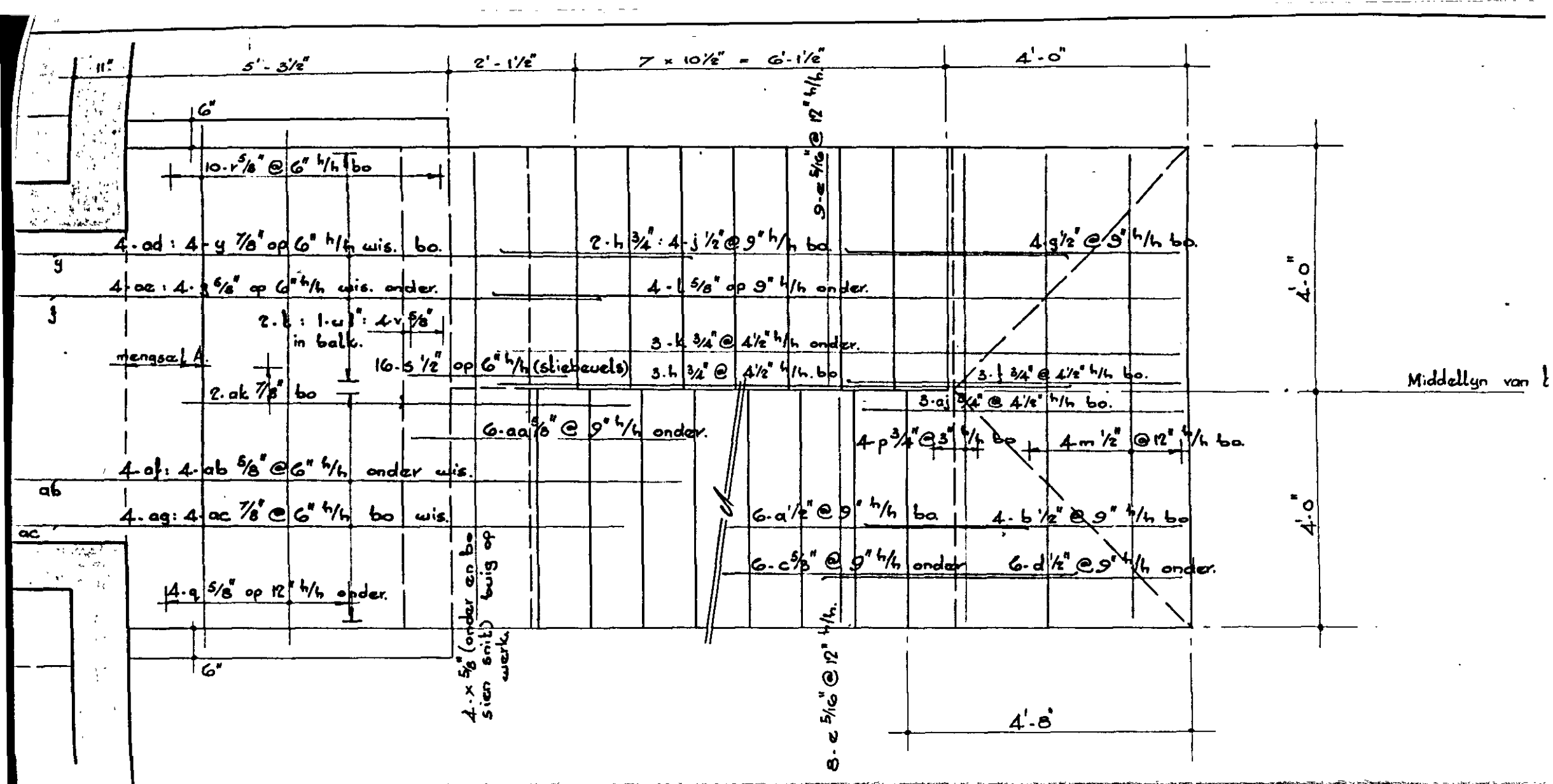

½" Skaal PLAN vanaf 8de tot 9de VLOER

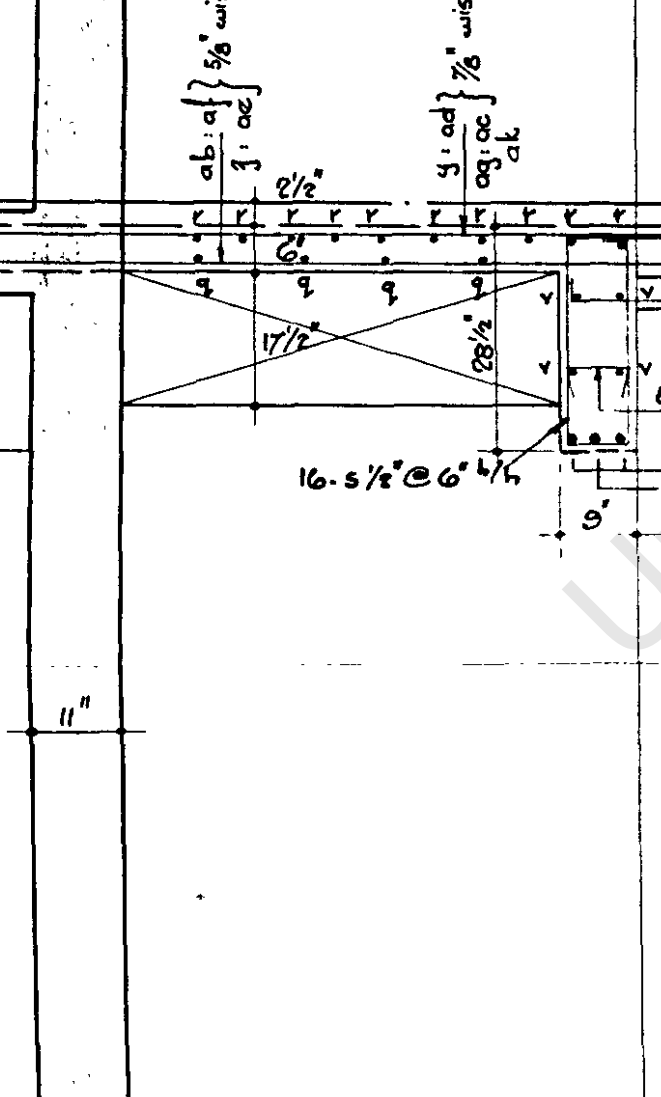

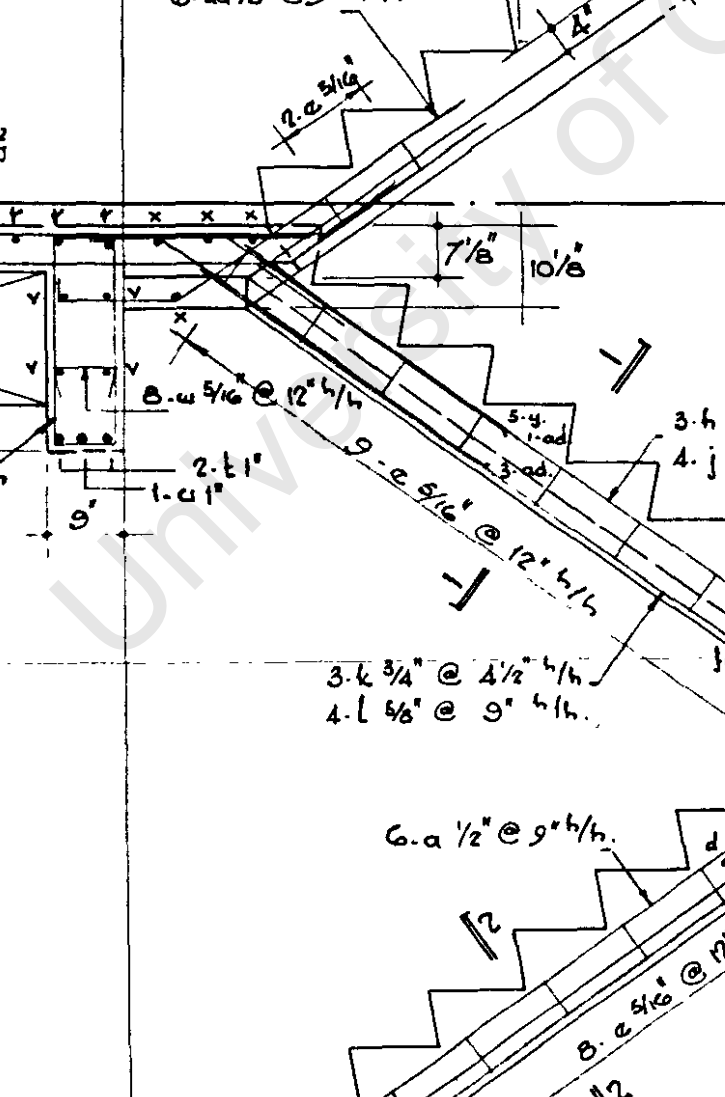

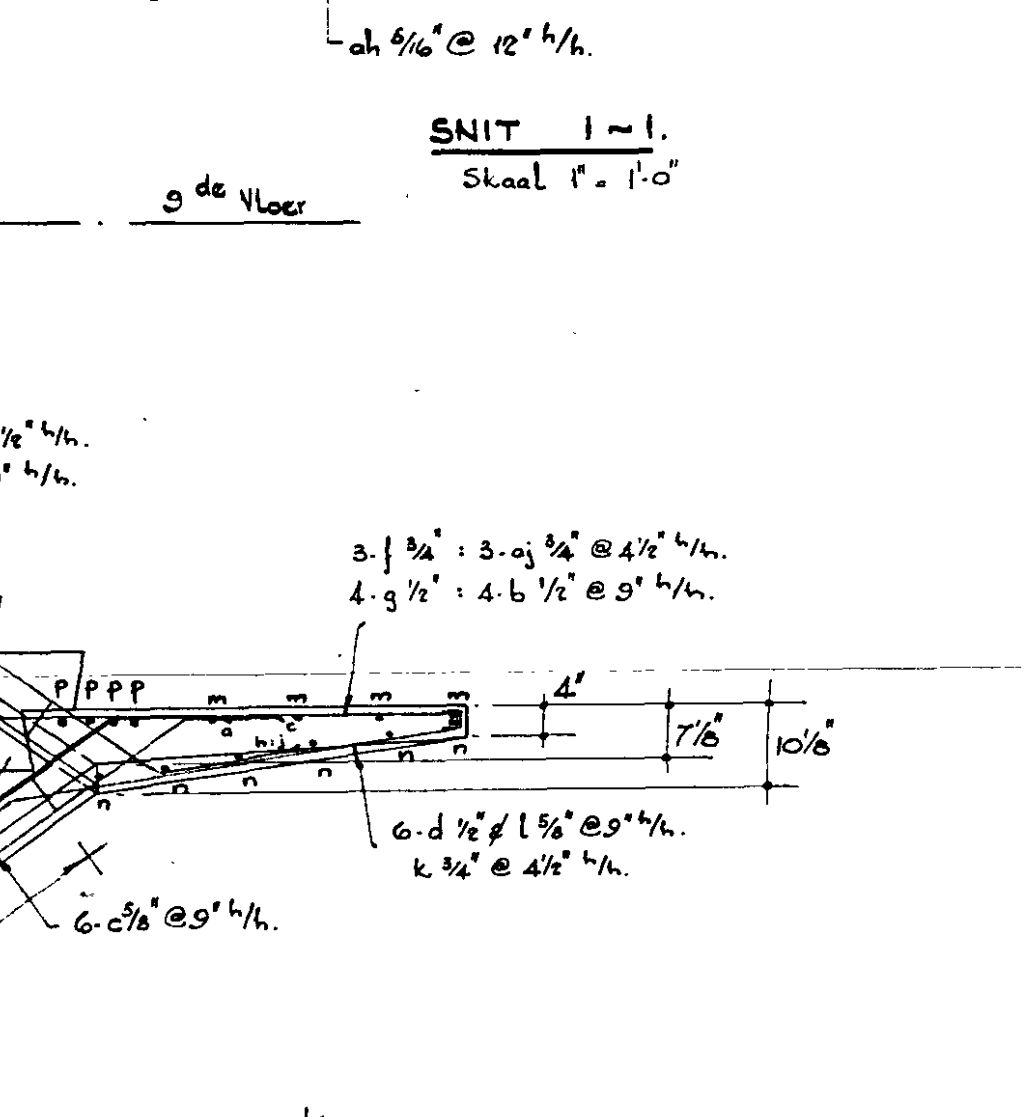

SNIT 1 ~ 1.

Skaal 1" = 1'-0"

½" Skaal AANSIG.

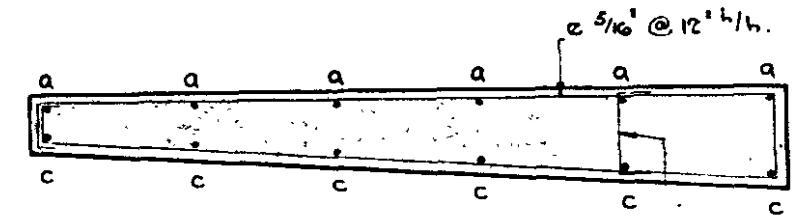

SNIT 2 ~ 2

Skaal 1" - 1'-0"

fig. 23c.

Betonmengsel: 8

APPENDICES

TO BOOK I

APPENDIX I - 1

NOTATION OF BOOK I - PART 1

B = Span length of landing.

b = Width of stair flight.

c = Horizontal gap between flights.

D = Total depth of landing slab, including screeding.

E = Young's modulus for concrete

E_F = Maximum extensional force per unit width in flights at intersection with landing.

E_L = Maximum extensional force per unit width in landing at intersection with flight.

E_{F1} = Extensional force at outside edge of flight at intersection with landing.

E_{F2} = Extensional force at inner edge of flight at intersection with landing.

E_{L1}, E_{L2} = Extensional forces in landing at intersection with flights and corresponding with E_{F1}, E_{F2}.

K_2 = Parameter depending on continuity of stair flights.

K_3 = Parameter depending on support conditions of loading.

$L = l$ = Horizontal span.

M = Width of landing.

R_F = Vertical reaction per unit width due to bending forces at intersection line Z_1Z_1 in fig. 5.2A(i).

R_V = Vertical resultants of extensional forces E_F and E_L.

S_1 = Horizontal shear force in flights.

S_2 = Horizontal shear force between supporting wall and landing.

ω = Uniformly distributed load per unit horizontal area.

ω_f = Uniformly distributed load applied to the stair flights per unit horizontal area.

ω_l = Uniformly distributed loading per unit area of landing.

$\frac{\delta}{\cos\theta}$ = Correction to deflection δ measured by suspended weight deflectometer where θ is angle of wire with vertical.

θ = Inclination of stair flights.

NOTATION OF BOOK I - PART 2

a = Width of landing.

b = Width of flight.

c = Width of gaps between flights.

D_{FCD} = the reaction at CD due to the local direct forces in the flight acting in the plane of the flight.

E_{FC} = The extensional force per unit length in the flight at C not including the local direct force.

E'_{FC} = The extensional force per unit length in the flight at C including the local direct force.

E_{LC} = The extensional force per unit length in the landing at C.

e = Eccentricity of resultant extensional force in flight.

h = Vertical height of stair flight.

k_1, k_2 = Factors depending on continuity of flights.

l = Horizontal span of flight.

M_{AB}, M_{CD}, M_{EF} = Bending moments at sections AB, CD and EF, respectively.

m, m_1, m_2 = Reaction per unit width due to bending forces at intersection of landing and flights.

$R_{\beta CD}$ = The resultant reaction due to the secondary bending force system and local direct forces acting at the intersection line CD at an angle β with the vertical.

R_{FCD} = The reaction at CD due to the bending forces in the flight acting at right angles to the flight.

R_{LCD} = The reaction at CD due to the bending forces in the landing acting at right angles to the landing.

RE_{FCD} = The resultant extensional force in the flight at CD due to the reaction $R_{\beta CD}$ but not including the effect of the local direct forces in the flight.

RE'_{FCD} = The resultant extensional force in the flight at CD due to the reaction $R_{\beta CD}$ and including the effect of the local direct forces in the flight.

RE_{LCD} = The resultant extensional force in the landing at CD.

S_{CD} = The shear force acting along the intersection line CD due to the primary force system but not including the effect of local direct forces.

S'_{CD} = The shear force acting along the intersection line CD due to the primary force system and including the effect of local direct forces.

ω = Uniformly distributed knife edge load.

ω_1 = Distributed load on flight per unit horizontal area.

ω_2 = Distributed load on landing per unit area.

W_F = Total load on flight.

X = Dimension indicating position of extensional forces in landings.

x = Variable measured horizontally from lower support of flight.

α_1, α_2 = Angles that the resultant extensional forces make with the centre-lines of the flights.

β = Angle which reaction $R_{\beta CD}$ makes with the vertical.

θ = Inclination of stair flight.

NOTATION OF BOOK I - PART 3

AS FOR PART 2 WITH IN ADDITION :-

E = Young's modulus.

EI_{DG} = Effective modulus of rigidity of the edge DG of the landing if subjected to bending moments acting along DG about axes parallel to the X-axis.

eb = Effective reduction due to M_t of the lever arm about O of the resultant reaction $m'b$.

GC = Torsional rigidity of flights.

m' = Vertical component of reaction at intersection line of flights and landing due to secondary bending force system.

m'' = Additional load supported by bending forces.

M_t = Torsional moment in flights.

$M_{x,o}$ = Bending moment at O about the X-axis.

s = Length of stair flight.

ω' = Portion of uniformly distributed load resisted by extensional forces.

Δ_{CH} = Sideway of the stairs at CH.

δ_o = Vertical deflection of point O .

ε_{uo} = Displacement of O in plane of upper flight.

$\varepsilon_{FC}, \varepsilon_{FD}$ = Extension of the flight at C and D, respectively.

λ = Relative vertical deflection at intersection line of flight edges.

ρ = Rotation of landing about the Z-axis.

$\mathcal{T}$ = Relative deflection at intersection line of the flight edges measured at right angles to the plane of the flight.

ϕ = Angle in Williott diagram.

NOTATION OF BOOK I - PART 4

f_u = Ultimate tensile strength of material of model stairs.

W = Point load.

NOTATION OF BOOK I - PART 5

A = Constant depending on end conditions of beam.

a = Width of landing.

B = Constant depending on end conditions of beam.

C = Constant depending on end conditions of beam.

D = Constant depending on end conditions of beam.

d = Effective thickness of flights.

d_1 = Thickness of landing.

E = Young's modulus.

I = Moment of inertia of beam.

I_x = Effective moment of inertia of landing.

k = Modulus of the analogous foundation.

$\frac{1}{k_1}$ = Parameter defining effective length of flight.

M_o = Couple acting at left hand extremity of analogous beam.

P_o = Shear force acting at left hand extremity of analogous beam.

s = Length of flights.

x = Variable measured along beam.

y = Vertical deflection of beam.

β = Parameter defined by $\sqrt[4]{\frac{k}{4EI}}$.

θ = Inclination of flights.

APPENDIX I-2

Extracts from design calculations for fire-escape stairway illustrated in figs. 23A, 23B and 23C.

Determination of Loads.

Dead Weight - Flights.

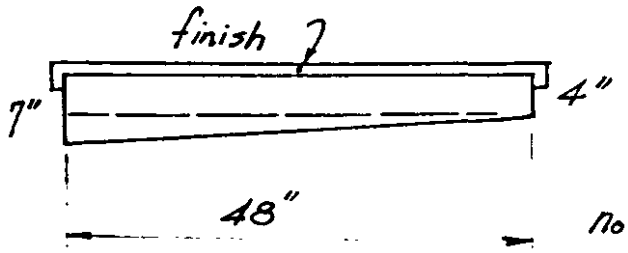

Cross Section of flight

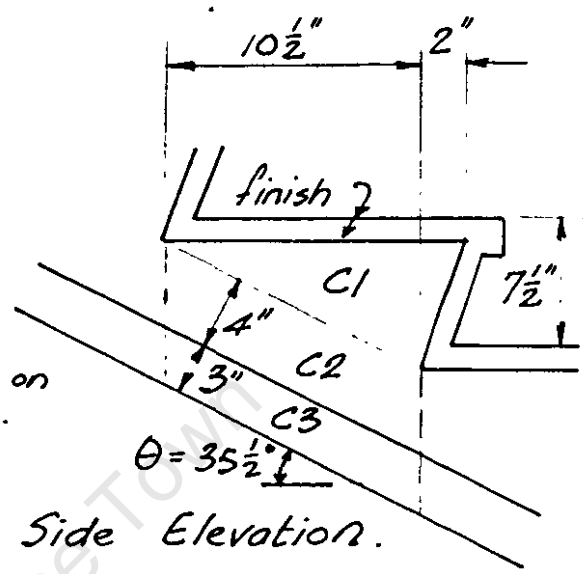

Side Elevation.

Weight of Concrete

C1	$1.04 \times 12.5 \times 7.6 \times 0.5 \times 4$	=	195 lb.
C2	$1.04 \times 4 \times 10.5 \times \frac{1}{\cos 35\frac{1}{2}^\circ} \times 4$	=	217
C3	$1.04 \times 3 \times 10.5 \times \frac{1}{\cos 35\frac{1}{2}^\circ} \times \frac{4}{2}$	=	81
			493

$\times \frac{12.5}{10.5} = 590$ lb

Finish $25 \times \frac{20.5}{10.5} \times 4.2 = 205$ lb

∴ Dead Weight of flights = 795 lb per horiz. ft run.
≒ 200 lb per horiz □ ft.
(neglecting eccentricity due to shape.)

Dead Weight - Landing.

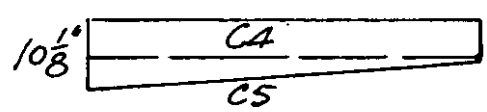

finish		15 lb/□'
Concrete C4	≒	50
" C5	≒	35
		100 lb/□'

Live Load = 100 lb/□'

Bending Moments due to "secondary" system.

Landing Cantilever: (neglecting non-uniform distribution)

dL $M_c = 100 \times 4^2 \times 6 = 9,600$ lb. ins. per ft (average)

LL + dL $M_c = 200 \times 4^2 \times 6 = 19,200$ " " " "

"Free" span moment

dL $M_s^{free} = 200 \times 7^2 \times 1.5 = 14,700$

LL + dL $= 300 \times 7^2 \times 1.5 = 22,000$

Fixed end moments.

dL $M_s^F = 200 \times 7^2 \times 1.0 = 9,800$

LL + dL $= 300 \times 7^2 \times 1.0 = 14,700$

APPROXIMATE BENDING MOMENT ENVELOPE

assuming stairs fixed at main landing and negligible deflection at intermediate landing.

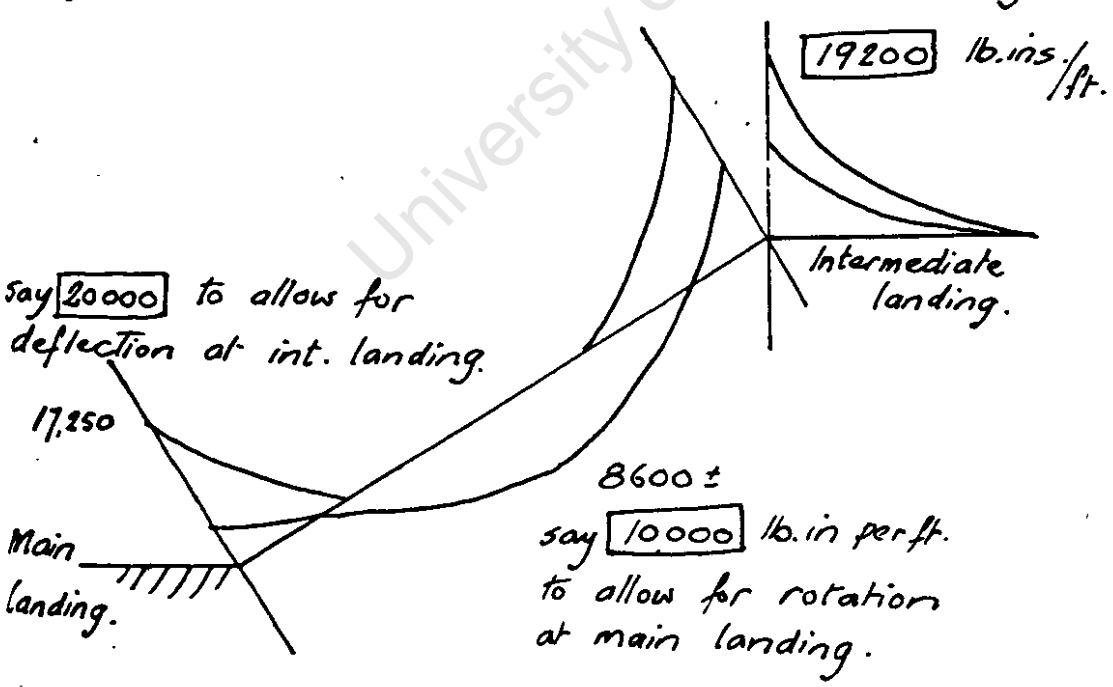

Note The eccentricity of load due to the shape of the flights is to be taken into account when detailing the steel reinforcement.

Maximum Reaction m' at intermediate landing "support" provided by Primary force system. (approximate method)

dL + LL	Landing	$200^{\#} \times 4$	= 800	lb per ft.
	Flights	$300 \times 7/2$	= 1050	" " "
	Reaction due to B.M.	$4000 \times \frac{1}{7}$ say	= 570	" " "
			£ = 2420	" " "

Extensional forces in upper flight at intersection with intermediate landing (see part 2.)

$$E'_{FG} = \frac{m'}{\sin\theta}\left[1 + \frac{3(b+c)}{b}\right] - \frac{w_1 l \sin\theta}{2}$$

$$= \frac{2420}{\sin 35\frac{1}{2}^\circ}\left[1+3\right] - \frac{300 \times 7 \sin 35\frac{1}{2}}{2} \qquad (c=0)$$

$$= 16700 - 600$$

$$= 16100 \text{ lb. per ft} \longrightarrow \text{Use stress concentration factor of 2.0}$$

$$E'_{FH} = \frac{m'}{\sin\theta}\left[1 - \frac{3(b+c)}{b}\right] - \frac{w_1 l \sin\theta}{2}$$

$$= -8350 - 600$$

$$= -8950 \text{ lb. per ft} \longrightarrow \text{can reduce due to above-mentioned stress concentration.}$$

Extensional forces in upper flight at intersection with main landing

$$E'_{FJ} = \frac{m'}{\sin\theta}\left[1 + \frac{3(b+c)}{b}\right] + \frac{w_1 l \sin\theta}{2}$$

$$= 16700 + 600 = 17300 \text{ lb. per ft} \longrightarrow \text{Use stress concentration factor of 2.0}$$

$$E'_{FK} = -8350 + 600$$

$$= -7750 \text{ lb. per. ft.} \longrightarrow \text{can reduce.}$$

Similarly Extensional forces in lower flight

$$E'_{FD} = -16700 + 600 = -16100 \text{ lb. per ft.}$$

$$E'_{FC} = +8350 + 600 = 8950 \text{ " " "}$$

$$E'_{FB} = -16700 - 600 = -17300 \text{ " " "}$$

$$E'_{FA} = +8350 - 600 = +7750 \text{ " " "}$$

4.

Transverse Bending Moments in the intermediate landing acting along intersection line COGH about X-axis.

Maximum bending moment (if torsion in flights is neglected)

$$\leq \frac{m'b(b+c)}{2}$$

$$= 2420 \times \frac{4^2}{2} \times 12 = 230,000 \text{ lb.ins.}$$

Determination of deflection δ_o of mid-point of intersection line COGH of flights and interm. lndg.

From Part 3 (if torsion in the flights is neglected)

$$\delta_o = \frac{m'l}{EdSin^2\theta Cos\theta}\left[1+3\frac{(b+c)^2}{b^2}\right]$$

$$= \frac{2420 \times 7 \times 4}{4{\cdot}2\times10^6 \times 7\tfrac{1}{2}" \times (0{\cdot}58)^2 \times 0{\cdot}81}$$

$$= \underline{0{\cdot}008"}$$

$E \doteq 60\,000\sqrt{u}$

$= 60\,000\sqrt{5000}$

$= 4{\cdot}2\times10^6 \text{ lb/in}^2$

$d \doteq 7\tfrac{1}{2}"$ allowing for cross-sectional shape, steps and reinforcemt.

Load Test on Prototype

The deflection of the above point was measured in a full-scale load test carried out before the finish had been applied. For an applied load of 100 lb per sq. ft the recorded deflection was 0·004". Assuming a linear load-deflection relationship the additional deflection due to dead weight would result in a total deflection of approximately 0·009", which is in good agreement with the theoretical value above.

The deflection of the extremities of the intersection line (At positions C and H) were of similar order which justifies the assumptions made.

APPENDIX I-3

EXTRACT FROM CONTRIBUTION

TO DISCUSSION OF

PAPER BY SIEV

Published in the Journal of the Structural Division, Proceedings of the American Society of Civil Engineers, Vol. 88, No. ST 6, December, 1962.

ANALYSIS OF FREE STRAIGHT MULTI-FLIGHT STAIRCASES[a]

Discussion by A. C. Liebenberg

A. C. LIEBENBERG,[7] M. ASCE.—Siev's extension of the theory to include the determination of secondary stresses resulting from the compatibility condition at the intersection of the flights and the intermediate landing has been studied with great interest. It would, however, appear that the assumptions made in the analysis may result in errors that are of the same order as the calculated secondary stresses.

In determining the relative displacements of the corners of the flights in order to establish the twist of the flights for substitution into Eq. 29, the deformation of the landing has apparently been neglected because the equations used in establishing this compatibility equation had been derived with the landing in a "rigid" state. Eq. 29 is not correct because the bending deformation of the landing edge 3 - 10 (see Fig. 7) would correspond only with the additional twist $w_3''' - w_4'''$ of the flights after relaxing of the rigid condition assumed in the first stage of the calculation. The twist $w_3' - w_4'$ corresponds with a rotation of the landing in a horizontal plane when in the "rigid" condition, and it is not related to the bending of 3 - 10. Furthermore, $w_3^{iv} - w_4^{iv}$ would equal zero as the component $M_{\overline{z}}$ is acting in the plane of the flight.

The author's resolution of the moment M_x into the components $M_{\overline{z}}$ and $M_{\overline{x}}$ is correct since the absence of any other external forces on the landing makes this the only feasible solution.

The additional deflection of the flights as a result of bending deformation of the landing edge may be of an equal order of magnitude to that of δ_o, the deflection caused by extension of the flights, and cannot be neglected in the compatibility equation. In determining the torsional rigidity, the author has neglected the stiffening effect caused by the bending of the flights,[8] which for the flights in the numerical example $\left(\frac{s}{b} = 2.8\right)$ would result in a 20% increase in torsional rigidity if the effect of the steps is neglected.

The compatability problem in stairs of this type is actually one of great complexity. The Bernouilli-Euler, or so-called straight-line stress distribution, does not apply at the intersection lines, as assumed, because of the fact that the bending stiffness of the landing is relatively small compared with the

---

[a] June 1962, by A. Siev (Proc. Paper 3168).

[7] Liebenberg and Stander, Cons. Civ. and Structural Engrs., Cape Town, South Africa.

[8] "The Torsional Rigidity of Rectangular Slabs," by K. H. Gerstle, and R. W. Clough, Journal, American Concrete Institute, November, 1953.

ANALYSIS OF FREE STRAIGHT MULTI-FLIGHT STAIRCASES[a]

Discussion by A. C. Liebenberg

A. C. LIEBENBERG,[7] M. ASCE.—Siev's extension of the theory to include the determination of secondary stresses resulting from the compatibility condition at the intersection of the flights and the intermediate landing has been studied with great interest. It would, however, appear that the assumptions made in the analysis may result in errors that are of the same order as the calculated secondary stresses.

In determining the relative displacements of the corners of the flights in order to establish the twist of the flights for substitution into Eq. 29, the deformation of the landing has apparently been neglected because the equations used in establishing this compatibility equation had been derived with the landing in a "rigid" state. Eq. 29 is not correct because the bending deformation of the landing edge 3 - 10 (see Fig. 7) would correspond only with the additional twist $w_3''' - w_4'''$ of the flights after relaxing of the rigid condition assumed in the first stage of the calculation. The twist $w_3' - w_4'$ corresponds with a rotation of the landing in a horizontal plane when in the "rigid" condition, and it is not related to the bending of 3 - 10. Furthermore, $w_3^{iv} - w_4^{iv}$ would equal zero as the component $M_{\overline{z}}$ is acting in the plane of the flight.

The author's resolution of the moment M_x into the components $M_{\overline{z}}$ and $M_{\overline{x}}$ is correct since the absence of any other external forces on the landing makes this the only feasible solution.

The additional deflection of the flights as a result of bending deformation of the landing edge may be of an equal order of magnitude to that of δ_o, the deflection caused by extension of the flights, and cannot be neglected in the compatibility equation. In determining the torsional rigidity, the author has neglected the stiffening effect caused by the bending of the flights,[8] which for the flights in the numerical example $\left(\frac{s}{b} = 2.8\right)$ would result in a 20% increase in torsional rigidity if the effect of the steps is neglected.

The compatability problem in stairs of this type is actually one of great complexity. The Bernouilli-Euler, or so-called straight-line stress distribution, does not apply at the intersection lines, as assumed, because of the fact that the bending stiffness of the landing is relatively small compared with the

---

[a] June 1962, by A. Siev (Proc. Paper 3168).

[7] Liebenberg and Stander, Cons. Civ. and Structural Engrs., Cape Town, South Africa.

[8] "The Torsional Rigidity of Rectangular Slabs," by K. H. Gerstle, and R. W. Clough, Journal, American Concrete Institute, November, 1953.

extensional stiffness of the flight. This results in a stress concentration at points 4 and 9, as illustrated by a photo-elastic experiment on a model stair made of Araldite B casting resin (Figs. 10, 11, and 12) conducted in the Mechanical Engineering Department of the University of Cape Town. The approximate stress distribution at various sections as compared with the straight line theory is illustrated in Fig. 13. Although a pure state of plane stress was not achieved in this experiment, as a result of secondary deformation, the qualitative result leaves no doubt regarding the nature of the stress concentration. In the analysis of stairs of this type, some allowance should be made

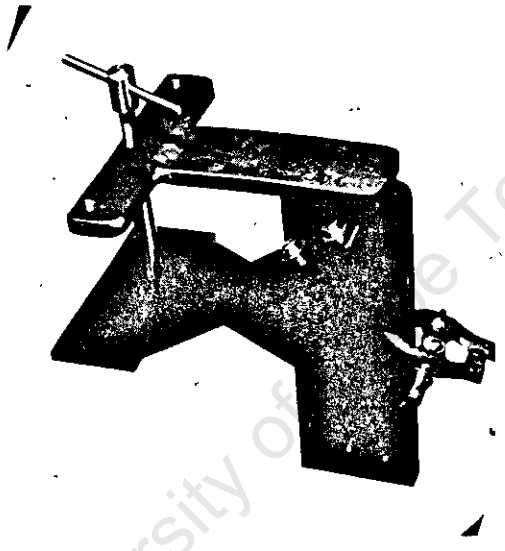

FIG. 10.—MODEL STAIRS MADE OF ARALDITE B CASTING RESIN SHOWN IN LOADING JIG

for this stress concentration in assessing the primary stresses. For reinforced concrete, a factor of 2.0 should cover most cases occurring in practice. For the determination of secondary stresses, however, the straight line assumption may be used as it will result in a conservative estimate.

As concluded by the author, the secondary stresses are usually negligible, and this formed the basis of the writer's analysis.[9] In the design of a stairway recently undertaken by the writer the value of the dimension c almost equalled b, and an assessment of the "secondary" stresses was essential. The approximate procedure adopted for the solution of the symmetrical case was as follows:

The stiffness of the landing was assumed to be infinite in its own plane so that points 3,4,9, and 10 remained co-linear in the plane of the landing. Bend-

[9] "The Design of Slab Type Reinforced Concrete Stairways," by A. C. Liebenberg, The Structural Engineer, May, 1960.

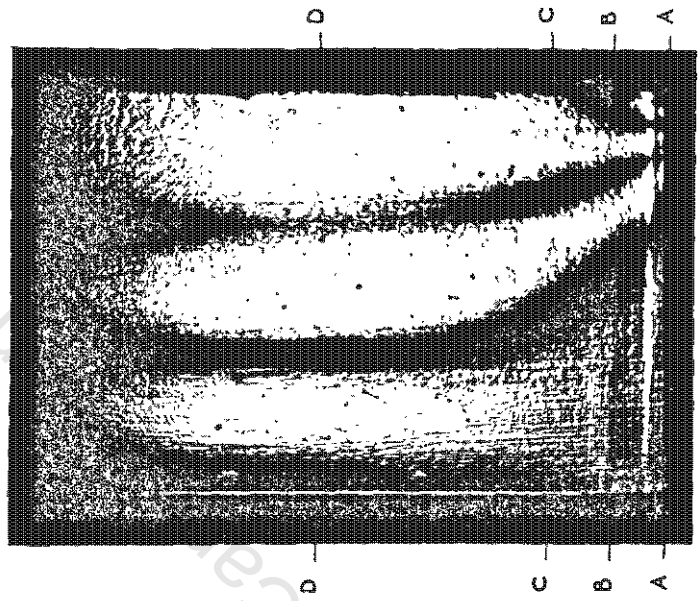

FIG. 12.—FRINGES OBTAINED IN LOWER FLIGHT WITH STAIR MODEL SUBJECTED TO 50-1/2 LB AS IN FIG. 10 (DARK FIELD)

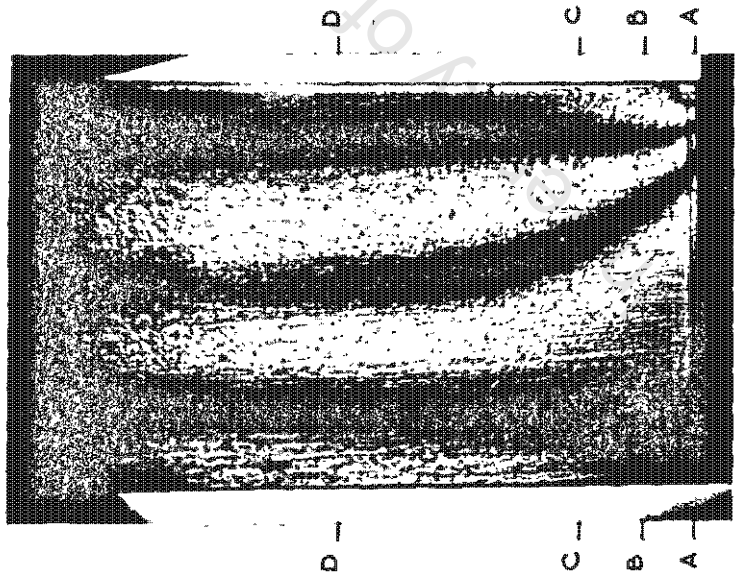

FIG. 11.—FRINGES OBTAINED IN LOWER FLIGHT WITH STAIR MODEL SUBJECTED TO 50-1/2 LB AS IN FIG. 10 (LIGHT FIELD)

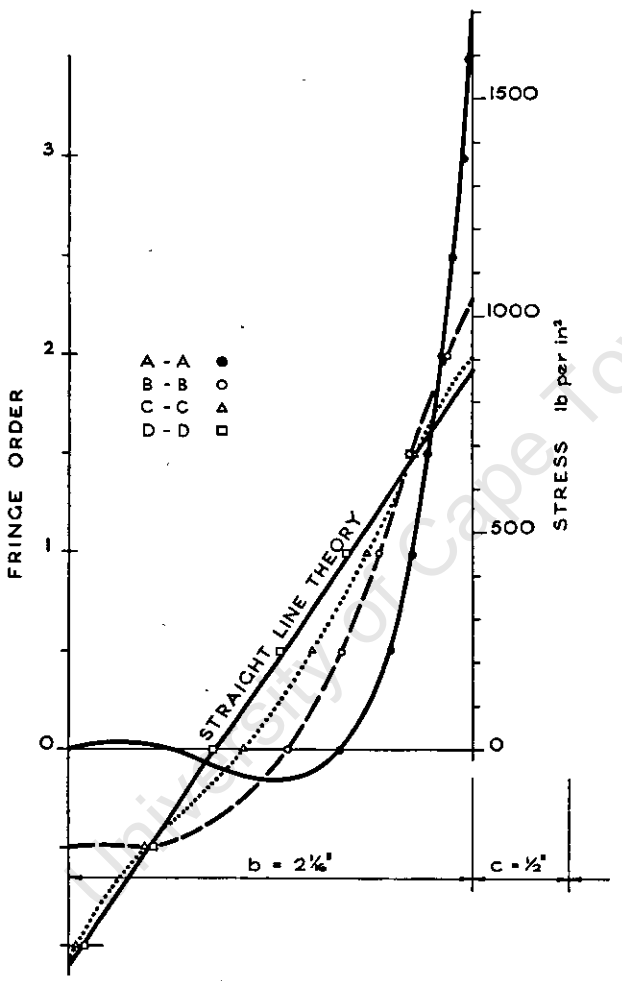

FIG. 13.—STRESS DISTRIBUTION AT VARIOUS SECTIONS OF LOWER FLIGHT SHOWING CONCENTRATION AT INTERSECTION WITH LANDING

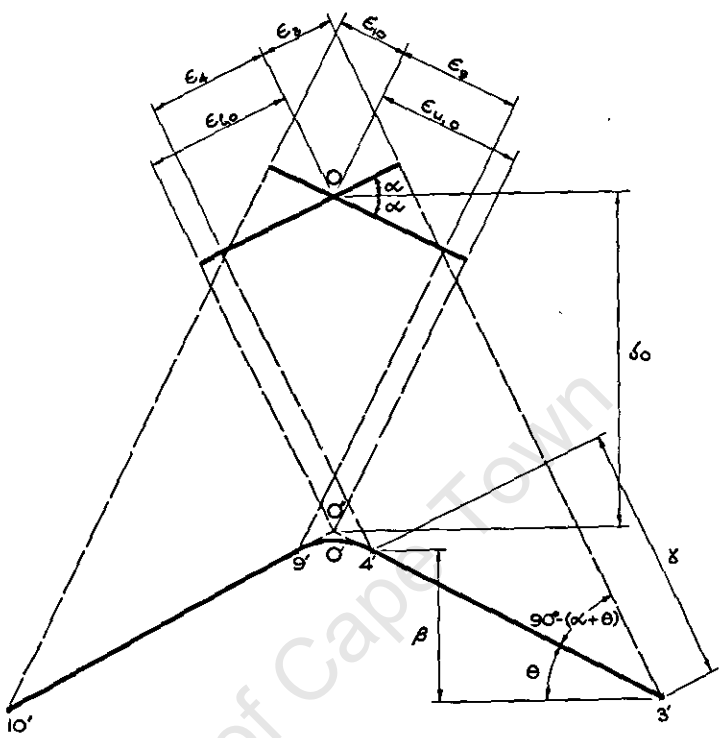

FIG. 14.—WILLIOT DIAGRAM OF DISPLACEMENTS DUE TO STRAIN IN PLATES FOR SYMMETRICAL LOADING

ing deformation of the landing about the x-axis was assumed to be confined to the neighborhood of the interval 4 - 9. Tests have indicated that this approximates to the truth because of the great stiffness caused by the interaction of the flights and landing in the intervals 3 - 4 and 9 - 10. As the dimension c increases relative to b, the accuracy of this assumption will increase. The compatability calculation is essential only for cases in which c is large so that the assumption is justified.

The resultant Williot diagram is shown in Fig. 14 [Fig. 6 (f)]. The extension of lines 3 - 4 and 10 - 9 meet at 0 because of the requirements of symmetry and the assumption that the landing is infinitely stiff in its own plane. Using the author's notation and with reference to Fig. 14, the following equations express the conditions of equilibrium of forces and compatability of deformations at the intersection line 3 - 10:

Bending equilibrium at o about x-axis is expressed by

$$M_{x,o} = R' \frac{b(b+c)}{2} - \frac{M_{\bar{x}}}{\cos \alpha} \quad \ldots\ldots\ldots \quad (47)$$

Bending deformation of edge 3 - 10 of landing is expressed by

$$\frac{\beta}{b} = \frac{M_{x,o}\, C}{2\, E\, I_b} \quad \ldots\ldots\ldots\ldots\ldots\ldots \quad (48)$$

The torsional twist of a flight (about the x-axis in its own plane) is equal to

$$\frac{\gamma}{b} = \frac{\beta \sin(\alpha + \theta)}{b \sin \theta} \quad \ldots\ldots\ldots\ldots \quad (49)$$

Therefore,

$$\beta = M_{\bar{x}} \frac{b\, s \sin \theta}{G\, C \sin(\alpha + \theta)} \quad \ldots\ldots\ldots\ldots\ldots\ldots \quad (50)$$

From the geometry of Fig. 14

$$\frac{\epsilon_3 - \epsilon_4}{\beta} = \frac{\cos(\alpha + \theta)}{\sin \theta} \quad \ldots\ldots\ldots\ldots\ldots \quad (51)$$

Therefore,

$$\frac{R's}{E\, t\, \beta \sin \alpha} \; 6\left(\frac{b + c}{b}\right) - \frac{12\, M_{\bar{x}} \tan \alpha\, s}{E\, t\, b^2\, \beta} = \cos \alpha \cot \theta - \sin \alpha \ldots \quad (52a)$$

and

$$\cot \theta = \frac{6\, R's\, (b + c)}{E\, t\, b\, \beta \sin \alpha \cos \alpha} - \frac{12\, M_{\bar{x}} \tan \alpha\, s}{E\, t\, b^2\, \beta \cos \alpha} + \tan \alpha \ldots \quad (52b)$$

By equating

$$M_{\bar{x}} = R'\, b^2\, e \quad \ldots\ldots\ldots\ldots\ldots\ldots \quad (53)$$

it can be shown that

$$e = \frac{\left[\dfrac{6\, s\, (b + c)}{E\, t\, b \cos \alpha} + \dfrac{b^2 c\, (b + c)(\sin \alpha \tan \alpha + \cos \alpha)}{4\, E\, I_b}\right]}{\left[\dfrac{b^3 s}{G\, C} + \dfrac{12\, s \tan^2 \alpha}{E\, t} + \dfrac{b^3 c\, (\sin \alpha \tan \alpha + \cos \alpha)}{2\, E\, I_b \cos \alpha}\right]} \quad \ldots\ldots \quad (54)$$

and that

$$\cot \theta = \frac{24\, S\, I_b \left[\frac{b+c}{\sin \alpha} - 2\, b\, e \tan \alpha\right]}{t\, b^3\, c\, [(b+c) \cos \alpha - 2\, b\, e]} + \tan \alpha \ldots\ldots (55)$$

Eqs. 54 and 55 can be evaluated by direct substitution of known parameters and are thus independent of the magnitude of loading. They are, however, dependent on the type of loading. Using these values, the unknowns $M_{\bar{x}}$, β, and $M_{x,o}$ can be determined in terms of R'.

Now

$$R' + R'' = R \ldots\ldots (56)$$

and the vertical deflection at the midpoint of (3 - 4) is equal to

$$\delta_o + \beta \left(\frac{1}{2} + \frac{c}{2\, b}\right) = \frac{4\, R''\, l^2 s}{E\, t^3} \ldots\ldots (57)$$

in which

$$\delta_o = \frac{\epsilon_{u,o}}{\sin \alpha} = \frac{R' s}{E t \sin^2 \alpha} \left[1 + 3 \left(\frac{b+c}{b}\right)^2\right] - \frac{6\, M_{\bar{x}}\, s \tan \alpha}{E t\, b^2 \sin \alpha} \left(\frac{b+c}{b}\right) \ldots (58)$$

Accordingly, a solution of all the unknowns can be obtained to give compatibility of deformation at the intersection line 3 - 10 in terms of the assumptions made.

The solution of the numerical example given by the author results in the following forces if the values for I_b and C are used (the author's results are given in brackets for comparison):

R' = 156.3 lb per in. (156.8)
R'' = 1.7 lb per in. (1.2)
M_x = 9,500 lb - in. (18,550)
$M_{x,o}$ = 213,800 lb - in. (205,300)

For stairs in which the dimension c is large, the discrepancies may be greater. Similar arguments apply in the case of assymmetrical loading.

127

ANALYSIS OF FREE STRAIGHT MULTIFLIGHT STAIRCASES[a]

Closure by Avinadav Siev

AVINADAV SIEV.[12]—The examples from New-Zealand practice, especially the design shown in Fig. 15, are interesting. When confronted, in 1960, with the assignment of a staircase of this type, the writer was unable to find confirmation for his conclusion that torsional stresses are not essential for equilibrium. Liebenberg's article was not published until after the draft of the paper was ready, and still another[13] only after its publication. Yet even today (1963) the writer knows of engineers who find it difficult to reconcile the rational explanation with their intuitive conviction regarding the presence of torques. The staircase shown in Fig. 15 should therefore be regarded as a daring attempt at maximum exploitation of this type of design.

The writer doubts that Glogau's recommendation in regard to possible LL in preference to code LL ("because most of the spare redundancy is already being utilized by this design method") is indispensable. In the codes the specified LL exceeds the actual LL, and they are on the safe side. Moreover, there are many systems without "spare" redundancy such as cantilever beams, tension bars in trusses, etc. The permissible stresses are based on the safety factor designed to account for, inter alia, accidental excessive load. In fact, the safety factor should rather be regarded as a factor of uncertainty.

As uncertainty in regard to structural behavior decreases, the trend in the codes is toward a reduced safety factor, and the building designer is allowed a much higher factor of uncertainty than his counterpart in the aircraft industry where the safety factor is only 1.5 (except where fatigue is involved), although risk of life is involved. In the missile industry, etc., the factor of safety is lower.

Liebenberg refers to the following points:

1. The stiffening effect on the torsional rigidity caused by bending of the flight plates has been disregarded;
2. the assumption of linear stress distribution at the intersection lines is not exact;
3. bending of beam 3-10 is confined to the neighborhood of the interval 4-9; and
4. Eq. 29 should be corrected.

---

[a] June 1962, by Avinadav Siev (Proc. Paper 3168).

[12] Senior Lecturer, Technion, Israel Inst. of Technology, Haifa, Israel.

[13] "Columnless Stairs," by L. H. Mitchell and F. S. Shaw, Architectural Science Review, July, 1960, p. 80.

As for the first three points, the writer did not claim that the proposed analysis was "exact." It was only intended as an indication that the order of magnitude of the secondary stresses is small, so that they can safely be neglected. No attempt was made to study stresses beyond the "secondary," i.e., of a third order.

The edge conditions of the flights are certainly not those assumed in Reference 8. The degree and character of fixity of the flight in the landing is quite complex and form the subject of a separate study, in progress at present.

The stress distribution shown in Fig. 13 is extremely interesting. Yet nonlinearity is only local and the deviation from linearity at section B-B (which is near A-A) is quite small, as it should be according to the St. Venant principle. In any case, the stress resultant in the flights is the same, and it seems therefore that Eqs. 19 and 17 yield a satisfactory approximation. The local high stresses at points 4 and 9 are of secondary importance, because the membrane or plate stresses are only a fraction of the total stresses, including the slab bending moments. There is also reason to believe that this stress concentration is of the type accounted for by plastic flow of the material at high stresses.

The mode of deflection of beam 3-10 is of the utmost importance, because (as already indicated in the paper) this deflection is the dominant factor contributing to the torque. It will be shown in the following how different assumptions relating to beam bending change entirely the order of magnitude of the torsional moments.

However, the problem of beam bending is related to that of determining moment of inertia of the latter. When writing the paper, it was assumed that the assumption of the contribution of one half of the landing width to an average I_b at the entire beam length will safely replace the true state of unknown varying rigidities. Experimental data[13] published in the meantime indicate that the assumption of beam 3-10 as comprising one half of the landing width is quite realistic, so that a smaller value than specified in Eq. 23 could have been taken for $\delta''_3 - \delta''_4$. The true value should lie somewhere between that shown in Fig. 7(b) (Eq. 23) and Fig. 14 (Eq. 48), depending on the value of c, as noted by Liebenberg.

Eq. 29 should be corrected as follows:

$$w'''_3 - w'''_4 = \left(w'_3 - w'_4\right) + \left(w''_3 - w''_4\right) + \left(w^{IV}_3 - w^{IV}_4\right) \quad \ldots . \quad (59)$$

and as

$$w'''_3 - w'''_4 = \frac{M_{\bar{x}}\, b\, s}{G\, C} \quad \ldots\ldots\ldots\ldots\ldots (60)$$

and the writer sincerely thanks Liebenberg for drawing his attention to this error.

Eq. 59 coincides exactly with the corrected formula suggested by Liebenberg. It is easily seen that Fig. 14 includes Fig. 6(f) with the effect of $M_{\bar{x}}$ taken into account (Eq. 52a) as well as Fig. 7(d) in a slightly modified form; β used by Liebenberg is exactly $\delta''_3 - \delta''_4$ and γ equals the left side of Eq. 59.

Substituting the values of the numerical example into Eq. 59 yields $M_{\overline{x}} = 25{,}000$ lb-in.

Using Liebenberg's third point, relating to the bending of beam 3-10, Eq. 24 is replaced by

$$w''_3 - w''_4 = \frac{\delta''_3 - \delta''_4}{\cos \alpha} = R' \frac{b\, c^2 (b+c)}{4\, E\, I_b \cos \alpha} - M_{\overline{x}} \frac{b\, c}{2\, E\, I_b \cos^2 \alpha} \quad \ldots . \quad (61)$$

Substitution of these values into Eq. 59 yields a result coincident with that of Liebenberg. Substituting

$$\sin \alpha \cdot \tan \alpha + \cos \alpha = \frac{1}{\cos \alpha} \quad \ldots\ldots\ldots\ldots \quad (62)$$

into Eq. 54, and dividing the denominator by b^2, Eq. 53 becomes

$$M_{\overline{x}} = R' \frac{\frac{6\, s\, (b+c)}{E\, t\, b \cos \alpha} + \frac{b^2 c\, (b+c)}{4\, E\, I_b \cos \alpha}}{\frac{b\, s}{G\, C} + \frac{12\, s \tan^2 \alpha}{E\, b^2\, t} + \frac{b\, c}{2\, E I_b \cos^2 \alpha}} \quad \ldots\ldots\ldots \quad (63)$$

The first term of the denominator is exactly the coefficient of Eq. 22, the first term of the numerator is that of Eq. 25, the last terms correspond to these of R' and $M_{\overline{x}}$ in Eq. 61, etc. The writer believes that no similar discrepancy exists in the case of asymmetrical load.

To conclude, there are many uncertainties in addition to those mentioned, such as the value of the torsional rigidity C in cracked reinforced concrete, the behavior of the landing as a cantilever notfixed at section 4-9, the stress-strain curves in reinforced concrete, etc.; still, it is clear that torsional and secondary stresses are normally negligible and can be disregarded, except when c is relatively large.

Errata.

Page 207, line 2: By Avinada Siev should read By Avinadav Siev

Page 209, line 4: $X = \overline{X} \cos \alpha$ and $Z = \overline{X} \sin \alpha$

Page 221, line before Eq. 24: in the directions normal to the flight plane

Page 221, line after Eq. 24: should be w''' instead of w''.

Page 222, Eq. 33: $\delta_o = \frac{R''\, l^2\, s}{3\, E \left(\frac{t^3}{12}\right)} = \frac{4\, R''\, l^2\, s}{E\, t^3}$

Page 224, Fig. 8(g): Deformation of beam $\overline{3.\ 10}$

Page 226, line 6 from bottom: . . . a cross section of 24 in. by 8 in. is assumed. . . .

B O O K II

A STRESS-STRAIN FUNCTION

FOR CONCRETE

REPRINTED FROM *MAGAZINE OF CONCRETE RESEARCH*. VOL. 14, No. 41. JULY 1962. pp. 85–90.

UDC 624.043 : 666.97

A stress-strain function for concrete subjected to short-term loading

by A. C. Liebenberg, B.Sc.(Eng.), A.M.I.C.E., A.M.I.Struct.E., A.M.Asce., A.M.(S.A.)I.C.E.

UNIVERSITY OF CAPE TOWN

SUMMARY

The author develops a function relating stress and strain for concrete subjected to short-term non-repetitive uniaxial loading. The function is based on well established empirical relations and its mathematical form corresponds with the suspected nature of the physical behaviour of concrete under stress.

Introduction

Various stress-strain functions for concrete have been produced which either are rather complex[1] or require more than one function[2] to cover the full range of strengths commonly obtained with " ordinary " concretes. These functions do not correspond directly with the peculiar physical behaviour of concrete under stress and have been produced by arbitrary processes. An attempt is made in this paper to develop a simple function for concrete subjected to short-term non-repetitive uniaxial loading, in which well established empirical relations are utilized and which has a mathematical form corresponding to the suspected nature of deformation.

Material properties of concrete

The extreme complexity of concrete as a structural material due to its heterogeneous composition and the resultant mechanical-rheological behaviour has been investigated in considerable detail. Several theories and formulae have been suggested expressing the behaviour patterns of various phenomena such as shrinkage and deferred strain in terms of time and other relevant parameters. The fact that these formulae seem to agree well with the observed behaviour suggests that they correspond with the physical nature of the phenomena which they express in mathematical form. No attempt appears to have been made to derive a stress-strain function on a similar basis.

Suggested physical basis for the stress function

It has been well established by experiment that, for the range of strengths commonly obtained with " ordinary " concretes, prisms or cylinders subjected to uniaxial loading at a moderate and continuous rate exhibit the following behaviour characteristics.

(1) The initial modulus of elasticity, for concretes with no marked shrinkage history, is approximately proportional to the square root of the cube strength (or cylinder strength).

(2) The peak stress is attained at an approximately constant strain for any particular rate of loading, no matter what the crushing strength.

(3) Failure or disintegration occurs at a particular strain for any particular cube strength and rate of loading.

(4) It is furthermore suspected[3] that the descending branch of the stress-strain curve—a phenomenon apparently found only in concrete and some timbers—is caused by progressive irreversible micro-cracking so that, with further increasing strain, a progressively smaller number of uncracked particles is called upon to resist load.

Brandtzaeg's theory of failure[3] presents a concept of " critical load " at minimum volume which occurs at approximately 80% of ultimate load. At this point it is assumed that a progressive internal splitting is initiated on minute sections scattered throughout the concrete. With due regard to this concept it may nevertheless be argued that the deviation from the linear stress-strain relation at an earlier stage is due to a similar process on a smaller scale, perhaps involving " slipping " rather than " splitting ", and that the degree of deviation is principally a function of strain. This is the physical behaviour pattern which forms the basis of the function derived below.

Magazine of Concrete Research : Vol. 14, No. 41 : July 1962

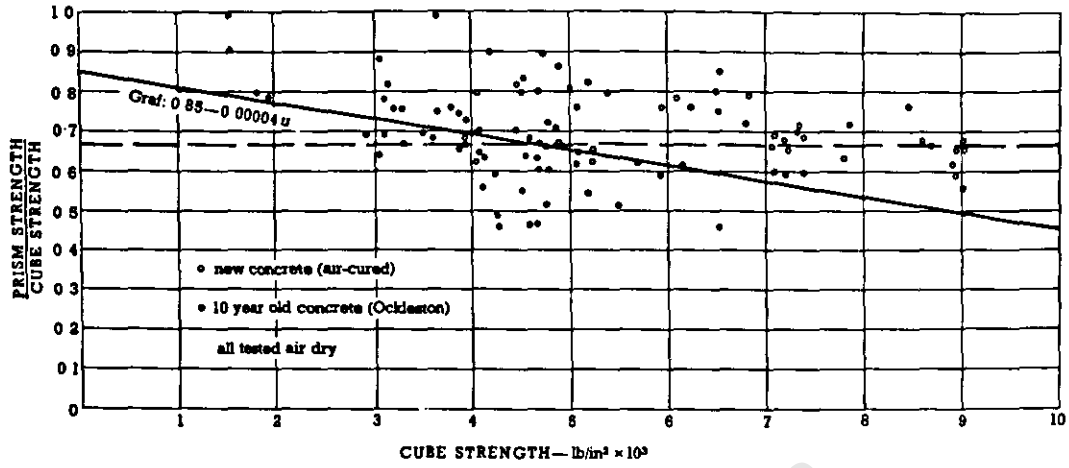

Figure 1

Mathematical form of the stress function

Using the concept stated above, we can express the stress-strain relation in the form $f = E_c(\varepsilon - \varepsilon_d)$ where ε_d is the deviation of strain (Figure 2) and E_c is the initial modulus of elasticity or

$$f = E_c[1 - \varphi(\varepsilon)]\varepsilon \ldots\ldots\ldots\ldots\ldots (1)$$

where $\varphi(\varepsilon)$ is a function of strain.

Before expanding this function it is necessary to deal briefly with various concepts and relations.

Relations between prism strength, cube strength and cylinder strength

It was established by Graf[4] that the prism strength can be related to the cube strength by the formula

$$f_{max}/u = 0{\cdot}85 - 0{\cdot}00004\,u$$

where f_{max} is the ultimate stress of a $30 \times 30 \times 130$ cm prism and u the crushing strength of a 20 cm cube, both values expressed in lb/in². The mean values of tests carried out by the author on 4×4 in. prisms in accordance with B.S. 1881:1952 (Figure 1) are slightly higher and appear to agree approximately with comparable American values of cylinder strength[3] if L'Hermite's formula[5] for the ratio of cylinder strength to cube strength

$$\frac{\text{cylinder strength}}{\text{cube strength}} = 0{\cdot}76 + 0{\cdot}20 \log \frac{u}{2844} \simeq 0{\cdot}8$$

is applied.

For the purposes of this paper it is assumed that the prism strength is two-thirds of the cube strength. This is sufficiently accurate for the normal range of concretes, considering the usual scatter pattern, but rather low for low-strength concretes as shown in Figure 1. The values plotted are based on students' tests on laboratory-made 4×4 in. prisms and 6 in. cubes together with values calculated by the author from results obtained by Professor A. J. Ockleston and Mr I. R. Scott [6]on specimens ten years old cut from the Old Dental Hospital building in Johannesburg. Values obtained by the author on specimens from the stairs[7] of the same building as well as from the Old Alliance House in Cape Town (30 years old) are also included. All these tests were in accordance with B.S. 1881:1952.

Initial modulus of elasticity

It has been established that the initial modulus of elasticity $E_c \simeq A\sqrt{u}$ where the coefficient A appears to depend primarily on the conditions of curing and exposure to which the concrete has been subjected. Authorities differ as to the mean value but the author, after analysing the results of tests carried out by various workers as well as tests done under his supervision, has come to the conclusion that the mean value of A if E_c and u are expressed in lb/in² approximates to 75,000 lb$^{\frac{1}{2}}$/in. for water-cured concretes tested wet. The value decreases with partial curing to 60,000 for air-cured concretes less than a year old tested air-dry. Long periods in an air-dry state appear to reduce the value to as low as 40,000, but insufficient test data are available to draw definite conclusions. The results of this investigation are represented in Figure 4, for which it must be noted that Graf expressed the modulus of elasticity in the form $E_c = \alpha/(\beta + \gamma/u)$, not in terms of $\sqrt{u}$. The curves shown were derived by the author from the results of 600 tests[4] carried out by Graf on water-cured concretes. Graf later revised his formula which, if expressed in the form $A\sqrt{u}$, gives $A \simeq 55{,}000$ lb$^{\frac{1}{2}}$/in. This reduction agrees with relations established by him between water- and air-cured concretes so that the latter formula apparently applies to air-cured concretes. Walker actually suggested[8] the formula $E_t = 66{,}000\sqrt{u_{cyl}}$, where u_{cyl} is the cylinder strength and E_t is the tangent modulus at 25% of ultimate stress, which approximates[5] to $E_s = 66{,}000\sqrt{u}$ where u is the cube strength and E_s is the secant modulus at 25% of ultimate stress. The value of A for the initial tangent modulus could therefore be expected on this basis to exceed 66,000 for water-cured concretes.

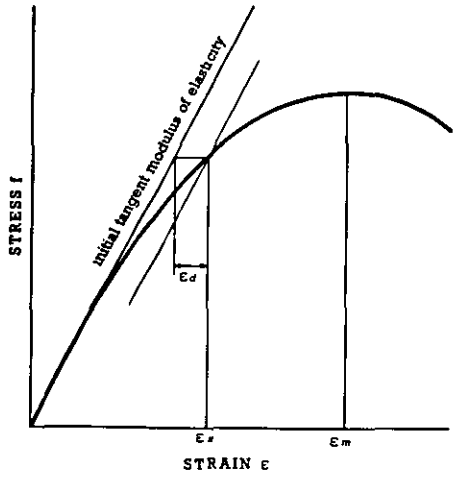

Figure 2

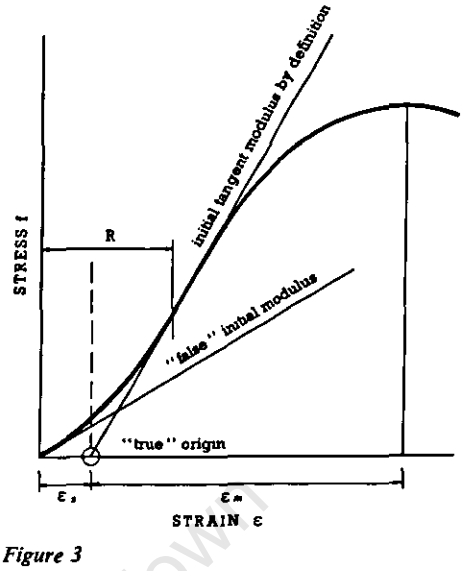

Figure 3

It is important to define the initial modulus of elasticity clearly as various authorities use different concepts. In this paper the initial modulus is taken to mean the value represented by the slope of the tangent to the curve at the origin as indicated in Figure 2.

The use of secant moduli at various arbitrary stresses or strains may lead to considerable confusion. On the other hand, care has to be taken in determining the initial modulus. Concretes with a marked pre-history of shrinkage often exhibit a " false " initial modulus and it may be difficult to determine the precise value. This phenomenon has apparently received little attention, although it is of great practical importance. Tests carried out by the author on specimens cut from full-scale structures and on air-cured laboratory specimens indicate that concrete may have a low initial modulus (Figure 3) bearing little or no relation to its other properties: the effect usually disappears after the first loading cycle. That this phenomenon is common knowledge but is usually ignored is apparent from the instructions given in B.S. 1881:1952 for determining the modulus of elasticity of concrete in which the results of the first cycle are discarded if they exhibit this phenomenon. Actually this first cycle tells a great deal, and its relation to later cycles will be determined principally by the method of curing up to the time of loading. This phenomenon is not often found in water-cured concrete: it is apparently related to the mode of shrinkage which in turn is influenced by the method of curing or the degree of exposure, the material properties of the concrete and the shape and boundary conditions of the specimen. The effect is probably caused by internal micro-cracking which reduces the effective cross-sectional area. These micro-cracks close up during the first cycle of loading and only partially re-open when the load is removed so that the effect is reduced in later cycles. It should be even more noticeable in specimens that have hair cracks and, in tests carried out on concrete with a just-visible hair crack, a considerable reduction in the initial modulus was recorded. The S-shaped stress-strain curve of Figure 3 can accordingly be accounted for as follows. Initially, over range R, the modulus of elasticity is low, owing to micro-cracking. The modulus increases as these micro-cracks and extremely small voids close up and remains approximately constant over the linear (or so-called elastic) range, with a gradually increasing deviation as mentioned previously, until the so-called plastic range is reached. This non-linear range and recoverable and permanent, instantaneous and deferred (or creep) strains have been the subject of much recent research.

The size of the " apparent shrinkage strain " ε_s which determines the position of the " true " origin of the stress-strain curve (Figure 3) cannot as yet be predicted. For experimental stress-strain curves where no " shrinkage strain " was apparent, the initial modulus of elasticity was taken for the purposes of this paper as that indicated in Figure 2. Where the effect was marked, an estimate of the " apparent shrinkage strain " ε_s was made by drawing a tangent to the curve at the point of change of curvature, as shown in Figure 3. This tangent was then assumed to be the initial tangent modulus, as it passed through the " true " origin as defined above. The values established for the coefficient A were established by the author from old concretes on the above basis, as in most cases the specimens exhibited a marked " apparent shrinkage strain ". This corresponds with the procedure laid down in B.S. 1881:1952.

The exact basis and methods of interpretation of the tests by Graf, Roš, Guyon, Walker, Jensen and Viest are not clear. As there is no accepted method for computing the initial value of Young's modulus for concrete, any direct comparison of the results obtained by different research workers may be misleading and can at best only indicate trends. This is well borne out by Figure 4. A more precisely defined procedure may considerably reduce the scatter.

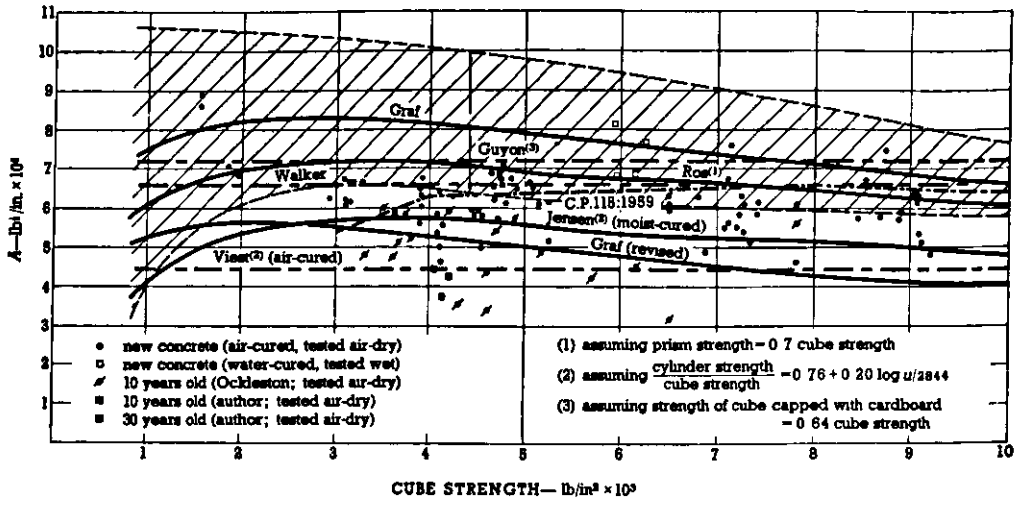

Figure 4

Expansion of the stress function for prisms in terms of known parameters

The author has found that the stress function given in equation 1 corresponds closely with test results if $\varphi(\varepsilon)$ is expressed in the form $B\varepsilon^n$. As discussed above, E_c can be equated with $A\sqrt{u}$. The function therefore becomes

$$f = A\sqrt{u}(1-B\varepsilon^n)\varepsilon \quad \ldots\ldots\ldots\ldots\ldots (2)$$

To establish the values of the parameters B and n, the concept given above in (2) can be utilized.

Therefore $df/d\varepsilon = A\sqrt{u}[1 - (n+1)B\varepsilon^n] = 0$ when $\varepsilon = \varepsilon_m$ where ε_m is the strain at peak stress f_{max}.

Therefore $$B = \frac{1}{(n+1)\,\varepsilon_m{}^n}$$

also $$f_{max} = A\sqrt{u}(1-B\varepsilon_m{}^n)\varepsilon_m$$

Therefore $$\tfrac{2}{3}u = A\sqrt{u}\left[1 - \frac{1}{(n+1)}\right]\varepsilon_m$$

and $$n = \frac{\tfrac{2}{3}u}{A\sqrt{u}\varepsilon_m - \tfrac{2}{3}u}$$

where $\varepsilon_m = 0{\cdot}0020$ for a rate of loading approximating to 0·001 strain/min. This value of ε_m has been found to be fairly constant for the concrete strengths normally used. The family of curves represented by equation 2 for $A = 60{,}000$ lb$^{\frac{1}{2}}$/in. and various values of u are illustrated in Figure 5. Curves for $A = 75{,}000$ and 40,000 lb$^{\frac{1}{2}}$/in. at $u = 6{,}000$ lb/in^2 are also given.

Ultimate strain

Although there is a wide divergence of opinion as to the ultimate strain attained by a prism before disintegration or rupture occurs, the indications are that it depends primarily on the rate of loading and the cube strength. Concretes with low strength disintegrate at a higher strain so that the stress-strain curves terminate approximately as indicated in Figure 5. The termination line could probably be expressed as a function of cube strength and rate of loading, but may also depend on the curing and exposure. For purposes of analysis the ultimate strain can be assumed to approximate to $\varepsilon_u = 0{\cdot}004 - u/(8{\cdot}3\times10^6)$ which is derived from a similar empirical function developed by Hognestad, Hanson and McHenry[3] in terms of the cylinder strength by assuming that $u = u_{cyl}/0{\cdot}78$.

Comparison of curves with experimental values

The theoretical curves agree remarkably well in shape with the results of a statistical study made by Kriz and Lee[1] of the concrete stress-strain curves obtained experimentally by Hognestad, Hanson and McHenry[3]. Their curves are, however, based on tests done in flexure and on concentrically loaded cylinders and not prisms so that the ratio of peak stress to cylinder strength is different. The stress-strain function can be expressed in terms of cylinder strength in the form

$$f = A_s\sqrt{u_{cyl}}(1 - B\varepsilon^n)\varepsilon \quad \ldots\ldots\ldots (3)$$

where $A_s = \dfrac{60{,}000}{\sqrt{0{\cdot}8}} = 67{,}000$ lb$^{\frac{1}{2}}$/in.

u_{cyl} = cylinder strength in lb/in^2

$$B = \frac{1}{(n+1)\,\varepsilon_m{}^n} \text{ and } n = \frac{f_{max}}{A_s\sqrt{u_{cyl}}\varepsilon_m - f_{max}}$$

where f_{max} depends on the cylinder strength and usually exceeds $0{\cdot}90u_{cyl}$. For comparison this theoretical function has been calculated for strengths corresponding with the above-mentioned statistical curves. The superimposed curves are illustrated in Figure 6. The experimental values of f_{max} have been adopted.

Hognestad, Hanson and McHenry found a striking similarity between the results of the flexural and the cylinder stress-strain curves.

For concretes of higher strength the aggregate is increasingly more important than the cement paste and the function would probably have to be amended

APPENDIX II - 1

NOTATION OF BOOK II

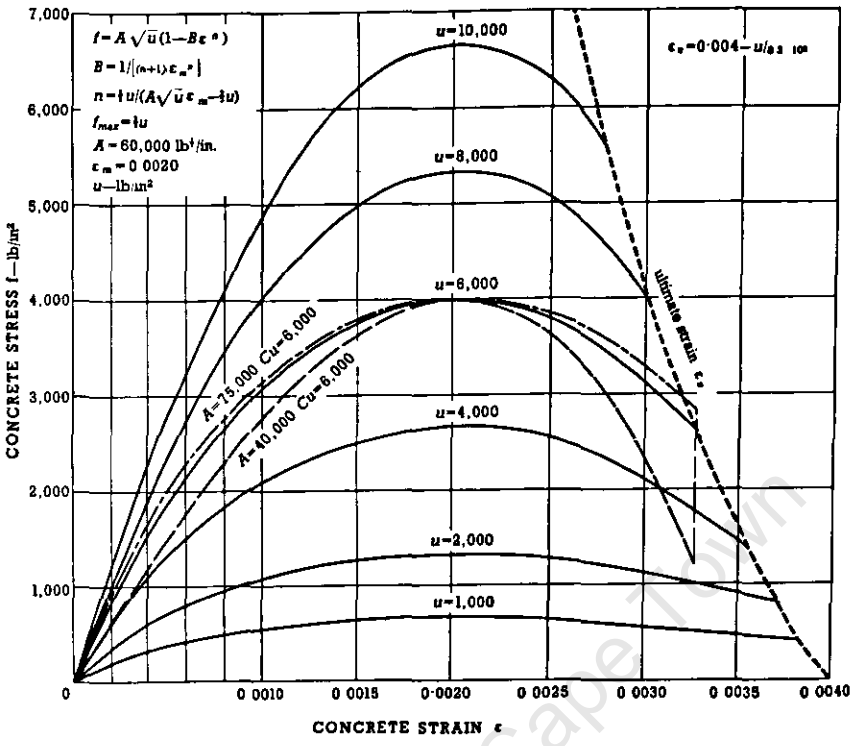

Figure 5

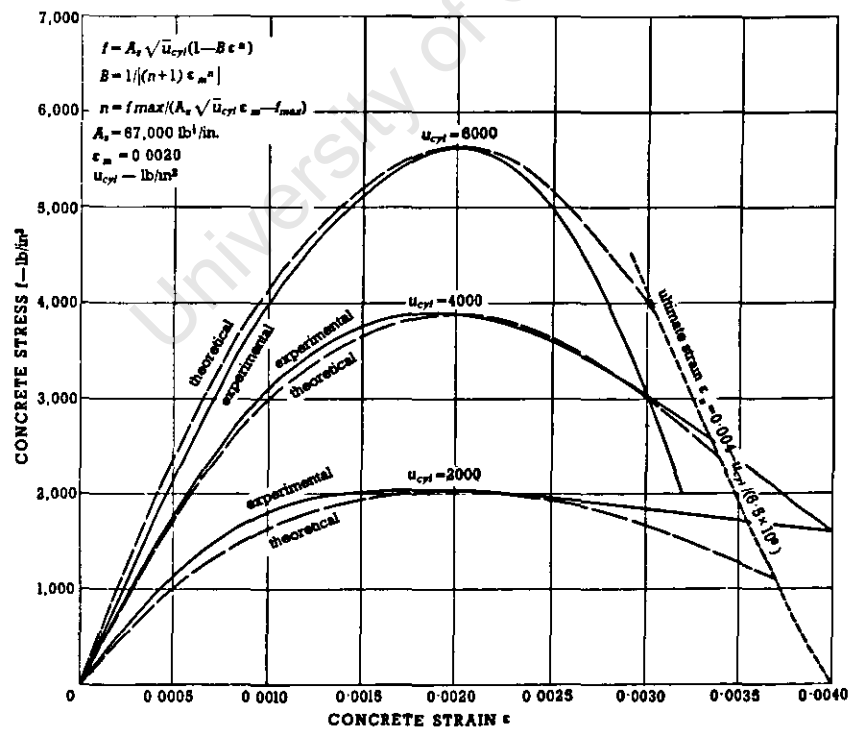

Figure 6

as well as the value of ε_m. Although the author lacks the experimental data, it may be possible to express ε_m as a function of parameters such as the cube strength and the aggregate strength.

The stress-strain function would apply only for a continuous rate of loading of the order of 0·001 strain/min. The complexity of the behaviour of concrete with time, owing to its peculiar mechanical-rheological properties, requires more fundamental research in order to expand the function for general application.

Application of the function to flexural theory

It is generally accepted that compressive strain of concrete in flexure conforms very closely to a linear

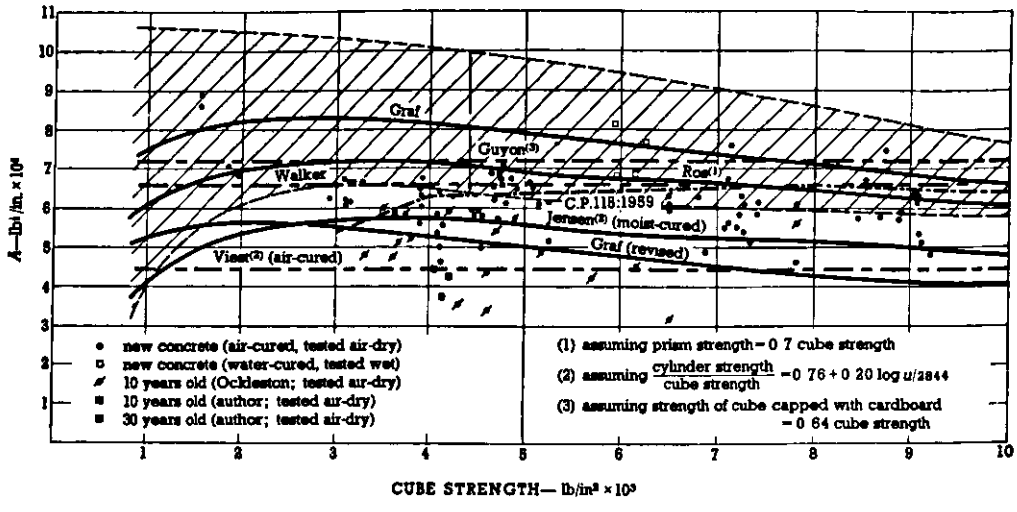

Figure 4

Expansion of the stress function for prisms in terms of known parameters

The author has found that the stress function given in equation 1 corresponds closely with test results if $\varphi(\varepsilon)$ is expressed in the form $B\varepsilon^n$. As discussed above, E_c can be equated with $A\sqrt{u}$. The function therefore becomes

$$f = A\sqrt{u}(1-B\varepsilon^n)\varepsilon \quad \ldots\ldots\ldots\ldots\ldots (2)$$

To establish the values of the parameters B and n, the concept given above in (2) can be utilized.

Therefore $df/d\varepsilon = A\sqrt{u}[1 - (n+1)B\varepsilon^n] = 0$ when $\varepsilon = \varepsilon_m$ where ε_m is the strain at peak stress f_{max}.

Therefore $$B = \frac{1}{(n+1)\,\varepsilon_m{}^n}$$

also $$f_{max} = A\sqrt{u}(1-B\varepsilon_m{}^n)\varepsilon_m$$

Therefore $$\tfrac{2}{3}u = A\sqrt{u}\left[1 - \frac{1}{(n+1)}\right]\varepsilon_m$$

and $$n = \frac{\tfrac{2}{3}u}{A\sqrt{u}\varepsilon_m - \tfrac{2}{3}u}$$

where $\varepsilon_m = 0{\cdot}0020$ for a rate of loading approximating to 0·001 strain/min. This value of ε_m has been found to be fairly constant for the concrete strengths normally used. The family of curves represented by equation 2 for $A = 60{,}000$ lb$^{\frac{1}{2}}$/in. and various values of u are illustrated in Figure 5. Curves for $A = 75{,}000$ and 40,000 lb$^{\frac{1}{2}}$/in. at $u = 6{,}000$ lb/in^2 are also given.

Ultimate strain

Although there is a wide divergence of opinion as to the ultimate strain attained by a prism before disintegration or rupture occurs, the indications are that it depends primarily on the rate of loading and the cube strength. Concretes with low strength disintegrate at a higher strain so that the stress-strain curves terminate approximately as indicated in Figure 5. The termination line could probably be expressed as a function of cube strength and rate of loading, but may also depend on the curing and exposure. For purposes of analysis the ultimate strain can be assumed to approximate to $\varepsilon_u = 0{\cdot}004 - u/(8{\cdot}3\times10^6)$ which is derived from a similar empirical function developed by Hognestad, Hanson and McHenry[3] in terms of the cylinder strength by assuming that $u = u_{cyl}/0{\cdot}78$.

Comparison of curves with experimental values

The theoretical curves agree remarkably well in shape with the results of a statistical study made by Kriz and Lee[1] of the concrete stress-strain curves obtained experimentally by Hognestad, Hanson and McHenry[3]. Their curves are, however, based on tests done in flexure and on concentrically loaded cylinders and not prisms so that the ratio of peak stress to cylinder strength is different. The stress-strain function can be expressed in terms of cylinder strength in the form

$$f = A_s\sqrt{u_{cyl}}(1 - B\varepsilon^n)\varepsilon \quad \ldots\ldots\ldots (3)$$

where $A_s = \dfrac{60{,}000}{\sqrt{0{\cdot}8}} = 67{,}000$ lb$^{\frac{1}{2}}$/in.

u_{cyl} = cylinder strength in lb/in^2

$$B = \frac{1}{(n+1)\,\varepsilon_m{}^n} \text{ and } n = \frac{f_{max}}{A_s\sqrt{u_{cyl}}\varepsilon_m - f_{max}}$$

where f_{max} depends on the cylinder strength and usually exceeds $0{\cdot}90u_{cyl}$. For comparison this theoretical function has been calculated for strengths corresponding with the above-mentioned statistical curves. The superimposed curves are illustrated in Figure 6. The experimental values of f_{max} have been adopted.

Hognestad, Hanson and McHenry found a striking similarity between the results of the flexural and the cylinder stress-strain curves.

For concretes of higher strength the aggregate is increasingly more important than the cement paste and the function would probably have to be amended

APPENDIX II - 1

NOTATION OF BOOK II

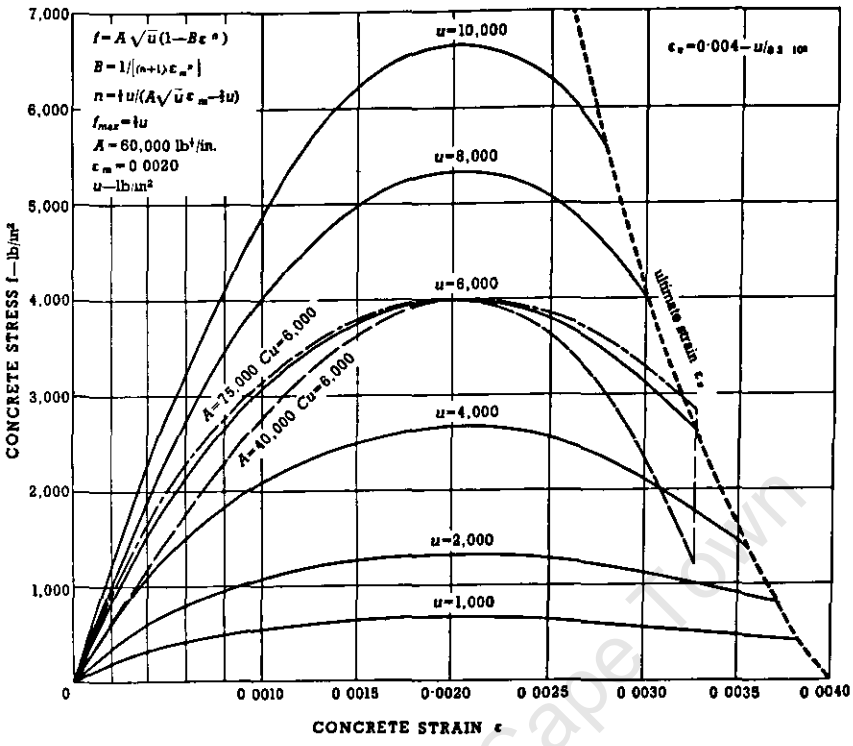

Figure 5

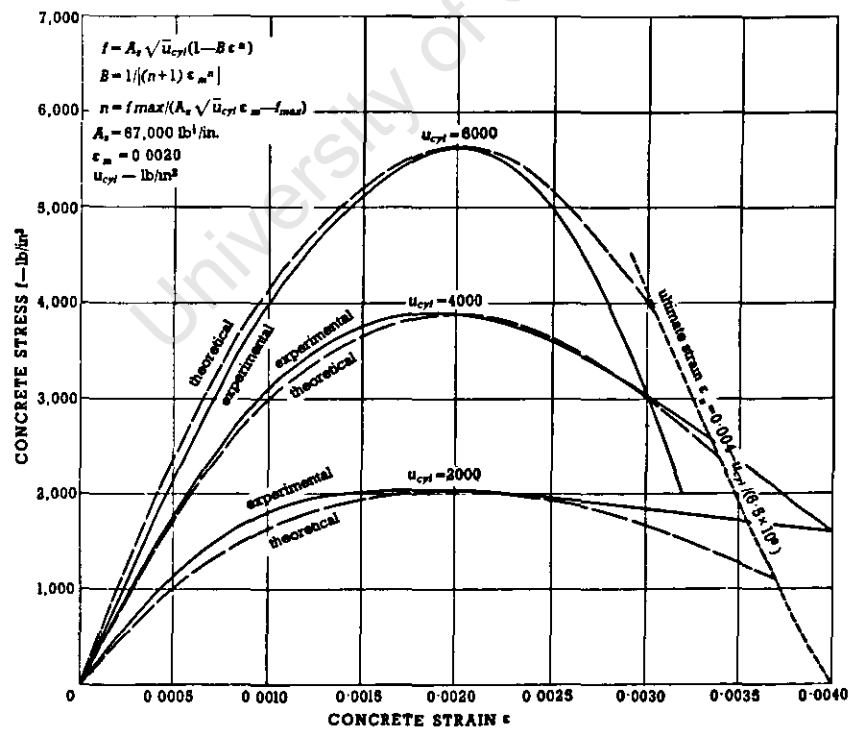

Figure 6

as well as the value of ε_m. Although the author lacks the experimental data, it may be possible to express ε_m as a function of parameters such as the cube strength and the aggregate strength.

The stress-strain function would apply only for a continuous rate of loading of the order of 0·001 strain/min. The complexity of the behaviour of concrete with time, owing to its peculiar mechanical-rheological properties, requires more fundamental research in order to expand the function for general application.

Application of the function to flexural theory

It is generally accepted that compressive strain of concrete in flexure conforms very closely to a linear

B O O K III

ARCH ACTION IN REINFORCED CONCRETE FLOOR SLABS

ACKNOWLEDGEMENTS

The author carried out this work on a part-time basis and its completion could not have been possible without much assistance from many sources for which he is greatly indebted.

He wishes to acknowledge the assistance received from the South African Council for Scientific and Industrial Research in the form of research grants for payment of assistants and running expenses, for the loan of instruments and for undertaking the publication of this work. He wishes to express his appreciation to Prof. R.G. Robertson, of the Department of Civil Engineering at the University of Cape Town who has in many ways assisted the author and who together with Mr. D.J. McCaw of his department sacrificed valuable time in order to participate in the Alliance House tests. The author also wishes to thank the other members on the staff of the Civil Engineering Department and students who assisted with the laboratory work.

The Allied Building Society is thanked for permitting the tests on the Old Alliance House and the co-operation of the demolition contractors, Messrs. Clifford Harris (Pty.) Ltd., is duly acknowledged.

ARCH ACTION IN CONCRETE SLABS

SYNOPSIS

The author summarizes the historical background to the discovery of arching or dome-action in concrete slabs and briefly discusses progress made in research in this field.

The basic principles are enumerated and the nature of the problems involved in developing a theory of arching are described. Alternative approaches are discussed and an empirical theory, developed by the author from a statistical analysis of full scale and laboratory tests, is explained.

A description of these tests and an analysis of the results clearly demonstrates a consistent pattern in the behaviour of slabs which comply with the conditions which are necessary for arch action to occur. Although the problem is extremely complex the theory as developed appears to give reasonably accurate predictions of the ultimate load-carrying capacity in certain cases.

The paper is concluded by a discussion of the limitations of the theory and the probable advantages of an extended knowledge which will require additional research.

PART I

1.1 INTRODUCTION

All accepted theories of the strength of reinforced concrete slabs including both elastic and ultimate load theories, such as Johansen's yield-line theory, are based on the assumption that slabs behave as plates and that the effects of so-called secondary extensional forces are negligible. During the last decade, however, there have been various reports of full scale tests on slabs in which the ultimate loads greatly exceeded the predictions of the yield-line theory, in some cases by factors in excess of 3.0. This necessitated serious reconsideration of the basic assumptions and has resulted in the development of the theory of arching or dome action in slabs.

1.2 HISTORICAL BACKGROUND

Engineers have been aware of the phenomenon of "arching" in beams, walls and thick slabs for a long time. A beam restrained against movement at its ends can in a sense be considered to be a flat arch and it was considered logical to think in terms of compressive forces acting along an arch profile contained within the beam dimensions. There are many references to the phenomenon dating back several decades[1]. The so-called discontinuity in the behaviour of a flat arch at the limit when it becomes a prismatic beam served furthermore to cloud the issue. In fact no such discontinuity exists if secondary forces and deformations are properly accounted for.

The circumferential or Smulski (S.M.I.) system of reinforcing for flat slabs[2] developed and patented by Edward Smulski before 1920 relied on a system of compressive forces acting within rings of reinforcement and is probably the first attempt to utilize arching forces in slabs. Although the system required approximately 25% less reinforcement than the two-way or four-way system it does not appear to have found favour.

3/ The ...

The facts appear to be different as regards arching in concrete slabs of the dimensions normally used in practice. Although there had been various reports in the past[3] of tests on what were relatively thin normally reinforced concrete slabs in which unexpectedly high ultimate loads were attained, no satisfactory explanations were forthcoming. The discrepancies found between theory and test results were usually ascribed to strain-hardening of the reinforcement and positive membrane action or the so-called "catenary" effect, but these phenomena provided no satisfactory explanation.

It was with the advent of prestressed concrete runways that the phenomenon attracted the attention of Freyssinet as a result of tests carried out on a trial length of runway for the Orly Airport in 1945[4]. Similar results were obtained by Guyon when testing prestressed concrete deck slabs for bridges. He has described[5] in great detail the various stages in the behaviour of continuous prestressed concrete slabs subjected to concentrated transverse loading, as revealed by tests to failure. He suggests practical rules for designing such slabs to resist point loads, taking into account the resistance provided by arch action. This work has been incorporated by M. Guyon in Volume II of his text-book on Prestressed Concrete[6] published during 1960.

The tests carried out on the Old Dental Hospital Building in Johannesburg prior to demolition in 1952 lead to the recognition of the phenomenon in normally reinforced concrete and demonstrated the great value of full scale tests to destruction. In tests on both the South stairway[7] and the two-way spanning slabs[8] the ultimate load exceeded the prediction of Johansen's yield-line theory by factors of the order of 3.0. The deflection behaviour of the stairs was such as to lead to the conclusion that arching action was taking place. During tests to destruction on the lower flight the intermediate landing deflected downwards initially,

4/but ...

but after the flight had developed cracks it deflected upwards as a result of the thrust action of the arching forces. Ockleston has shown[9] that arching forces can account for the high ultimate load of the two-way spanning slabs tested by him.

Arch action has also been observed in brickwork panels[10] subjected to transverse loading and has been the subject of experimental investigations from which an approximate theory based on idealized elasto-plastic assumptions has been developed by McDowell, McKee and Sevin.[11] [12]

In co-operation with Prof. R.C. Robertson and Mr. D.J. McCaw of the University of Cape Town, the author carried out tests[13] to destruction on fifty two-way spanning panels of the old "Alliance House", an eight-storey reinforced concrete framed building in Cape Town, prior to its demolition towards the end of 1957. In these tests which are described in more detail later, vertical deflections at various positions on the slab panels were recorded for increments of loading up to total failure as well as the corresponding horizontal deflections and rotations at the boundaries. These tests were probably the first in which such readings were taken and clearly illustrated the nature and importance of arch action and provided an unique opportunity for analysis. As a first step in the analysis, tests were carried out in the laboratories of the Civil Engineering Department of the University of Cape Town on both one-way and two-way model slab panels. The boundary restraints necessary for the simulation of arch action were provided by specially designed equipment.

From the results of these full scale and laboratory tests an empirical-phenomenological theory of arching for certain types of normally reinforced concrete slabs has been developed by the author. Although no experimental work has been done by the author on prestressed concrete slabs he has attempted to indicate a line of approach in order to develop a more general theory.

5/ Various ...

Various research workers have been studying the problem in recent years and R.H. Wood devotes a chapter of a recent text-book[14] to the phenomenon. He prefers to retain the plate analogy instead of the concept of arching and develops instead the idea of enhanced bending resistance due to a change in the yield criterion. His approach basically amounts to an extension of rigid-plastic plate theory and a solution for a clamped circular slab is developed. Wood points out "that the results obtained must be treated as the idealized results of plastic theories, and will have to be modified in the light of test results to account for neglected elastic strains and instability." This so-called instability which is not predicted by this theory arises due to his refusal to accept the arch action analogy and necessitates the introduction of reduction factors. The author doubts the correctness of describing the sudden violent failure as a buckling phenomenon.

D.L. Marriott[15] carried out tests on unreinforced square slab panels and one-way spanning slab elements and developed an idealized elasto-plastic theory for one-way spanning and square slabs with an empirical extension thereto for rectangular slabs. In order to develop the theory many simplifying assumptions are made which do not necessarily correspond with reality. Due to the implicit relationship of the equations developed solutions can only be found by successive approximations which process requires forced convergence due to the fact that the equations are not well conditioned. In spite of the above-mentioned complexities the theory does not correspond well with the practical results and Marriott concludes that the true stress-strain curve for concrete should be taken into account.

All the above-mentioned theories assume absolute rigidity at the perimeter supports, a condition that would rarely exist in practice. An approximate theory for one-way spanning slab elements to explain the effect of horizontal spread has been suggested by Robertson-Liebenberg-McCaw[13] and this was

subsequently .../6

subsequently extended by the author for an idealized elasto-plastic slab as described in section 2.2

K.P. Christiansen[16] has developed a theory for one-way spanning slab elements or beams which is basically similar to the above-mentioned theory except that the basic equations differ and are in the author's opinion[17] not quite correct.

1.3 THE GENERAL PRINCIPLES OF ARCH ACTION

The general principles of arching or dome action in plane slabs can be formulated as follows:

Arch action in plane slabs under transverse loading can be defined as the resistance developed by a system of compressive forces distributed in such a manner as to resemble the action of an arch or dome, as indicated in figure 1, and generated in the slab after the development of some form of articulation, such as localised cracking, by geometric deformation of the slab elements bounded by these lines of articulation. These compressive forces, which are superimposed on the pure bending forces, are balanced either by external forces at the support boundaries which are induced by reaction against "abutments" or by peripheral tensile forces. Tensile forces and the complimentary compressive forces acting in the same vertical plane in the elements of the slab itself, whether due to normal reinforcement or prestressing cables cannot be considered to be part of the arching system as they belong to the internal system of bending forces whether of a simple or of a complex nature. The basic requirements for arching action to occur are therefore that one or more degrees of articulation should develop, that there should be external or peripheral restraint against horizontal spread of the support boundaries and that deformation and the resultant change of geometry of the slab elements should induce compressive forces which are arched in the opposite direction to the loading.

Arching action cannot occur in continuous thin slabs made of a material of which stress strain relationships in

compression and tension are similar. If the boundaries of a slab constructed of such a material are restrained, deflection will cause extension of the central plane and result in the development of tensile membrane stresses. This action is called the catenary effect.

Arch action can however occur in a plane slab made of such material if an artificial articulation or cut or a reduction in section is provided. One and three degrees of articulation are illustrated in figures 2 and 3 respectively. The approximate stress distribution at various sections are given together with the profile of the discontinous neutral axis or plane. Only two-dimensional cases are illustrated but the same basic arguments will apply in the case of two-way spanning slabs. The mechanics of arching is clearly illustrated by these diagrams. It is essential that the diagonal lines AC and CB should be inclined upwards and as long as this is the case and sufficient restraint is provided at the supports, arch action can occur. In the "ideal" case to be dealt with later the action will disappear when AC and CB become horizontal and the load on a one-way spanning element will have attained its maximum value at a central deflection of 0.423d. A perspex model with artificial cuts along the "yield lines" is illustrated in figure 4. If the compressive modulus of elasticity of the material should exceed the tensile value, articulation is not essential for arch action to occur.

An important principle regarding the pattern and number of articulations can be formulated, viz. that no matter how many articulations are developed the system remains stable until the critical deflection has been attained. Even the application of a different mode of loading, including the reversal of part of the loading at any stage prior to failure, will not upset the stability. The reason for this is that the articulations

8/ differ ...

differ from the usual concept of a pin-joint in that they are uni-directional. Any reversal of the rotation at such an articulation will tend to close the crack whereupon the articulating action at that position will cease. Any attempts to compare arching collapse with buckling collapse are accordingly fallacious. The suddeness of the failure that does occur at peak load is not unlike normal crushing failure if the load-deformation characteristics are compared.

The cases dealt with above were provided with artificial articulations which approximate to the "ideal" because the contact areas between the elements are small and the forces are concentrated at the extreme fibres. Arch action can, however, also occur in materials which develop "articulation zones". Reinforced concrete is typical of this class and may develop well defined single cracks with a relatively small contact area or a zone of smaller cracks depending mainly on the percentage of reinforcement, the degree of restraint and the mode of loading. The arching efficiency is directly related to these factors.

Until cracking has occurred the behaviour of concrete approximates to that of the material described above and no arching can occur. Laboratory tests however indicate that arch action commences before any cracks become visible, apparently due to the formation of micro-cracks. It is consequently not purely an ultimate phenomenon.

The various stages of behaviour of a reinforced concrete slab subjected to a gradually increasing transverse loading and complying with the conditions for arch action to occur can be summarised as follows :

Initially bending action of an almost purely elastic nature will resist the load with concrete and steel resisting tensile forces at all sections until a second stage is reached,

9/ when as ...

when as a result of micro-cracking and the formation of one or more "articulations", the bending forces are supplemented by gradually increasing arching forces. The nature of the bending action will alter and after considerable deformation, with visible cracking followed by the yielding of the steel reinforcement a third stage is reached with the formation of a virtually new structure not unlike an arch or dome, "articulated" at the major crack lines with inclined thrust forces acting in the intermediate slab elements as illustrated in figure 1. Thereafter the bending resistance remains approximately constant over a large deflection range and provided premature failure due to crushing or shearing of the concrete does not occur, the arching resistance increases until a critical stage is reached at which the arching mechanism collapses. After collapse of the arching and bending systems the slab may still be capable of resisting load by virtue of a "catenary" action of the reinforcement. The various stages as applicable to a typical one-way spanning slab element are illustrated graphically in figure 5.

In connection with the behaviour mode described above, it is interesting to consider what happens at the instant a crack develops. In the case of a reinforced concrete slab without horizontal restraint a sudden increase in deflection occurs and some energy is dissipated mainly in the form of heat energy which is non-recoverable while the steel absorbs additional energy which is recoverable if yield has not yet occurred so that portion of the sudden increment is permanent provided the direction of the total force is not reversed. In the case of a slab which develops arch action the sudden increase is very much reduced due to the fact that the release of tensile strain energy is partially converted to compressive strain energy.

Provided that premature crushing or shear failure does not occur, the arching action reaches its peak value at a

10/ deflection . ...

deflection, depending on various factors to be dealt with later, which is usually equal in magnitude to about 1/4 the slab depth for one-way spanning slabs. If this peak value is attained after yielding of the steel, the total maximum load-bearing capacity will equal the sum of the maximum bending and arching resistances. In slabs with large span/depth ratios the arching peak which will be relatively small may occur prior to yielding of the reinforcement in which case the two peak values cannot be simply added.

It appears that the crack pattern is primarily determined by the distribution of bending forces. The crack pattern will in turn determine the nature of the arching action which will also depend on

(a) the shape and dimensions of the slab,

(b) the restraint at the boundaries against horizontal spread and rotation,

(c) the mode of loading,

(d) the structural properties of the concrete and

(e) the percentage steel reinforcement and its distribution.

The structural properties of the concrete are in turn affected by various factors to be briefly discussed in the next section.

In most of the theories of arch action suggested in connection with reinforced and prestressed concrete and brickwork panels referred to previously the assumption is made that the abutments are perfectly rigid. The full scale tests referred to above indicated that this condition would rarely occur in practice. The actual spread measured at the level of the horizontal "abutment" reactions was of the same order but usually exceeded the "rib-shortening" of the slab elements. The "spread" was principally caused by (a) rotation at the supports about a centre of rotation at a different

11/ level ...

level, (b) radial compression of the surrounding slabs similar to the "rib-shortening" of the elements of the slab panel itself, accompanied by circumferential extension and by (c) bending deformation in the plane of the slabs acting as horizontal girders.

Although this spread may cause a considerable reduction of the compressive forces, the arching resistance may still be significant. Several of the slabs tested resisted a load more than three times in excess of the ultimate load predicted by the yield-line method.

The failure of arching action can occur due to (a) the deflection exceeding the critical deflection at which the maximum load carrying capacity due to arching action is developed, i.e. collapse of the arching mechanism due to yielding of the supporting abutments and/or "rib-shortening" of the slab elements, (b) crushing failure of the concrete and (c) shear failure of the concrete.

The same arguments would apply to prestressed concrete, but here the commencement of arching action would occur at a later stage as the formation of a crack pattern and the development of the necessary articulations would be delayed by the initial prestress.

1.4 THE PROBLEMS INVOLVED IN DEVELOPING A THEORY OF ARCHING IN PLANE REINFORCED CONCRETE SLABS

Ultimate theories which take only the bending resistance of slabs into account, such as Johansen's yield-line theory, require no accurate knowledge of the deformation of the slab elements on account of the fact that the maximum moment of resistance attained at the yield point of the steel remains approximately constant over a large deflection range, and allows the maximum moments to develop over almost the full extent of the yield lines corresponding closely to the

conditions assumed in the rigid-plastic theory. The cube strength of the concrete and the yield strength of the steel are the only material properties which are required to be known and the analytical problem is largely confined to predetermining the crack pattern, which unfortunately cannot be readily established in all cases. An accurate theory of arching, on the other hand, requires a far greater knowledge of the properties of concrete and of the boundary conditions which will determine the distribution and magnitude of the thrust forces and requires knowledge of the crack pattern as a starting point.

The complexity of concrete as a structural material due to its heterogenous composition and the resultant mechanical-rheological behaviour precludes the development of a comprehensive and accurate theory of arching from first principles. Unfortunately arch action is highly sensitive to deformations so that an accurate stress-strain function is an essential requirement. The author has succeeded in developing a stress-strain function[14] for concrete subjected to short-term non-repetitive uni-axial loading which agrees well with experimental work on prisms and cylinders but more fundamental research into stress-strain relationships and especially into methods of determining crack patterns and of estimating the influence of the past history of the concrete and the effects of long term and repetitive loading are required before anything more than approximate theories can be developed.

Apart from the complexity of concrete as a material, the problem of arching in slabs is in itself extremely complex and difficult to solve even for idealized materials. Idealized rigid-plastic or elasto-plastic theories do not however produce satisfactory results. Even these over-simplified theories in most cases yield extremely complex

equations which require further simplifying assumptions as regards boundary conditions and the distribution of forces. On account of the implicit nature of the equations based on the elasto-plastic theory, solutions can only be found by indirect methods such as the method of successive approximations. Convergence is invariably slow and must be forced artificially. Although elasto-plastic theory is more complex than rigid-plastic theory, the former is for obvious reasons in better agreement with the actual behaviour of slabs but both theories require empirical factors to correct for the inaccurate assumptions made in order to obtain solutions and for various secondary effects not incorporated in the basic theory.

The inaccuracy in spite of the complexity of theories such as the above makes it appear extremely doubtful whether any satisfactory progress can at this stage be made along these lines.

After examining various channels the author has come to the conclusion that the most practical procedure at present is an empirical-phenomenological approach as is adopted in parts 2 and 3.

1.5 THE DEVELOPMENT OF A STRESS-STRAIN FUNCTION FOR THE EMPIRICAL-PHENOMENOLOGICAL THEORY

As indicated above the incorporation of an accurate stress-strain function in arching theory is essential if progress is to be made. The function developed by the author and described elsewhere[18] is not extremely complicated but due to its uni-axial nature and the complexities in the theory of arching it cannot be applied by direct analysis to formulate a theory using an element as starting point.

As a first step in developing a theory the author has accordingly used an approach which is based on the same empirical-phenomenological principles that were used to

14/ develop ...

develop the above-mentioned stress-strain function, but is expressed in terms of arbitrary concepts of stress and strain.

In order to reduce the complexity of the problem a elemental uni-directional strip of slab was used as starting point and its behaviour established by experiment for a large range of conditions in which arch action was simulated. The basis of this analysis is the so-called Ideal Arching Slab element which is indicated in figure 6 and is used to define terms such as "arching stress" and "arching strain" as developed in Part 3 and from which the so-called arching stress-strain function was developed.

This function bears a marked similarity to the stress-strain function developed for prisms and is based on the same concepts. These have been described elsewhere[18] but can be briefly summarized as follows :

(a) Concrete is a complex material with solid, semi-solid and liquid phases which impart to it a peculiar mechanical-rheological behaviour.

(b) Although the solid components are basically elastic, the composite material does not deform linearly even under short term stress application.

(c) The above-mentioned "deviation" from the linear law can be partly accounted for by a gradual process of disintegration commencing in the form of micro cracks which eventually initiate internal splitting on minute sections scattered throughout the concrete so that a progressively smaller number of uncracked particles is called upon to resist the load until the peak stress is attained to be followed by the peculiar descending branch of the stress-strain curve and eventually complete disintegration.

(d) The above-mentioned micro-cracks are often present before application of stress, having been caused

by shrinkage forces and which explains the low initial modulus often found in air-cured concretes. The existence of such micro-cracks has, subsequent to the development of this theory which was at that stage based on conjecture, been established by electron microscope[19] analysis.

(e) Tests indicate that the characteristics of the stress-strain curve of concrete can be expressed in a simple way as functions of the crushing strength or the strain. The initial modulus of elasticity for moderate rates of loading is very nearly proportional to the square root of the crushing strength, the constant of proportionality depending on the maturity or age and environment in terms of temperature and humidity. The deviation from this initial linear relationship (See figure 7) can be expressed as a function of strain in the form

$$f_c = E_c\left(1-\phi(\epsilon)\right)\epsilon$$

The peak stress is attained at a strain which is approximately constant irrespective of the crushing strength and apparently depends only on the rate of loading. Complete disintegration occurs at a strain which for any particular rate of loading can be expressed as a function of the crushing strength.

The above empirical relations were used to develop the following stress-strain function for concrete prisms as described in the above-mentioned reference.

$$f_c = A\sqrt{u}\left[1-B\epsilon^n\right]\epsilon \qquad \ldots\ldots (1)$$

where f_c = mean stress on cross-section of prism in lb. per in^2

A = constant of proportionality

$\doteq$ 75,000 lb$^{\frac{1}{2}}$/in. for water-cured concretes tested wet

A = 60,000 $lb^{\frac{1}{2}}/in.$ for air-cured concretes (dry atmosphere) less than 1 year old tested air-dry decreasing to 40,000 $lb^{\frac{1}{2}}/in.$ for air-cured concretes (dry atmosphere) 10 years old tested air-dry.

u = cube strength in lb. per in^2.

$$B = \frac{1}{(n+1)\varepsilon_m^n}$$

ε = strain

$$n = \frac{\frac{2}{3}u}{A\sqrt{u}\,\varepsilon_m - \frac{2}{3}u}$$

ε_m = 0.0020 for moderate rates of loading (0.001 $\pm$ strain/min.)

This function could probably be extended along similar lines to include the effects of time, rate of loading and previous loading cycles, but the experimental data available at present are insufficient to establish the necessary relationships.

1.6 THE DETERMINATION OF THE CRACK PATTERN

In order to develop a theory of arching it is necessary to be able to predict the development and pattern of cracks at the various stages of loading. For the reasons already enumerated this cannot be accomplished with great accuracy and simplifying assumptions are accordingly made as follows:

(a) It is assumed that the crack pattern is caused entirely by bending forces and that arching forces are secondary effects which have no influence on the pattern other than reducing the size of the cracks and the rate of relative rotation of adjacent elements at a crack.

(b) It is furthermore assumed that the cracks are well defined and can be represented by the intersection of two plane sections. The existence in practice of micro-cracks

or a series of closely spaced cracks in heavily reinforced slabs to form a crack zone, is allowed for in the empirical theory by the incorporation of efficiency parameters.

As regards the determination of the configuration of the cracks the procedures developed for yield-line theories[14, 1 will be adopted and it will for convenience be assumed that this applies even in the early stages of micro-cracking. It naturally follows that arching theory is therefore an extension of yield-line theory and will be limited to those cases for which the latter theory has produced solutions until improved methods of crack prediction are developed.

1.7 THE COMPATIBILITY EQUATION

It follows from the nature of arch action that the equations expressing the compatibility of horizontal spread of the slab panel and the corresponding deformations of the perimeter elements at the slab boundaries must be the starting point of any theory of arching. There are various ways of formulating these equations and since the problem is a three-dimensional one, any suitable perimetral axis within the slab section can be selected as a boundary such as (i) the middle axis (ii) the neutral axis of the cracked section (iii) the line of intersection of the resultant compressive force and the slab cross-section at the perimeter, or (iv) the extreme compressive fibre on the slab soffit. The relative positions of these boundaries at a particular section are illustrated in fig. 8. For idealized theories where the assumption is made that no rotation of the external elements takes place at the perimeter there is little to choose between these methods.

In method (i) the equation states that the deformation of the middle axis at the perimeter (Δ_p) equals the extension of the middle plane due to the opening of cracks (Δ_c) less the shortening effect of arch compression (Δ_s) and membrane deflection (Δ_ω), i.e.

$$\Delta_p = \Delta_c - \Delta_s - \Delta_\omega \quad \ldots\ldots\ldots (2)$$

18/ In method ..

In method (ii) the equation states that Δ_p equals the spread of the perimetral neutral axis Δ_θ due to rotation of the slab elements less the shortening effect of arch compression and bending (Δ_s) and (Δ_b) i.e.

$$\Delta_p = \Delta_\theta - \Delta_s - \Delta_b \quad \ldots (3)$$

Methods (iii) and (iv) are similar to (ii) except that the magnitudes of the terms differ.

Rotation of the external elements at the perimeter complicates the issue and since the axis of rotation does not necessarily coincide with either the middle axis or neutral axis, Δ_p may be increased by a component due to rotation.

In the approximate equation originally developed by Robertson-Liebenberg-McCaw[13] to demonstrate the basic principles of arch action, method (iii) was used. In the semi-analytical theory developed in 2.2 method (i) is used. In the empirical theory developed later method (iv) is used for convenience as it has a special significance and the quantities involved can be determined by direct measurement.

158.A

*

It is not however the intention to discard this theory as an empirical development thereof in a simplified form may produce good results, as is stated on page 214.

PART 2

THE THEORY OF ARCHING IN ONE-WAY SPANNING CONCRETE SLAB ELEMENTS OR BEAMS

2.1 GENERAL

Although the arching phenomenon in slabs is mostly associated with two-way spanning slabs, the problem is greatly simplified by studying the behaviour of one-way spanning elements or beams. Even if concrete is assumed to have the properties of an idealized elasto-plastic material it is necessary on account of the complexity of the problem to make further simplifying approximations in order to obtain a solution by analytical means. A semi-analytical theory based on these assumptions was developed by the author, but it was not pursued* due to its inaccuracy in spite of great complexity. An extension of rigid-plastic theory as proposed by Wood[14] is simpler but does not in the author's opinion give a sufficiently accurate reflection of the actual behaviour of reinforced concrete slabs. The empirical-phenomenological theory developed below is favoured as it is more realistic and the various arbitrary concepts formulated can be established by direct measurement which makes it eminently suitable for empirical development. It does not, however, yield direct solutions and successive approximations or graphical methods have to be employed but these are not very tedious. Certain fortuitous relationships have greatly increased the value of this theory and facilitated its extension to two-way spanning slab panels.

2.2 AN EMPIRICAL-PHENOMENOLOGICAL THEORY OF ARCHING IN ONE-WAY SPANNING CONCRETE SLAB ELEMENTS OR BEAMS

2.2.1 The Ideal Arching Slab

In order to establish the behaviour pattern of arch action in reinforced concrete slabs the author has used the concept of the Ideal Arching Slab in

20/ relation ...

relation to the actual slab. The Ideal Arching Slab is defined as a slab with perfectly defined cracks corresponding with the theoretical positions of the cracks in the prototype as determined by yield-line theory and with contact at these cracks confined to the extreme compressive fibres as illustrated in fig. 6. For the purpose of this analogy the actual behaviour of the Ideal Arching Slab in terms of the material properties and its dimensions need not be investigated as it is more convenient to establish arbitrary concepts which allow a more direct analysis.

For a slab with three articulations as illustrated in fig. 6 the unrestrained spread Δ_u can be expressed approximately in terms of the vertical deflection ω_c as C as follows :-

$$\Delta_u \doteq \int_0^{\omega_c} \frac{d-y}{x}\,dy + \int_0^{\omega_c} \frac{d-y}{L-x}\,dy$$

$$= \frac{\omega_c L \left(d - \frac{\omega_c}{2}\right)}{x(L-x)} \qquad \ldots\ (4)$$

It will be assumed that this equation is precisely correct for the purposes of this theory, thereby rigidly defining Δ_u .

For a restrained slab the actual spread Δ_a will be less than the unrestrained spread as defined above by an amount Δ_r , i.e.

$$\Delta_a = \Delta_u - \Delta_r \qquad \ldots\ (5)$$

where Δ_r can by analogy be called the horizontal component of the rib-shortening effect.

As in the case of the idealized elasto-plastic slab described in Appendix III - 1 the determination of Δ_r results in implicit functions which require indirect methods for solution. In order to eliminate these procedures we shall arbitrarily define the "arching strain" e_a in terms of the above concepts such that

$$e_a = \frac{\Delta_r}{L} = \frac{\Delta_u - \Delta_a}{L} \qquad \ldots\ (6)$$

This function will serve as the basis of the theory developed below.

If we define "arching stress" f_a in terms of the horizontal component of the arching compressive force: H_a and the gross cross-sectional dimensions such that $f_a = \frac{H_a}{bd}$ we can also formulate the concept of "arching modulus" m_a such that

$$m_a = \frac{f_a}{e_a} = \frac{H_a L}{bd\Delta_r} \doteq \frac{E_i}{2.0} \qquad \ldots\ldots \quad (7)$$

where E_i is the modulus of elasticity of the material of the ideal slab. If the moduli of horizontal restraint at the supports acting at the level of the soffit of the slab are R_A and R_B respectively then

$$H_a = R_s \Delta_a \qquad \ldots\ldots \quad (8)$$

where $R_s = \frac{R_A R_B}{R_A + R_B}$ is the total modulus of the horizontal support restraints in force units per unit spread per width b of slab.

We can relate R_s with the properties of the slab by means of the non-dimensional parameter

$$R_F = \frac{R_s L}{m_a bd} \qquad \ldots\ldots \quad (9)$$

which can again be expressed as a function of the ratio

$$R_e = \frac{\Delta_r}{\Delta_u} = \frac{\Delta_u - \Delta_a}{\Delta_u} \qquad \ldots\ldots \quad (10)$$

as follows :-

$$R_F = \frac{R_s L}{m_a bd} = \frac{H_a L}{m_a \Delta_a bd}$$

$$= \frac{\Delta_r}{\Delta_a} = \frac{\Delta_u - \Delta_a}{\Delta_a} = \frac{R_e}{1 - R_e} \qquad \ldots\ldots \quad (11)$$

It will be noted that the factor R_F includes the dimensional properties of the slab, the arching modulus, and the restraint R_s against horizontal spread, whereas R_e is a function of deformation only. If the above-mentioned properties of the slab are known, R_s can accordingly be determined by measurement of the deformation of the slab. The factors R_F and R_e thus provide an indirect method of determining the horizontal

22/ restraint ...

restraint R_s and were applied in the analysis of full-scale tests described in 3.3. Before this could be done however it was necessary to know the arching modulus m_a for any particular case under consideration. The laboratory tests described in 2.3 were carried out with this object in mind.

2.2.2 <u>The Reinforced Concrete Slab in relation to the Ideal Arching Slab</u>

After the formation of cracks a reinforced concrete slab with restraint against horizontal spread at the supports behaves in a manner similar to that of the ideal arching slab when subjected to transverse loading. Contact at the articulations is however not confined to the extreme fibres but extends to the neutral axis. This together with the additional bending induced by the support moments and the localized plastic deformation at the articulations reduces the arching efficiency.

In the case of a reinforced concrete slab it is convenient to separate the resistance due to bending forces from that due to arching forces and this can readily be done at the ultimate stage by subdividing the total compressive force C_T acting in the concrete into C_s and C_a where C_s is the compression due to bending at the section and $C_a = H_a$ is the compression due to arch action.

If the compressive stress block (fig. 11) is subdivided in such a manner that C_s acts in the outer portion then the moment of resistance due to bending $M_B = C_s l_a$, where l_a is the lever arm, is identical to the total moment if arching forces were absent. The resistance due to C_a would then be the increase in resistance due to arching.

The depths of the neutral axis at any of the major cracks and the positions of the resultant forces C_a

23/ and ...

and C_s depend on the shape of the compressive "stress block". If we equate the actual stress distribution to that of an equivalent uniform stress βu (where u is the cube strength) applied over a depth γd_n where d_n is the depth of the neutral axis we have :-

$$d_{nA} = \frac{A_{SA} f_y + H_a}{\beta \gamma b u} \quad \text{.... (12)}$$

where d_{nA} is the depth of the neutral axis at A,

A_{SA} is the area of tensile mild steel reinforcement per width b at A,

f_y is the yield stress of the steel, and

u is the cube strength of the concrete.

$$l_{aA} = d_1 - \frac{0.5 A_{SA} f_y}{\beta u b} \quad \text{.... (13)}$$

where l_{aA} is the lever arm of the steel at A about C_s, and d_1 is the effective depth of the steel.

$\therefore$ M_B = moment of resistance at A due to bending

$$= C_{SA} l_{aA} = T_A l_{aA} = A_{SA} f_y l_{aA}$$

$$= A_{SA} f_y \left[d_1 - \frac{0.5 A_{SA} f_y}{\beta u b} \right] \quad \text{.... (14)}$$

Also $$d_{aA} = d - \frac{(A_{SA} + A_{sc}) f_y + H_a}{\beta u b} \quad \text{.... (15)}$$

where d_{aA} is the effective depth of slab available for arching between A and C.

Using the yield "stress block" as adopted by the British Code of Practice CP 114 (1957) and as confirmed by recent tests[20] the above parameters

24/ approximate ...

to the following values :-

$$\beta = {}^{2}/_{3}$$

$$\gamma = 0.85$$

These relationships only apply in the ultimate range and vary slightly with cube strength but for the purpose of this theory they will be assumed to apply throughout the loading and empirical corrections will be introduced. Where compressive reinforcement is used these equations can quite simply be adapted and it is convenient to include the compressive steel force in the bending resistance moment. The latter is also assumed to resist the total self weight of the slab.

It will be assumed that the applied loading can be expressed in the form $p = b\eta\phi(x)$ where p, the intensity of load, is a function ϕ of x multiplied by a parameter η which corresponds with a particular stage in the loading. The "shape" of the load diagram is accordingly similar at all stages of loading as the arrangement and ratios of intensities are fixed.

With reference to fig. 10 it can be shown that for a slab with equal mild steel tensile reinforcement at supports and midspan, η_B, the parameter associated with the peak load resisted by bending forces only, can be expressed in terms of the ultimate bending moments per width b at the yield lines (M_B) as follows

$$\eta_B = \frac{2M_B - p_d\frac{bL^2}{8} + \frac{p_d b}{2}\left(\frac{L}{2}-x_c\right)^2}{\frac{bx_c}{L}\int_0^L \phi(x)(L-x)dx - b\int_0^{x_c}\phi(x)(x_c-x)dx} \qquad \ldots(16)$$

where p_d is the self weight per unit area.

For a uniformly distributed loading $p = p_1$, where p_1 is a constant, equation (16) becomes

$$\eta_B = \frac{2M_B - p_d\frac{bL^2}{8}}{p_1\frac{bL^2}{8}} \qquad \ldots (16A)$$

i.e. $M_{fc}^{A} = M_{fc} - M_{fc}^{B}$

$$= M_{fc} - \left(\frac{L-x_c}{L} A_{SA} l_{aA} + \frac{x_c}{L} A_{SB} l_{aB} + A_{Sc} l_{ac}\right) f_y + p_d \frac{bL^2}{8} - \frac{p_d b}{2}\left(\frac{L}{2} - x_c\right)^2$$

$$= M_{fc} - \left\{ \frac{L-x_c}{L} A_{SA}\left(d_1 - \frac{0.5 A_{SA} f_y}{\beta u b}\right) + \frac{x_c}{L} A_{SB}\left(d_1 - \frac{0.5 A_{SB} f_y}{\beta u b}\right) + A_{Sc}\left(d_1 - \frac{0.5 A_{Sc} f_y}{\beta u b}\right)\right\} f_y + p_d \frac{bL^2}{8} - \frac{p_d b}{2}\left(\frac{L}{2} - x_c\right)^2$$

$$= M_{fc} + \frac{f_y^2}{2\beta u b L}\left((L-x_c) A_{SA}^2 + x_c A_{SB}^2 + L A_{Sc}^2\right) - \left(\frac{L-x_c}{L} A_{SA} d_1 + \frac{x_c}{L} A_{SB} d_1 + A_{Sc} d_1\right) f_y + p_d \frac{bL^2}{8} - \frac{p_d b}{2}\left(\frac{L}{2} - x_c\right)^2$$

∴ from 18 a

$$\frac{1}{2\beta}\left\{ \frac{H_a (A_{SA} + A_{Sc}) f_y + H_a^2}{0.5 u b} - \frac{x_c}{L} \cdot H_a \cdot \frac{(A_{SA} - A_{SB})}{u b} f_y + \frac{L-x_c}{u b L} A_{SA}^2 f_y^2 + \frac{x_c}{u b L} \cdot A_{SB}^2 f_y^2 + \frac{A_{Sc}^2 f_y^2}{u b} \right\}$$

$$= H_a (d - \omega_c) - M_{fc} + \left[\frac{L-x_c}{L} A_{SA} + \frac{x_c}{L} A_{SB} + A_{Sc}\right] d_1 f_y - p_d \frac{bL^2}{8} + \frac{p_d b}{2}\left(\frac{L}{2} - x_c\right)^2$$

$$\therefore \alpha = \frac{1}{2\beta}$$

$$= \frac{u b \left\{ H_a (d - \omega_c) - M_{fc} - p_d \frac{bL^2}{8} + \frac{p_d b}{2}\left(\frac{L}{2} - x_c\right)^2 + \left(\frac{L-x_c}{L} A_{SA} + \frac{x_c}{L} A_{SB} + A_{Sc}\right) d_1 f_y \right\}}{2 H_a (A_{SA} + A_{Sc}) f_y + 2 H_a^2 - \frac{x_c}{L} H_a (A_{SA} - A_{SB}) f_y + \frac{L-x_c}{L} A_{SA}^2 f_y^2 + \frac{x_c}{L} A_{SB}^2 f_y^2 + A_{Sc}^2 f_y^2}$$

... (19)

Equation 19 can be used to verify $\alpha = \frac{1}{2\beta}$ (which is the only empirical factor in these equations) by experiment, in which H_a is determined by direct measurement. Using the stress block as assumed in the British Code of Practice CP. 114 (1957), $\alpha = 0.75$. For a central point load P applied to a slab with symmetrical reinforcement

$$\alpha = \frac{u b \left\{ H_a (d - \omega_c) - \frac{PL}{4} - p_d \frac{bL^2}{8} + \left[A_{SA} + A_{Sc}\right] d_1 f_y \right\}}{2 H_a (A_{SA} + A_{Sc}) f_y + 2 H_a^2 + A_{SA}^2 f_y^2 + A_{Sc}^2 f_y^2} \quad \text{...(19a)}$$

27/ An analysis ...

An analysis of 74 tests described later gave a mean value for α which was in close agreement with the above value but the coefficient of variation was 28%. In particular cases the value deviated considerably from the mean as can be seen from Table 1. This is due to the sensitivity of equation 19 rather than the inaccuracy of the parameter as the equation unfortunately includes small differences of large quantities. Conversely it can be shown that the arching load calculated by the theory is not influenced greatly by variations in α, so that $\alpha = 0.75$ is sufficiently accurate for all cases. This was borne out by a statistical analysis of the ratio P_E/P_T which gave a mean value of 0.99, with a coefficient of variation of only 9%.

2.2.3 The "Arching Stress" function for reinforced concrete

It will be obvious after studying Appendix III - 1 that an accurate arching stress function $f_a = \phi_a(\epsilon_a)$ is too complex for analytical solution. It is evident that ϕ_a depends on the slab dimensions, the material properties including the quantity and distribution of steel reinforcement, the type of loading and the boundary restraint. The first series of laboratory tests described in 2.3 were carried out to establish various relationships in order to develop an empirical function which could be of practical application.

There appeared to be a marked similarity between the "arching stress vs. arching strain" curve as indicated in fig. 13 and that of the stress-strain relationship of a prism subjected to uni-axial loading, indicated in fig. 7. A prism stressed along a diagonal would have even a closer relationship. It was accordingly assumed that the arching stress function for a one-way spanning slab element could be formulated along similar lines to that developed in 1.5 in the form

$$f_a = G\sqrt{\mu}\left[1 - D(\epsilon_a)^p\right]\epsilon_a \qquad \ldots\ldots (20)$$

where the parameter G depends on the depth-span ratio, the quality and distribution of steel reinforcement, the type of loading and the end restraint. The parameters D and p correspond with B and n of equation (1) but have different values as f_a and e_a are not true stresses but are based on the arbitrary concepts as defined in 2.2.1.

2.2.4 The deviation of arching strain

The laboratory tests covered a fairly wide range of cases and indicated definite trends. A statistical analysis of the shape of the arching stress vs arching strain curve produced the result illustrated in fig 24. The corresponding histograms together with the relevant statistical values are illustrated in fig. 23. It will be noted that the standard deviations do not greatly exceed that usually obtained for the stress-strain relation of a prism subjected to uni-axial loading.

Similarly as for the function developed in 1.5 it can be shown that

$$D = \frac{1}{(p+1)(e_{ap})^p} \qquad \ldots (21)$$

where e_{ap} is the arching strain at which the peak arching stress is attained.

The statistical analysis (fig. 23) has indicated that e_{ap} approximates to 0.0015.

Insufficient test data are as yet available to relate p with the cube strength and other varisbles. The problem is extremely complex and does not at this stage warrant full consideration. The influence of the cube strength, the depth/span ratio, the reinforcement and the restraint on the deviation from the initial modulus has been disregarded, but the determination of p has been based on a statistical analysis of a large number of tests, as shown in fig. 23.

29/ Assuming ...

Assuming that e_{ap} = 0.0015 and that e_{ad}, the mean deviation of arching strain at peak stress is 0.0006, then

$$p = \frac{e_{ap} - e_{ad}}{e_{ad}} = 1.5 \quad \ldots (22)$$

The curve obtained from equation 20 using the above value is shown in fig. 24. It will be noted that the mean values obtained from the statistical analysis are in close agreement with this curve.

2.2.5 The initial modulus of arching and the determination of G

Values obtained for the initial modulus of arching m_{ai}, defined by $\frac{df_e}{de_a}$ at $e_a = e_{am}$, arching strain at minimum R_e, are shown in figs. 21 and 22 for two types of loading. The reason for selecting the above value of e_a for defining m_{ai} will be evident from the R_e vs e_a curves (see figs. 17 to 20). For a linear horizontal restraint R_s it would appear that arch action commences to behave according to a particular pattern at this stage. For other non-linear restraints the R_e -curve will have a different shape which may not have an equivalent minimum value so that e_{am} will be tentatively equated to 0.0004 to cover all cases.

It would appear that $\frac{m_{ai}}{\sqrt{u}}$ can be approximately expressed by $\frac{G}{1+3.5r_s}$ for the mean of a large number of tests as indicated in figs. 21 and 22 where the value of G depends primarily on the type of loading and the end restraint (R_s).

It is not inferred that this function has any fundamental basis at all but is tentatively proposed until more data are available. It should more correctly be a more complex function of r_s, R_s, $\frac{d}{L}$, the mode of loading and the rotational restraint at the supports. The full-line curves drawn on the above-mentioned diagrams (figs. 21 and 22) represent the assumed values of $\frac{m_{ai}}{\sqrt{u}}$ for R_s = 300,000 lb. per in. spread per foot width of

slab expressed as $\frac{G}{1+3.5r_s}$ where, for air-cured concrete slab elements subjected to this restraint,

$G \doteqdot$ 18,000 lb$^{\frac{1}{2}}$/in. for mid-point loading ... (23)

$\doteqdot$ 22,000 lb$^{\frac{1}{2}}$/in. for third-point loading ... (24)

The effects of the rate of loading and creep with passage of time are beyond the scope of this work, all the above values applying to tests of a few hours' duration.

The arching stress function can accordingly be expressed as follows :

$$f_a = \frac{G\sqrt{u}}{1+3.5r_s}\left[1 - D(e_a)^p\right]e_a \quad \text{... (25)}$$

$$= \frac{G\sqrt{u}}{1+3.5r_s}\left[1 - 6890\, e_a^{1.5}\right]e_a \quad \text{... (26)}$$

where G depends on R_s , r_s and the mode of loading. For the two types of loading undertaken in the laboratory tests the value $\frac{G}{1+3.5r_s}$ is determined from figs. 21 and 22.

2.2.8 The most probable ultimate load P_p .

The relations established above enable us to develop an approximate method of analysis by which the most probable ultimate load of a one-way spanning slab element can be predicted by successive approximations or by graphical construction provided the horizontal restraint is known and can be expressed as a function of Δ_a in the form $H_a = \psi(\Delta_a)$. In this method the mode of loading, the end restraint, the slab dimensions, the cube strength, the distribution of the steel reinforcement and its yield strength are all taken into account. Shear failure has not been taken into account however and required separate consideration.

The procedure can be summarized as follows :-

(1) Determine the positions of the yield lines and the ultimate load P_B resisted by the steel reinforcement in bending by yield-line analysis taking the self weight of the slab into account.

(2) Assume a value for the arching strain at which failure is likely to occur, say e_a = 0.0010.

(3) Determine the average arching stress by substitution of this value together with the other known parameters in the equation

$$f_a = \frac{G\sqrt{u}}{1+3.5r_s}\left[1 - 6890\, e_a^{1.5}\right] e_a$$

Where $\frac{G}{1+3.5r_s}$ is determined from figs. 21 and 22

(4) Determine $H_a = f_a b d$

(5) Determine $d_{aA} = d - \frac{(A_{sA} + A_{sc}) f_y + H_a}{\frac{2}{3} u b}$

(6) Determine the actual spread from the relationship $H_a = \psi(\Delta_a)$ Note: For laboratory tests: $H_a = R_s . \Delta_a$

(7) Determine Δ_u by substitution in the formula $e_a = \frac{\Delta_u - \Delta_a}{L}$

(8) Determine the deflection ω_c at the midspan articulation by solution of the equation

$$\Delta_u = \frac{\omega_c L \left(d - \frac{\omega_c}{2}\right)}{x_c (L - x_c)}$$

(9) The load corresponding with the assumed value for e_a and the calculated value for ω_c can now be determined, i.e. $P_p = P_B + P_A$ where P_A is determined from equation (18) for the particular mode of loading, e.g. for a central point load applied to a slab element with symmetrical reinforcement

$$P_A = \frac{4 H_a}{L} \left(d_{aA} - \omega_c\right) \quad \text{.... (28)}$$

(10) By repeating the procedure for a series of values of e_a a portion of the curve for P_p vs. ω_c can be plotted from which the peak value and the corresponding deflection can be determined.

It must be noted that the maximum total load will equal the sum of the maximum loads carried by the two systems only if the arching peak is attained after the yielding of the steel reinforcement. For large span/depth ratios and/or where deformation is accompanied by considerable rotation at the supports the steel may yield at a later stage in which case the total load carrying capacity of the slab is reduced. It is therefore necessary to determine at what deflection yielding of the steel occurs so as to relate it with the arching load. The theory of deformation of reinforced concrete slabs subjected to bending forces has unfortunately not been developed sufficiently to

35/ enable ...

enable us to make accurate predictions. The procedure adopted by the author is to assume a load deflection curve which initially approximates to that of an uncracked slab incorporating the reinforcement as an equivalent concrete area, but deviates at an increasing rate to equal two thirds the theoretical deflection of a fully cracked section as yielding of the steel commences. This method can obviously at best only be very approximate.

2.3 FIRST SERIES OF LABORATORY TESTS

2.3.1 Description of Tests

The laboratory tests described in this paper were carried out in order to study the behaviour of one-way spanning slab elements subjected to transverse loading with controlled restraint at the supports. A large range of 12" wide concrete specimens were cast varying in cube strength from under 1,500 lb/in^2 to more than 12,000 lb/in^2. The age of the concrete when tested varied from 3 days for some Ciment Fondu specimens to a maximum age of 165 days for Ordinary Portland Cement specimens. The slab thickness varied from 2½" to 4" and the spans from 4'0" to 8'0". The influence of the reinforcement was studied by testing slabs with two types of reinforcement illustrated in figure 16. The quantity of reinforcement was varied to cover a large range. Plain concrete slabs were also tested. In all these tests a linear elastic horizontal restraint was applied at the supports, i.e. the horizontal restraint was applied in such a manner that the ratio of the horizontal force generated at the supports to the actual measured spread was constant for any particular test. In addition to applying a wide range of restraints up to 1,500,000 lb/in. spread, the behaviour of unrestrained slabs was investigated in terms of various factors influencing arch action. Two modes of tranverse

37/ loading ..

loading were applied, viz. concentrated at mid-span and at third points.

In most of the tests of this series, the "end blocks" of the slab elements were restrained against rotation to approximate to "fixed-end" conditions. Tests to a smaller scale were also carried out on 1½" thick 3-span slabs to investigate the effects of rotation at the supports.

The apparatus used for carrying out these tests is illustrated in figures 13, 14 and 15. The horizontal restraint was applied by hydraulic jack in such a manner that the force applied was proportional to the horizontal spread measured at the level of the soffits at the supports. Vertical loading was applied in small increments and the horizontal force adjusted to correspond with the restraint/spread relationship for the particular test. The smaller these increments the more closely the behaviour would correspond with the ideal. It was found that, with a small amount of experience, the vertical and horizontal loading could be applied simultaneously to give readings which necessitated only very minor adjustments to the loading.

The gauges measuring the rotation at the supports gave the mean rotation of the soffit of the slab immediately beyond the points of support as shown in fig. 15. It is necessary to clarify this point as considerable distortion of the "end block" occurs. The horizontal spread was also measured at these positions as shown in figure 15. Vertical deflections were measured at various positions on the span and in some tests strain-recordings by Huggenberger-type gauges were made.

The ends of the slabs were bedded on mortar in special steel seatings mounted on accurately machined plates and rollers and clamped in such a manner so as to allow free horizontal movement but only a very small degree of rotation.

38/ The ...

The tests were carried out with the assistance of students over a period of three years with the standard of work varying considerably.

The cube strength has been used as the basis to define the concrete as it is in general usage, but it is realized that there are severe limitations to this method. Three 6" cubes were tested for each slab. Prisms for carrying out modulus or rupture tests and for determining the elastic modulus in accordance with B.S. 1881 : 1952 were cast in some of the series.

Both ordinary Portland cement of South African manufacture and imported Ciment Fondu, a high-alumina cement, were used. The coarse aggregate consisted throughout of Malmesbury blue-stone which is a hard but poorly shaped crushed quartzite or hornfels. The maximum size used was -½" with poor grading as commonly used commercially in Cape Town. The fine aggregate used was Cape Flats sand which has a fineness modulus varying between 1.80 and 2.20 and normally falls within grading zone 3 of B.S. 882 but which nevertheless is an excellent sand on account of its rounded shape. The standard of mix design and control varied considerably depending on the students concerned but gsnerally speaking the deviation in cube strength was not excessive.

The accuracy of moisture content control varied from accurate control, including moisture content determination of the sand by weighing, to approximate control by slump, and compacting factor apparatus. Only weigh batching was used, the concrete being mixed in a rotary pan mixer. Compaction was carried out by hand tamping or vibration. Accurately made steel moulds were used throughout.

All test specimens including the cubes were air-cured after the initial 24 hours under samp sacks. The temperature and relative humidity in the laboratory during the period of testing varied approximately as follows. During the

39/ summer ...

summer months the temperatures ranged from 60°F to 80°F and the relative humidity from 73% to 55%. During the winter months the temperature ranged from 45°F to 65°F and the relative humidity from 95% to 50%. The cubes were tested immediately after completion of the test on the slab specimen.

Before carrying out the main test the moduli of elasticity of some of the slab specimens were determined in the testing apparatus by applying horizontal force at the ends only. The stress applied did not exceed 15% of the cube strength.

The slab dimensions were checked by measurement and after completion of the test the exact positions of the reinforcing bars were located by cutting open the slabs. Only round mild steel bars were used.

2.3.2 Analysis of Results

The results of a typical series of tests are given in Table 1. Curves giving the most important relationships for test M1 are illustrated in fig. 17 and typical calculations are given in Appendix III - 4. A detailed analysis was made of 83 single-span slabs and 12 three-span slabs, and all tests have been included in the statistical analysis with the exception of certain readings where it was perfectly clear that a gauge was at fault or some other experimental error had occurred. The pressure cell recording vertical loading was found to be at fault when tested after test M15 and in addition the crack at one support occurred at an angle across the support which obviously affected the readings for horizontal spread. Certain readings such as those at which visible spalling occurred, were not always recorded.

Most of the items of Table 1 are self explanatory if read in conjunction with the foregoing text but a few points need further clarification.

40/ rows ...

Rows 1 & 13 : The average values of the slab depth d, and of the effective depth of the steel d_1, were obtained by determining the mean value at the supports and then averaging this value with the depth at midspan.

Row 3 : The notation gives the number of reinforcing bars, the diameter of the bars and the type of the reinforcement. The two types used are illustrated in fig. 16. The bars of type A were cranked at approximately quarter-points of span for mid-point loading and at a distance of one-sixth span from the supports for third point loading.

Row 4 : The force, $A_s f_y$, is the sum of the yield strengths of the reinforcing bars. In the earlier tests average values were used but it was found that the errors resulting therefrom were considerable on account of the fact that the yield strength varied a great deal within one batch. In the later tests a test specimen was cut from each bar and the individual yield strengths added.

Row 14 : The effective arching depth, d_a, was calculated in accordance with the theory developed above assuming $\beta = \frac{2}{3}$ and using H_E, the experimental value of H_a as recorded by pressure cell.

Row 15 : The above value of β was also used in the determination of the lever arm l_a of the bending forces acting at any yield line. The theoretical load P_B resisted by bending forces was calculated by yield-line theory after allowing for the self-weight of the slab.

Row 16: The theoretical arching load P_A, was

41/ determined ..

determined using the above values of d_a and H_E .

Row 17 : It was assumed that the total theoretical load $P_T = P_A + P_B$

Rows 23 & 24 : Rotations taken at the loading coinciding with the minimum value of R_e .

Row 27 : The elastic modulus, m_{it} , was determined on the slab during the initial test described elsewhere.

Row 28 : The initial modulus of arching, m_{ai} , is the initial tangent modulus as illustrated in fig. 17 taken as the value of $\frac{df_a}{de_a}$ at $e_a = e_{am}$, i.e. at minimum R_e or $e_a = 0.0004$ whichever is the lesser.

Rows 33, 34 & 35 : Arching strains e_{am} , e_{ac} and e_{ap} were determined experimentally.

Rows 36 and 38 : The most probable load, P_p , and the most probable central deflection , w_{cp} , were determined in accordance with the theory developed above. The stress function used in the calculation of these values was corrected for the $\frac{R_s}{b}$ ratio. In an initial statistical analysis of 74 tests a stress function differing from the final expression suggested in equation 26a, of the form

$$f_a = \frac{12000\sqrt{u}}{1 + 2r_s}\left[1 - 6890\, e_a^{1.5}\right] e_a$$

with no correction for $\frac{R_s}{b}$ had been applied. The mean values of the ratios $\frac{P_E}{P_p}$ and $\frac{w_{ce}}{w_{cp}}$ were 1.00 and 1.23 with coefficients of variation of 14% and 32% respectively.

Application of the revised function with corrections for $\frac{R_s}{b}$ would have improved the histograms very considerably.

42/ The accuracy ..

The accuracy of the theory depends primarily on the stress-function and the value of the initial modulus of arching m_{ai}. The influence on m_{ai} of the cube strength and the steel reinforcement, expressed by the factor $r_s = \frac{A_s d}{bd^2} \times 100$, is illustrated in figs. 21 and 22 for mid-point and third-point loading respectively. The relationships established from the pattern of the experimental results were incorporated in the stress function to give equation 26a. The influence of other parameters such as the span/depth ratio and the magnitude of the horizontal restraint R_s was discussed in 2.2.5. Rotation of the supports did not appear to have any marked influence unless it was masked by the general scatter pattern and no definite conclusions could be drawn as insufficient data were available It would appear from the results of tests M9 and M10 that for a $\frac{L}{d}$ ratio of 36 the arching peak load in a clamped slab with $\frac{R_s}{b} = 300{,}000$ lb/in/ft. width is attained slightly before the three yield lines are fully developed.

The influence of the mode of loading can be readily explained by the particular bending deformation which in the case of a distributed loading has the effect of increasing the effective modulus of arching relative to that for a concentrated load at midspan. In the function for uniformly distributed loading the parameter G will probably slightly exceed that for third-point loading as discussed in 2.2.5. The greater scatter of the values of the modulus of arching evident at lower steel percentages can be accounted for by the greater variation in the form of cracks and the positions, which, for such slabs, depend for their precise configuration on the localized variation in tensile strength of the concrete. As the theory is based on a single crack at the point of maximum bending moment, it is understandable that a different crack pattern will cause a considerable deviation from the theory.

43/ This is ...

This is particularly true for cracks at the supports as the readings for horizontal spread may be greatly affected. This would not however apply in practice where a sudden change of section at perimeter beams would tend to control the crack positions. The experimental accuracy would have been greatly increased if concrete end-blocks of increased depth had been cast onto the slab elements. In heavily reinforced slabs, the crack positions can be predicted more precisely, but on the other hand, the arching efficiency is reduced due to the greater bending deformation of the slab and the zone of smaller cracks which effectively reduce the modulus. Whereas greater horizontal restraint at the support boundaries will increase the arching modulus as discussed in 2.2.5 it will at the same time reduce the effective arching depth, and thereby the efficiency of arching, due to the greater depth of stress block.

As the development of well defined cracks increases the arching effect, it follows that steel reinforcement with a low yield strength will increase the arching efficiency.

Test M11 in table 1 was a repetition test consisting of ten loading cycles. The maximum load applied for the consecutive cycles was increased in gradual stages with the maximum load being attained in the eighth cycle and total collapse occurring during the last cycle. There was visible spalling in the eighth cycle, with an apparent decrease in the ultimate load as indicated by the empirical theory. The deflection at which the peak load was attained was also apparently increased by the repetition. The load-deflection curves and stress-strain relationships revealed typical hysteresis envelopes as illustrated in figs. 25 and 26. The linear elastic law for R_s was maintained throughout the test which resulted in increasing residual horizontal reactions subsequent to each cycle. The residual forces would no doubt reduce with passage of time due to creep.

PART 3

THE THEORY OF ARCHING FOR TWO-WAY SPANNING SLABS

3.1 GENERAL

Whereas in the case of a one-way spanning element it was possible to obtain solutions based on idealised assumptions the problem is far more complex in two-way spanning slabs. Even if idealized assumptions regarding the material properties and the boundary restraints were to be made analytical solutions would be difficult. It might be possible to use methods of successive approximation to achieve compatibility of stress and strain in terms of whatever basic assumptions are made, but such procedures would be extremely tedious and bearing in mind the variability of concrete, cannot be justified at this stage except as a purely academic exercise.

The only feasible solution would appear to be an extension of the empirical method developed in Part 2. Tests on model slab panels and full scale tests have given some indication of the nature of dome action in panels. This knowledge has been incorporated in the theory developed below.

3.2.1 Empirical-phenomenological theory for two-way rectangular slab panels

It would appear from tests that the crack pattern developed in rectangular slab panels is primarily determined by bending forces. This deduction also follows from the fact that dome action depends on articulation and accordingly must be secondary. It does not however follow that dome-action has no bearing on the crack pattern at all, in fact the propagation of cracks in the latter stages may well be considerably influenced by the superimposed compressive arching forces. We shall however ignore much effect at this stage and adopt the methods used

yield-line analysis, in so far as they have been successfully developed, for determining the most probable crack pattern.

The problem that remains therefore is to determine the distribution of stress at the articulations. No direct analysis is practicable and it will be necessary to resort to simplification by making various approximate assumptions.

The actual distribution of the arching forces depends on many factors but principally on the shape of the panel, the depth-span ratio, the degree of boundary restraint and the distribution of loading. It does not remain constant but varies with increasing load. The extent of this variation depends largely on the bending stiffness of the slab in relation to the dome action or the ability of the slab to transfer the applied loading by bending forces to the lines of articulation so as to achieve efficient dome action. It is obvious from inspection and tests have confirmed that the greatest arching stiffness exists across the corners of the panel normal to the diagonal yield-lines where the effective span is reduced. There will consequently be a tendency for these diagonal arches to act as supports thereby reducing the effective panel size as illustrated in fig 27. This action is analogous to what is usually referred to as corner lever action in yield-line analysis. The result is that greater arching forces tend to develop towards the corners but are again reduced in the immediate vicinity of the corners due to flexibility of the acute-angled ends of the slab elements. If the slab elements bounded by the articulations could be imagined to have infinite bending stiffness the arching forces would be greatest in the corners, but due to the above-mentioned flexibility we find that the actual distribution of horizontal forces at the boundaries

*

FOOTNOTE TO PAGE 185

The author wishes to acknowledge the fact that this test was carried out by a student under the supervision of the staff of the Civil Engineering department whose assistance and observations made the successful procedure possible.

is approximately as indicated in fig. 27. The precise shape depends on the factors mentioned above.

It has been demonstrated in the laboratory* on perspex and steel models that the slab can in certain cases carry increasing loads even after total arching collapse across the centre of the short span. For point loads applied at third points on the long span centre-line it was found that in an artificially articulated panel (fig. 4) increasing loads were carried even after a visible gap had formed in the crack between the two loads. This load was clearly resisted by bending forces in conjunction with the diagonal arching across the corners. At this stage all internal arching forces were concentrated across the diagonal articulations but the distribution of fig. 27 would still apply approximately at the external boundary although the forces would be more concentrated towards the corners.

Tests carried out on a square slab panel made of steel plate with artificial articulations similar to that illustrated in fig. 4 demonstrated the significance of this corner effect very clearly. A series of tests in which a central concentrated load was applied were carried out to study this effect. After the first test the contact faces of the diagonal articulations were filed to prevent contact for a small distance from the panel corners. After each test the length of the "gap" was gradually increased and the effect on the load carrying capacity noted. At first the reduction in load was small but as the extent of the gaps approached a third of the length along the diagonals a marked drop in load was noted. It is clear that this was the region of maximum arching across the corners and that it played a significant part in the dome action as described previously.

47/ Taking the ...

Taking the above known behaviour into account it is immediately obvious that if we were to assume a uniform distribution of stress along the outer boundary we would in most cases be conservative in our estimate of the load-carrying capacity if we were to base the calculation on the maximum arching force attained across the centre of the short span. This conclusion must be qualified by the fact that it also depends on the shape of the panel and the applied loading. For a large span-ratio and a single concentrated load the bending stiffness may not be sufficient to give the assumed distribution and the boundary forces will in fact tend to be as illustrated in fig. 28.

Although certain fortuitous results as described later greatly simplify the empirical theory for the slab types tested, it would be dangerous to extrapolate without verification by further tests.

3.2.2 Normally reinforced concrete slab panels

With the results of the full-scale tests carried out on the Old Alliance House available as well as supplementary laboratory tests it has been possible in conjunction with the theory developed for one-way spanning elements to get some idea of the order of magnitude of the arching forces acting in rectangular two-way spanning normally reinforced concrete slab panels. The basic assumption made in this analysis is that the distribution of the horizontal component of the arching forces acting normally to the yield lines can be represented by an equivalent uniformly distributed force system. The theoretical load-carrying capacity of the arching forces in any slab can readily be established in terms of this simplified force system. This can be done for any particular deflected shape by considering the equilibrium of the slab elements bounded by the yield-lines. As in yield-line analysis the

48/ assumption ..

assumption is made that bending deformation of these elements is negligible. The equivalent mean intensity of arching stress can accordingly be determined for any load-deflection values found by experiment.

As explained in 3.2.1 this uniform distribution does not necessarily occur in practice so that a correction must be applied. This is done by extending the parameter G in equation 26a to G_e which includes a correction factor. The value of G_e can be determined experimentally if the stress function is expressed in terms of the deformation of the slab at a particular section in the panel. It has been found convenient to use the centre-line across the short span as the reference section for studying the behaviour of slab panels. The correction factor will not necessarily be constant so that G_e becomes a function of the deformation which can most usefully be expressed in terms of the arching strain e_a. The method used for determining G_e is explained in 3.3.9. In a similar manner the restraint against horizontal spread at the boundary can be expressed in terms of R_e as a function of e_a at the same section across the short span.

If both G_e and R_e are known it is possible to calculate the load for any deflection of the panel by adopting the method explained in 2.2.4 and as indicated in 3.2.3 from which the maximum load can be determined graphically or by successive approximations.

Both G_e and R_e depend on a large number of variables and it follows that they are highly complex functions. The full scale tests described in 3.3 did however indicate that whereas both functions vary initially they tend in most cases to constant values as the ultimate load is approached. This greatly simplifies the problem as it is in such cases only necessary to specify the limiting values. Where this

49/ does not ...

does not apply a solution can however be obtained by the same method provided the functions are known in graphical form. Much can be learnt from these curves about the behaviour of a slab if analysed in terms of established patterns.

It accordingly remains to establish the functions G_e and R_e for a wide variety of cases. This can naturally only be done by empirical methods. The tests described in 3.3 only covered a few cases and much more information is required before the method can be used for design purposes. Because of its phenomenological nature the method is not amenable to extrapolation. In the meantime it may however serve as a useful tool to research into this phenomena.

3.2.3 Calculation of the most probable ultimate load P_p for two-way spanning rectangular slabs

Using the relations established for the empirical theory and with reference to fig 29, the most probable ultimate load for a two-way spanning slab can be calculated as follows if the functions G_e and R_e for the particular slab in terms of a particular cross-section are known.

The crack pattern and the ultimate superimposed load that can be resisted by bending forces P_B is calculated by yield-line theory taking due account of the dead load.

The ultimate arching load P_A is calculated by adapting the procedure described in 2.2.8 in which the calculation of the deformation is done for a particular cross-section, usually at the centre line across the short span in terms of which the parameters G_e and R_e apply. The expression for P_A is derived by considering the equilibrium of the elements bounded by the major cracks. Contrary to yield-line theory applied to bending forces, arching forces will in most cases induce vertical shear forces at the diagonal yield lines, the resultant of which

50/ is shown ...

is shown for three-point loading in fig. 29.

For this type of loading the arching load P_A can be expressed in terms of the equivalent uniformly distributed arching force H_a (lb. per foot) by considering the equilibrium of the elements as follows :

$$P_A \frac{L_1}{4} = \frac{H_a}{12}\left\{q(d_a - w_c) + 2a\left(d_a - \frac{w_c}{2}\right)\right\} + 2S.c$$

Also $2S.d = \frac{H_a}{12} L_1 \left(d_a - \frac{w_c}{2}\right)$

$$\therefore P_A = \frac{H_a}{3L_1}\left\{q(d_a - w_c) + 2a\left(d_a - \frac{w_c}{2}\right)\right\} + \frac{H_a c}{3d}\left(d_a - \frac{w_c}{2}\right)$$

Now $\frac{c}{d} = \frac{L_1}{2a}$

$$\therefore P_A = \frac{H_a}{3}\left\{\left(d_a - \frac{w_c}{2}\right)\left(\frac{2a}{L_1} + \frac{L_1}{2a}\right) + \left(d_a - w_c\right)\frac{q}{L_1}\right\} \quad \ldots (28a)$$

which replaces equation (28) in 2.2.7.

3.3 TESTS TO DESTRUCTION ON SLAB PANELS OF THE OLD ALLIANCE HOUSE

3.3.1 General

The tests described below were carried out on the Old Alliance House in Cape Town during September and October of 1957 by the author in co-operation with Prof. R.G. Robertson and Mr. D.J. McGaw of the Department of Civil Engineering of the University of Cape Town. Fifty slab panels were tested to destruction prior to demolition of the building.

The building had been constructed some 30 years previously and was an eight storey reinforced concrete framed structure consisting of slab panels with secondary and main beams supported on columns forming 15 ft. by 17 ft. bays as illustrated in figs. 30, 31 and 32.

Due to the extremely short period available for testing and the lack of adequate assistance and funds only two alternative programmes could be considered. As first alternative a few slab panels could be tested with great thoroughness in order to get detailed information about a limited number of tests or, secondly, a larger number

could be tested with less detailed recordings in order to assess the consistency of certain basic behaviour patterns. The latter alternative was decided on and this decision has probably been justified by the results. At the time when these tests were undertaken to investigate arch action very little was known about the phenomenon. With the knowledge gained since, it would be possible to improve considerably on the testing procedure for a similar series of tests.

3.3.2 Description of the tests

Loading was applied by hydraulic jacks and in most tests consisted of two-point loading as illustrated in figs. 33 and 34. Single-point loading and three-point loading were applied in some tests as shown in fig. 35. The reaction to the jacking forces was obtained by providing specially made props supported against the floor above. In this manner two tests were in fact carried out simultaneously, the upper slab being loaded upwards until it failed, at which stage propping at several higher levels was added to enable the test on the lower slab to be completed without damage to the upper floor panels, or vice versa if the lower slab failed first. Modified Ewing gauges were attached to the tubular struts and calibrated to read the jacking forces. During the loading procedure it was endeavoured at all stages to apply equal forces at the loading points. It was not always easy to achieve this in the three-point tests as the relative decrease in load at the central point immediately prior and subsequent to attaining the peak load was so rapid that a considerable amount of pumping of the central jack was required to maintain equal loads. Readings of deformation were taken at three sections across the short span (viz. at centre and quarter-points of the long span) as illustrated in fig. 33. Relative vertical deflections, horizontal spread and rotations were recorded by means of the apparatus illustrated

in figure 36. From these readings it was possible to calculate ω_c the differential vertical deflection and Δ_a the actual spread at soffit level at the supports (see fig 36) on the assumption that the distortion of the beam cross-section was negligible.

In most tests a single run to failure over a period of approximately one hour was carried out. In a few cases several load cycles slightly less than the failure load were applied in order to study the effects of repetitive loading. Short term creep tests were carried out by leaving the jacks on overnight, which amounted to applying constant deformation resulting in a decrease of load with passage of time.

3.3.3 Description of slab panels

The slabs varied in thickness from approximately $4^7/8$" to 5½" including the screed topping which was usually less than 1/2" in thickness. For the purposes of this analysis the screed has of necessity to be included in the effective slab thickness and accordingly adds an unfortunate but unavoidable inaccuracy to the analysis. The slab panels tested varied slightly in size being approximately 8'0" by 14'0" clear span in all cases except for four on the seventh floor which were approximately 5'4" by 13'6".

The reinforcement in all cases consisted of 7 no. 1/2 inch and 7 no. 3/8" diameter mild steel bars placed alternatively at 12" c/c in the bottom only across the short span with the only reinforcement in the longitudinal direction being two 1/4" diameter lacing bars tied to the main steel at approximately quarter points of the short span as indicated in fig. 32.

3.3.4 Beams and columns

The main beams spanning between columns were 20" deep, including the slab and screed topping, by 9½" wide and a typical beam which was cut open was reinforced with 1 no.

$1\frac{1}{8}$" and 3 no. 7/8" diameter mild steel bottom bars of which 2 no. 7/8" diameter bars were cranked up near the columns to act as top steel over these supports. The stirrups were 3/8" diameter spaced at 12" c/c with 2 no. 3/8" tying bars in the top of the beam.

The secondary beams were 18" deep including the slab and screed topping by $7\frac{1}{2}$" wide and a typical beam which was cut open was reinforced with 1 no. 3/4" diameter and 2 no. 5/8" diameter mild steel bottom bars with both 5/8" diameter bars cranked near the supports to act as top steel. The stirrups were 3/8" diameter at 12" c/c with 2 no. 3/8" diameter tying bars in the top of the beam. The stirrups to these internal beams were open at the top while stirrups to perimeter beams were closed, the top arm being however too short to act effectively as top steel in the adjacent slabs.

Columns cut open at various levels were reinforced with 4 no. 3/4" diameter main bars and 1/4" ø binders at 12" c/c being 18" x 18" or slightly larger in cross-section.

3.3.5 Material properties of concrete and steel

The quality of the concrete was fair in spite of the fact that sea sand with a high percentage of sea shells had been used as fine aggregate. The coarse aggregate consisted of crushed quartzite (alternatively described as a hornfels, being a highly metamorphosed arenaceous shale from the Malmesbury series).

Concrete samples were collected and cut by Emery wheel into 3" x 3" x 6" prisms and 4" cubes. All surfaces were checked and if found not to be true to plane the bearing surfaces were made good with cement mortar as well as all chipped corners and other irregularities. All dimensions were accurately recorded. Although the maximum deviation from the specified overall dimensions was as much as 0.40" the accuracy generally was very much greater and the surfaces were invariably parallel to within 0.05".

54/ All tests ...

All tests on the above specimens were carried out in accordance with B.S. 1881 : 1952, the concrete being in an air-dry state. The results are indicated in table 2. Prior to crushing, the cubes were subjected to tests by the Schmidt impact-hammer. These tests indicated a mean rebound number of 43 as against the number 29 corresponding with 4,000 lb./in^2 on the manufacturers' calibration curve for 28-day concrete. The shift is slightly greater than that found by Ockleston and Scott for 10 year old concrete(22) which seems to indicate that a family of calibration curves for this apparatus could readily be established to cover the full range of concretes in terms of maturity. Samples of the reinforcing steel were collected and tested in accordance with BS 785-1938 with the results indicated in table 3.

3.3.6 Brick partition walls

Slabs supported by partition walls were not tested until after these had been removed by the demolition contractors. Partition walls either directly on or under the perimeter beams or immediately adjacent to the beams as indicated in fig. 36 did however have a marked effect on the results due to a clamping effect whereby the beam rotations were considerably reduced and the effective restraint of the slab increased. A typical layout of brick partitions over and under the seventh floor slab is indicated in fig. 31.

3.3.7 Analysis of results

A brief analysis in summary form with typical results only will be given in this report. Typical calculations are given in Appendix III - 5.

The ultimate loads attained in the various tests are shown in tabular form in table 4. The tables are to be read in conjunction with fig. 31 on which the reference grid is indicated. The number in the table preceding the grid reference denotes the floor, e.g. 7-C1 refers to the panel of the seventh floor slab in the third row parallel to Castle Street and the first row parallel to St. George's Street.

55/ The total ..

The total ultimate applied load is indicated to the nearest short ton (2,000 lb.) and the mode of loading by the number of point loads and the direction of application, e.g. 20 refers to 2-point loading acting upwards. Single concentrated loads were either applied at the centre of the panel or on the longitudinal centre line approximately 3'0" from the short span centre line in which case the letter e is added to the symbols denoting the mode of application. The date of the tests and the sequence numbers prefixed by the letter T are given because the condition of adjacent panels previously tested to destruction obviously influenced the results.

Three-point-loading was applied symmetrically on the longspan centre line spaced at 30" intervals.

The letter R denotes a repetition test, the letter d a delayed test and the adjacent panels marked S were tested simultaneously. Shear failure is indicated by S.F. Typical results expressed in terms of the various concepts developed for the empirical theory discussed in 3.2.2. are indicated in figs. 37 an 39. R_e is calculated directly from the recorded deflections but G_e is calculated indirectly as explained in 3.3.9.

3.3.8 General observations and conclusions

A discussion of the full significance of the various tests would require a detailed analysis in relation to the precise conditions pertaining in the vicinity of the slab perimeter. This would be beyond the scope of this paper. This section will accordingly be confined to general observations and conclusions.

The test results confirmed without exception that arch action is a reliable load-carrying system for short-term loads provided the necessary conditions previously defined are present. The effects of repetitive loading and delay tests were similar to the laboratory results and it would appear that creep seriously decreases the arching

56/ capacity ...

capacity of a slab. This was clearly demonstrated by tests on panel 2-D1.

The first test was carried out on the 12th September by applying 3-point loading downwards. After attaining a load of 48 short tons the load was removed. The residual deflection implied that the slab even after removal of load might be subjected to horizontal perimetral forces. These forces if of considerable magnitude would decrease with passage of time as a result of creep resulting in a corresponding reduction in the arching capacity of the slab. This was confirmed by a repeat test carried out on 26th October in which the slab failed at a load of only 24 short tons. The contribution due to bending forces as calculated by yield-line theory could not have exceeded 8 short tons so that arching was still significant but the reduction is disturbing and clearly demonstrates that this phenomenon will require more investigation.

The effects of shrinkage were evident in two respects; firstly, in the form of various diagonal corner cracks which tended to reduce the arching capacity of the relevant panels very slightly and secondly in the reduction of the elastic modulus of the concrete which had a value according to tests on prisms cut from concrete samples (table 2) approximating closely to $40{,}000\sqrt{u}$ as compared with the value $60{,}000\sqrt{u}$ normally found for 28-day air-cured concrete tested in an air-dry state. This reduction may be due to internal micro-cracking developed during the life-time of the structure. As very few results of prism tests on concrete of this age are available these conclusions need verification. The tests carried out by Ockleston and Scott[22] on samples of ten-year old concrete indicated a proportionate reduction to give a mean value of $50{,}000\sqrt{u}$. This reduction of the modulus of

57/ elasticity ...

elasticity with time means that the arching capacity of a slab decreases with passage of time at a reducing rate in accordance with the shrinkage-time relationship.

The significance of rotational restraint was clearly borne out by the increase in the load-carrying capacity of panels that were effectively clamped by partitions on one or more boundaries. This applied particularly to corner panels which had an amazingly large arching capacity approaching that of internal panels. The mechanism of arch action in corner panels can be explained by the fact that the perimeter beams act as ties restraining the external corner which acts as a buttress to the elements of the panel. The arching forces on the two external boundaries are accordingly concentrated at the corners as indicated in fig. 40.

The fact that the cement screed acted monolithically with the concrete greatly complicated the analysis. For the purposes of this paper it has been assumed that the total thickness of slab including the screed consisted of concrete with a cube strength of 4,000 lb. per in^2. The total slab thickness varied from $4\frac{7}{8}$" to $5\frac{1}{4}$" but as only a limited number of measurements were taken it has been assumed that the total effective thickness throughout was 4.8 inches and that the effective depth of the steel was 4.2 inches. The dimensions of all slab panels in plan were measured.

Using the procedure described in 3.3.9 the results of these tests were used to calculate G_e and R_e, typical curves of which are given in figs. 38 and 39.

The analysis of the larger size panels indicated that G_e was only slightly smaller for slabs tested upwards than for those tested downwards, but that it increased as the number of point loads were increased due to the fact that the distribution of load was improved. For corner panels and semi-internal panels subjected to symmetrical

58/ loading ...

loading G_e varied from 5,000 to 9,000 $lb^{\frac{1}{2}}/in.$ For internal panels G_e varied from 8,000 to 10,000 $lb^{\frac{1}{2}}/in.$ For corner panels R_e varied from 0.25 to 0.35. For semi-internal and internal panels R_e varied from 0.30 to 0.60. For single eccentric point loading the value of G_e in terms of the centre-line across the short span increased but the value of R_e decreased, both by $50\pm$ %.

The above values were greatly influenced by the positions ofthe partitions relative to the perimeter beams as discussed previously and the state of the adjoining slab panels.

The smaller panels were tested with two-point loading upwards and the arching resistance of 7AB2 with all the other adjoining panels intact gave G_e = 8,000 $lb^{\frac{1}{2}}/in.$ and R_e = 0.30. The values for the other three small panels decreased according to the sequence of the tests apparently due to the damaged state of the adjoining slabs. Lack of time did not permit accurate records being kept of crack formation in all cases. A fairly consistent pattern for each type of loading was however apparent and usually corresponded reasonably well with yield line theory applied to the point-loading. The cracks were usually well defined due to the low steel ratio but were not always symmetrical which fact considerably effected the above-mentioned parameters.

Cracks were in many cases observed in adjacent panels and from the configuration could be ascribed to extensional forces caused by the perimeter arching forces. The cracks were usually consistent with deep girder action of the surrounding panels combined with circumferential tensile forces. A typical example is illustrated in fig. 41.

In the case of some single point loads failure by shear occurred with characteristic violence. The above values of G_e would probably be larger by 50% for 28-day concrete slabs but the values of R_e would not be effected to the same extent.

59/ 3.3.9 Calculation ...

3.3.9 Calculation of G_e from full scale tests

The theory proposed in 3.2.3. is based on the assumption that G_e and R_e for the particular slab are known. These functions cannot at present be determined analytically, but can however be derived indirectly from tests such as those described in 3.3. By recording the relevant deformations corresponding with any particular applied loading the theory applied in reverse in order to determine G_e. Typical curves for G_e are given in fig. 38.

The procedure adopted is as follows :-

(i) Determine $P_A = P_T - P_B$

where P_T is the applied total load and P_B is the applied load resisted by bending forces in accordance with yield-line theory taking dead load into account.

(ii) Determine d_{aB} the effective depth of slab available for arching between C and B in terms of H_a from the equation (15)

$$d_{aB} = d - \frac{(A_{sB} + A_{sc}) f_y + H_a}{\frac{2}{3} u \times 12}$$

where with reference to fig. 29

A_{sB} = area of steel at B per foot width

A_{sc} = area of steel at C per foot width

(iii) Determine H_a by substitution of the above equation in equation 28a and hence

$$f_a = \frac{H_a}{bd} = \frac{H_a}{12d}$$

(iv) Determine e_a from equation 6.

(v) Determine $G_e = \frac{f_a (1 + 3.5 r_3)}{[1 - 6890 e_a^{1.3}] e_a \sqrt{u}}$

R_e is determined directly from equation 10 and typical curves are given in fig. 38. Typical calculations are given in Appendix III - 5.

3.3.10 Application of Theory to tests on slabs of the Old Dental Hospital Building

The theory has been checked for the two-way spanning slab tested by Ockleston in the single-panel test. (See Appendix III-6.)

60/ For ...

For G_e = 10,000 lb$^{\frac{1}{2}}$/in. and R_e = 0.40 the theoretical load deflection curve coincides almost exactly with the experimental values in the ultimate range as shown in fig. 42. It could be reasoned that the initial self weight deflection is approximately three times that indicated due to creep in which case the deflections would correspond still closer as the true origin used for plotting the empirical curve is shifted further to the left. The theory if correct indicates that the magnitude of the equivalent uniform horizontal arching force acting at the perimeter at the ultimate load was of the order of 15,000 lb. per ft., that the spread at soffit level on the centre line across the short span was of the order of 0.15 in and that the arching strain was approximately 0.00060. The fact that the theoretical and experimental curves do not diverge appreciably after the peak load had been attained indicates that G_e and R_e remained constant over a large deflection range. The flatness of the experimental curve and the ability of the slab to resist the applied load over such a large deflection range can probably be accounted for by the corner effect previously discussed.

3.4 LABORATORY TESTS ON TWO-WAY SPANNING MODEL SLABS

Various tests were carried out on both plain concrete and steel slabs to investigate certain aspects of arching.

Plain concrete slabs 24" x 24" in plan by 1½" thick with slab surrounds varying in width from 3" to 15" and reinforced with one ¼" diameter M.S. bar per 3" width fixed parallel to the edges in the middle plane and lapped at the ends to provide a continuous circumferential band, were subjected to central point loading to investigate the effectiveness of the perimeter restraint. A special testing frame was designed to provide partial rotational restraint at the support boundaries.

The increase in the load carried by arching corresponding

/61 with ...

with increasing widths of surround was clearly evident. The arching action of slabs of this type is highly complex and for plain concrete slabs extremely sensitive to the particular crack pattern. As in the case of one-way spanning plain concrete slabs the crack patterns were not always perfectly symmetrical. This influenced the behaviour considerably. At the time these tests were carried out the empirical theory had not been fully developed and the horizontal spread of the slab soffit at the support could not be calculated with sufficient accuracy from the recorded deflections. These tests could accordingly not be used to extend the theory but they did nevertheless provide valuable information. The tests clearly demonstrated the various stages of behaviour for this type of slab which can be summarized as follows:

(a) An initial linear load deflection relationship until development of tensile perimeter cracks in the top of the slab and radial cracks in the soffit which was usually accompanied by a deviation from the linear behaviour mode until a sudden decrease in load was recorded.

(b) Thereafter the load built up once more to a new peak as arching forces became effective. The ratio of the above-mentioned peak loads depended on the tensile strength of the concrete and the arching restraint and for high strength concretes the initial peak was higher.

(c) The complexity of arch action across the diagonals due to the previously mentioned corner effect resulted in some cases in the load attaining a series of peaks as the crack pattern was extended in definite stages. The slabs were able to resist load at central deflections approaching the total thickness of the slab when arch-action across the midspan could no longer be effective, due to corner arch action in conjunction with bending forces and secondary arching forces.

62/ Tests ...

Tests were also carried out on a 6" square model slab made from 1/4" steel plate in which artificial perimetral and diagonal articulations were provided similar to the perspex model shown in fig. 4. The investigation of the corner effect has already been referred to in 3.2.1. The effect of boundary restraint was investigated by varying the width of the surround from 5.5" to 0.75". The effectiveness of the restraint was clearly analogous to the thick cylinder effect if the slab surround is imagined to be a slice from a square tube with pressure applied at the internal perimeter as can be seen from fig. 43. The scatter of results can be accounted for by the lack of perfect fit of the triangular parts. Unfortunately repetition recordings with the same model could not be carried out as this would have resulted in further damage to the edges.

The initial load deflection relationships were related to the perimeter restraints in a similar manner as the ultimate load, but as the central deflection approached the plate thickness the load-deflection relationship for all cases tested had identical gradients. This can be explained by the fact that at this stage the deflection was mainly due to bending of the triangular cantilevers supported by the corner arches.

If no rotation were to occur at the boundaries of a slab we could accordingly conclude that the additional restraint provided by panels other than those immediately surrounding the particular slab is negligible. In most cases occurring in practice a considerable portion of the effective spread at the perimeter of the slab is due to rotation of the supporting beams. It would appear therefore that the boundary restraint problem can for all practical purposes be confined to that of investigating the rotational stiffness of the perimeter beams and the effect of the surrounding slabs within a boundary at a distance from the slab supports not exceeding about 1.5 times the short span or the long span whichever is the lesser.

PART 4

CONCLUSIONS

4.1 ANALYSIS OF PRESENT KNOWLEDGE

The discovery of the phenomenon and the development of various theories of arching was briefly covered in 1.2. The problem involved in the development of such theories was discussed in 1.4. Although the nature of arch action is well understood, no satisfactory analytical solutions have been developed for two-way spanning slab panels. Various solutions for one-way spanning slab elements or beams have been suggested but these are either extremely complex or over simplifications and would rarely find direct application in practice as arching is in most cases a two-way phenomenon. The empirical theory suggested by the author could be developed to cover a wide range of conditions but this would require much more research as it is not amenable to extrapolation.

The effects of repetitive loading need further investigation as loading cycles terminating well below the ultimate attained in a single run, may under particular circumstances have a marked influence on the ultimate load factor. The development of a shake down analysis on an empirical-theoretical basis would appear essential if repetitive loading is to be taken into account as the reduction in the true load factor could be critical. Arch action is particularly prone to such reduction as any decrease in the boundary restraints causes increased vertical deflections which in turn requires greater horizontal reactions.

The effects of dynamic loads would be an interesting field of study about which little is known as there are obvious applications in this direction as discussed below.

The influence of shrinkage and creep is of very considerable importance and will require special study.

64/ Very little ...

Very little is known about these phenomena in relation to this problem except that they are of great importance due to the sensitivity of arching to small changes in the planar dimensions.

4.2 PROBABLE FUTURE DEVELOPMENTS

Various research workers throughout the world have in recent years become interested in this problem and different approaches will probably be adopted. At present there appear to be two lines of thought, firstly in terms of the arching analogy and secondly by retaining the plate analogy[14] and using the concept of enhanced bending resistance due to a change in the yield criterion. The author doubts whether the second approach will produce useful results unless a complete range of empirical correction factors is introduced.

Rigid-plastic theory using either analogy does not appear very promising as the true peak value of the load cannot be assessed, the theoretical value occurring at zero deflection.

Idealized elasto-plastic theories are more promising but are extremely complex as illustrated in Appendix III - 1. After doing a considerable amount of work in this direction Marriott[15] concluded that a more accurate stress function was required. At present this can only be done by some method similar to that proposed by the author. A more fundamental method would however be preferred and this could probably be done in the same way as for the idealized elasto-plastic theory but using instead a more accurate stress function for concrete, incorporating calculated crack patterns and a true analysis of steel stress at all stages. Such a theory could be formulated in terms of definite basic assumptions but the difficulties involved in finding solutions would be extreme.

At present this could only be justified as an interesting academic exercise. Development in methods of

65/ analysis ...

analysis may however change the picture in the future. The biggest obstacle to a precise theory will always be the variability of the material properties of concrete and it therefore remains to decide how much effort should be expended in the development of the theory. Practical considerations would indicate the limit at that stage when the theoretical accuracy is of the same order as the predictability of the material properties of concrete made to the highest standard of control that is economically justifiable. Much more research is however required to attain such a standard of accuracy. This could most economically be done by carrying out tests prior to demolition of building structures. As the cost involved in such tests is not excessive and reinforced concrete structures are more often demolished these days there is no reason why an extensive knowledge of a wide range of conditions could not be gained within a reasonable period of time provided tests are systematically undertaken and the work is properly co-ordinated.

4.3 PRACTICAL APPLICATIONS AND THE ECONOMIC IMPLICATIONS

For normally reinforced concrete slabs the problem is at this stage primarily of academic interest as it is doubtful whether any governing authority would be prepared to incorporate design procedures based on arching theory in its code of practice until much more is known about the phenomenon. In the case of prestressed concrete Guyon has succeeded in convincing the French authorities of the feasibility of its application by conducting full scale tests. His method however is limited to the utilization of horizontal restraint forces not exceeding that of the cable forces and can accordingly only be considered as a partial application of the arching forces. It is however a considerable advance and general interest in the theory will gain momentum when the economic advantages become evident.

In considering the application of this theory in practice it is necessary to classify structures into three

basic types. Firstly, those which would serve a useful purpose even if they could withstand the design forces only once and suffer severe disfiguration and cracking in the process. Under these we can classify magazines for explosives, defence installations and air raid shelters.

The second type of structure is that which has to withstand repetitive loadings without suffering any visible signs of distress such as normal building structures, bridges and roads in which hair cracks may however be permissible.

The third type should preferably not develop any cracks at all, viz. water-retaining structures.

It is obvious that arching theories have no application to the third type, have a limited application in the case of the second type and could be applied to full advantage to the first type.

The limited application to the second type is probably of most importance as these structures are far more numerous. Application would probably be restricted to adopting a reduction in the factor of safety or load factor F as determined by conventional methods of design. As F usually exceeds 2.0, even a reduction of only 25% would still give a load factor of 1.5 in terms of conventional methods. This may result in a considerable saving in cost. A reasonable approach would therefore be to design such slabs to satisfy three requirements, viz.

(i) A reduced load factor of say 0.75F in terms of conventional methods provided that

(ii) the ultimate load as calculated by arching theory in conjunction with yield-line theory gives a load factor of at least 1.5F and

(iii) that visible cracks are unlikely to occur at the design load. The application of load factors in terms of arching resistance would require greater study than conventional systems as it is far more essential that the effects of dead

67/ loads ...

loads, non-dynamic superimposed loads, dynamic loads and cyclic loads should receive separate consideration.

The theory would have special application to structures such as bridge decks where large concentrated loads due to exceptionally heavy wheel loads may occur rarely in the lifetime of the structure. Even in large panels arching resistance to concentrated loads is very significant due to the "spreading" effect. The design of concrete road pavements and aircraft runways could be adapted to include arching theory as tests[4] [23] have indicated a very considerable increase of load-carrying capacity above that predicted by conventional bending theories.

As regards application of the theory to the first type the obvious procedure would be to so proportion the structure that the slab panels would have the highest possible arching resistance in terms of the material available as the problem in this case can be reduced to that of getting the optimum result as the magnitude of the forces may not be predictable with any accuracy. Where the maximum probable forces are known an application of the theory with a load factor of say 3.0 may be reasonable but so many factors are involved that a detailed discussion is beyond the scope of this work.

APPENDICES

TO BOOK III

APPENDIX III-1

A SEMI-ANALYTICAL THEORY OF ARCHING BASED ON IDEALIZED ELASTO-PLASTIC ASSUMPTIONS

III-1.1 Normally reinforced and plain concrete slab elements

As was explained previously crack formation is essential for arch action to develop. It may however be initiated at an early stage due to micro-cracking prior to the development of a well defined crack at any section when the steel reinforcement is still in the elastic range and the concrete compressive stresses are low. An accurate assessment of internal forces would accordingly require recognition of these facts. The incorporation of a stress-strain function for concrete which is initially linear but gradually deviates therefrom until the so-called plastic stress block is attained would however result in equations which are too complex for a direct analytical approach.

It will accordingly be assumed that the behaviour of a reinforced concrete slab can be equated to that of an idealized system consisting of perfectly elastic slab elements between the main cracks at which both the concrete in compression and the steel in tension are for an infinitesimal length assumed to be perfectly plastic. The inaccuracy of the assumption that no secondary cracks occur in these elements together with the non-linearity of the concrete stress-strain relationship is allowed for by an equivalent modulus of elasticity which is applied in conjunction with the Bernoulli-Euler theory as is common practice in the calculation of the deformation of concrete. The external elements or members providing the horizontal restraints are assumed to be perfectly elastic. Since conditions approximating to the assumed yield criteria only exist subsequent to yield of the steel reinforcement this theory can only apply in the ultimate range and it is necessary to establish an equivalent zero deflection ω_z as

indicated in fig. 9 to correct for the inefficiency of the arch action in the initial stages. This deflection parameter cannot be accurately determined by analytical methods.

Using the assumptions made in 1.6 and furthermore assuming that no differential deflection or rotation of the external elements at the supports takes place we can accordingly proceed to develop the compatibility equation.

With reference to fig. 10 the extension of the middle plane subsequent to the development of yield-lines can be expressed as follows :

$$\Delta_a = \Delta_L + \Delta_R$$

$$= \Delta_{cL} + \Delta_{cc} + \Delta_{cR} - \Delta_e - \Delta_\omega \qquad \ldots (29)$$

where $\Delta_a = \Delta_L + \Delta_R$ is the total horizontal spread of the supports at middle plane level,

$\Delta_{cL} + \Delta_{cc} + \Delta_{cR}$ is the sum of the crack widths at middle plane level.

Δ_e is the horizontal component of the elastic shortening of the elements

Δ_ω is the reduction in length of the horizontal component of the middle plane, or the so-called membrane shortening effect, due to deflection.

If R_L and R_R are respectively the moduli of horizontal restraint at middle plane level at the left and right supports expressed in force units per width b per unit deflection, and if the horizontal component of the arching compressive forces is H_a per width b then

$$\Delta_a = \Delta_L + \Delta_R$$

$$= \frac{H_a}{R_L} + \frac{H_a}{R_R}$$

$$= H_a \cdot \frac{R_L + R_R}{R_L R_R} = \frac{H_a}{R_a} \qquad \ldots (30)$$

*

FOOTNOTE TO PAGE 210

For the assumptions made, equations (33a) and (33c) are not accurate as the effect of rotation at the supports due to elastic deformation of the uncracked portions of the slab as derived from equations (38) and (39) should be incorporated. The magnitude of these rotations will depend on the loading and the reinforcement. However, the assumption of no rotation of the supports is not realistic either and if this is amended to read that the rotation of the supports is assumed to be of such magnitude as to give compatibility of bending rotations for the uncracked slab, then equations (33a) and 33c) become more precise. The total crack width would then be due to plastic deformation only. The actual rotations of the supports could be incorporated in the theory if the rotational restraints of the supports are known, but this would result in further complication.

where R_a is the "total modulus" of the support restraints per width b .

Using the same notation as in 2.2 and the yield stress block adopted by the B.S. Code of Practice C.P. 114 (1957) as indicated in fig. 11,

d_n = the depth of the neutral axis

$$= \frac{A_s f_y + H_a}{\frac{2}{3} u b \times 0.85} \qquad \ldots (31)$$

where

A_s = area of mild steel per width

f_y = yield stress of steel

u = cube strength of concrete

If the stress block is subdivided as shown

$$M_B = A_s f_y \left[d_1 - \frac{0.5 A_s f_y}{\frac{2}{3} u b} \right] \qquad \ldots (32)$$

where d_1 = effective depth of steel

If no rotation* or deflection of the supports takes place as in fig. 10 then the width of the cracks at middle plane level can be expressed as follows

$$\Delta_{cL} \doteq \left(\frac{d}{2} - d_n \right) \frac{\omega_p}{x_c} \qquad \ldots (33a)$$

$$\Delta_{cc} \doteq \left(\frac{d}{2} - d_n \right) \left(\frac{\omega_p L}{(L - x_c) x_c} \right) \qquad \ldots (33b)$$

$$\Delta_{cR} \doteq \left(\frac{d}{2} - d_n \right) \frac{\omega_p}{(L - x_c)} \qquad \ldots (33c)$$

where ω_p is the deflection at $x = x_c$ due to plastic rotation at the yield lines.

The horizontal component of the elastic shortening of the elements approximates to

$$\Delta_e \doteq \frac{H_a L}{E_c b d} \qquad \ldots (34)$$

The membrane shortening approximates to

$$\Delta_\omega \doteq \frac{\omega_c^2 L}{2 x_c (L - x_c)} \qquad \ldots (35)$$

where ω_c is the total deflection at $x = x_c$

Equation (29) then becomes

$$\frac{H_a}{R_a} \doteq \left(\frac{d}{2} - \frac{A_s f_y + H_a}{0.567\, ub}\right)\frac{2\omega_p L}{x_c(L-x_c)} - \frac{H_a L}{E_c bd} - \frac{\omega_c^2 L}{2x_c(L-x_c)} \quad \text{... (36)}$$

This equation is only applicable when the assumed yield criteria are attained after yielding of the steel. It can be expressed in differential form as was done using method (ii) for expressing compatibility but the accuracy is reduced thereby as several simplifying assumptions are necessary in order to obtain solutions which are only slightly less complicated than those obtained by this method.

If ω_e is the deflection at $x = x_c$ due to elastic deformation of the elements then

$$\omega_c = \omega_p + \omega_e + \omega_z \quad \text{.... (37)}$$

where ω_z is the equivalent zero deflection referred to above. Using the concepts previously established

$$\omega_e = -\frac{L-x_c}{L}\int_0^{x_c}\frac{Mx\,dx}{E_c I} - \frac{x_c}{L}\int_{x_c}^{L}\frac{M(L-x)dx}{E_c I} \quad \text{.... (38)}$$

where at any position x

$$M = M_B - \frac{b(\eta_B+\eta_a)x}{L}\int_0^L \phi(x)(L-x)dx - p_d\frac{bLx}{2} + b(\eta_B+\eta_a)\int_0^x \phi(x_1)(x-x_1)dx_1 + p_d\frac{bx^2}{2} + H_a\left(\frac{d}{2} - \frac{A_s f_y + 0.5H_a}{\frac{2}{3}u} - \omega_x - r_m\omega_p\right) \quad \text{.... (39)}$$

where η_a is the parameter associated with the load due to arching

x_1 is a dummy variable between the limits 0 and x

$$\omega_x \doteq -\frac{L-x}{L}\int_0^x \frac{Mx\,dx}{E_c I} - \frac{x}{L}\int_x^L \frac{M(L-x)dx}{E_c I} \quad \text{.... (40)}$$

I is the equivalent moment of inertia of the uncracked slab element including the steel reinforcement in terms of an effective modulus of elasticity of concrete, E_c.

$$r_m = \frac{x}{x_c} \quad \text{in the range} \quad x = 0 \text{ to } x = x_c$$

$$= \frac{L-x}{L-x_c} \quad \text{in the range} \quad x = x_c \text{ to } x = L$$

It will tentatively be assumed that $\omega_z = 0.5\,\omega_{ey}$ ... (41)

where ω_{ey} is the value of ω_e as given by equation (39) for the case $\eta_a = H_a = 0$

By taking moments about C and considering the left element we get, with reference to figs. 10 and 11

$$H_a\left(d - \frac{2A_s f_y}{\frac{2}{3}ub} - \frac{H_a}{\frac{2}{3}ub} - \omega_c\right) = b\eta_a\left[\frac{x_c}{L}\int_0^L \phi(x)(L-x)\,dx - \int_0^{x_c}\phi(x)(x_c-x)\,dx\right] \quad \text{... (42)}$$

where ω_c is the total deflection at C.

The interdependence of equations (39) and (40) makes the formulation of $\omega_x = \phi_2(x)$ extremely tedious and since $\omega_z \ll r_m\omega_p$ in the ultimate range we can with sufficient accuracy replace equation (40) by

$$\omega_x = r_m\,\omega_e \quad \text{... (40a)}$$

An additional justification for this assumption is the fact that the second term in the last bracket of equation (39) that is affected hereby is empirical with a variation in magnitude of similar order to the probable error in the above.

To find a solution for a particular slab complying with the assumptions made above the procedure is briefly as follows:

(a) Determine M_B from equation (32), and from equation (17) in 2.2 find the ultimate load P_B that the slab can resist in bending and the positions of the major cracks to establish x_c.

(b) For any particular loading $p = b\eta\phi(x) > b\eta_B\phi(x)$ find η_a from $\eta_a = \eta - \eta_B$ where η_B is found from equation (16) in 2.2

(c) Determine ω_z from equation (41)

(d) Assume a value for ω_c

(e) Solve for H_a from equation (42)

(f) Solve for ω_p from equation (36)

(g) Solve for ω_e from equation (37)

(h) Determine M as a function of x from equation (39) using the approximations of equation (40a)

(i) Check for ω_e from equation (38). Repeat procedure (d) to (i) by assuming different values for ω_c until (g) and (i) produce similar results.

By selecting a series of values η_a the relationship P (the total load) vs. ω_c can be established graphically from which $P_{max.}$, the maximum total load, and $\omega_{max.}$ the corresponding deflection can be determined by inspection. For low restraints (R_a), ω_e is not sensitive to variations in ω_c so that the procedure can be simplified by changing the order of operations.

The author did not pursue this method due to the fact that various empirical corrections were required and it did not at that stage appear to warrant the labours involved in finding solutions. Its application to two-way spanning slabs could only be done by making various approximate assumptions by which its fundamental nature would be lost in relation to the interpretation of test results. A more direct approach as presented in 2.2 was accordingly preferred.

D.L. Marriott[15] has recently (1963) presented a thesis in which he developed a method very similar to the above except that he assumed complete rigidity against horizontal spread at the supports and did not apply the correction ω_z . The results of laboratory

tests on plain concrete slabs and beams were compared by him with theoretical curves. His conclusions coincide with those stated above and confirm that a more realistic stress-function is required.

It is not the author's suggestion that fundamental theories should be permanently discarded but in the interim, until methods of coping with the various complexities are developed, the method developed in 2.2 may be useful.

APPENDIX III-2

NOTATION OF BOOK III

A = Constant of proportionality in stress function for concrete prisms.

A_s = Cross-sectional area of tensile steel reinforcement.

A_{sA}, A_{sB}, A_{sc} = Cross-sectional areas of tensile steel reinforcement at support A, at support B, and in the span at position C, respectively.

a = Dimension in two-way spanning slab panel defining crack pattern (See fig. 29).

B = Parameter used in stress function for concrete prisms.

b = Width of an element of slab

C_a = Compressive force acting at any particular section of a slab element induced by arch action.

C_s = Compressive force acting at any particular section of a slab element induced by bending in conjunction with the tensile steel reinforcement.

$C_T = C_s + C_a$ = Total compressive force acting at any particular section of a slab element.

C_{sA} = Compressive force acting in a slab element at A induced by bending in conjunction with the tensile steel reinforcement

c = Dimension in two-way spanning slab panel dependent on crack pattern (See fig. 29).

D = Parameter in arching stress function.

d = Total depth of slab

d = Dimension in two-way spanning slab panel, dependent on crack pattern (See fig. 29).

d_1 = Effective depth of tensile steel reinforcement measured from the outer compressive fibre.

d_a = Effective depth of slab available at any particular section for arch action after considering the bending resistance in conjunction with the tensile steel reinforcement.

d_{aA} , d_{aB} = effective depths of slab available for arch action at sections A and B, respectively.

d_n = Depth of neutral axis of slab at any particular section measured from the outer compressive fibres.

d_{nA} = Depth of neutral axis of slab at support A measured from outer compressive fibre.

E_c = Young's modulus for concrete

E_i = Young's modulus for the material of the hypothetical ideal slab.

e_a = Arching strain, which is not a true strain but is defined by arbitrary concepts.

e_{ap} = Arching strain at which the peak arching stress is attained

e_{ad} = Mean deviation of arching strain at peak stress from the initial linear relationship.

e_{at} = "True" arching strain which is the actual mean value of strain due to arching forces integrated over the whole span of the slab element.

e_{ac} = Arching strain calculated from experimental values at the first visible signs of local crushing of concrete at a major articulation.

e_{am} = Arching strain at the minimum value of R_e .

f_a = Arching stress by arbitrary definition (not a real stress value).

f_c = Compressive stress in concrete prisms subjected to uni-axial load.

f_y = Yield stress of tensile steel reinforcement.

F = Load factor

G = Parameter in arching stress function for one way spanning slab element.

G_e = Parameter in arching stress function as applied to two-way spanning slab panels and includes a correction factor.

H_a = Horizontal component of the arching force acting in a slab element.

H_E = Experimental value of H_a as determined in experiment by pressure cell.

I = Moment of inertia.

K_1 = $\frac{E_c}{m_{ait}}$

L = Span of one-way spanning slab element

L_1 = Short span of two-way spanning slab panel.

l_a = Lever arm of slab in bending

l_{aA} = Lever arm of slab in bending at support A.

m_{at} = Modulus of the "true" arching stress-strain curve.

m_a = Modulus of arching by arbitrary definition

m_{ai} = Initial modulus of arching.

m_{ait} = Initial modulus of the "true" arching stress-strain curve.

m_{it} = Initial elastic modulus of test slab (not directly related to arching modulus).

M = Bending moment

M_B = Moment of resistance due to bending at any particular section.

M_{fc} = The equivalent free-span bending moment at C due to the total load.

M_{fc}^A = The equivalent free span bending moment at C due to load P_A supported by arching forces.

M_{fc}^B = The equivalent free span bending moment at C due to the load P_B supported by bending forces.

n = Parameter in stress function for concrete prisms.

p = Parameter in arching stress function

p_d = Self weight of slab including finish (if any).

p = Intensity of uniformly distributed loading.

P = Unit concentrated load.

P_A = Ultimate load resisted by arching forces.

P_B = Ultimate load resisted by bending forces.

P_E = Total ultimate load determined by experiment.

P_T = Total theoretical ultimate load calculated by using measured value of H_E.

P_P = Most probable ultimate load predicted by arching theory in conjunction with yield-line theory.

q = Dimension in two-way spanning slab defining crack pattern (See fig. 29).

R_A, R_B, R_L, R_R = Moduli of horizontal restraints at the supports A, B, left support and right support, respectively.

R_a = Total modulus of support restraints per width b in semi-analytical theory.

R_e = Non-dimensional parameter giving horizontal restraint in terms of deformations of the slab.

R_F = Non-dimensional parameter giving horizontal restraint in terms of the slab properties.

R_s = Total modulus of horizontal restraint at supports.

R_{eo} = The apparent internal restraint factor for no restraint against horizontal spread.

R_{et} = The "true" internal restraint factor.

r_s = Steel ratio: $\frac{A_s d_1}{bd^2} \times 100$

r_m = $\frac{x}{x_c}$

S = Resultant vertical shear force due to arching forces acting across diagonal yield lines in slab panel.

T_A = Tensile force due to steel reinforcement at yield point.

Δ_{a04} = Actual spread of the equivalent unrestrained slab corresponding with $\Delta_u = 0.0004L$

Δ_b = Horizontal component of shortening effect due to bending in slab element.

Δ_c = Extension of the middle plane of slab due to opening of cracks.

Δ_{cc} = Horizontal spread due to crack opening in the span at C.

Δ_{cL} = Horizontal spread due to crack opening at left-hand support.

Δ_{cR} = Horizontal spread due to crack opening at right hand support.

Δ_e = Horizontal component of the elastic shortening of the slab elements .

Δ_L = Horizontal spread of left-hand support.

Δ_p = Horizontal deformation or spread at the perimeter or ends of slab measured at a particular level.

Δ_R = Horizontal spread of right hand support.

Δ_r = Horizontal component of "rib-shortening" effect due to arch action.

Δ_s = Shortening of the middle plane of slab due to arch compression.

Δ_u = Theoretical unrestrained spread of slab elements.

Δ_w = Effective shortening of horizontal component of middle plane of slab due to membrane deflection.

Δ_θ = Spread of the perimetral neutral axis of slab due to rotation of slab elements.

ε = Concrete strain.

ε_m = Concrete strain at peak stress.

η = Parameter defining magnitude of applied load.

η_B = Parameter defining magnitude of load resisted by bending forces.

η_a = Parameter defining magnitude of load resisted by arching forces.

ξ_1, ξ_2 = Unknown functions relating the initial arching modulus and the cube strength of the concrete.

ϕ = A function of strain giving the deviation of strain in the stress function for concrete prisms.

ϕ_a = Arching stress function in terms of arching strain.

ϕ_2 = is a function for ω_x in terms of x .

ψ = the modulus of restraint R_s expressed as a function of Δ_a .

APPENDIX III-3

REFERENCES

1. TAYLOR, THOMPSON & SMULSKI. Concrete plain and reinforced. Vol. 1. John Wiley & Sons. pp. 115.

2. TAYLOR, THOMPSON & SMULSKI. Concrete plain and reinforced. Vol. 1. John Wiley & Sons. pp. 367.

3. THOMAS, F.G. Studies in reinforced concrete VIII. The strength and deformation of some reinforced concrete slabs subjected to concentrated loading. Technical Ppaer No. 25. H.M.S.O. London.

4. HARRIS, A.J. Prestressed concrete runways: History, practice and theory. Proc. Inst. Civil Engrs. January 1957. pp. 46.

5. GUYON, Y. Essai sur des dalles continues précontraintes. Annales de l'institut technique du batiment et des travaux publics. November 1955.

6. GUYON, Y. Prestressed Concrete. Vol. 2. John Wiley & Sons.

7. LIEBENBERG, A.C. Load tests on stairways of a reinforced concrete building in Johannesburg. The Concrete Association - Johannesburg. December 1956. pp. 22.

8. OCKLESTON, A.J. Load tests on a three storey reinforced concrete building in Johannesburg. The Structural Engineer. October 1955. pp. 304.

9. OCKLESTON, A.J. Arching action in reinforced concrete slabs. The Structural Engineer. June 1958. pp. 197.

10. THOMAS, F.G. The strength of brickwork. The Structural Engineer. February 1953. pp. 44.

11. McDOWELL, E.L., MCKEE, K.E. & SEVIN, E. Arching action theory of masonry walls. Proc. Am. Soc. Civil Engrs. Vol. 82. No. ST.2 March 1956. pp. 915 - 1.

12. McKEE, K.E. & SEVIN, E. Design of masonry walls for blast loading. Proc. Am. Soc. Civil Engrs. No. ST1. January 1958. pp. 1512 - 1.

13. ROBERTSON, R.G., LIEBENBERG, A.C. McGAW. D.J. Contribution to discussion on paper 'Arching action in reinforced concrete slabs' by Prof. A.J. Ockleston. The Structural Engineer. Dec. 1958.

14. WOOD, R.H. Plastic and elastic design of slabs and plates. Thames and Hudson. London pp. 245 - 261.

15. MARRIOTT, D.L. The behaviour of plain concrete slabs under transverse load and lateral restraint. Thesis for degree of MSc. University of Natal. 1963.

16. CHRISTIANSEN, K.P. The effect of membrane stresses on the ultimate strength of the interior panel in a reinforced concrete slab. The Structural Engineer. August 1963. pp. 261 - 265.

17. LIEBENBERG, A.C. Correspondence on 'The effect of membrane stresses on the ultimate strength of the interior panel in a reinforced concrete slab' by K.P. Christiansen. The Structural Engineer. January 1964.

18. LIEBENBERG, A.C. A stress-strain function for concrete subjected to short term loading. Magazine of Concrete Research No. 41. July 1962. Cement & Concrete Association. pp. 85 - 90.

19. SLATE, F.G. & OLSEFKI, S. X-rays for study of internal structure and micro-cracking of concrete. Journal of the American Concrete Institute. May 1963. No. 5. Proceedings V. 60. pp. 575.

20. FERGUSON, P.M. Recent trends in ultimate strength design. Proc. A.S.C.E. Vol. 87. No. ST1. January 1961.

21. JOHANSEN, K.W. Yield-line theory translated from the Danish. Cement and Concrete Association.

22. OCKLESTON, A.J. & SCOTT, I.R. The determination of the properties of materials from the Old Dental Hospital. The Concrete Association, Johannesburg. October 1956. Paper No. 2.

23. LIEBENBERG, A.C. Contribution to discussion 'load-carrying capacity of concrete pavements' by G.G. Meyerhof, Journal of the Soil Mechanics & Foundations Division of the Proceedings of the A.S.C.E. Vol. 88. June 1962 Part I.

APPENDIX III - 4a.

Analysis of Laboratory Tests.

SLAB M1 (See Table 1 and Fig. 17.)

Row.

14 $$d_a = d - \frac{(A_{SA} + A_{SC})f_y + H_E}{\frac{2}{3}ub}$$

$$= 3.19 - \frac{2 \times 5750 + 7230}{\frac{2}{3} \times 1870 \times 12} = 1.94 \text{ ins.} \rightarrow$$

15. $$l_{aA} = d_1 - \frac{0.5\, A_{SA} f_y}{\frac{2}{3}ub}$$

$$= 2.41 - \frac{0.5 \times 5750}{\frac{2}{3} \times 1870 \times 12} = 2.22 \text{ ins.}$$

$$P_B = \frac{8}{L}\left(A_s f_y \times l_a - p_d \frac{L^2}{16}\right)$$

$$= \frac{8}{72}\left(5750 \times 2.22 - 40 \times \frac{6^2}{16} \times 12\right) = 1300 \text{ lb.} \rightarrow$$

16. $$P_A = \frac{4 H_E}{L}(d_{aA} - w_{ce})$$

$$= \frac{4 \times 7230}{72}(1.94 - 0.61) = 535 \text{ lb.} \rightarrow$$

17. $$\therefore P_T = P_B + P_A = 1835 \text{ lb.} \rightarrow$$

18 $$\therefore \frac{P_E}{P_T} = \frac{2000}{1835} = 1.09 \rightarrow$$

19 $$\alpha = \frac{ub\left[H_E(d - w_{ce}) - P_E\frac{L}{4} - p_d\frac{bL^2}{8} + (A_{SA} + A_{SC})f_y d_1\right]}{2H_E(A_{SA} + A_{SC})f_y + 2H_E^2 + A_{SA}^2 f_y^2 + A_{SC}^2 f_y^2}$$

$$= \frac{1870 \times 12\left[7230(3.19 - 0.61) - 2000\frac{72}{4} - 40 \times \frac{12}{8} \times 6^2 + (2 \times 5750)2.41\right]}{2 \times 7230(2 \times 5750) + 2(7230)^2 + 2(5750)^2}$$

$$= 0.55 \rightarrow$$

Row 36.

Calculation of the Most Probable Load P_p.

(1) $P_B = 1300$ lb. (see previous page)

(2) Assume $e_a = 0.0008$

(3) $\therefore f_a = \frac{G\sqrt{u}}{(1+3.5r_s)}\left[1 - 6890\, e_a^{1.5}\right] e_a$

From fig. 21 $\frac{G}{1+3.5r_s} = 7700$ lb/in.

for $r_s = 0.289$ and $R_s/b = 200.000$ lb/in.

$\therefore f_a = 7700 \times \sqrt{1870}\left[1 - 6890(0.0008)^{1.5}\right]0.0008$

$= 220$ lb/□"

(4) $\therefore H_a = f_a bd = 220 \times 12 \times 3.19 = 8420$ lb.

(5) $\therefore d_{aA} = d - \frac{(A_{sA} + A_{sc})f_y + H_a}{\frac{2}{3}ub}$

$= 3.19 - \frac{(2 \times 5750) + 8420}{\frac{2}{3} \times 1870 \times 12} = 1.86$ in.

(6) $H_a = \psi(\Delta_a) = R_s \cdot \Delta_a = 200.000 \times \Delta_a$ lb.

$\therefore \Delta_a = \frac{8420}{2 \times 10^5} = 0.0421$"

(7) $\therefore \Delta_u = (0.0008) \times 72 + 0.0421 = 0.0997$ in.

(8) $\Delta u = \frac{4w_c}{L}\left(d - \frac{w_c}{2}\right)$

$\therefore w_c = d\left(1 - \sqrt{1 - \frac{\Delta_u L}{2d^2}}\right) = 0.63$ in.

(9) $\therefore P_A = \frac{4H_a}{L}(d_a - w_c) = \frac{4 \times 8420}{72}(1.86 - 0.63)$

$= 580$ lb.

$\therefore P_T = P_A + P_B = 580 + 1300 = \underline{1880}$ lb.

By repeating the above procedure for a series of values of e_a the curve shown in fig. 21 was drawn from which the peak load and the corresponding deflection could be determined.

The values calculated above coincided almost exactly with the peak values. The shape indicated a very small increase up to $w_c = 0.68''$.

APPENDIX III - 4b.

Laboratory Tests. — Semi-analytical theory.

Slab No. M1 (see Table I. and Fig. 17)

Estimate of ultimate load by semi-analytical theory (see Appendix III - 1)

(a) $M_B = A_{sf}f_y\left(d_1 - \frac{0.5\,A_{sf}f_y}{\frac{2}{3}u.b}\right)$

$= 5750\left(2.41 - \frac{0.5\times 5750}{8\times 1870}\right)$

$= 12{,}750$ lb. ins.

$A_{sf}f_y = 5750$
$d_1 = 2.41''$
$b = 12''$
$u = 1870$ lb/in²
$d = 3.19''$
$L = 72''$

For concentrated midspan loading ($x_c = \frac{L}{2}$)

$P_B = \frac{2M_B - p_d L^2/8}{L/4}$

$= \frac{(2\times 12750) - (3.32\times \frac{72^2}{8})}{72/4}$ lb

$= 1{,}298$ lb.

$p_d = \left(\frac{12\times 3.19\times 150}{1728}\right)$ lb/ins.

$= 3.32$ lb/in.

(b) Try $P = 1700$ lb $\therefore$ $P_a = 402$ lb.

(c) w_{ey} for ordinary bending only ($H_A = H_A = 0$)

$M = M_B - \frac{P_B}{2}.x - \frac{p_d L}{2}.x + \frac{p_d x^2}{2}\left[+P_B\left(x-\frac{L}{2}\right)\right]$

[for $x > x_c = \frac{L}{2}$]

$w_{ey} = -\frac{1}{2E_cI}\int_0^{\frac{L}{2}}\left(M_B x - \frac{P_B x^2}{2} - \frac{p_d L x^2}{2} + \frac{p_d x^3}{2}\right)dx$

$-\frac{1}{2E_cI}\int_{\frac{L}{2}}^{L}\left(M_B L + \frac{P_B L}{2}.x - \frac{p_d L^2}{2}x + \frac{p_d L x^2}{2} - \frac{P_B L^2}{2}\right.$

$\left. - M_B x - \frac{P_B x^2}{2} + \frac{p_d L x^2}{2} - \frac{p_d x^3}{2} + \frac{P_B L x}{2}\right)dx$

$= -\frac{1}{2E_cI}\left(\frac{M_B L^2}{4} - \frac{P_B L^3}{24} - \frac{5}{192}p_d L^4\right)$

Equivalent Moment of Inertia I

$\bar{x}$ ↓ ↑ --

	A	x	Ax	$\frac{Ad^2}{12}$	$A(x-\bar{x})^2$
Concrete (12×3.19)	38.28	1.595	61.1	32.45	0.03
steel $(3 \times 0.049 \times \frac{30}{3.015})$	1.461	0.78	1.14	—	0.91
	39.74		62.24	32.45	0.94

$\bar{x} = 1.568''$ $\quad I = 33.39 \text{ in}^4$.

$$\therefore w_{ey} = -\frac{1}{2 \times 3.015 \times 10^6 \times 33.39}\left(\frac{12750}{4}.72^2 - \frac{1298.}{24}72^3 - \frac{5}{192} \times 332 \times 72^4\right) \text{ ins.}$$

$$= +0.0298 \quad \text{say } 0.03''.$$

Assume $w_z = 0.5\, w_{ey} = 0.015''$

1st trial :

(d) Try $w_t = 0.60$ ins. ..... where w_t is a trial value for w_c.

(e) $$H_a\left(d - \frac{2A_s f_y}{\frac{2}{3}u} - \frac{H_a}{\frac{2}{3}u} - w_t\right) = \eta_a\left[\frac{x_c}{L}\int_0^L \phi(x)(L-x)\,dx - \int_0^{x_c} \phi(x)(x_c - x)\,dx\right]$$

$$= \frac{\rho_a L}{4} - 0$$

$$\therefore 12H_a\left(3.19 - \frac{2 \times 5750}{\frac{2}{3} \times 12 \times 1870} - \frac{H_a}{\frac{2}{3} \times 1870} - 0.60\right) = \frac{402 \times 72}{4}$$

$$\therefore 0.0096\, H_a^2 - 21.84\, H_a + 7240 = 0$$

$$\therefore H_a = 401 \text{ lb/in.}$$

$$\therefore H_a b = 401 \times 12 = 4810 \text{ lb.}$$

(f) $$\frac{H_a b}{k_a} = \left(\frac{d}{2} - \frac{A_s f_y + H_a}{0.567\, u}\right) w_p \frac{2L}{x_c(L-x_c)} - \frac{H_a L}{E_c d} - \frac{w_t^2 L}{2x_c(L-x_c)}$$

$$\therefore \frac{4810}{200{,}000} = \left(1.595 - \frac{5750 + 4810}{12720}\right)\frac{w_p}{9} - \frac{401 \times 7.5}{10^6} - \frac{(0.60)^2}{36}$$

$$\therefore w_p = 0.436 \text{ ins.}$$

(g) $$\therefore w_c = 0.60 - 0.436 - 0.015 = 0.149 \text{ ins.}$$

(h) $M = M_B - \frac{P}{2}x - \frac{p_d L}{2}x + \left[P\left(x - \frac{L}{2}\right)\right] + \frac{p_d x^2}{2}$ (for $x > \frac{L}{2}$ only)

$+ H_A\left(\frac{d}{2} - \frac{A_s f_y + H_a}{\frac{2}{3}u} - \frac{2x}{L}(w_e + w_p)\right)$ ($L - x$ for $x > \frac{L}{2}$)

$= 12{,}750 - 969.5x + 1.66x^2$

$+ 4810\left(1.595 - \frac{5750 \times 2405}{8 \times 1870} - \frac{0.585}{36}x\right)$

$= 17{,}800 - 1047.6x + 1.66x^2$

(i) $\therefore \quad w_e = -\frac{1}{E_c I}\left[8900x^2 - 349.2x^3 + 0.415x^4\right]_0^{36}$

$= -\left(\frac{11.53 - 16.20 + 0.70}{3.015 \times 33.39}\right) = +0.041$ ins.

c.f. 0.149 ins.

Similarly.

2nd. Trial $w_t = 1.00$ in.

$w_p = 1.404'' > w_t$.

Final Trial $w_t = 0.87''$

$w_p = 0.815$

$w_e = 0.040$

and $w_e = 0.043$ } c.f. O.K.

i.e. $P = 1700$ lb $w_t = 0.87$ ins.

Similary. $P = 1500$ lb. $w_t = 0.13$ ins.

$P = 1600$ lb $w_t = 0.21$ ins.

$P = 1700$ lb $w_t = 0.31$ ins.

$P = 1750$ lb $w_t = 0.46$ ins

For curve see Fig. 17.

APPENDIX III - 5

Analysis of Alliance House Tests.

TEST NO. T13 on Panel 6-B4

(see Table 4(6) and Fig. 37)

Corrected Test Results.

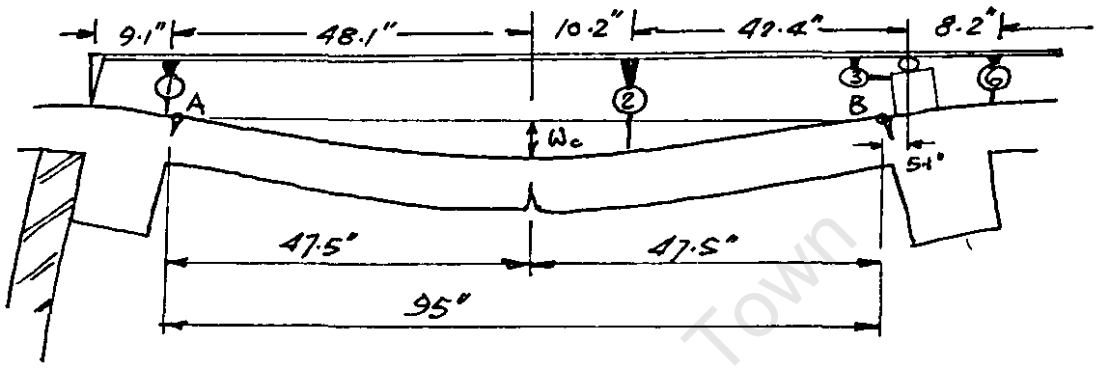

Correction Factor for ② for ℄ deflection

$$= \frac{47.5}{47.5 - 10.2} = 1.28 .$$

Deflection of pt. A below original line $= \frac{9.7}{9.1} \times ① = w_A$

" " " B " " " $= \frac{5.1}{8.2} \times ⑥ = w_B$

Then $w_c = 1.28\, w_2 - \left(\frac{w_A + w_B}{2}\right)$

Total Expansion : $\Delta_a = \frac{4.8}{9.1} \times ① + \frac{7.5}{8.2} \times ⑥ - ③$

Panel dimensions.

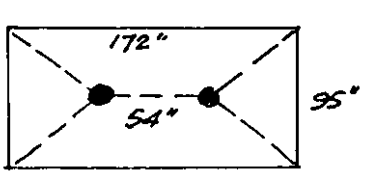

$L_1 = 95"$ $\quad d = 4.8"$

$L_2 = 172"$ $\quad d_1 = 4.2$

$q = 54"$ $\quad u = 4000\ lb/in^2$

$a = 59"$ $\quad A_{sc} f_y = 7598\ lb/ft.$

$$\therefore \frac{2a}{L_1} + \frac{L_1}{2a} = 1.24 + 0.804 = 2.045.$$

$$\frac{q}{L_1} = \frac{54}{95} = 0.57.$$

$\Sigma = 2.615$

5.2

Dials on Struts	Load P_T (kips)	Deflections 1	6	3	2 corr.**	w_A $\frac{9.7}{9.1}\times$①	w_B $\frac{9.1}{8.2}\times$⑥	$\frac{w_A+w_B}{2}$	w_c (ins. $\times 10^3$)	$\frac{4.8}{9.1}\times$①	$\frac{7.5}{8.2}\times$⑥	Δ_a* (ins. $\times 10^3$)
0	0	0	0	0	0	0	0	0	0	0	0	0
1	4.3	-0.7	1.5	0.8	-12.0	0.7	0.9	0.8	11.2	0.4	1.4	1.0
2	8.6	-1.6	3.2	1.9	-26.9	1.7	2.0	1.9	25.0	0.8	2.9	1.8
3	12.9	-2.3	5.0	3.3	-41.5	2.5	3.1	2.8	38.7	1.2	4.6	2.5
4	17.2	-3.0	7.1	5.3	-57.0	3.2	4.6	3.9	53.1	1.6	6.8	3.1
5	21.5	-3.7	10.2	7.1	-75.5	3.9	6.3	5.1	70.4	2.0	9.3	4.2
6	25.8	-4.1	12.9	9.4	-99.2	4.4	8.0	6.2	93.0	2.2	11.8	4.6
7	30.1	-4.2	17.8	11.5	-129.2	4.5	11.1	7.8	121.4	2.2	16.3	7.0
8	34.4	-4.2	25.0	14.0	-182.0	4.5	15.5	10.0	172.0	2.2	22.8	11.0
9	38.6	-3.8	33.6	16.2	-242	4.05	20.9	12.5	230	2.0	30.7	16.5
10	42.6	-3.2	44.6	19.2	-321	3.4	27.7	15.6	305	1.7	40.8	23.3
11	46.6	-2.7	57.7	22.1	-416	2.9	35.9	17.4	399	1.4	52.7	32.0
11.5	48.5	-2.0	71.2	24.5	-515	2.1	44.3	23.2	492	1.1	65.0	41.6
12 → 11.5	50.4	-1.4	83.7	26.5	-610	1.5	52.0	26.8	583	0.7	76.5	50.7
11.8 → 11.5	48.9	-1.1	89.3	27.6	-651	1.2	55.5	28.4	623	0.6	81.6	55.6
13	54.2	-0.3	109.1	30.8	-835	0.3	67.9	34.1	801	0.2	99.8	69.2
13.5	56.0	-0.9	114.2	11.4	-1258	1.0	71.0	36.0	1212	0.5	104.6	93.7
14	57.9	-	-	-	-2430	-	-	-	2400±	-	-	-
13.0 → 12.0	52.3	+22	118.5	-21.7	-3025	-23.5	73.6	25.1	3000	-11.6	108.3	124.4

* $\Delta_a = -③ + ⑥\frac{7.5}{8.2} - ①\frac{4.8}{9.1}$

** $2_{corr.} = 1.28 \times w_2$

---

(4) Determination of P_B

By yield-line theory if total self-weight is taken by bending forces

$P_B \doteq \underline{16500\ lb.} \rightarrow$

$$d_a = d - \frac{(A_{SA} + A_{SC})f_y + H_a}{2/3\,u\,b} \qquad A_{SA} = 0$$

$$= 4.8 - \frac{7598 + H_a}{32000}$$

$$= 4.56 - 0.312 \times 10^{-4} H_a$$

Now from equation 28a.

$$P_A = \frac{H_a}{3}\left\{(d_a - \frac{w_c}{2})(\frac{2a}{L_1} + \frac{L_1}{2a}) + (d_a - w_c)\frac{2}{L_1}\right\}$$

$$= \frac{H_a}{3}\left\{2.615(4.56 - 0.312\times10^{-4}H_a) - 1.59\,w_c\right\}$$

$$= -0.0000272\,H_a^2 + (3.97 - 0.53\,w_c)H_a$$

$$\therefore P_T = P_B + P_A = 16500 + (3.97 - 0.53\,w_c)H_a - 0.0000272H_a^2$$

$$\therefore H_a = \frac{(3.97 - 0.53\,w_c) \pm \sqrt{(3.97 - 0.53w_c)^2 - 0.0001088(P_T - 16500)}}{0.0000544} \rightarrow$$

$$e_a = \frac{\Delta_u - \Delta_a}{L}$$

$$= w_c\left(\frac{4d}{L^2}\right) - w_c^2\left(\frac{2}{L^2}\right) - \frac{\Delta_a}{L}$$

$$= w_c\left(\frac{4\times4.8}{95^2}\right) - w_c^2\left(\frac{2}{95^2}\right) - \frac{\Delta_a}{95}$$

$$= (21.3\times10^{-4})w_c - (2.22\times10^{-4})w_c^2 - \frac{\Delta_a}{95} \rightarrow$$

$$\Delta_u = 0.202\,w_c - 0.0211\,w_c^2 \rightarrow$$

$$r_s = \frac{A_{sc}\times d_1}{2bd^2}\times100$$

$A_{sc} = \frac{3}{8}"\phi + \frac{1}{2}"\phi$ alt @ 12"

0.11

0.195

0.305

$= 0.152$ □" per ft

$$= \frac{0.152\times4.2}{2\times12\times4.8^2}\times100$$

$$= 0.116 \rightarrow$$

$$f_a = \frac{G_e\sqrt{u}}{1+3.5r_s}\left[1 - 6890\,e_a^{1.5}\right]e_a$$

$$\therefore G_e = \frac{(1+3.5r_s)f_a}{\sqrt{u}\left[1-6890e_a^{1.5}\right]e_a} = \frac{0.022\,f_a}{\left[1-6890\,e_a^{1.5}\right]e_a}$$

$$= 0.386\times10^{-3}\,\frac{H_a}{X}$$

where $X = \left[1 - 6890\,e_a^{1.5}\right]e_a$

$$R_e = \frac{\Delta_u - \Delta_o}{\Delta_u}$$

Total Ld. P_T lb.	w_c ins.	Δ_a ins.	Δ_u ins.	e_a ins./ins. $\times 10^{-3}$	X ins/in $\times 10^{-3}$	H_a lb./ft.	G_e lb/in.	R_e
4,300	0·011	0·0010	0·0022	0·013	0·013	−2900	−86,000	0·545
8,600	0·025	0·0018	0·0051	0·035	0·035	−1900	−21,000	0·647
12,900	0·039	0·0025	0·0079	0·057	0·057	−800	−5.400	0·683
17.200	0·053	0·0031	0·0106	0·079	0·078	+260	+1280	0·708
21,500	0·070	0·0042	0·0140	0·103	0·102	+1400	+5100	0·700
25800	0·093	0·0046	0·0186	0.147	0.145	+2500	+6600	0-753
30 100	0·121	0·0070	0·0241	0.180	0.177	+3700	+8000	0·710
34,400	0·172	0·0110	0·0342	0·244	0·238	+4900	+7800	0·679
38,600	0·230	0·0165	0·0454	0·304	0·293	+6100	+8000	0·636
42600	0·305	0·0233	0·0595	0·381	0·362	+7.400	+7,800	0·609
46,600	0·399	0·0320	0·0771	0·475	0·440	+8,600	+7500	0·585
48.500	0·492	0·0416	0·0943	0·555	0·505	+9200	+7,000	0·559
50, 400	0·583	0·0507	0·1107	0·632	0·583	+10,000	+6800	0·543
48900	0·623	0·0556	0·1178	0·655	0·579	+9600	+6400	0·529
54 200	0·801	0·0692	0·1483	0·833	0·695	+11,500	+6350	0·533
57, 900	2.4 (approx.)	—	0·363	—	—	+18500	—	—

L.

APPENDIX III - 6.

Estimate of ultimate load for two-way spanning slab of the Old Dental Hospital building, Johannesburg tested by Prof. A.J. Ockleston.

(see reference 9.)

Slab dimensions: Short span $L_1 = 13'6'' = 162''$

Long span $L_2 = 15'10\frac{1}{2}'' = 190.5''$

Mean overall thickness of slab $d = 5.3''$.

(including 0.75" thick top screed.)

Mean cover over reinforcement in short span direction:

Top, including screed = 2.40"

Bottom = 0.55"

Effective depth d_1 at Midspan = 5.30 − 0.55 − 0.18 = 4.57"

Supports = 5.30 − 2.40 − 0.18 = 2.72"

Mean effective depth $d_1 = 3.65''$

Cube strength $u = 4200\ lb/\square''$

Area of steel reinforcement per foot width of slab:

Short span direction: Midspan 0.120; Supports 0.130 } Mean 0.125 $\square''/ft$.

	A_s ($\square''/ft$)	Yield stress (f_y)	$A_s f_y$ (lb/ft)
3/8" ϕ steel	0.0765	45,800	3500
5/16" ϕ " (av.)	0.0485	43,700	2120
	$\Sigma = 0.125$		5620

then

$$r_s = \frac{A_s d_1}{bd^2} \times 100 = \frac{0.125 \times 3.65 \times 100}{12 \times 5.30 \times 5.30} = 0.135$$

in short span direction

$$f_a = \frac{G\sqrt{u}}{(1+3.5r_s)}\left[1 - D(e_a)^p\right]e_a \quad \text{where} \quad D = 6890, \quad p = 1.5$$

Assuming $\boxed{G = 10{,}000\ ^{lb^{1/3}}/_{in} \qquad R_c = 0.40}$

then

$$f_a = \frac{10{,}000\sqrt{4{,}200}}{1+3.5(0.135)}\left[1 - 6890(e_a)^{1.5}\right]e_a$$

$$= 440{,}000\left[1 - 6890(e_a)^{1.5}\right]e_a$$

For $e_a = 0.0003$

$f_a = 127.1\ ^{lb}/_{\square"}$. $\therefore H_a = f_a bd$

$= 127.1 \times 12 \times 5.3$

$= 8{,}080$ lb. per ft.

$$\therefore d_{aA} = d - \frac{(A_{sA} + A_{sc})f_y + H_a}{\frac{2}{3}u.b}$$

$$\therefore d_a = 5.3 - \frac{(5620 \times 2) + 8080}{\frac{2}{3} \times 4200 \times 12} = 5.3 - 0.6$$

$= 4.7"$.

$$m_a = \frac{f_a}{e_a} = \frac{127.1}{0.0003} = 423{,}700\ ^{lb}/_{in^2}.$$

$$R_F = \frac{H_a L_1}{m_a bd \Delta_a} = \frac{R_c}{1-R_c} = \frac{0.40}{0.60} = 0.667$$

$$\therefore \Delta_a = \frac{8080 \times 162}{423{,}700 \times 12 \times 5.30 \times 0.667} = 0.073"$$

$$e_a = \frac{\Delta_u - \Delta_a}{L_1} \quad \therefore \Delta_u = e_a L_1 + \Delta_a$$

$= (0.0003 \times 162) + 0.073$

$= 0.122$ ins.

Also $\Delta_u = \dfrac{w_c L_1 (d - \frac{w_c}{2})}{x_c (L_1 - x_c)}$ $\qquad x_c = L_1 - x_c = \frac{L_1}{2}$

$$= \frac{4 w_c (d - \frac{w_c}{2})}{L_1}$$

$$\therefore 0.122 = \frac{w_c (5.30 - \frac{w_c}{2})}{40.5}$$

$$\therefore w_c^2 - 10.6\, w_c + 9.88 = 0$$

$$\therefore w_c = \frac{10.6 \pm \sqrt{112.4 - 39.4}}{2} = 1.025" \rightarrow$$

6.4

The curves plotted from the above values are given below. Fig. 42 was based on $G = 10{,}000$ lb½/in, $R_e = 0.40$

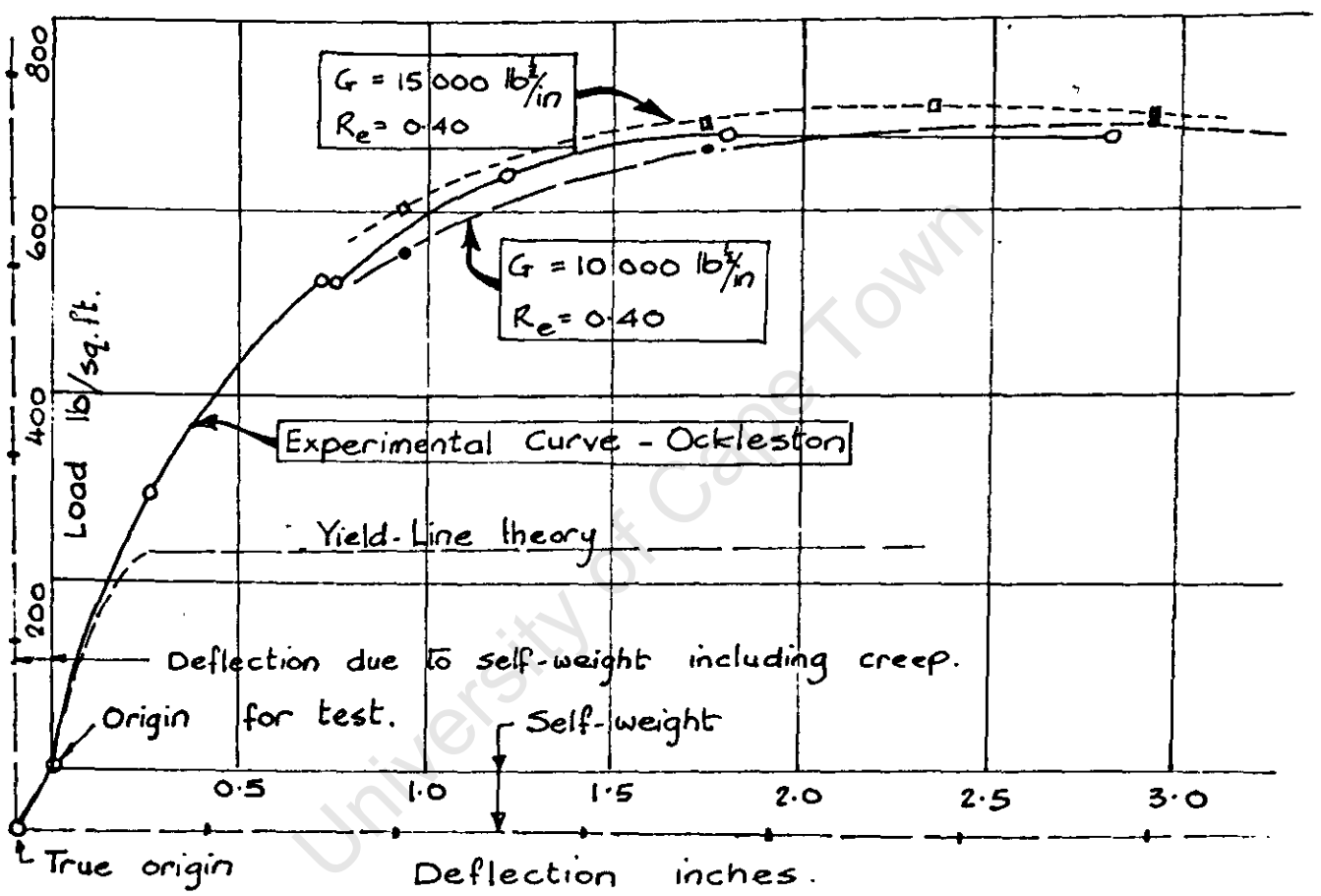

From the above curves it would appear that

$G = 13000$ lb½/in
$R_e = 0.38$

are the approximate values for the parameters of the above slab.

—

APPENDIX III-7

TABLES

AND

DIAGRAMS

OF

BOOK III

The author wishes to apologise for the odd sizes of the following diagrams and tables. These have been prepared for block-making for publication purposes.

✳

FOOTNOTE TO TABLE 1 ON PAGE 239

The ultimate load recorded for test M15 is almost certainly not the true maximum. The pressure cell recording vertical load began leaking immediately afterwards and the vertical load vs. vertical deflection graph showed a sudden drop which was not compatible with the horizontal force applied. The recorded value for the P_E/P_P ratio should therefore be discarded.

TABLE 1. ARCHING TESTS ON 12" WIDE SLAB ELEMENTS WITH CONCENTRATED MID-SPAN LOADING.

No	ITEM Detail	Symbol	Units	SLAB NUMBERS M1	M2	M3	M4	M5	M6	M7	M8	M9	M10	M11[xx]	M12	M13	M14	M15	M16	M17	M18
1	Average Depth	d	inches	3·19	3·22	3·11	3·20	3·17	3·06	3·13	3·03	3·19	3·08	3·13	3·33	3·22	3·19	3·14	3·04	3·23	3·05
2	Effective Span	L	inches	72	72	72	72	72	72	72	72	96	96	48	48	72	72	72	72	72	72
3	Reinforcement			3-¼-A	3-¼-A	3-¼-A	3-¼-A	3-¼-A	3-¼-A	3-¼-A	3-¼-A	3-¼-A	3-¼-A	3-¼-A	3-¼-A	3-⅜-A	3-⅜-A	NIL	NIL	5-⅜-A	5-⅜-A
4	Total Yield Force	Asfy	lb.	5750	5700	5475	5525	5275	5700	5475	5600	5700	6175	5150	5750	15250	15200	—	—	25100	25200
5	Concrete Mix by weight			1:4·12:4·34		1:1·54:2·04		1:2·18:2·88		1:2·24:2·98		1:2·23:3·07		1:2·20:3·03		1:2·27:2·97		1:2·27:2·97		1:2·27:2·97	
6	Water/Cement Ratio			0·93		0·41		0·55		·0·54		0·55		0·56		0·56		0·56		0·56	
7	Cube Strength	u	lb/in²	1870	1540	6530	6810	4810	4765	5180	5130	5210	5150	4690	4510	4480	3980	4720	3650	4025	3999
8	Age		days	41	48	45	46	55	47	49	43	60	61	61	62	51	29	42	46	28	29
9	Elastic Modulus of Prisms	E_c	lb/in²×10³	3015	3160	4860	4765	4700	4805	4190	4720	4245	—	4590	3950	4140	—	4460	—	—	4175
10	Horizontal End Restraint	Rs	lb/in×10⁻³	200	300	300	200	300	300	100	200	300	300	300	200	300	300	300	300	300	300
11	Maximum Vertical Load	P_E	lb	2000	2110	3230	3160	2430	2570	2290	2580	1640	1700	4750	4800	4540	4360	1440	1720	5800	5210
12	Horizontal Force corr. with P_E	H_E	lb	7230	8060	19060	16220	13500	17400	9380	13580	13680	13550	19400	19820	15170	14980	12110	19600	15380	11480
13	Average Effective Depth	d_1	inches	2·41	2·50	2·48	2·42	2·10	2·38	2·35	2·39	2·53	2·44	2·48	2·53	2·47	2·46	—	—	2·44	2·28
14	Effective Arching Depth	d_a	inches	1·94	1·64	2·53	2·70	2·55	2·31	2·64	2·45	2·59	2·46	2·34	2·46	1·95	1·76	2·82	2·37	0·90	1·11
15	Theoretical Load by Bending	P_B	lb	1300	1320	1360	1335	1070	1350	1270	1335	1010	1075	2000	2270	3710	3630	-118	-115	5590	5145
16	Theoretical Load by Arching	P_A	lb	535	495	1660	1580	1455	1350	850	1180	905	830	2310	2940	935	650	1430	1720	-161	-38
17	Total Theoretical Load	P_T	lb	1835	1815	3020	2915	2525	2700	2120	2515	1915	1905	4310	5210	4645	4280	1312	1605	5429	5107
18	Ratio P_E/P_T			1·09	1·16	1·07	1·09	1·04	0·95	1·08	1·03	0·86	0·89	1·10	0·92	0·98	1·02	1·10	1·07	1·07	1·02
19	Factor α	α		0·55	0·50	0·52	0·42	0·87	0·88	0·33	0·62	1·33	1·10	0·50	0·97	0·81	0·70	0·14	0·64	0·73	0·74
20	Load causing visible spalling	P_S	lb	MAX[x]	PM[x]	MAX	2900	2400	2400	2250	2500	1650	MAX	4400	4500	MAX	4000	PM	PM	5600	5000
21	Central Deflexion at spalling	W_{cs}	inches	0·61	0·79	0·96	0·66	0·60	0·60	0·92	0·68	0·95	0·96	0·60	0·48	0·84	0·60	0·80	0·86	0·78	0·68
22	Central Defln at Maxm Load	W_{ce}	inches	0·61	0·54	0·96	0·95	0·64	0·91	1·01	0·89	0·98	0·99	0·91	0·68	0·84	0·98	0·70	0·79	1·09	1·17
23	Rotation at Rem L.H.S.		rads/10³	1·6	1·8	1·5	3·4	1·7	3·6	2·4	0·7	1·2	3·0	4·8	2·4	1·7	3·3	0·3	4·4	6·0	6·1
24	" " " R.H.S.		"	0·5	2·6	1·2	0·5	1·0	1·7	0·5	0·2	7·6	0·2	0·7	1·2	1·9	2·5	2·4	1·3	4·2	6·8
25	" " Maxm Load L.H.S.		"	2·6	3·1	6·5	5·4	3·1	4·8	3·2	1·1	2·7	3·5	8·0	5·3	4·2	4·5	0·8	9·7	15·0	9·1
26	" " " " R.H.S.		"	1·2	3·7	2·6	1·3	1·5	2·7	0·9	0·5	9·5	0·5	2·3	2·5	4·2	4·5	7·0	2·5	12·1	8·2
27	Elastic Modulus Initial Test	m_{IT}	lb/in²×10³	2680	2350	4220	4500	4030	—	3140	3500	4730	—	5000	—	3240	—	4800	—	—	4450
28	Initial " of Arching	mai	"	308	295	761	636	630	610	440	620	650	700	550	530	500	480	1200	1090	390	350
29	Ratio $m_{ai}/\sqrt{u}$		lb½/in.	7140	7520	9420	7710	9100	8830	6120	8660	9000	9780	8030	7900	7470	7610	17300	18100	6150	5540
30	Reinforcement Factor	r_s		0·289	0·295	0·314	0·289	0·256	0·312	0·292	0·319	0·304	0·315	0·310	0·280	0·650	0·660	0	0	1·07	1·12
31	Minimum of Restraint Factor R_F	R_{Fm}		1·22	1·90	0·76	0·59	0·90	0·96	0·44	0·64	1·18	1·11	0·70	0·45	1·15	1·21	0·49	0·56	1·46	1·73
32	Minimum of Restraint Factor R_e	Rem		0·55	0·66	0·43	0·37	0·47	0·49	0·30	0·39	0·54	0·53	0·41	0·31	0·54	0·55	0·33	0·36	0·59	0·63
33	Arching Strain at Minm Re	e_{am}	%	0·015	0·035	0·020	0·040	0·030	0·050	0·038	0·040	0·028	0·037	0·040	0·040	0·020	0·025	0·010	0·012	0·040	0·010
34	" " " visible crushing	e_{ac}	%	0·080	0·120	0·110	0·055	0·070	0·070	0·066	0·055	0·090	0·062	0·120	0·110	0·105	0·095	0·100	0·08	0·105	0·100
35	" " " peak stress	e_{ap}	%	0·190	0·190	0·150	0·160	0·160	0·170	0·140	0·155	0·120	0·110	0·386	0·300	0·190	0·180	0·110	0·160	0·180	0·160
36	Probable Total Load	P_p	lb	1880	1840	3120	2980	2670	2720	2300	2470	1900	1890	4940	5170	4540	4340	2160	1680	5970	5980
37	Ratio P_E/P_p			1·06	1·15	1·04	1·06	0·91	0·95	1·00	1·05	0·87	0·90	0·96	0·93	1·00	1·01	0·67*	1·02	0·97	0·87
38	Central Deflexion at P_p	W_{cp}	inches	0·68	0·44	0·87	0·96	0·79	0·73	1·25	0·90	0·95	0·90	0·55	0·63	0·64	0·61	0·83	0·76	0·51	0·78
39	Ratio W_{ce}/W_{cp}			0·90	1·23	1·11	0·99	0·81	1·25	0·81	0·99	1·03	1·10	1·66	1·08	1·31	1·61	0·84	1·04	2·14	1·50
40	Ratio W_{ce}/d_a			0·32	0·33	0·38	0·35	0·25	0·39	0·38	0·36	0·38	0·40	0·39	0·28	0·43	0·56	0·25	0·33	1·21	1·05
41	$m_{ai}/\sqrt{u}$ from FIG. 21.		lb½/in.	7700	8800	8700	7700	9250	8700	6200	7100	8800	8700	8750	7750	5600	5550	18000	18000	4000	3700

MAX[x]: SPALLING COINCIDING WITH MAXM LOAD PM[x]: SPALLING OCCURRING AFTER MAXM LOAD [xx] REPETITION TEST

TABLE 1. ARCHING TESTS ON 12" WIDE SLAB ELEMENTS WITH CONCENTRATED MID-SPAN LOADING.

ITEM				SLAB NUMBERS															
No	Detail	Symbol	Units	M1	M2	M3	M4	M5	M6	M7	M8	M9	M10	M11[xx]	M12	M13	M14	M15	M16	M17	M18
1	Average Depth	d	inches	3·19	3·22	3·11	3·20	3·17	3·06	3·13	3·03	3·19	3·08	3·13	3·33	3·22	3·19	3·14	3·04	3·23	3·05
2	Effective Span	L	inches	72	72	72	72	72	72	72	72	96	96	48	48	72	72	72	72	72	72
3	Reinforcement			3-¼-A	3-¼-A	3-¼-A	3-¼-A	3-¼-A	3-¼-A	3-¼-A	3-¼-A	3-¼-A	3-¼-A	3-¼-A	3-¼-A	3-⅜-A	3-⅜-A	NIL	NIL	5-⅜-A	5-⅜-A
4	Total Yield Force	Asfy	lb.	5750	5700	5475	5525	5275	5700	5475	5600	5700	6175	5150	5750	15250	15200	—	—	25100	25200
5	Concrete Mix by weight			1:4·12:4·34		1:1·54:2·04		1:2·18:2·88		1:2·24:2·98		1:2·23:3·07		1:2·20:3·03		1:2·27:2·97		1:2·27:2·97		1:2·27:2·97	
6	Water/Cement Ratio			0·93		0·41		0·55		0·54		0·55		0·56		0·56		0·56		0·56	
7	Cube Strength	u	lb/in²	1870	1540	6530	6810	4810	4765	5180	5130	5210	5150	4690	4510	4480	3980	4720	3650	4025	3999
8	Age		days	41	48	45	46	55	47	49	43	60	61	61	62	51	29	42	46	28	29
9	Elastic Modulus of Prisms	Ec	lb/in²×10⁻³	3015	3160	4860	4765	4700	4805	4190	4720	4245	—	4590	3950	4140	—	4460	—	—	4175
10	Horizontal End Restraint	Rs	lb/in×10⁻³	200	300	300	200	300	300	100	200	300	300	300	200	300	300	300	300	300	300
11	Maximum Vertical Load	P_E	lb	2000	2110	3230	3160	2430	2570	2290	2580	1640	1700	4750	4800	4540	4360	1440	1720	5800	5210
12	Horizontal Force corr. with P_E	H_E	lb	7230	8060	19060	16220	13500	17400	9380	13580	13680	13550	19400	19820	15170	14980	12110	19600	15380	11480
13	Average Effective Depth	d_1	inches	2·41	2·50	2·48	2·42	2·10	2·38	2·35	2·39	2·53	2·44	2·48	2·53	2·47	2·46	—	—	2·44	2·28
14	Effective Arching Depth	da	inches	1·94	1·64	2·53	2·70	2·55	2·31	2·64	2·45	2·59	2·46	2·34	2·46	1·95	1·76	2·82	2·37	0·90	1·11
15	Theoretical Load by Bending	P_B	lb	1300	1320	1360	1335	1070	1350	1270	1335	1010	1075	2000	2270	3710	3630	-118	-115	5590	5145
16	Theoretical Load by Arching	P_A	lb	535	495	1660	1580	1455	1350	850	1180	905	830	2310	2940	935	650	1430	1720	-161	-38
17	Total Theoretical Load	P_T	lb	1835	1815	3020	2915	2525	2700	2120	2515	1915	1905	4310	5210	4645	4280	1312	1605	5429	5107
18	Ratio P_E/P_T			1·09	1·16	1·07	1·09	1·04	0·95	1·08	1·03	0·86	0·89	1·10	0·92	0·98	1·02	1·10	1·07	1·07	1·02
19	Factor α	α		0·55	0·50	0·52	0·42	0·87	0·88	0·33	0·62	1·33	1·10	0·50	0·97	0·81	0·70	0·14	0·64	0·73	0·74
20	Load causing visible spalling	P_S	lb	MAX[x]	PM[x]	MAX	2900	2400	2400	2250	2500	1650	MAX	4400	4500	MAX	4000	PM	PM	5600	5000
21	Central Deflexion at spalling	W_{cs}	inches	0·61	0·79	0·96	0·66	0·60	0·60	0·92	0·68	0·95	0·96	0·60	0·48	0·84	0·60	0·80	0·86	0·78	0·68
22	Central Defl^n at Max^m Load	W_{ce}	inches	0·61	0·54	0·96	0·95	0·64	0·91	1·01	0·89	0·98	0·99	0·91	0·68	0·84	0·98	0·70	0·79	1·09	1·17
23	Rotation at R_{em} L.H.S.		rads/10³	1·6	1·8	1·5	3·4	1·7	3·6	2·4	0·7	1·2	3·0	4·8	2·4	1·7	3·3	0·3	4·4	6·0	6·1
24	" " " R.H.S.		"	0·5	2·6	1·2	0·5	1·0	1·7	0·5	0·2	7·6	0·2	0·7	1·2	1·9	2·5	2·4	1·3	4·2	6·8
25	" " Max^m Load L.H.S.		"	2·6	3·1	6·5	5·4	3·1	4·8	3·2	1·1	2·7	3·5	8·0	5·3	4·2	4·5	0·8	9·7	15·0	9·1
26	" " " " R.H.S.		"	1·2	3·7	2·6	1·3	1·5	2·7	0·9	0·5	9·5	0·5	2·3	2·5	4·2	4·5	7·0	2·5	12·1	8·2
27	Elastic Modulus Initial Test	m_{IT}	lb/in²×10³	2680	2350	4220	4500	4030	—	3140	3500	4730	—	5000	—	3240	—	4800	—	—	4450
28	Initial " of Arching	mai	"	308	295	761	636	630	610	440	620	650	700	550	530	500	480	1200	1090	390	350
29	Ratio $m_{ai}/\sqrt{u}$		lb½/in.	7140	7520	9420	7710	9100	8830	6120	8660	9000	9780	8030	7900	7470	7610	17800	18100	6150	5540
30	Reinforcement Factor	r_s		0·289	0·295	0·314	0·289	0·256	0·312	0·292	0·319	0·304	0·315	0·310	0·280	0·650	0·660	0	0	1·07	1·12
31	Minimum of Restraint Factor R_F	R_{Fm}		1·22	1·90	0·76	0·59	0·90	0·96	0·44	0·64	1·18	1·11	0·70	0·45	1·15	1·21	0·49	0·56	1·46	1·73
32	Minimum of Restraint Factor R_e	Rem		0·55	0·66	0·43	0·37	0·47	0·49	0·30	0·39	0·54	0·53	0·41	0·31	0·54	0·55	0·33	0·36	0·59	0·63
33	Arching Strain at Min^m Re	e_{am}	%	0·015	0·035	0·020	0·040	0·030	0·050	0·038	0·040	0·028	0·037	0·040	0·040	0·020	0·025	0·010	0·012	0·040	0·010
34	" " " visible crushing	e_{ac}	%	0·080	0·120	0·110	0·055	0·070	0·070	0·066	0·055	0·090	0·062	0·120	0·110	0·105	0·095	0·100	0·08	0·105	0·100
35	" " " peak stress	e_{ap}	%	0·190	0·190	0·150	0·160	0·160	0·170	0·140	0·155	0·120	0·110	0·386	0·300	0·190	0·180	0·110	0·160	0·180	0·160
36	Probable Total Load	Pp	lb	1880	1840	3120	2980	2670	2720	2300	2470	1900	1890	4940	5170	4540	4340	2160	1680	5970	5980
37	Ratio P_E/P_p			1·06	1·15	1·04	1·06	0·91	0·95	1·00	1·05	0·87	0·90	0·96	0·93	1·00	1·01	0·67[#]	1·02	0·97	0·87
38	Central Deflexion at P_p	W_{cp}	inches	0·68	0·44	0·87	0·96	0·79	0·73	1·25	0·90	0·95	0·90	0·55	0·63	0·64	0·61	0·83	0·76	0·51	0·78
39	Ratio W_{ce}/W_{cp}			0·90	1·23	1·11	0·99	0·81	1·25	0·81	0·99	1·03	1·10	1·66	1·08	1·31	1·61	0·84	1·04	2·14	1·50
40	Ratio W_{ce}/da			0·32	0·33	0·38	0·35	0·25	0·39	0·38	0·36	0·38	0·40	0·39	0·28	0·43	0·56	0·25	0·33	1·21	1·05
41	$m_{ai}/\sqrt{u}$ from FIG. 21.		lb½/in.	7700	8800	8700	7700	9250	8700	6200	7100	8800	8700	8750	7750	5600	5550	18000	18000	4000	3700

MAX[x]: SPALLING COINCIDING WITH MAX[M] LOAD PM[x]: SPALLING OCCURRING AFTER MAX[M] LOAD [xx] REPETITION TEST

TABLE 1A. ARCHING TESTS ON 12" WIDE SLAB ELEMENTS WITH CONCENTRATED MID-SPAN LOADING.

ITEM No	Detail	Symbol	Units	SLAB NUMBERS M1	M2	M3	M4	M5	M6	M7	M8	M9	M10	M12	M13	M14	M16	M17	M18
42	Vertical load at first visible cracking	P_1	lb	310	800	1650	1180	950	1030	730	1000	390	750	1060	1550	1520	400	2600	1370
43	Vertical load.	P_2	"	1210	1250	2460	1940	1510	1870	1750	1690	1000	1320	2860	3200	3000	1200	4990	3060
44	" "	P_3	"	1730	1910	2840	2700	2050	2370	2180	2300	1530	1600	4020	4100	4060	1520	5550	4960
45	Maximum vertical load (P_E)	P_4	"	2000	2110	3230	3160	2430	2570	2290	2580	1640	1700	4800	4500	4360	1720	5800	5210
46	Vertical load.	P_5	"	1690	1710	2740	2610	2250	2000	1670	1930	1370	1420	3820	3210	3190	1420	5450	4920
47	Central deflection corr. with P_1	W_{c1}	inches	0·03	0·12	0·10	0·07	0·10	0·15	0·03	0·08	0·11	0·10	0·013	0·10	0·10	0·07	0·18	0·09
48	" " " " P_2	W_{c2}	"	0·16	0·17	0·26	0·19	0·18	0·29	0·23	0·19	0·32	0·32	0·16	0·29	0·31	0·30	0·47	0·29
49	" " " " P_3	W_{c3}	"	0·32	0·35	0·43	0·48	0·37	0·59	0·61	0·51	0·59	0·59	0·36	0·48	0·62	0·47	0·78	0·68
50	" " " " P_4	W_{c4}	"	0·61	0·54	0·96	0·94	0·61	0·91	1·01	0·89	0·98	0·99	0·68	0·80	0·98	0·79	1·09	1·17
51	" " " " P_5	W_{c5}	"	1·34	1·30	1·43	1·36	0·99	1·47	1·88	1·49	1·69	1·49	1·23	2·00	1·99	1·06	1·80	1·99
52	Horizontal force corr. with P_1	H_1	lb	520	2000	2740	1200	2560	3810	285	1400	2070	1220	400	2710	2810	2060	3800	1950
53	" " " " P_2	H_2	"	2540	3010	7240	3800	4710	7020	2440	3490	5360	4850	6680	6450	6560	9060	8820	5190
54	" " " " P_3	H_3	"	4460	5900	11650	9840	9230	13190	6440	9320	9300	9600	12560	10000	11630	12880	13060	9520
55	" " " " P_4	H_4	"	7230	8060	19060	16220	13500	17400	9380	13580	13680	13550	19820	14700	14980	19000	15380	11480
56	" " " " P_5	H_5	"	9660	10230	21600	19600	17620	20350	11540	16600	16800	15820	23490	16680	15190	21800	15150	7820
57	Horizontal expansion corr. with P_1	Δ_{a1}	inches	0·003	0·007	0·009	0·006	0·008	0·013	0·003	0·007	0·007	0·004	0·002	0·009	0·009	0·007	0·013	0·006
58	" " " " P_2	Δ_{a2}	"	0·013	0·010	0·024	0·019	0·016	0·024	0·024	0·017	0·018	0·017	0·033	0·022	0·022	0·030	0·030	0·018
59	" " " " P_3	Δ_{a3}	"	0·022	0·020	0·039	0·049	0·031	0·044	0·065	0·047	0·026	0·032	0·063	0·034	0·039	0·043	0·044	0·032
60	" " " " P_4	Δ_{a4}	"	0·036	0·027	0·064	0·081	0·045	0·058	0·094	0·068	0·045	0·045	0·099	0·050	0·050	0·063	0·052	0·038
61	" " " " P_5	Δ_{a5}	"	0·048	0·035	0·071	0·098	0·059	0·068	0·115	0·082	0·056	0·053	0·117	0·056	0·051	0·073	0·051	0·027

TABLE 2

TESTS ON CONCRETE SAMPLES

Test specimen	4" cubes	3" x 3" x 6" prisms
No of specimens	10	3
Mean density	142 lb/ft^3	140 lb/ft^3
Standard deviation	6 lb/ft^3	5 lb/ft^3
Mean crushing strength	4025 lb/in^2	
Standard deviation	787 lb/in^2	
Mean initial modulus of elasticity		2.67 x 10^6 lb/in^2
Standard deviation		0.23 x 10^6 lb/in^2

TABLE 3

TESTS ON STEEL SAMPLES

Nominal diameter	3/8"	1/2"
Number of samples	10	10
Mean yield strength	5,725 lb.	9,471 lb.
Standard deviation	77 lb.	207 lb.
Mean breaking strength	8,182 lb.	13,578 lb.
Standard deviation	141 lb.	214 lb.
	on 3"	on 4"
Mean elongation	27.0%	29.6%
Standard deviation	1.7%	2.6%

TABLE 4(a) - SEVENTH FLOOR

7-A4 T10 27.9.57 2U 23	7-B4 T13 1.10.57 2U 24		7-D4 T12 30.9.57 2U 23 SF	7-E4 T18 3.10.57 2U 23	
	7-AB3 T17 2.10.'57 2U 31	7-B3 T11 27.9.57 2U 31			
	7-AB2 T8 26.9.'57 2U 48	7-B2 T19 3.10.57 2U 20			
7-A1 T9 26.9.57 2U 20	7-B1 T15 2.10.57 2U 23	7-C1 T14 1.10.57 2U 30			7-F1 T7 25.9.57 2U 23

2 U = Two point loading upwards

Panel
Test No.
Date
Mode of Loading
Ultimate Load in short tons

Thickness $4\frac{7}{8}$" to 5"
including screed

TABLE 4(b) - SIXTH FLOOR

6-A4 T10 27.9.57 2D 27	6-B4 T13 1.10.57 2D 28		6-D4 T12 30.9.57 2D 28	6-E4 T18 3.10.57 2D 29	
		2D = Two point loading downwards Panel Test No. Date Mode of Loading Ultimate Load in short tons Thickness 5" to 5¼" including screed			
6-A1 T9 26.9.57 2D 24	6-B1 T15 2.10.57 2D 30	6-C1 T14 1.10.57 2D 32	6-D1 T1 10.9.57 3D 37		6-F1 T16 2.10.57 2D 21

TABLE 4(c) - FIFTH FLOOR

5-A4 T23 14/15.10.57 1-Ud 18	5-B4 T21 9.10.57 3-U 30 SF				
	5-B3 T30 22.10.57 3-U 23				
5-A2 T29 21.10.57 1-U 19	5-B2 T24 15.10.57 3-U 30				
5-A1 T22 11.10.57 1-U 22	5-B1 T20 4/7/8.10.57 2-U-SR 28 SF	5-C1 T20 4.10.57 2-U-S 31	5-D1 T27 17.10.57 1U 21	5-E1 T25 16.10.57 3U 31	5-F1 T28 18.10.57 1Ue 18

Panel
Test No.
Date
Mode of Loading
Ultimate Load in short tons

1 - Ud = Single central point load applied upwards - delay test

1 - Ue = Single eccentric point load applied upwards

2-U-SR = Two-point load applied upwards simultaneously with loading on adjacent panel. This panel subjected to repetition test subsequently.

SF = Shear failure

TABLE 4(d) - FOURTH FLOOR

4-A4 T26 16/18.10.57 1-Dd 25	4-B4 T21 9/10.10.57 3-Dd 30				
4-A3 T31 23.10.57 1-De 27	4-B3 T30 22.10.57 3-D 34				
4-A2 T29 21.10.57 1-D 20	4-B2 T24 15/16.10.57 3-DR 31				
4-A1 T22 11.10.57 1-D 17	4-B1 T20 4.10.57 2-DsR 27	4-C1 T20 7.10.57 2-Ds 38	4-D1 T27 17/18.10.57 1-DeR 27 SF	4-E1 T25 16.10.57 3-Dd 36 SF	4-F1 T28 18.10.57 1-De 19 SF

Panel
Test No
Date
Mode of Loading
Ultimate Load in short tons

1-De = Single eccentric load applied downwards

2-Ds = Two point simultaneous tests downwards

d = delayed test

R = repetition loading

SF = Shear Failure

TABLE 4(e) - THIRD FLOOR

		Panel Test No. Date Mode of Loading Ultimate Load in short tons			
		3-C1 T6 24.9.57 2-D 32	3-D1 T32 26.10.57 3-U 18		

TABLE 5: TYPICAL RESULTS OF LOAD TESTS ON SLABS OF THE OLD ALLIANCE HOUSE IN CAPE TOWN

NOTES:

1. Average cube strength u = 4,000 lbs. per in.^{2} (Tested air dry)
2. All panels reinforced as in FIG.32.
3. As the slab thickness 'd' was only measured in a few positions, an average value of 4·8 ins., including screed, has been assumed throughout.
4. The effective depth of steel 'd' has been taken as 4·2 ins.
5. Test numbers are in chronological order
6. Panel numbers indicate floor level and module number (See FIG.31)
7. Panel dimensions refer to the clear spans of the slabs.
8. The mode of loading is indicated as follows:-(See FIG.33)
   2U-54" = Two point loads at 54" cts. upward.
   3D-35" = Three point loads at 35" cts. downward.
9. Loading P_1 was at first observed cracking, P_2 & P_3 were intermediate loads, P_4 was the maximum load, P_5 was recorded subsequent to P_4.
10. All readings were taken along centre line of panel across the short span. (See FIGS. 33 & 36.)
11. Rotations θ_A refer to the support on the Castle street end of the panel (See FIG.31.) and θ_B to the opposite support.
12. Rotations are taken to be positive in the direction caused by hogging bending moment at the supports.
13. All figures indicated between brackets are approximate only.
14. → - Rotations recorded off the supports due to an obstructing wall, viz. on the slab panel immediately inside of the support crack.

	TEST Nº	DATE	PANEL Nº	DIMENSIONS		LOADING
Loads in lbs.	P	P_1	P_2	P_3	P_4	P_5
Central deflection in ins.	w_c	w_{c1}	w_{c2}	w_{c3}	w_{c4}	w_{c5}
Horizontal spread in ins.	Δ_a	Δ_{a1}	Δ_{a2}	Δ_{a3}	Δ_{a4}	Δ_{a5}
Rotation of support A in Rad	θ_A	θ_{A1}	θ_{A2}	θ_{A3}	θ_{A4}	θ_{A5}
Rotation of support B in Rad	θ_B	θ_{B1}	θ_{B2}	θ_{B3}	θ_{B4}	θ_{B5}

	T.13 A	1·10·'57	7B 4	95½" x 171"		2U - 54"
P	21 400	38 600	46 600	50 000	–	
w_c	0·093	0·366	0·891	1·659	–	
Δ_a	0·007	0·041	0·102	0·165	–	
θ_A	0·0014	0·0052	0·0127	0·0212	–	
θ_B	0·0008	0·0022	0·0136	0·0227	–	

	T 16	2·10·'57	6F 1	(100" x 169")		2D - 54"
P	30 000	38 600	42 700	44 400	44 400	
w_c	0·227	0·529	0·864	1·249	2·011	
Δ_a	0·035	0·080	0·125	0·164	0 294	
θ_A	0·0038	0·0051	0·0067	0·0075	0·0087	
θ_B	0·0059	0·0135	0·0220	0·0318	0·0542	

	T 8	26·9·'57	7AB 2	63½" x (162")		2U - 54"
Loads in lbs.	P	20 200	61 800	89 520	97 000	–
Central deflection in ins.	w_c	0·024	0·267	0·661	0·992	–
Horizontal spread in ins.	Δ_a	0·004	0·051	0·129	0·183	–
Rotation of support A in Rad	θ_A	0·0004	0·0020	0·0040	0·0048	–
Rotation of support B in Rad	θ_B	0·0004	0·0035	0·0082	0·0122	–

	T13 B	1·10·'57	6B 4	95" x 172"		2D - 54"
P	34 400	48 500	54 200	57 900	52 300	
w_c	0·172	0·492	0·801	(2·40)	(3·00)	
Δ_a	0·011	0·042	0·069	(0·10)	0·124	
θ_A	0·0031	0·0087	0·0133	(0·014)	0·0145	
θ_B	0·0005	0·0002	0·0000	–	+0·0024	

	T 18	3·10·'57	6E 4	94" x 177"		2D - 54"
P	50 000	56 000	58 000	59 000	53 000	
w_c	0·527	0·785	1·160	(1·30)	2·180	
Δ_a	0·028	0·048	0·072	(0·08)	0·096	
θ_A	0·0002	0·0004	0·0004	–	–	
θ_B	0·0032	0·0048	0·0065	–	0·0085	

	T10 B	27·9·'57	6A 4	97" x 170"		2D - 54"
Loads in lbs.	P	34 400	42 600	50 400	55 200	–
Central deflection in ins.	w_c	0·309	0·589	1·030	2·071	–
Horizontal spread in ins.	Δ_a	0·040	0·074	0·126	0·217	–
Rotation of support A in Rad	θ_A →	0·0064	0·0118	0·0205	0·0415	–
Rotation of support B in Rad	θ_B	0·0015	0·0022	0·0034	0·0052	–

	T14 A	1·10·'57	7C 1	93" x 179"		2U - 54"
P	13 000	42 600	58 300	60 900	–	
w_c	0·048	0·380	0·896	1·675	–	
Δ_a	0·005	0·048	0·120	0·150	–	
θ_A	0·0008	0·0045	0·0101	0·0162	–	
θ_B	0·0004	0·0030	0·0101	(0·0168)	–	

	T21 A	9·10·'57	5B 4	95" x 171"		3U - 30"
P	32 400	46 000	57 900	63 900	60 000	
w_c	0·155	0·361	0·650	1·073	–	
Δ_a	0·012	0·037	0·067	0·105	0·234	
θ_A	0·0020	0·0046	0·0089	0·0151	0·0250	
θ_B	0·0009	0·0025	0·0056	0·0103	0·0290	

	T12A	30·9·'57	7D 4	(94" x 171")		2U - 54"
Loads in lbs	P	30 100	38 000	46 200	48 000 S.F	36 000
Central deflection in ins.	w_c	0·282	0·499	1·010	1·882	2·817
Horizontal spread in ins.	Δ_a	0·032	0·056	0·113	–	0·143
Rotation of support A in Rad.	θ_A	0·0028	0·0063	0·0131	–	(0·0193)
Rotation of support B in Rad.	θ_B	0·0012	0·0026	0·0100	(0·0141)	0·0162

	T14 B	1·10·'57	6C 1	(95" x 170")		2D - 54"
P	34 400	54 200	61 700	64 700	–	
w_c	0·229	0·518	1·050	1·874	–	
Δ_a	0·029	0·068	0·124	0·182	–	
θ_A	0·0012	0·0026	0·0048	(0·0094)	–	
θ_B	0·0039	0·0083	0·0125	0·0153	–	

	T30 B	22·10·'57	4B 3	95" x 163"		3D - 35"
P	32 300	51 600	63 900	71 900	–	
w_c	0·162	0·468	0·793	2·162	–	
Δ_a	0·014	0·049	0·084	0·205	–	
θ_A	0·0027	0·0063	0·0082	0·0119	–	
θ_B	0·0005	-0·0006	-0·0006	0·0003	–	

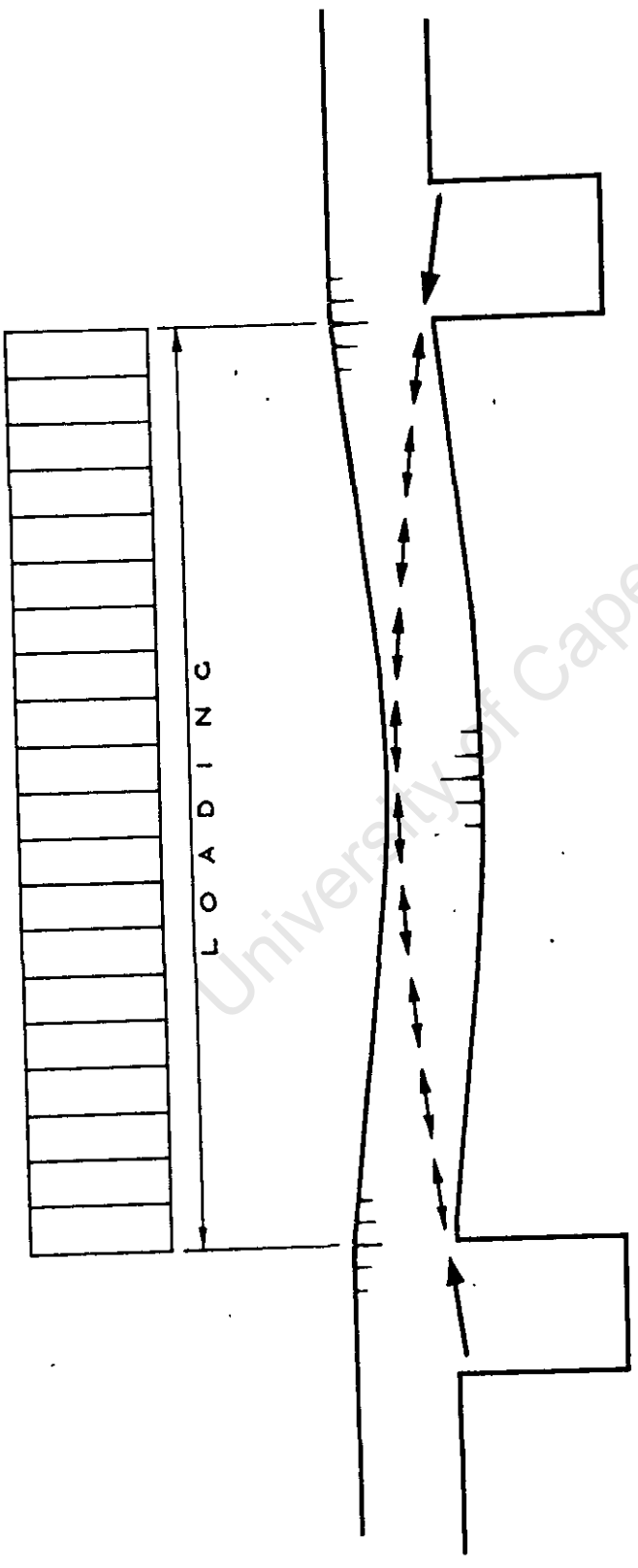

ARCHING ACTION IN REINFORCED CONCRETE SLAB

FIG. 1

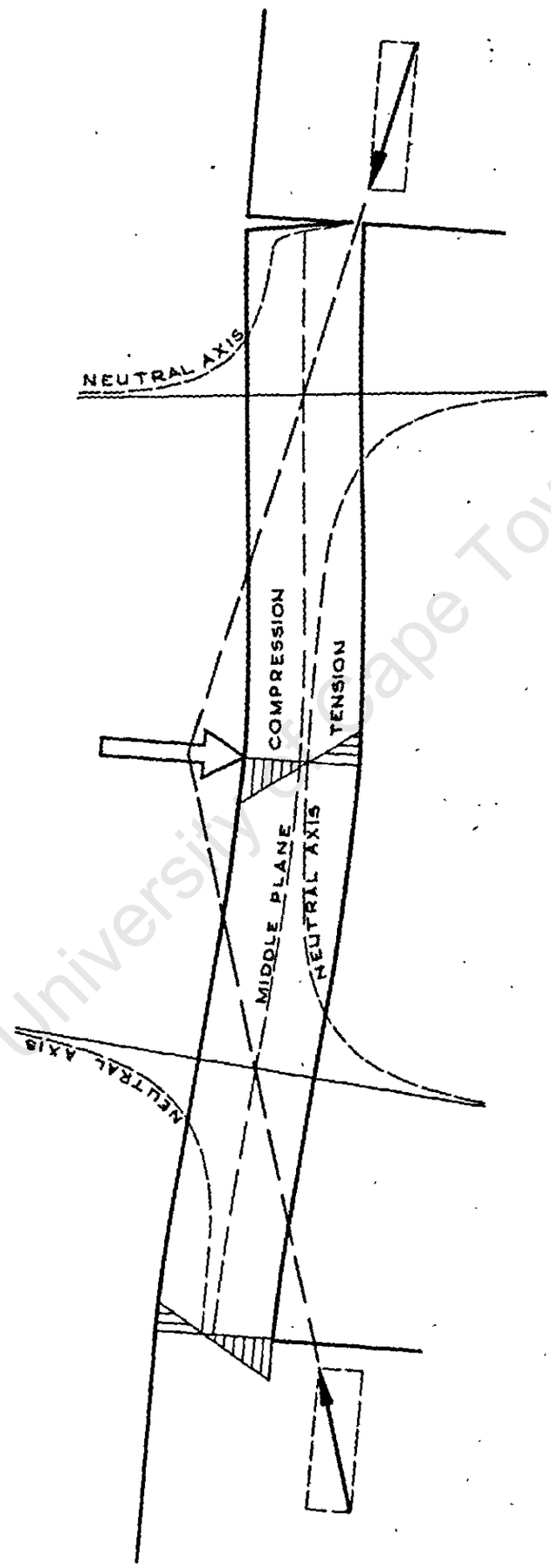

ARCHING ACTION OF SLAB WITH ONE ARTIFICIAL ARTICULATION

FIG. 2.

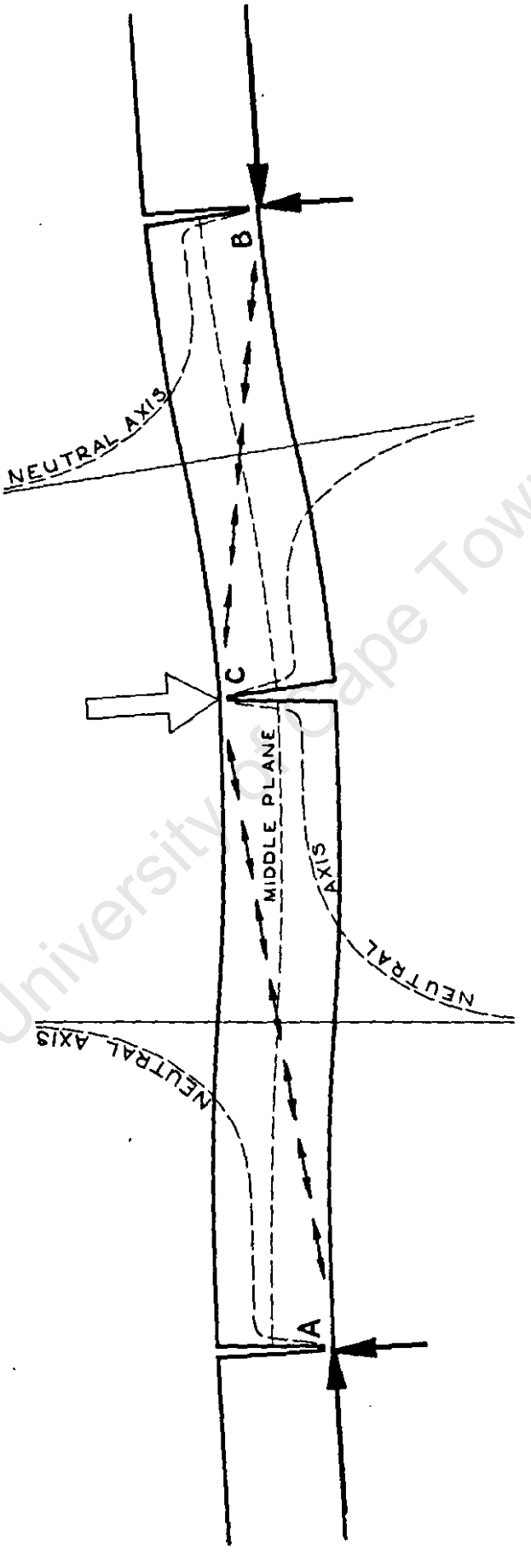

ARCHING ACTION OF SLAB WITH THREE ARTIFICIAL ARTICULATIONS

FIG. 3.

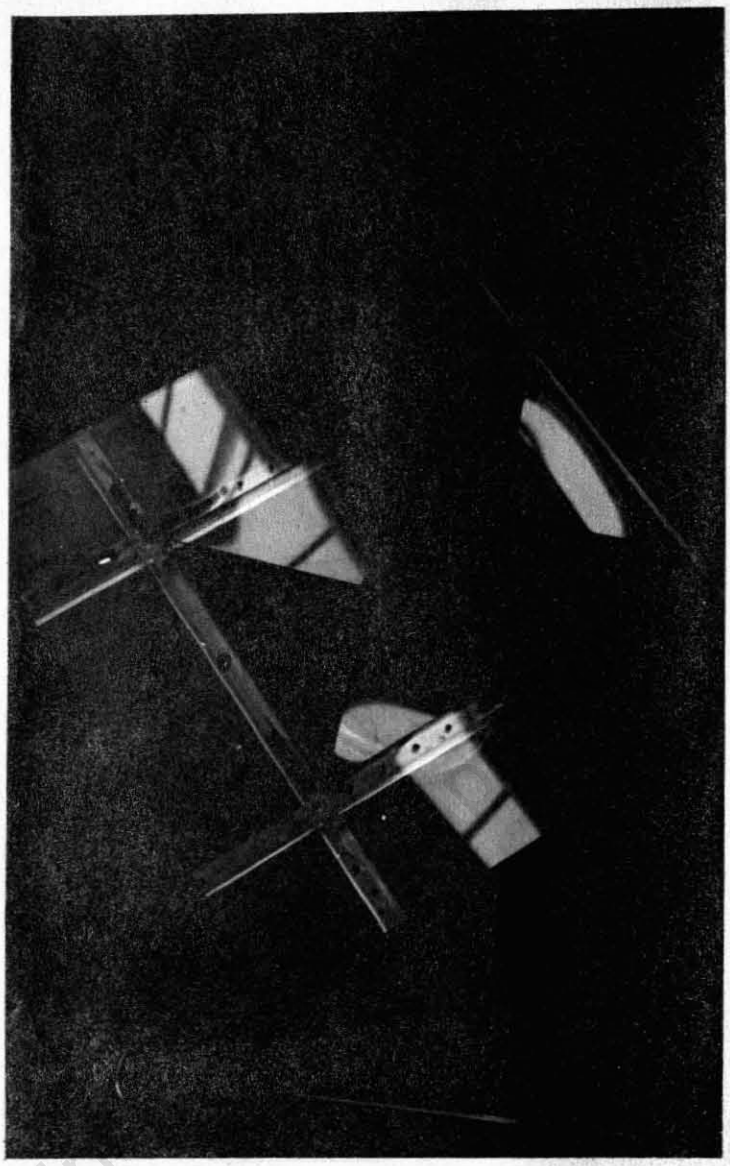

FIG. 4.

PERSPEX MODEL OF SLAB PANEL
WITH ARTIFICIAL ARTICULATIONS

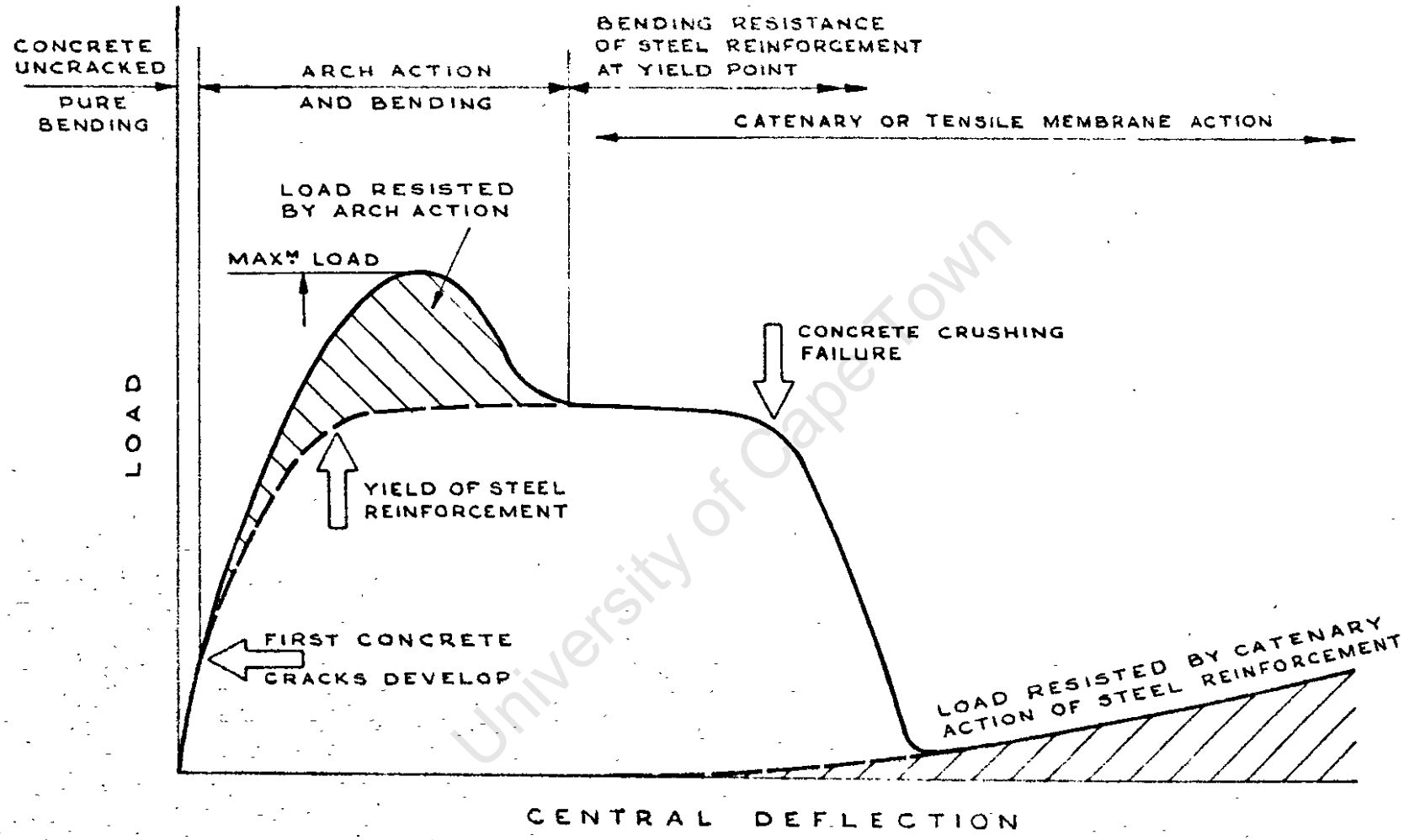

FIG. 5.

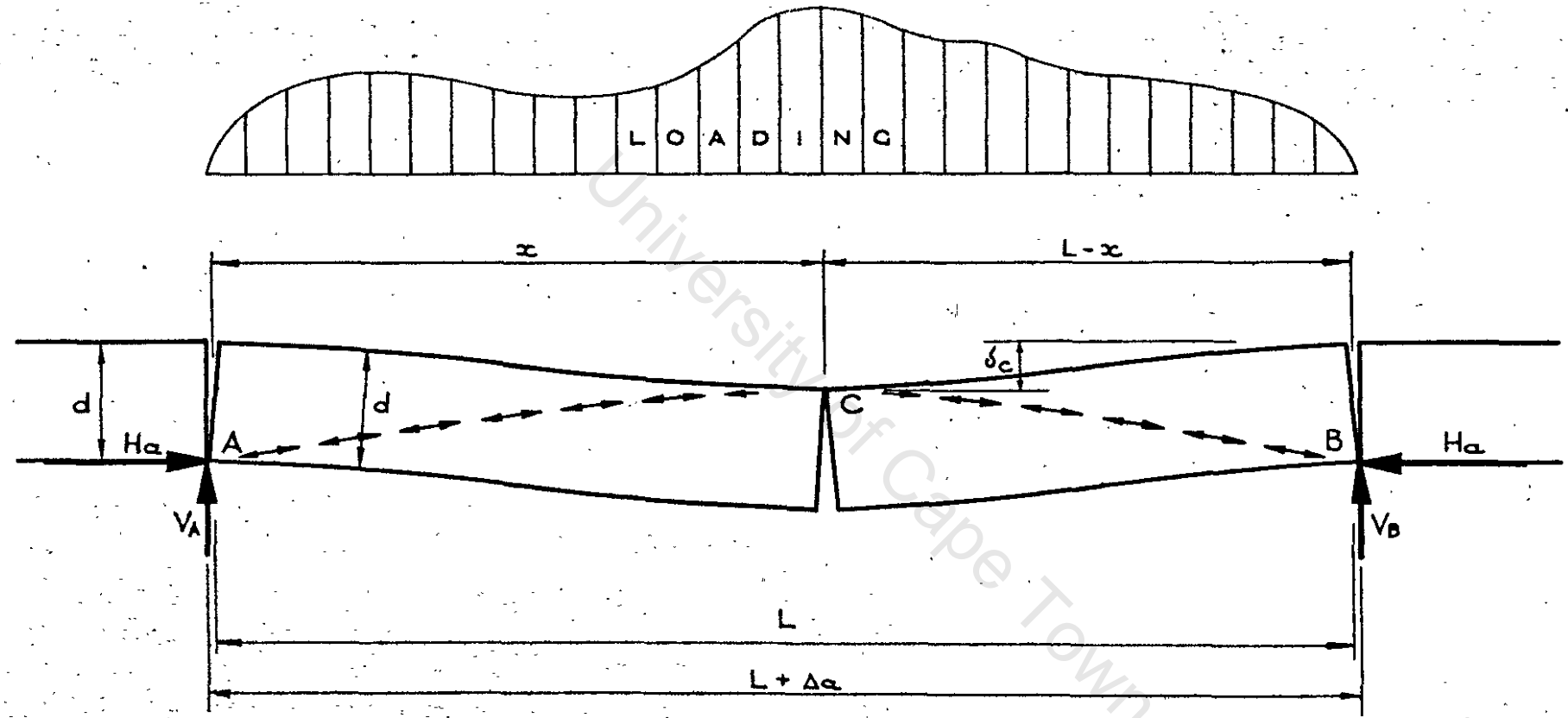

IDEAL ARCHING SLAB WITH THREE ARTICULATIONS

FIG. 6.

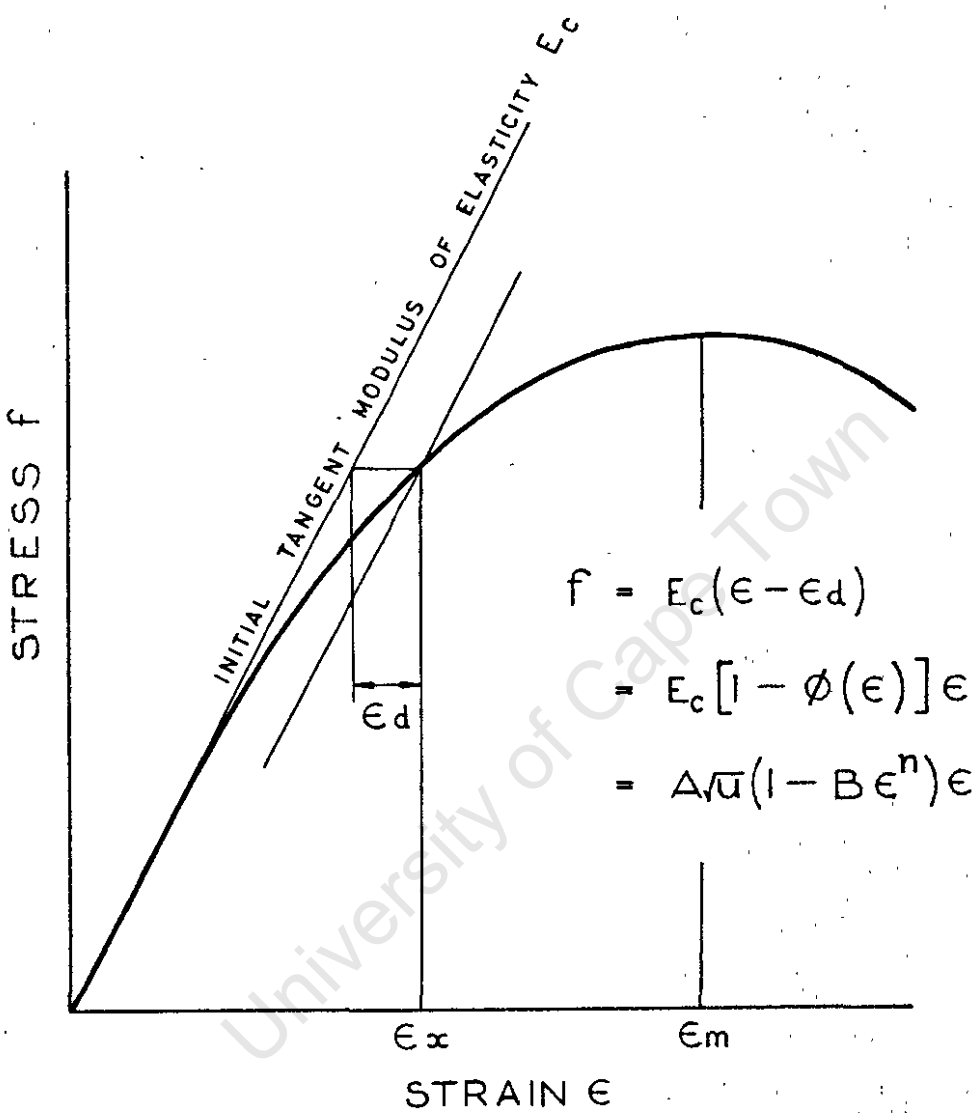

FIG.7.

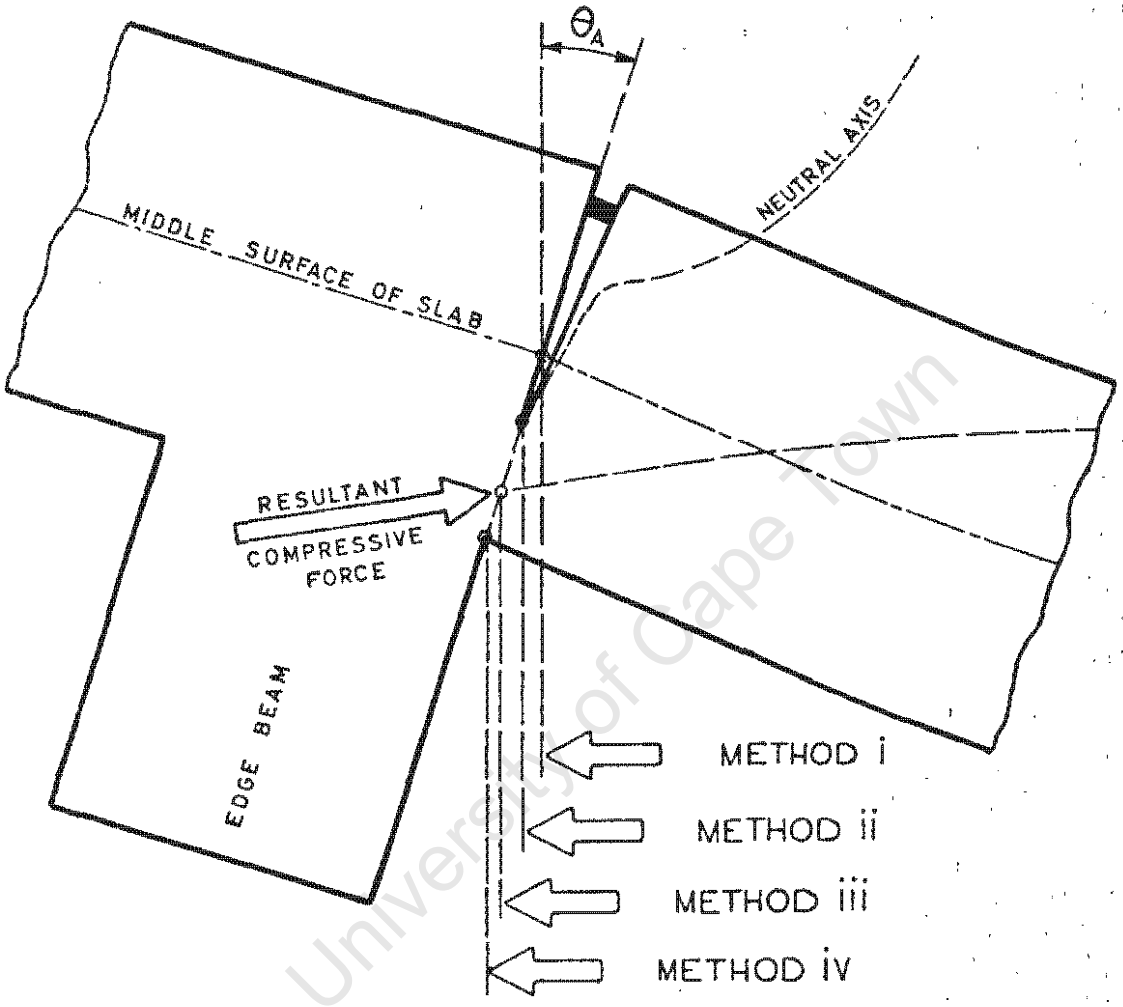

FIG.8.

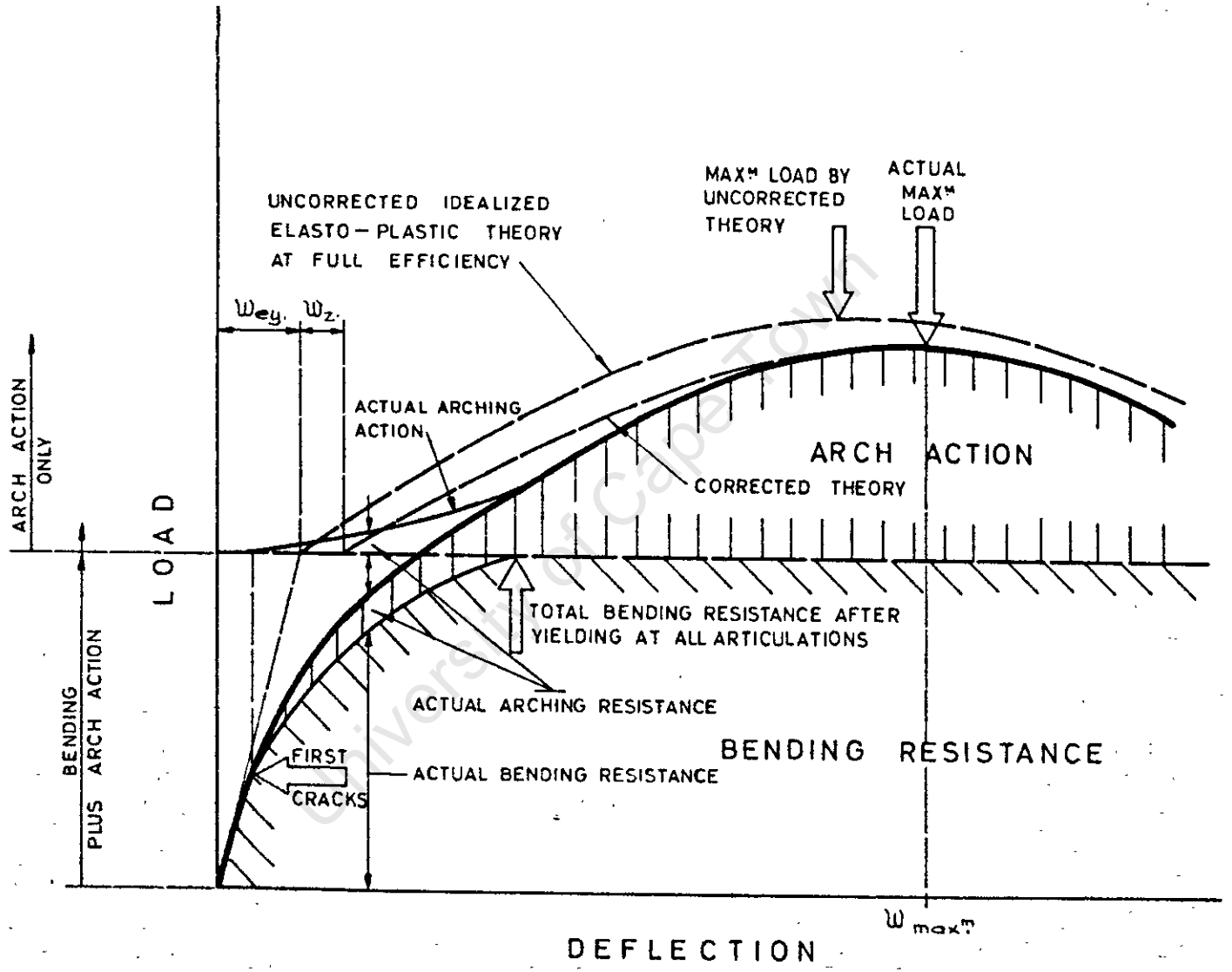

FIG. 9.

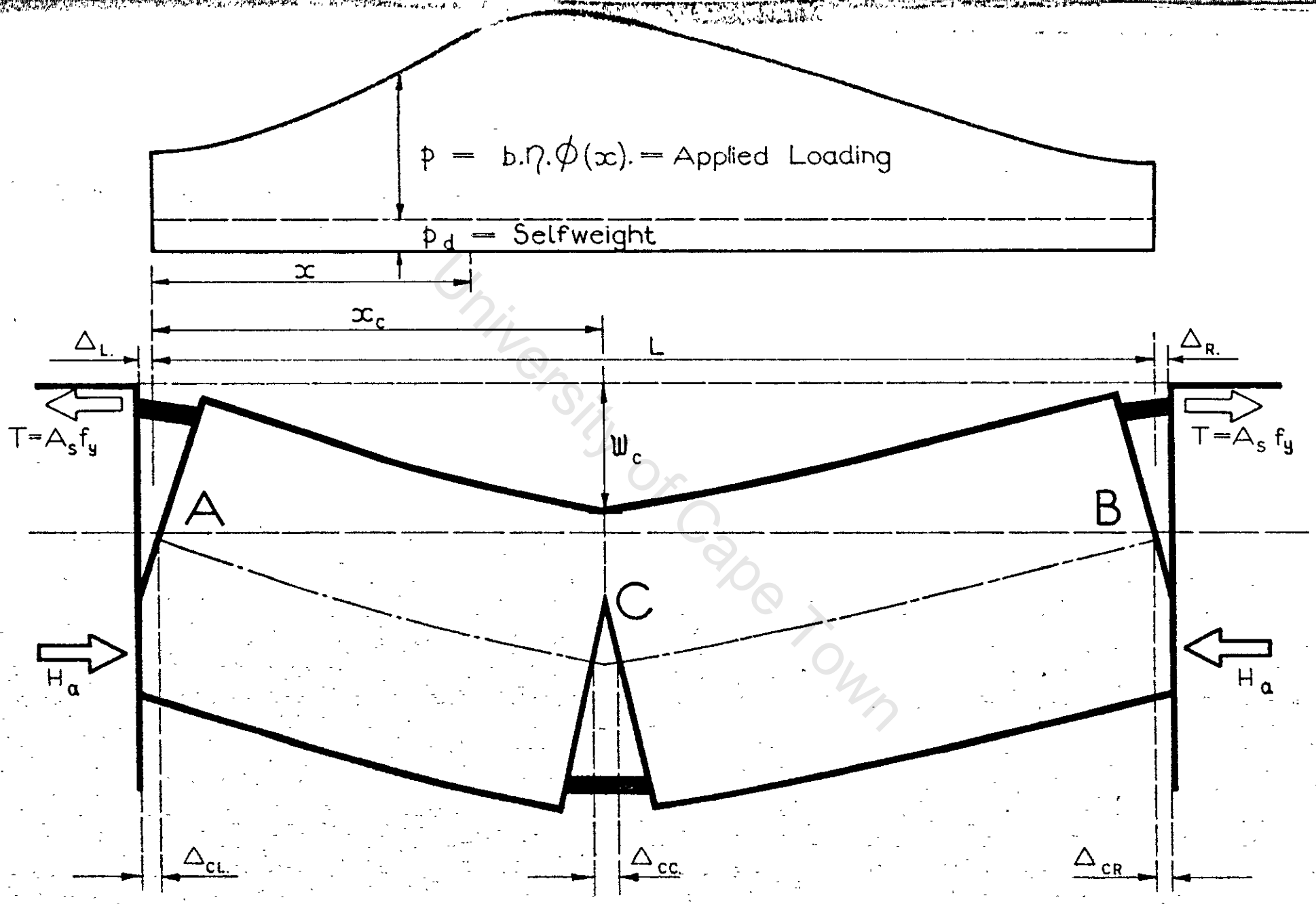

FIG. 10.

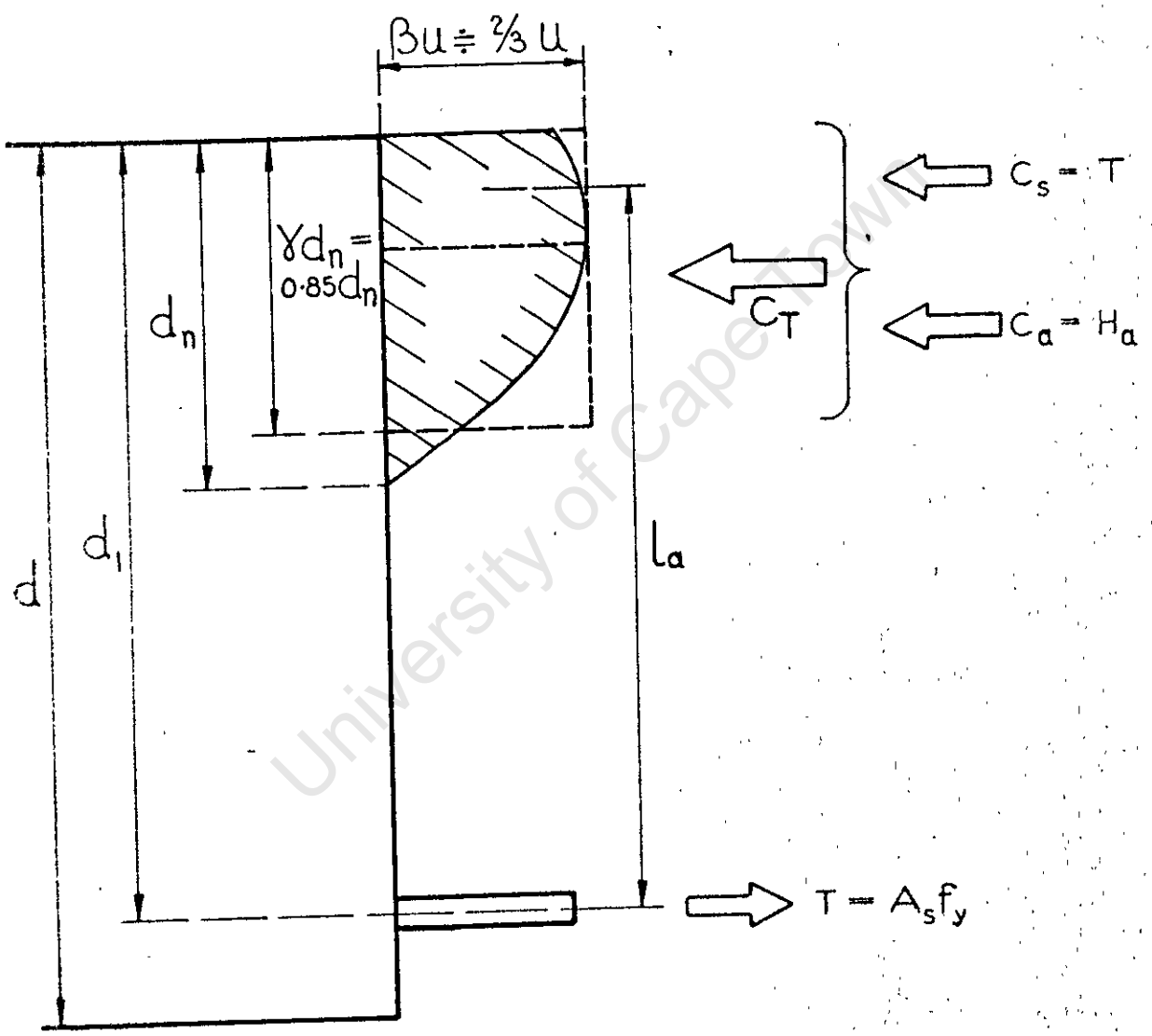

FIG. 11.

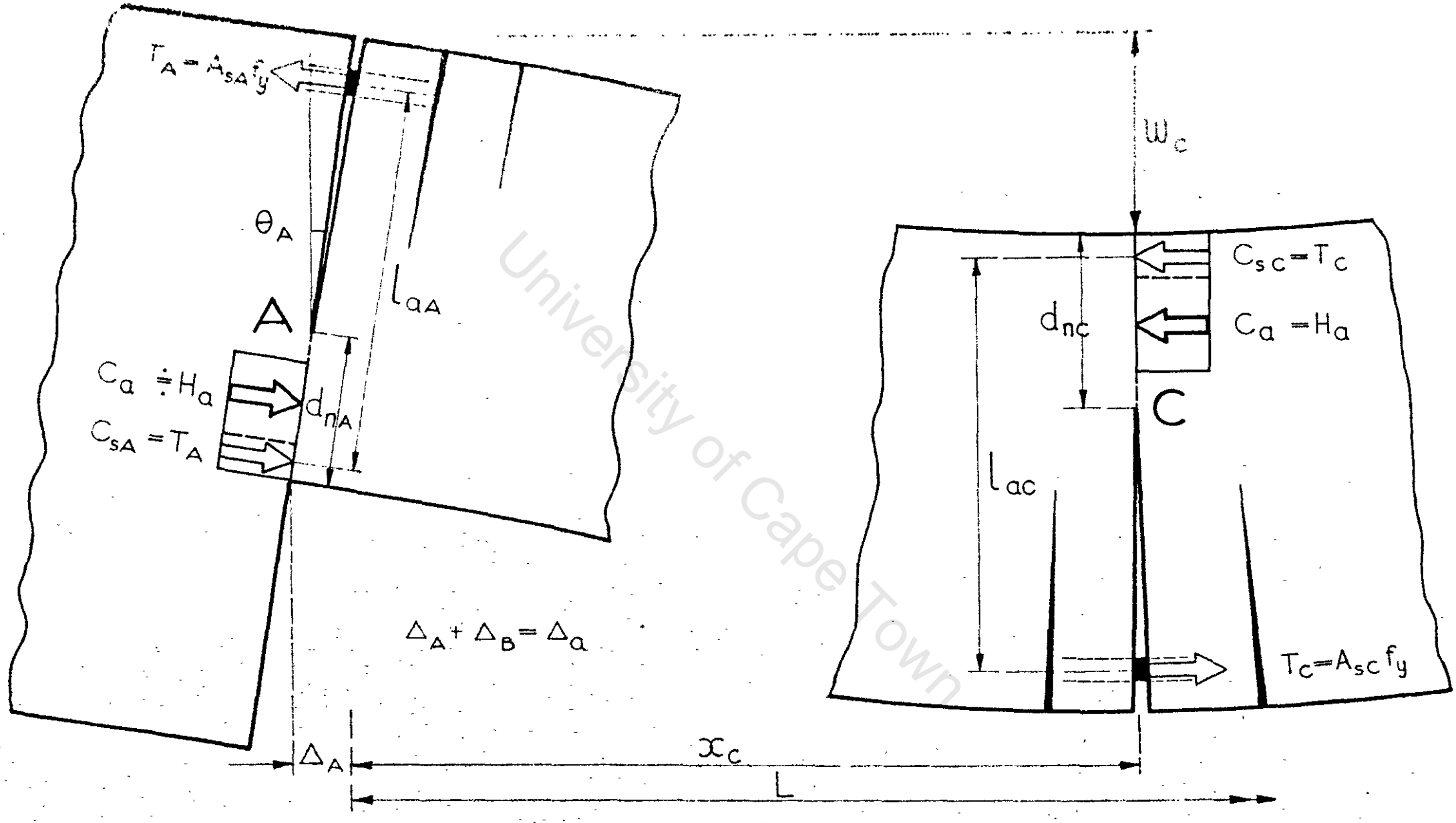

FIG.12.

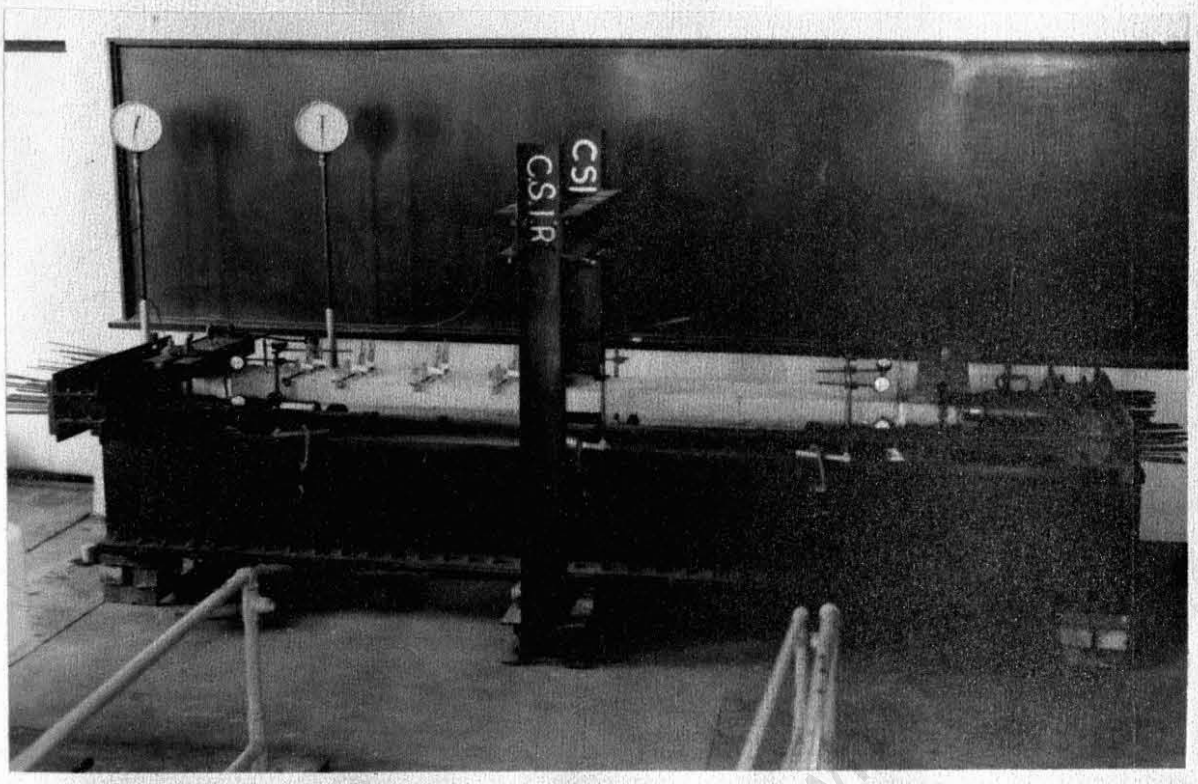

FIG. 13.

ARCHING TEST ON SINGLE SPAN SLAB ELEMENT

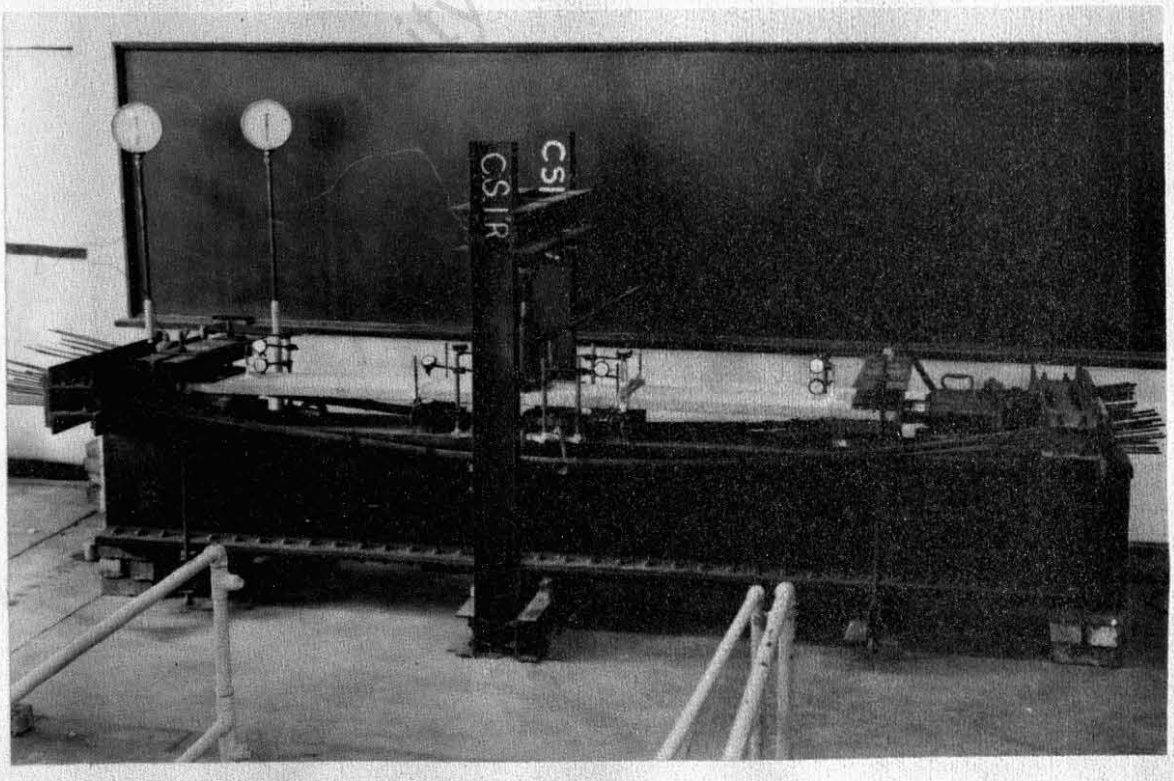

FIG. 14.

ARCHING TEST ON 3 SPAN SLAB ELEMENT

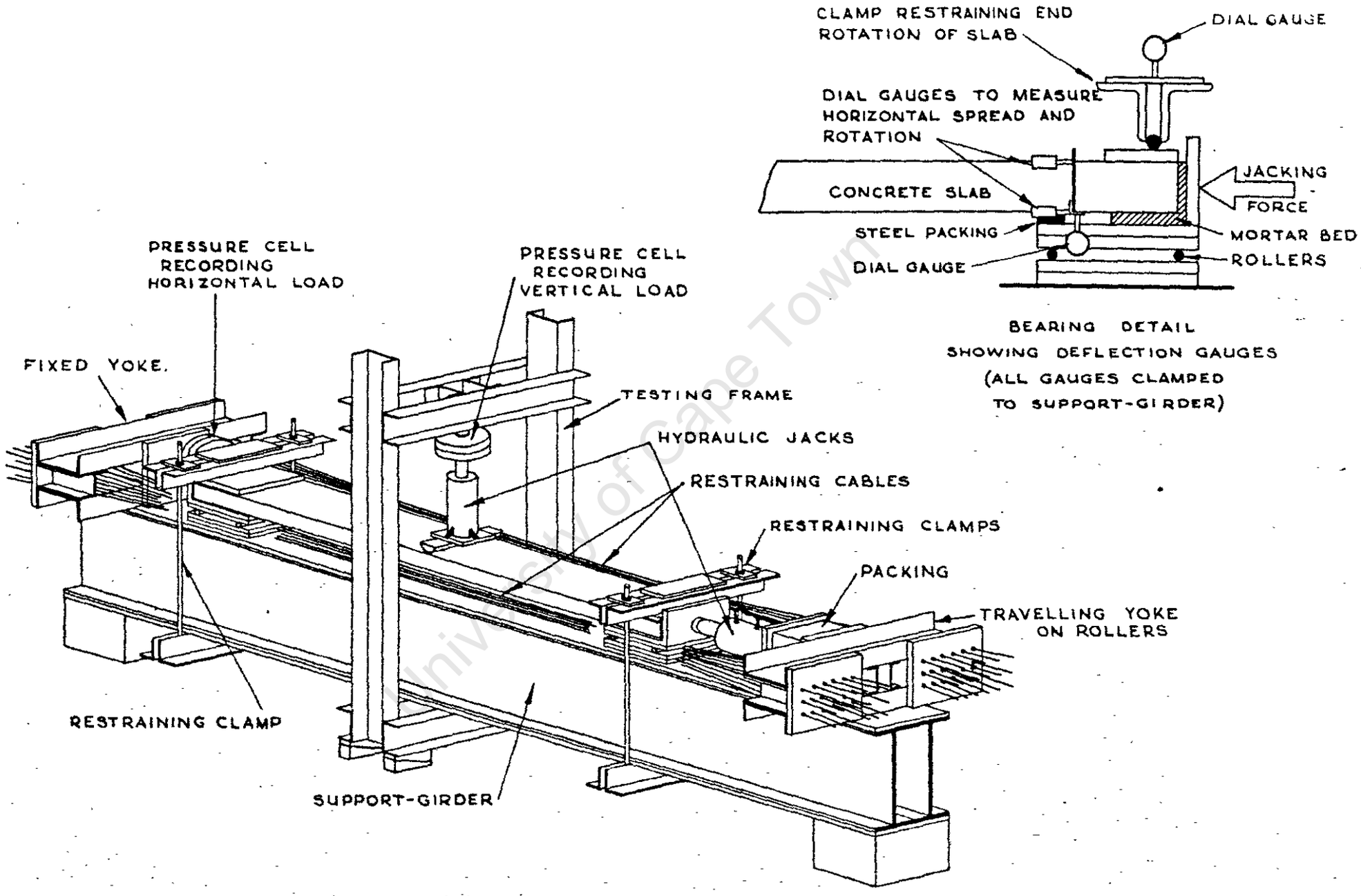

FIG. 15.

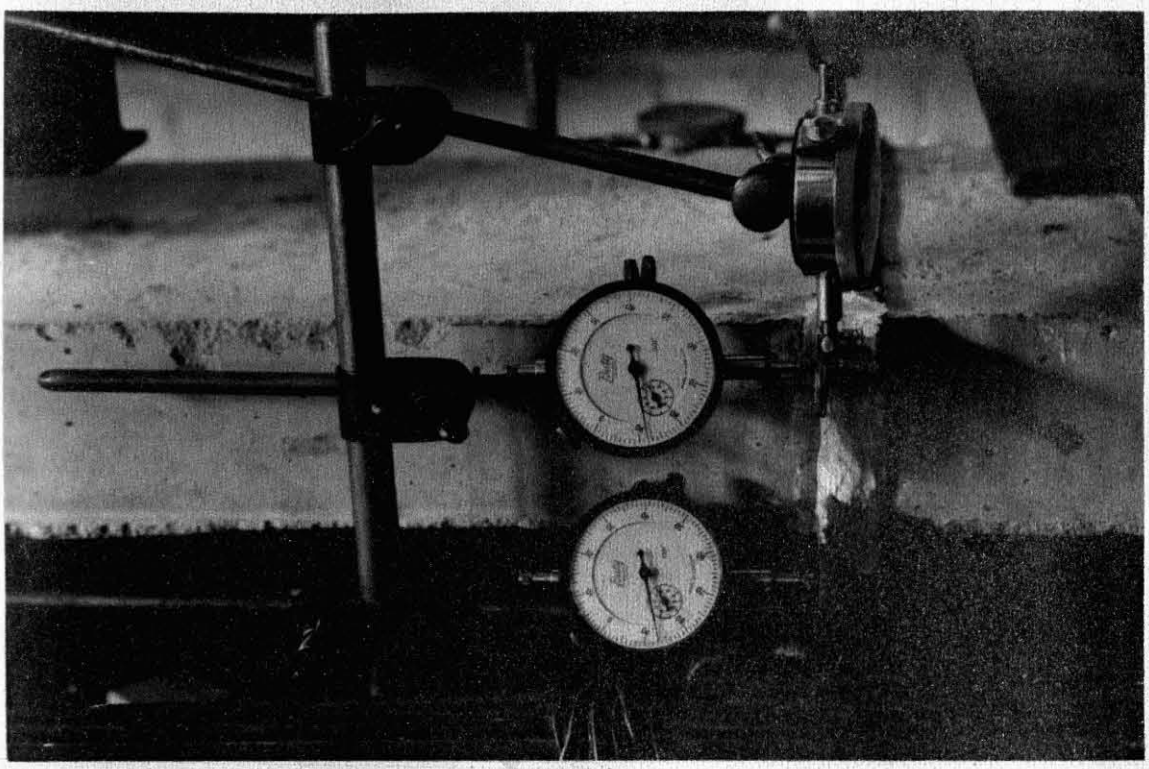

FIG. 15B.

Detail of dial gauges at right hand support to measure horizontal spread, vertical deflections and rotations. The vertical legs of the angle irons were cut away for the width of the slab element. The assembly was rigidly clamped and connected with Plaster of Paris to the end portion of the slab element as shown. Note the position of the support roller bearing relative to the assembly of gauges.

The alternative arrangement shown in fig. 15 with one horizontal angle-iron and a vertical extension was also used.

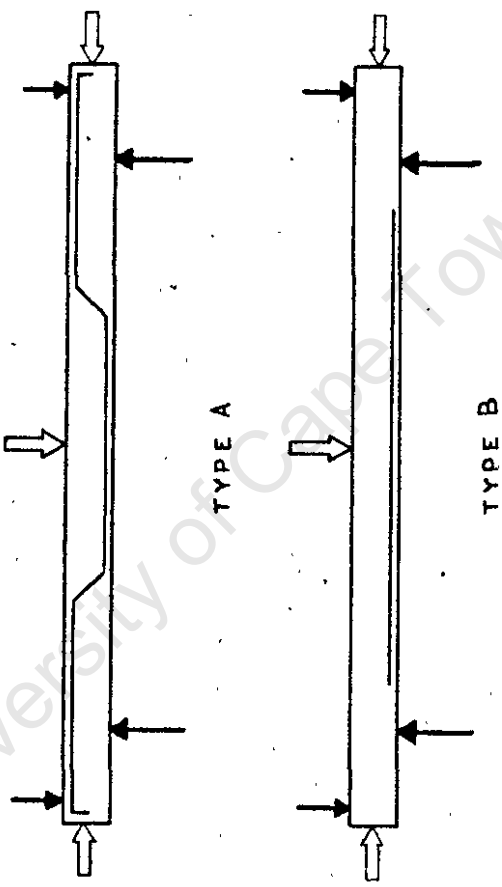

FIG. 16.

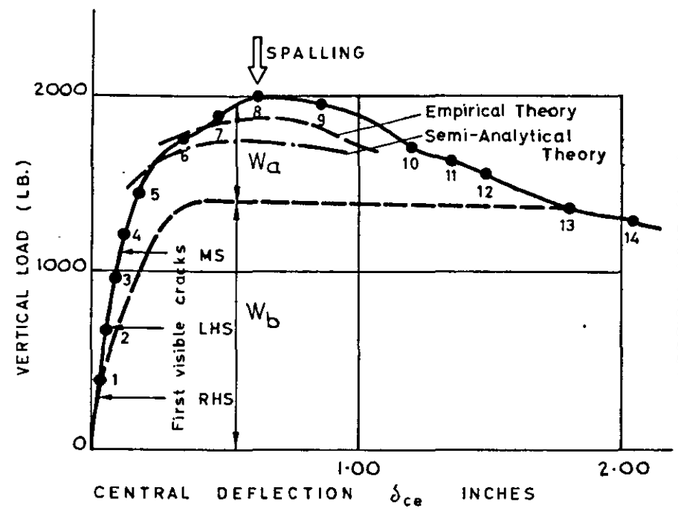

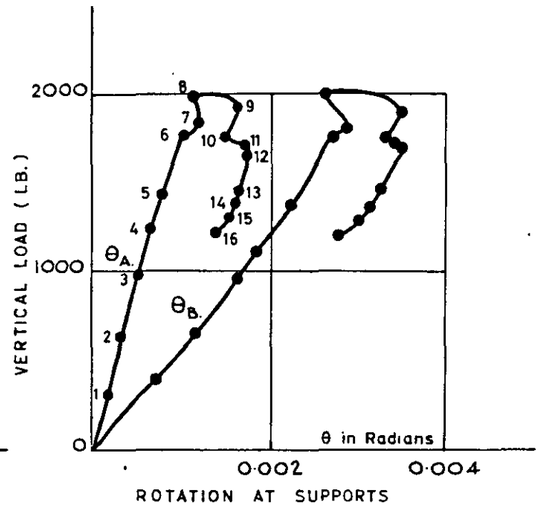

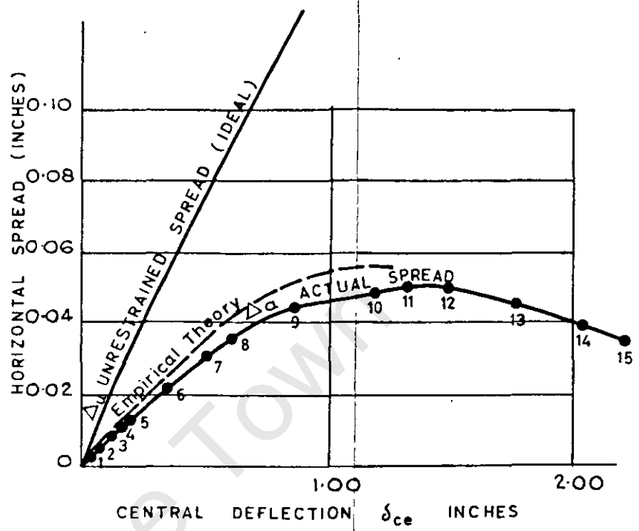

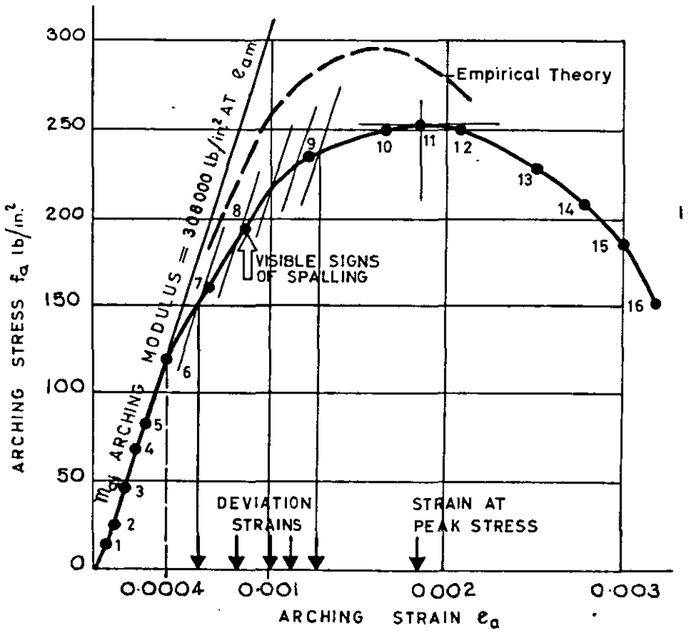

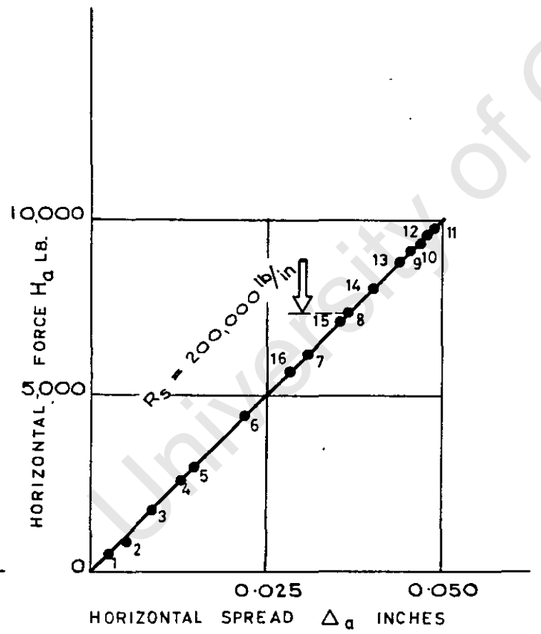

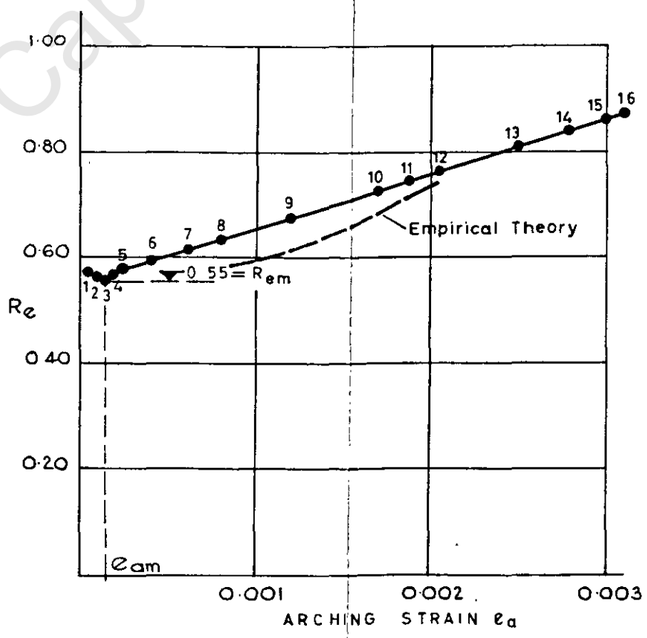

TYPICAL CURVES FROM RESULTS OF TEST M1

FIG. 17.

TEST ON TWO IDENTICAL 12 WIDE SLAB ELEMENTS WITH CONCENTRATED MID-SPAN LOADING TO DEMONSTRATE THE EFFECT OF HORIZONTAL RESTRAINT.

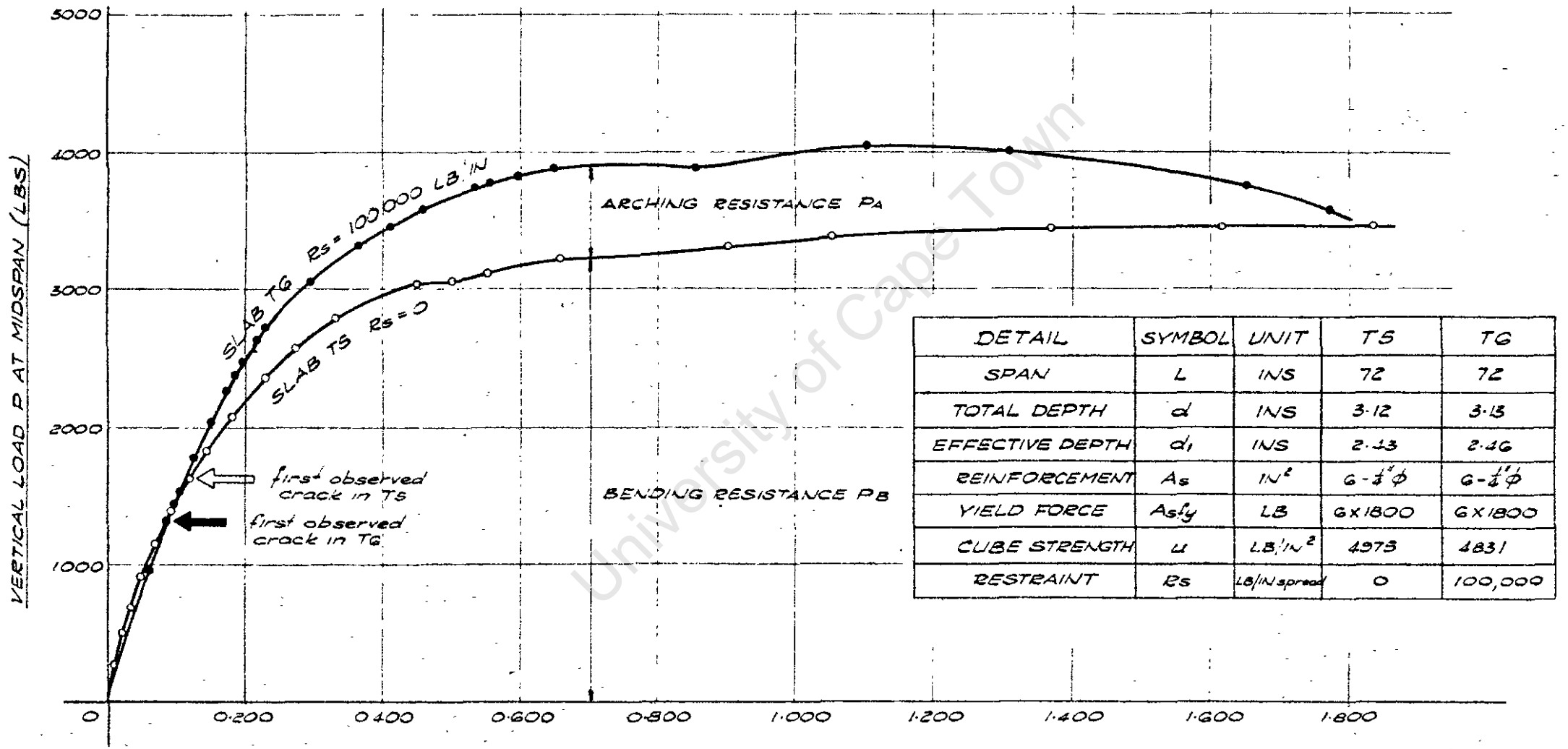

DETAIL	SYMBOL	UNIT	TS	TG
SPAN	L	INS	72	72
TOTAL DEPTH	d	INS	3·12	3·13
EFFECTIVE DEPTH	d_1	INS	2·43	2·46
REINFORCEMENT	A_s	IN^2	6-$\frac{1}{4}''\phi$	6-$\frac{1}{4}''\phi$
YIELD FORCE	$A_s f_y$	LB	6X1800	6X1800
CUBE STRENGTH	u	LB/IN^2	4973	4831
RESTRAINT	Rs	LB/IN spread	0	100,000

FIG 17A

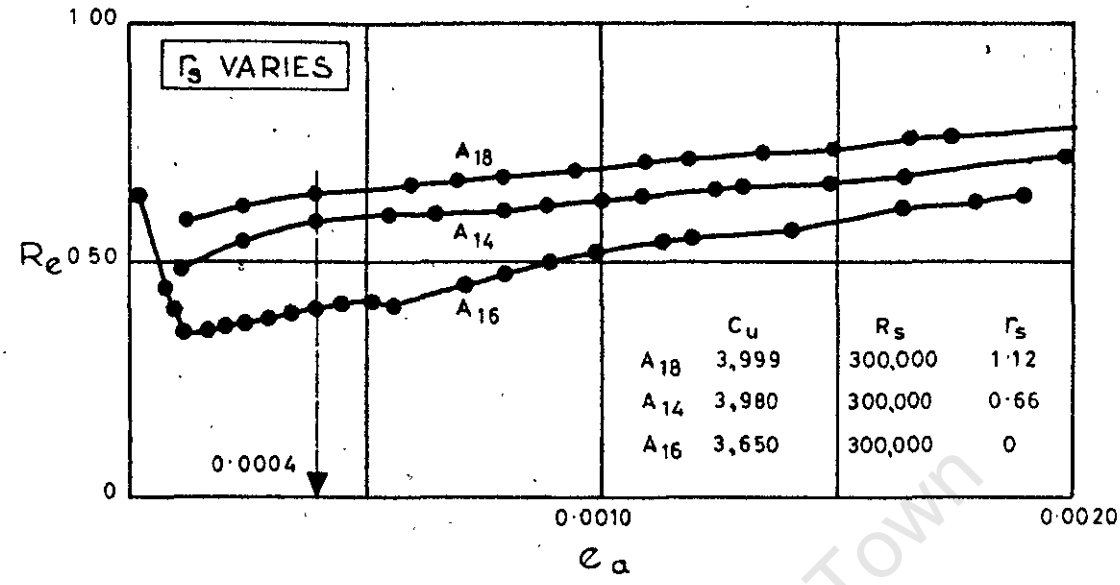

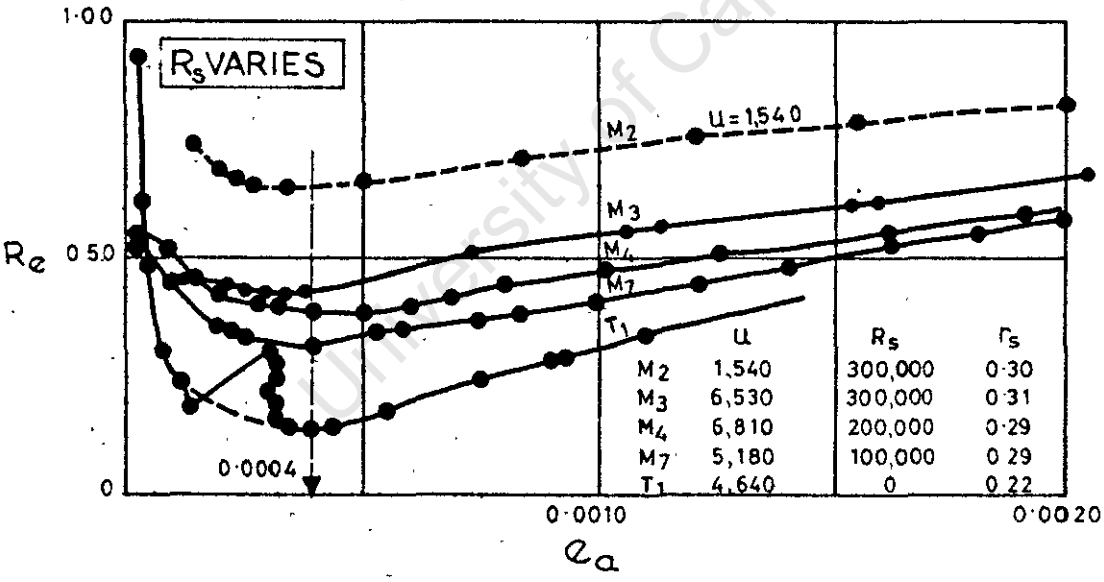

TYPICAL R_e CURVES

FIGS. 18(a) & 18(b).

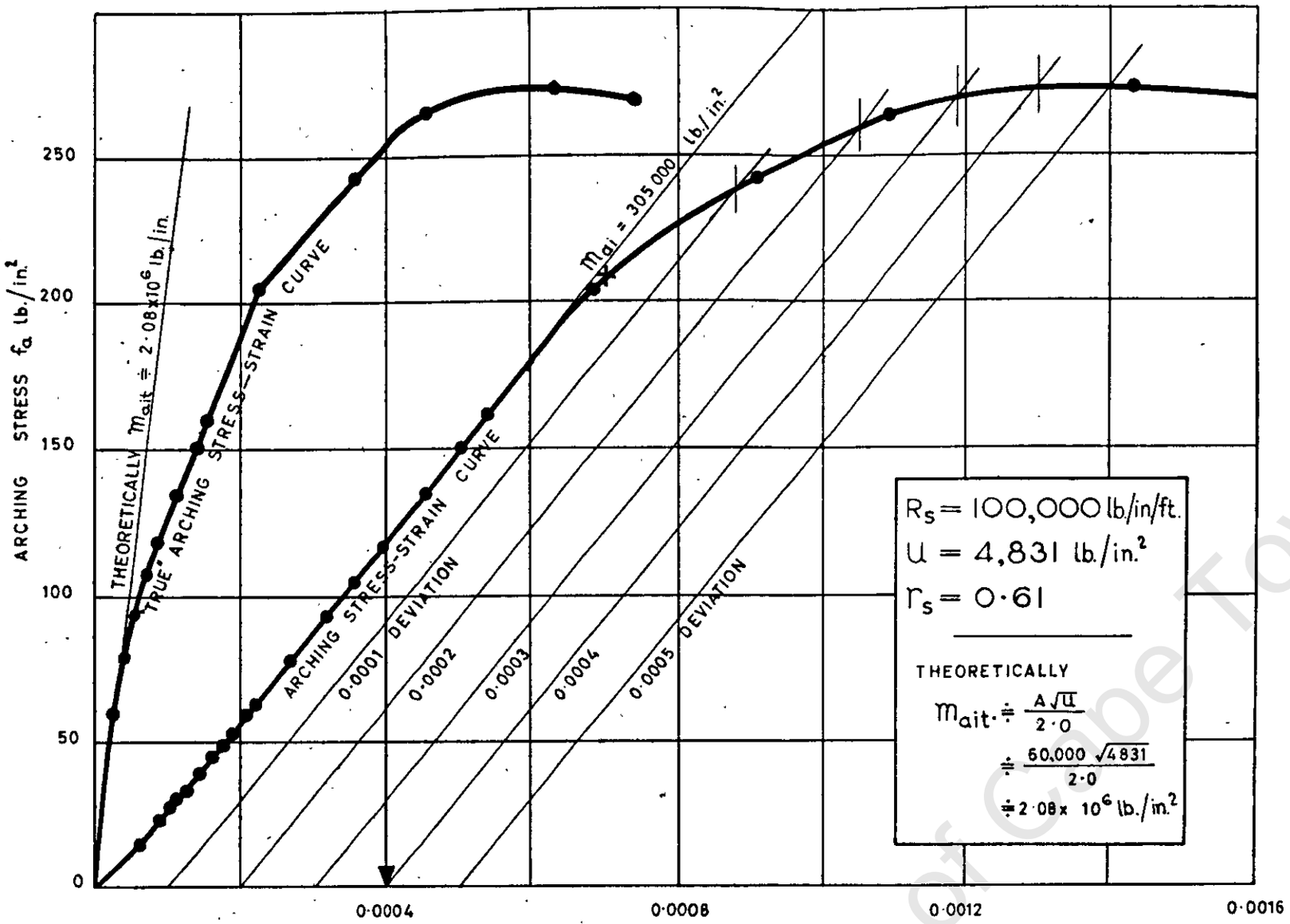

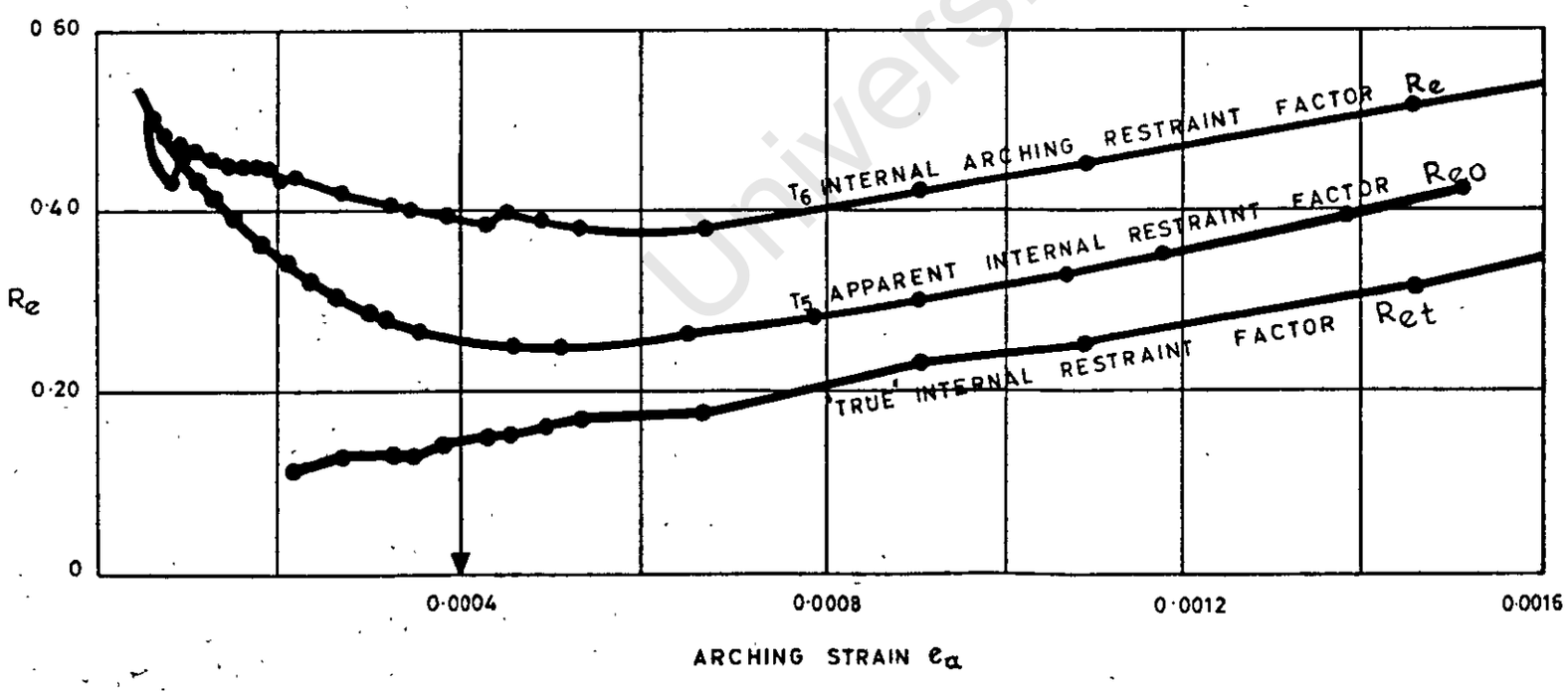

CURVES BASED ON 'TRUE' STRAIN VALUES DERIVED FROM TESTS T5 AND T6

FIG. 19.

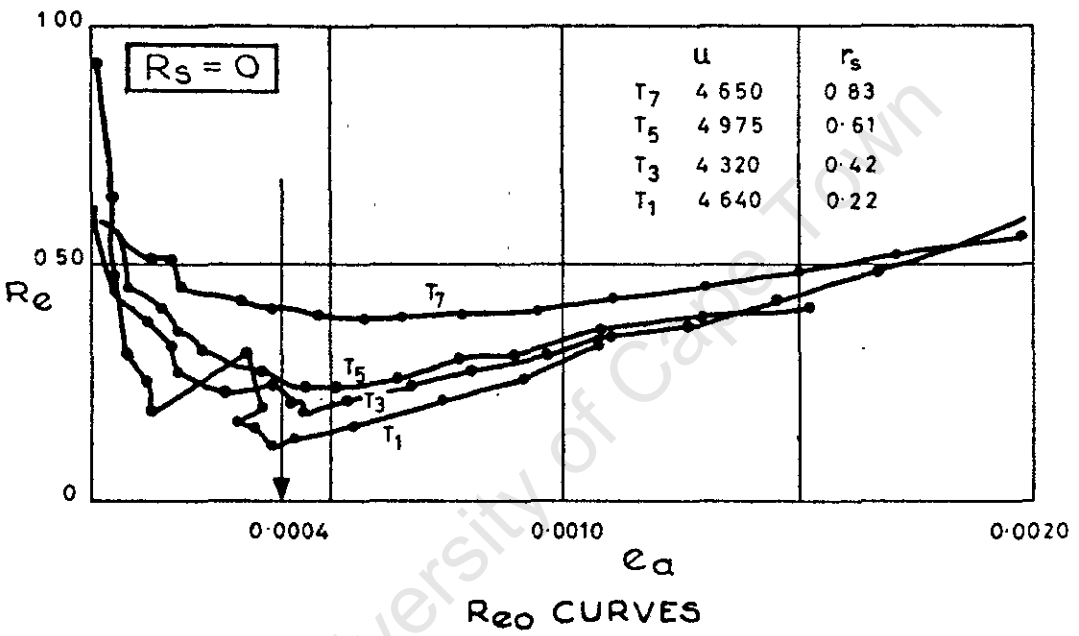

Reo CURVES

FIG.20.

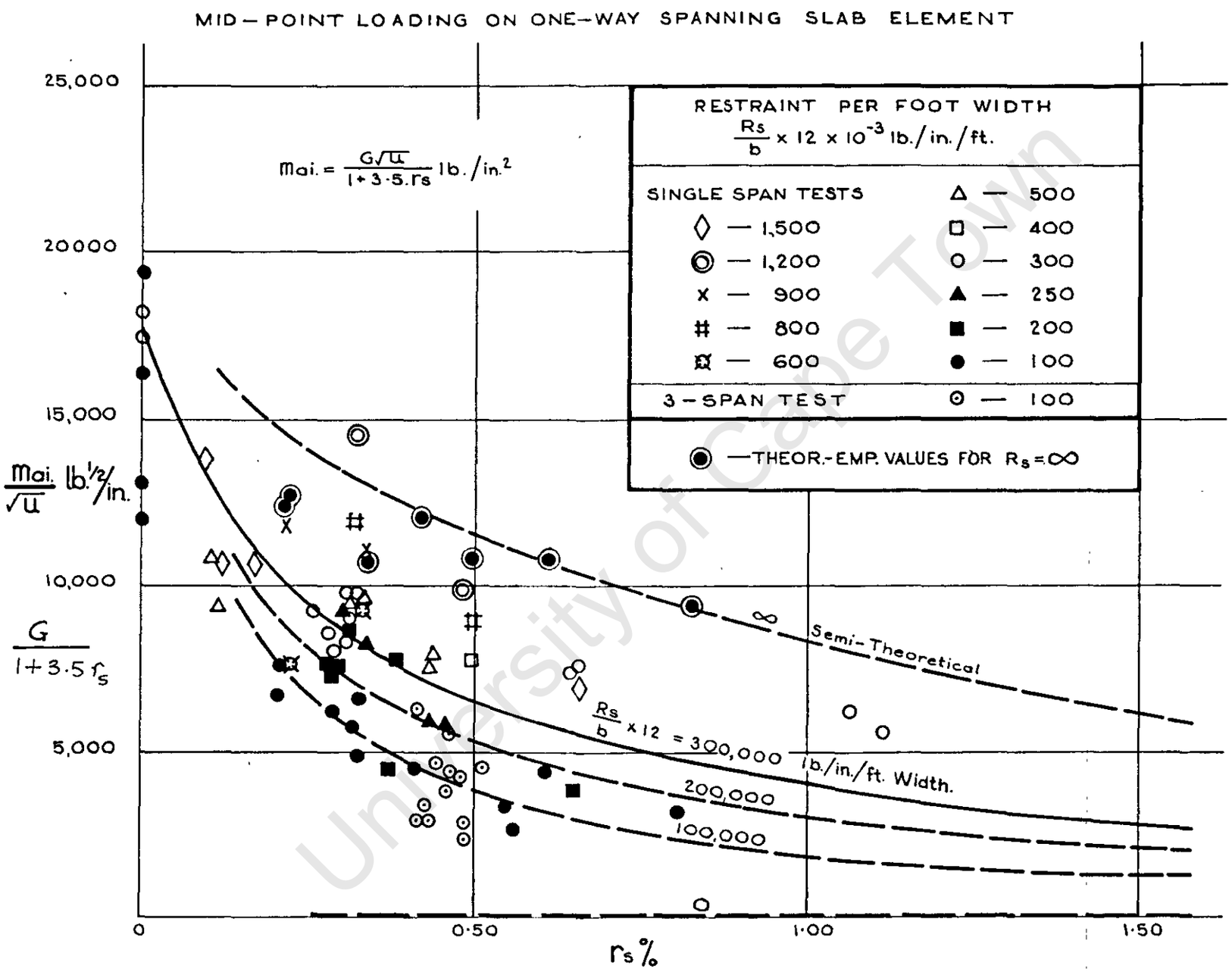

RELATION BETWEEN INITIAL INTERNAL MODULUS OF ARCHING m_{ai} AND CUBE STRENGTH, r_s AND $\frac{R_s}{b}$ FOR MID—POINT LOADING

FIG. 21.

$$r_s = \frac{A_s d_1}{bd^2} \times 100$$

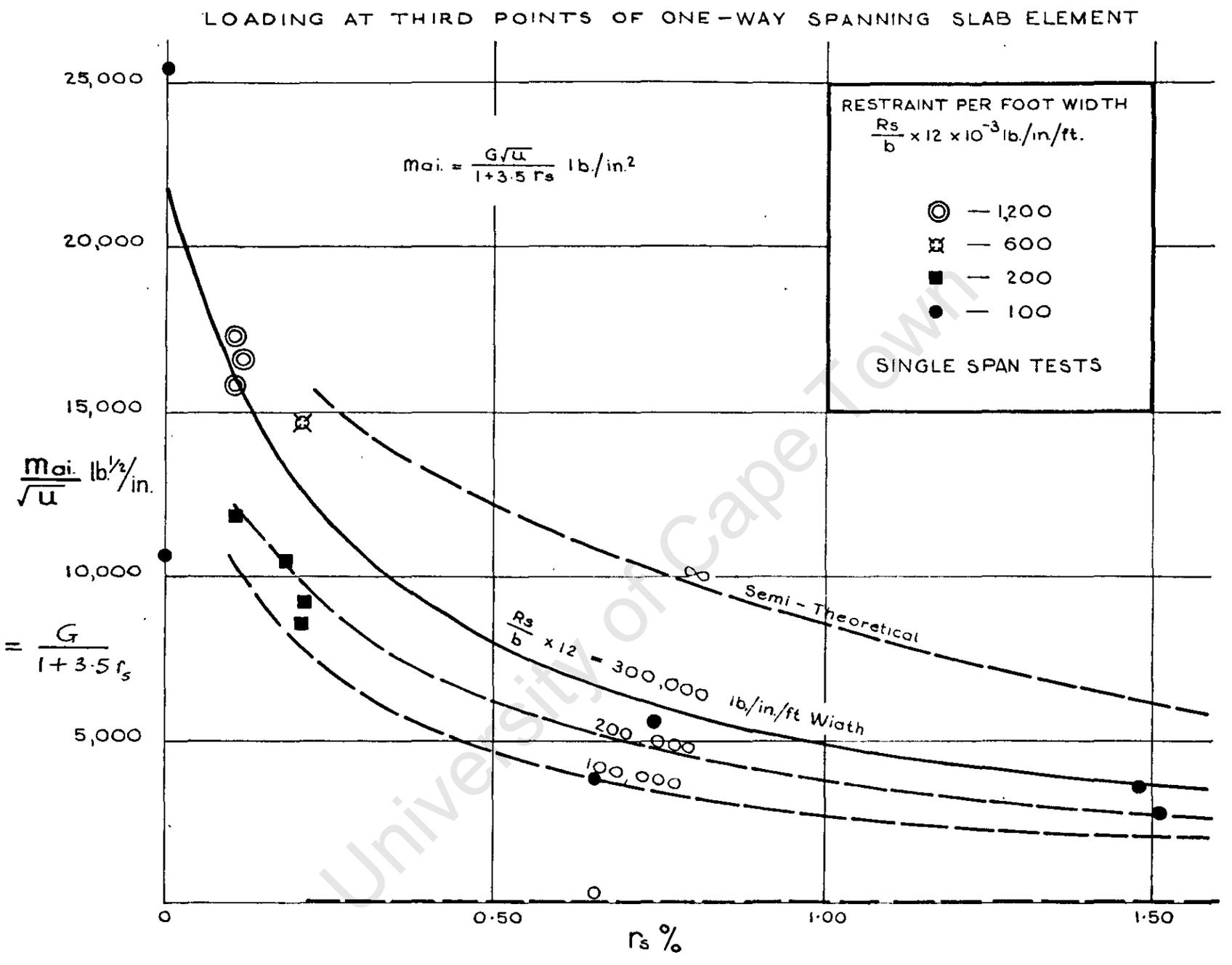

RELATION BETWEEN INITIAL INTERNAL MODULUS OF ARCHING m_{ai}. AND CUBE STRENGTH, r_s AND $\frac{R_s}{b}$ FOR THIRD-POINT LOADING

FIG. 22.

$$r_s = \frac{A_s d_1}{bd^2} \times 100$$

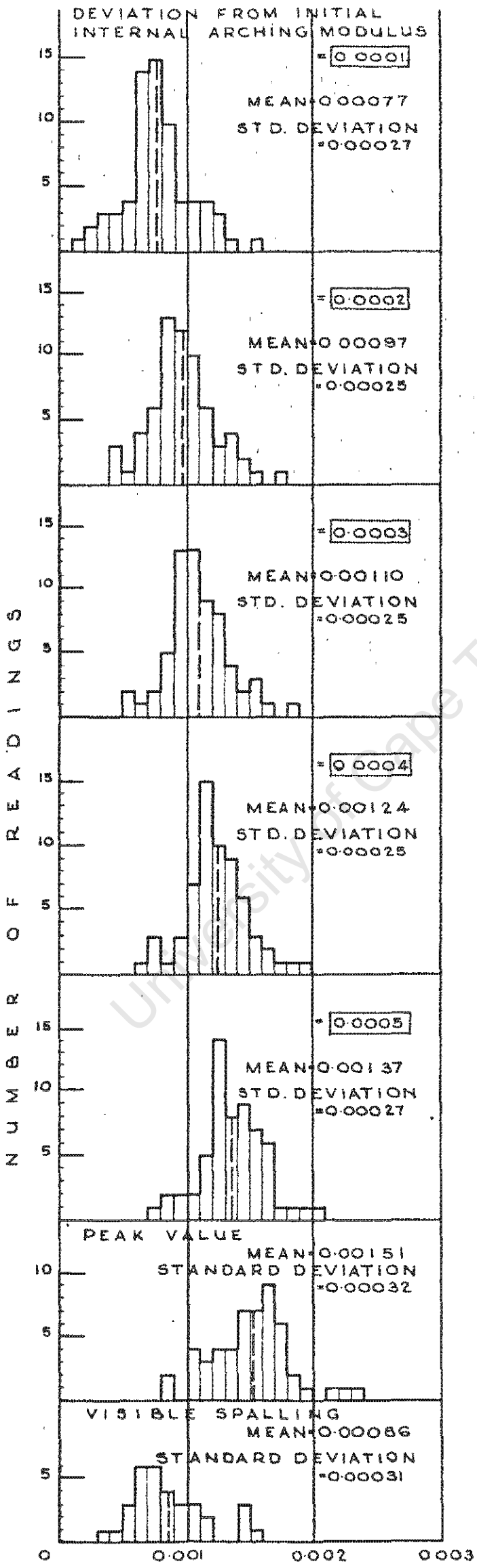

FIG. 23. HISTOGRAMS OF ARCHING STRAINS AT PARTICULAR DEVIATIONS OF STRAINS

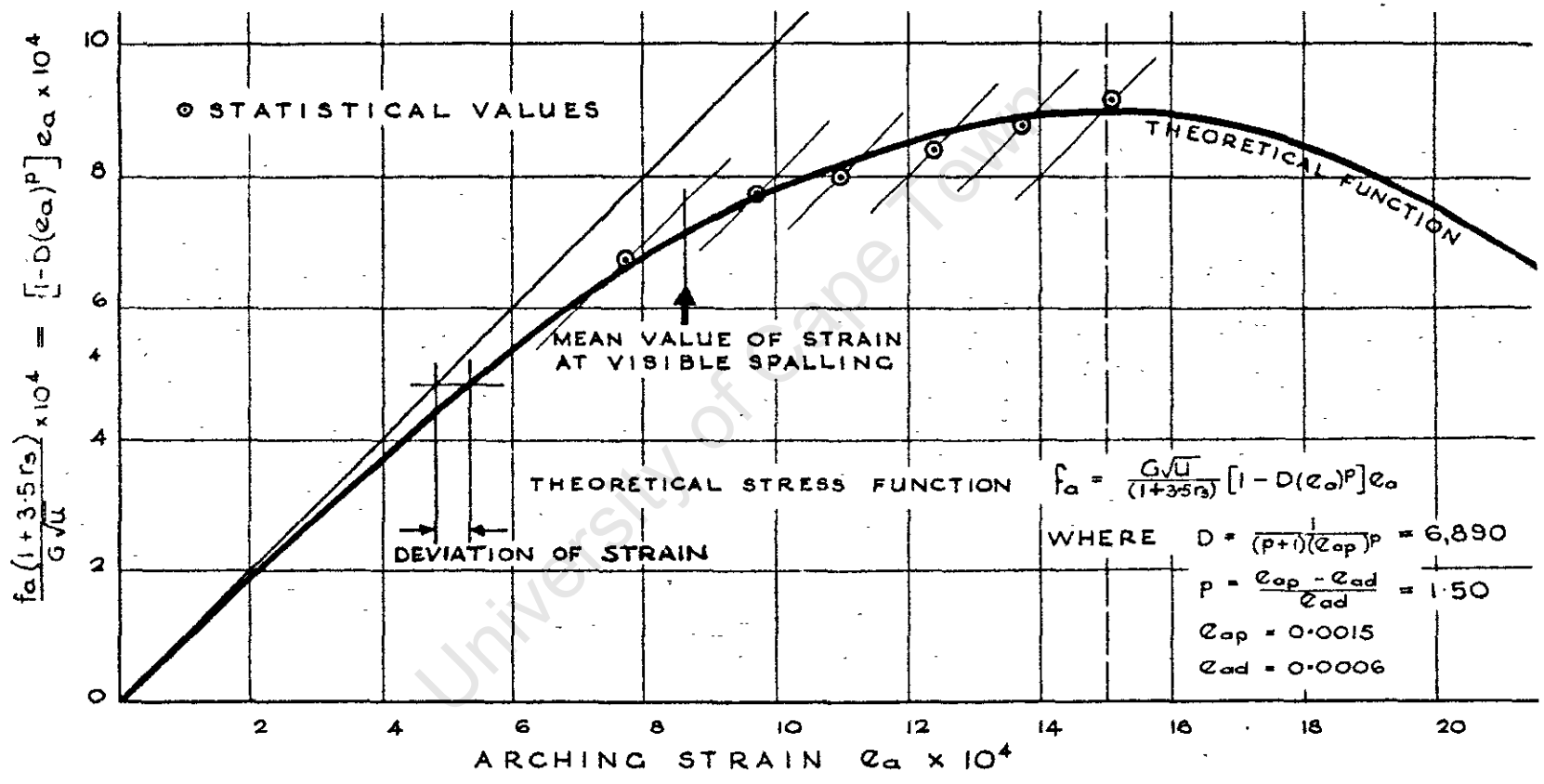

FIG.24. STRESS-STRAIN FUNCTION FOR ARCHING THEORY

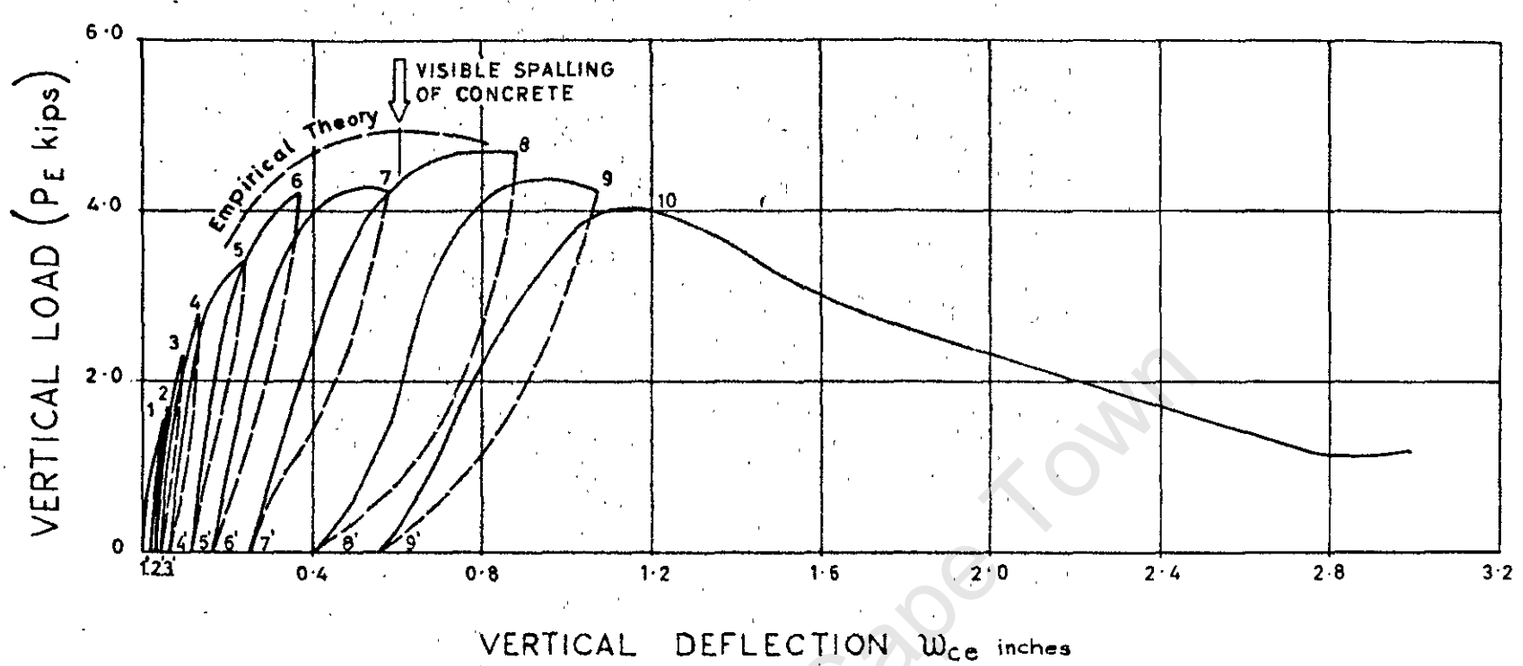

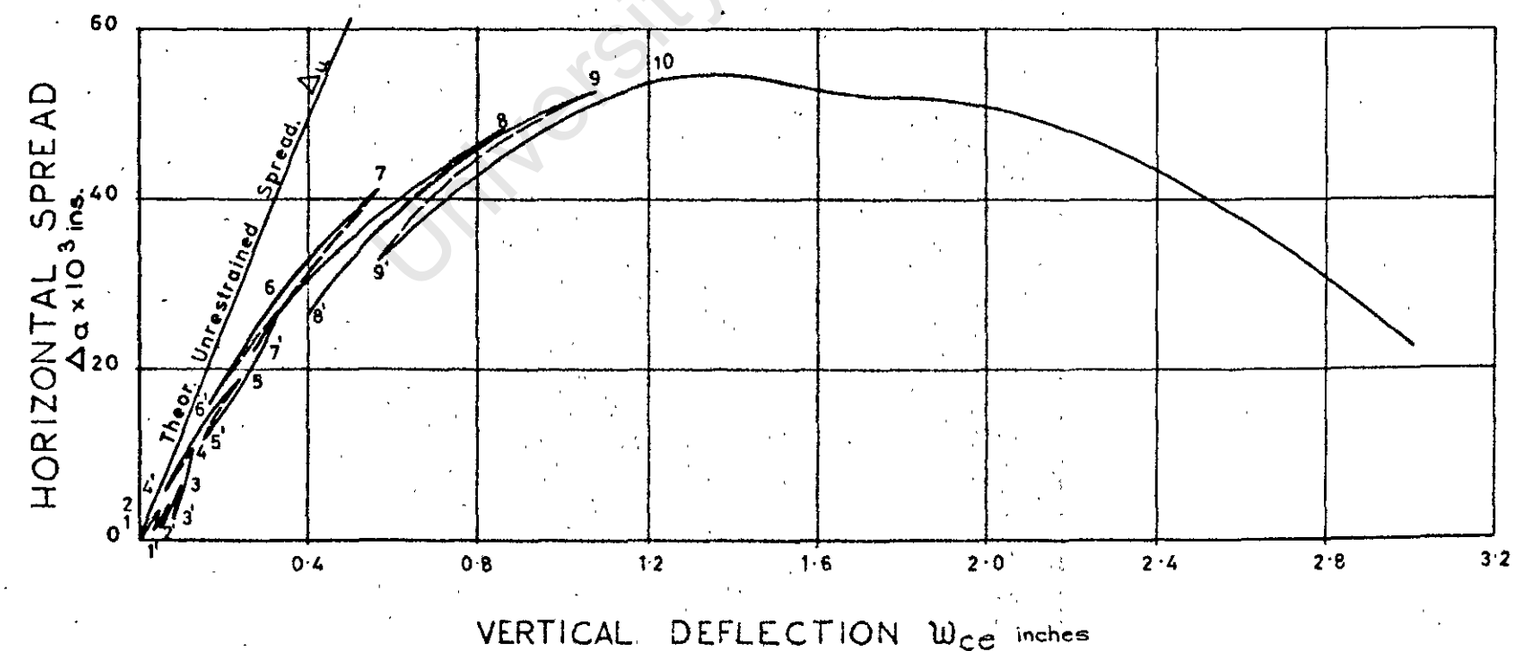

FIG. 25.

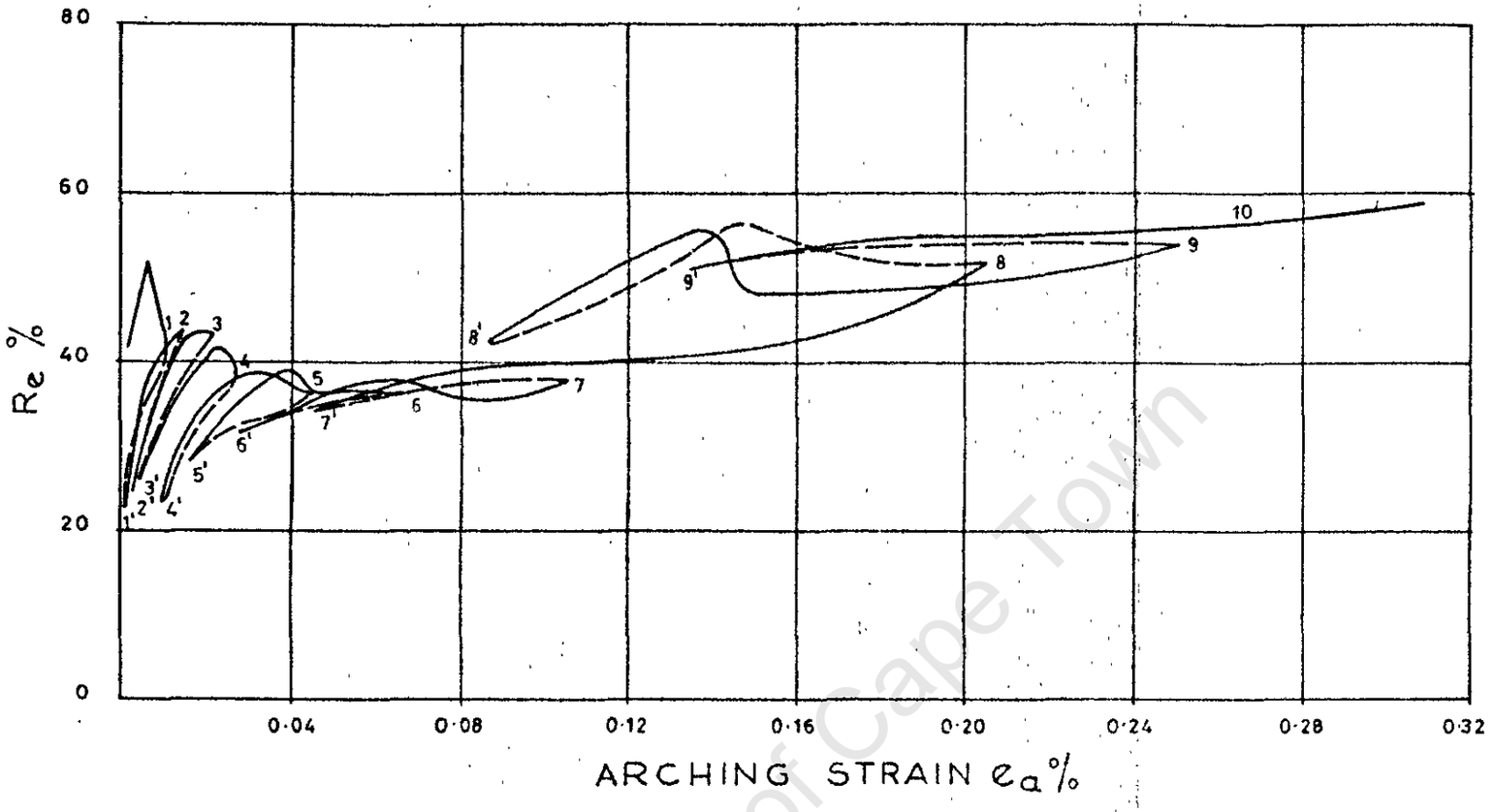

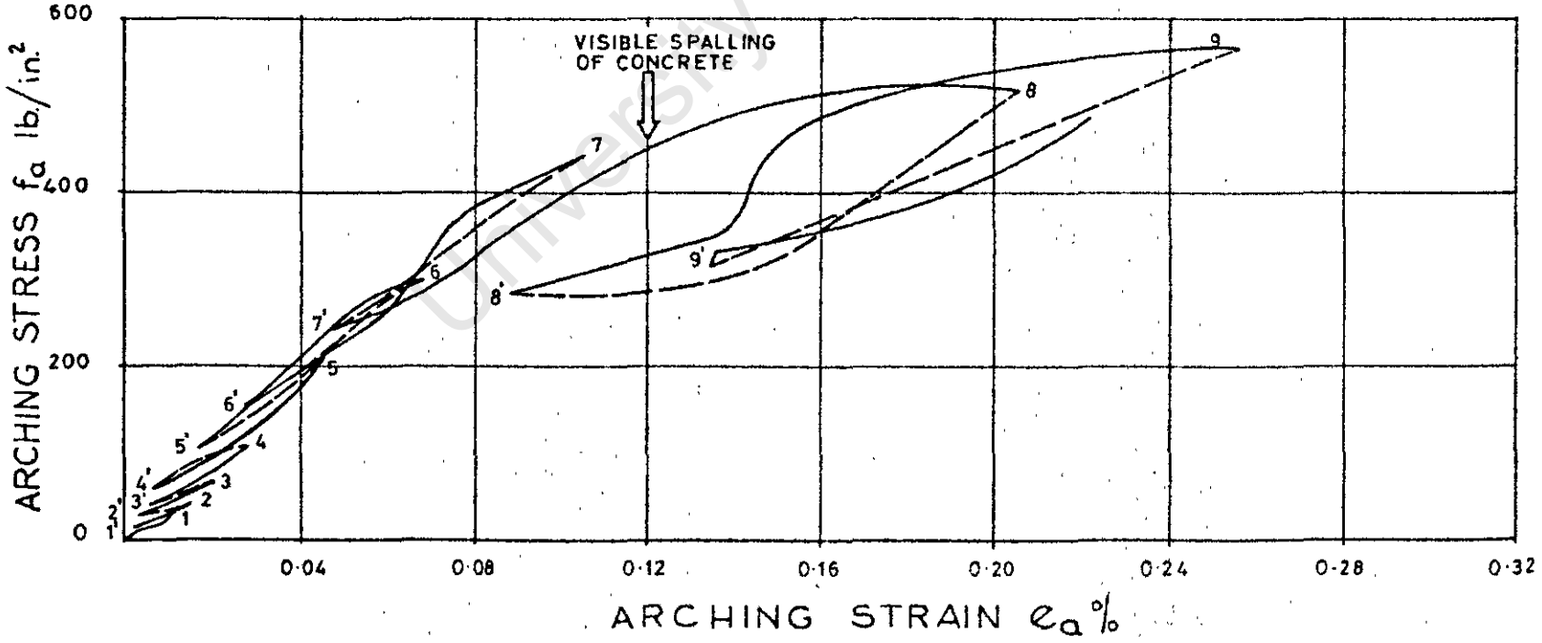

FIG. 26.

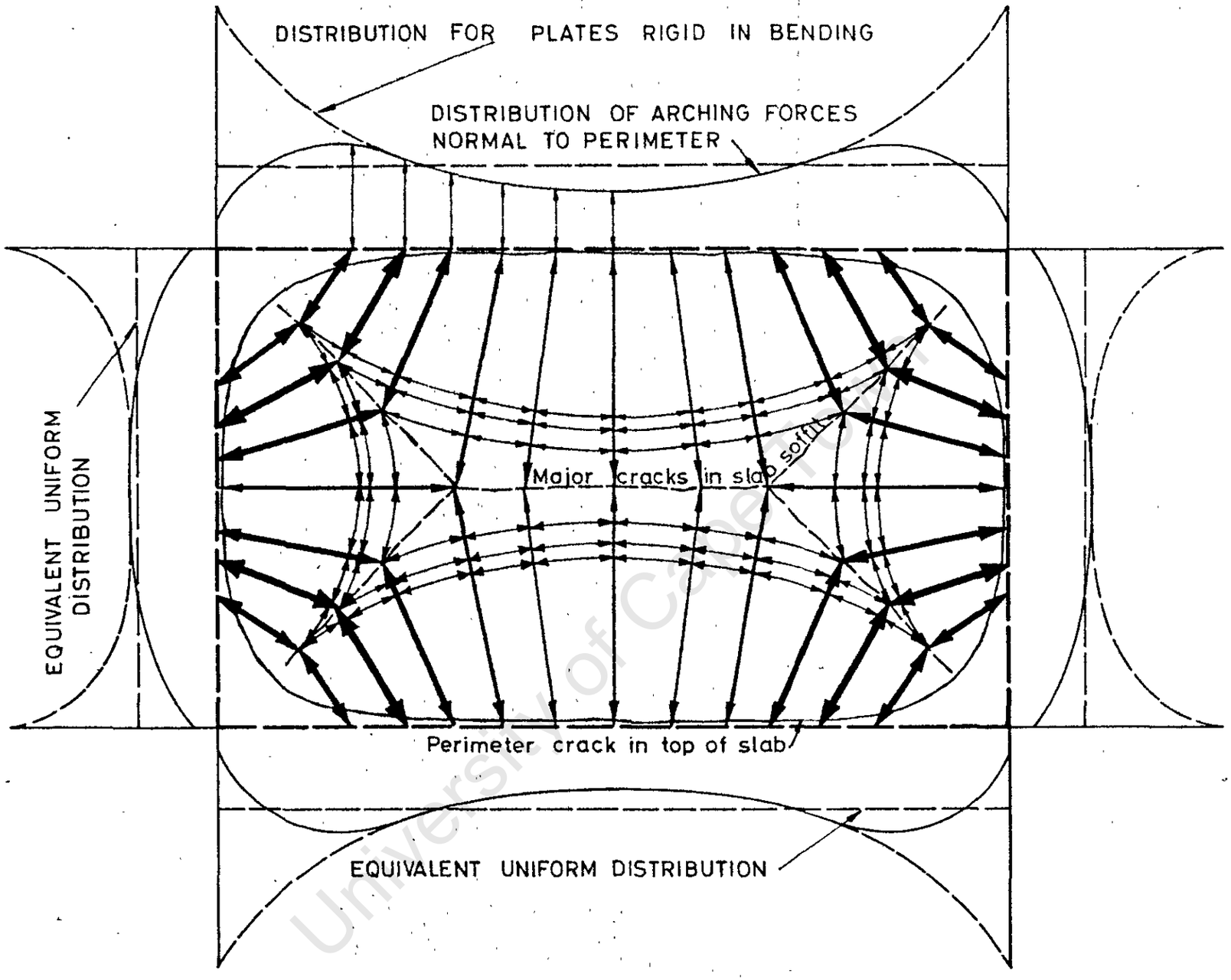

PROBABLE DISTRIBUTION OF THE PRINCIPAL ARCHING FORCES IN A SLAB PANEL WITH UNIFORMLY DISTRIBUTED LOADING

FIG. 27.

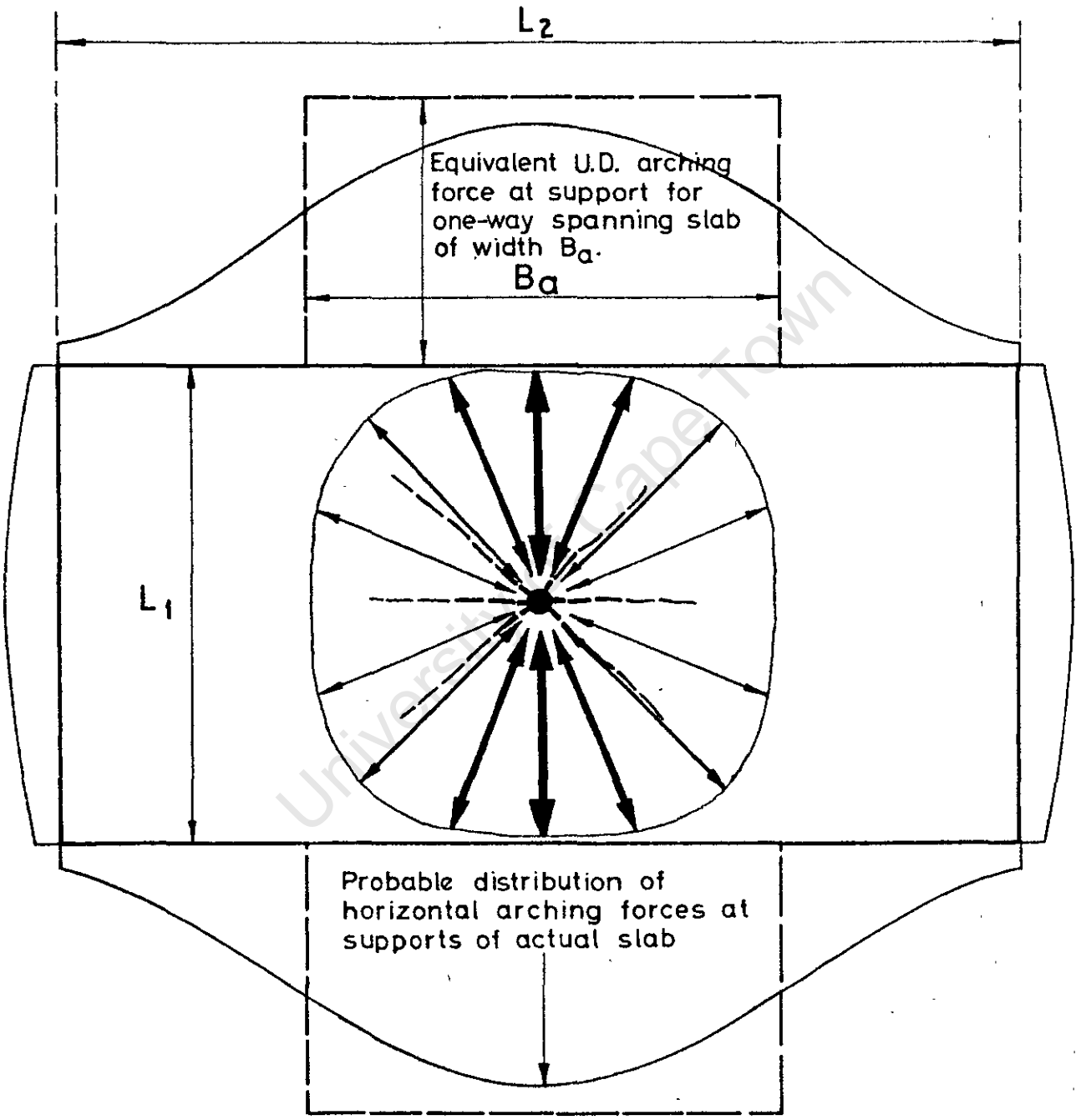

FIG. 28.

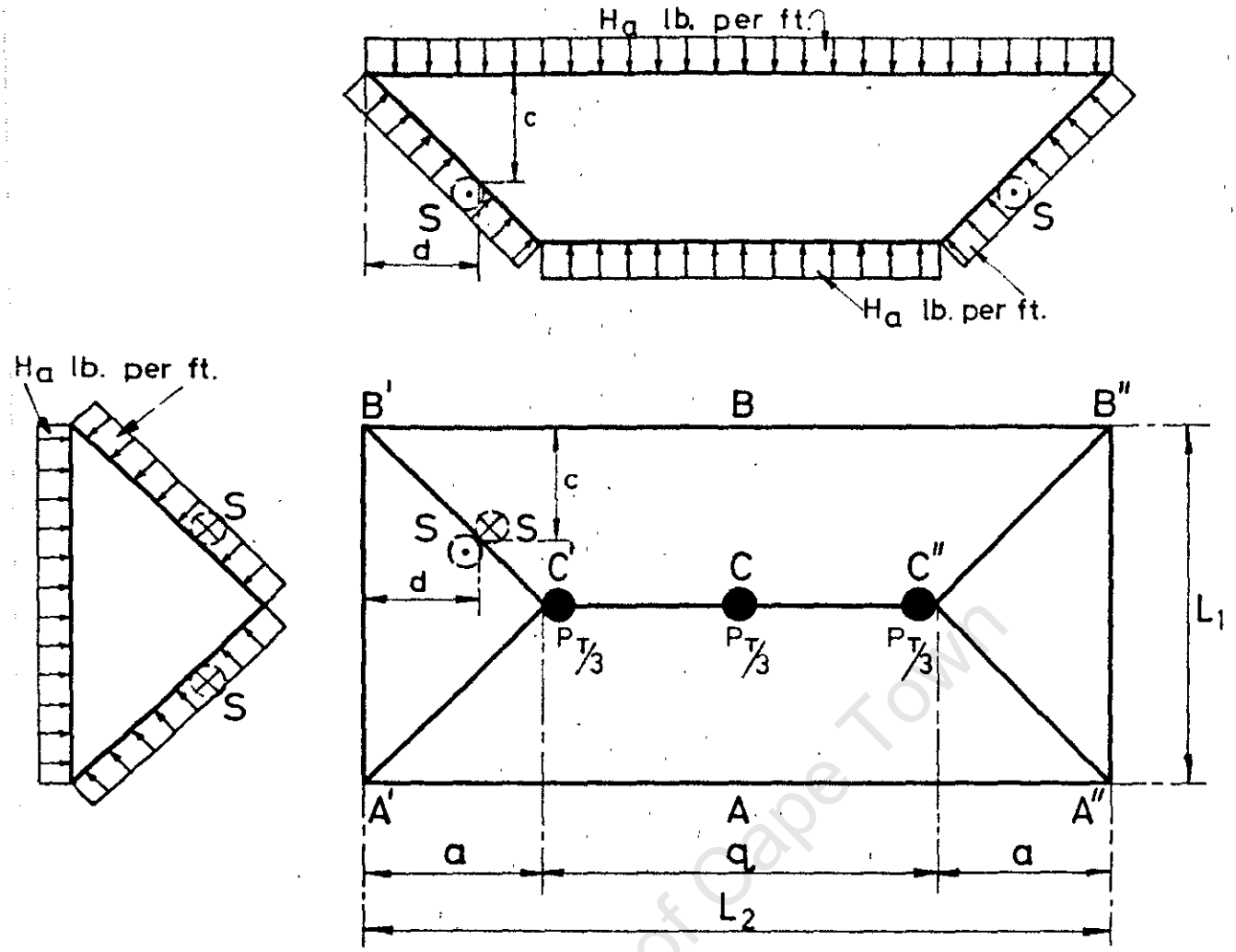

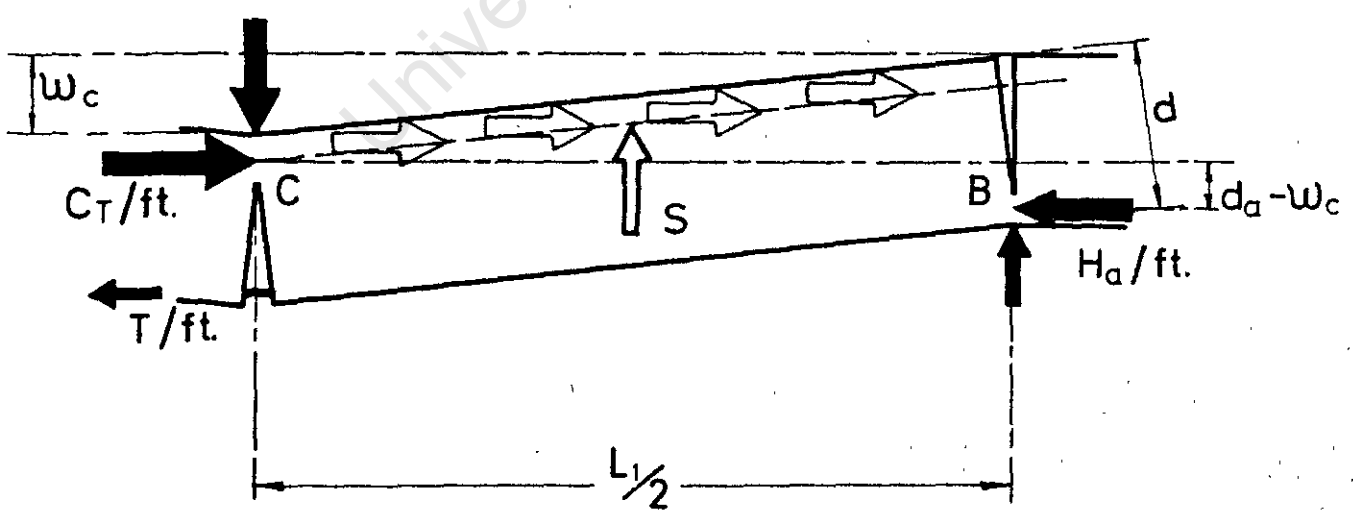

FIG. 29.

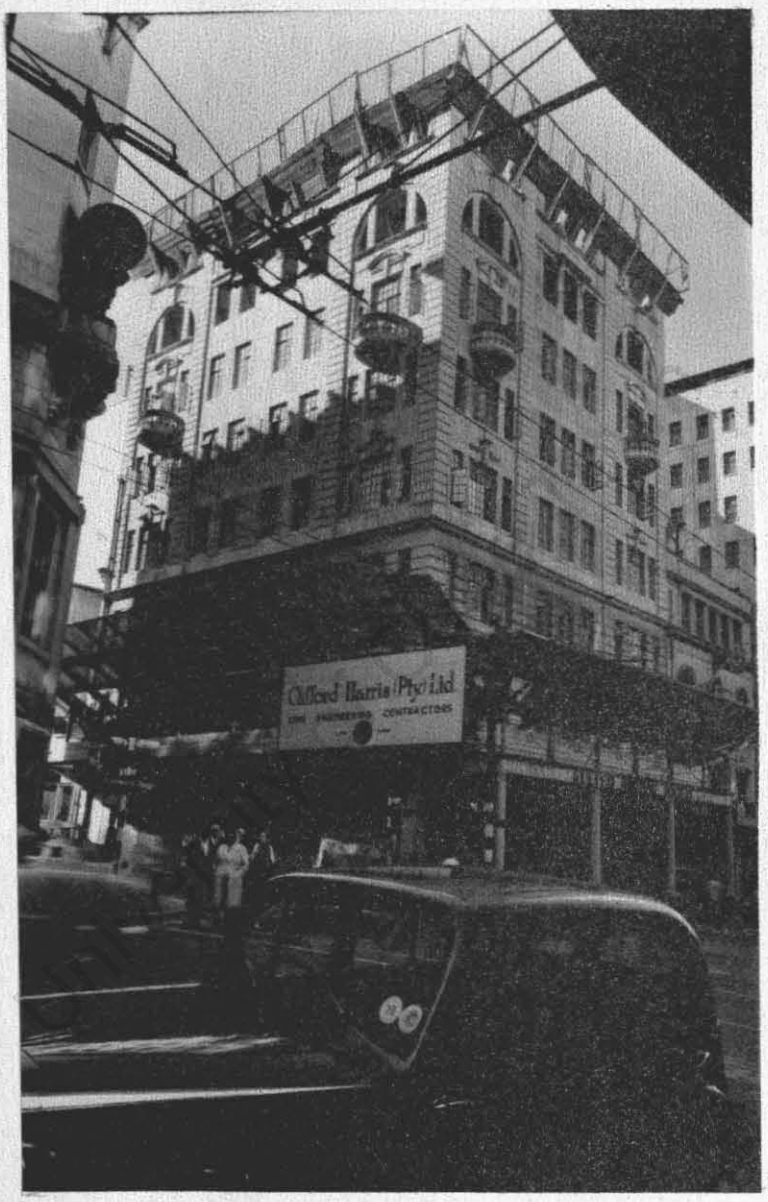

FIG. 30.

THE OLD ALLIANCE HOUSE CAPE TOWN

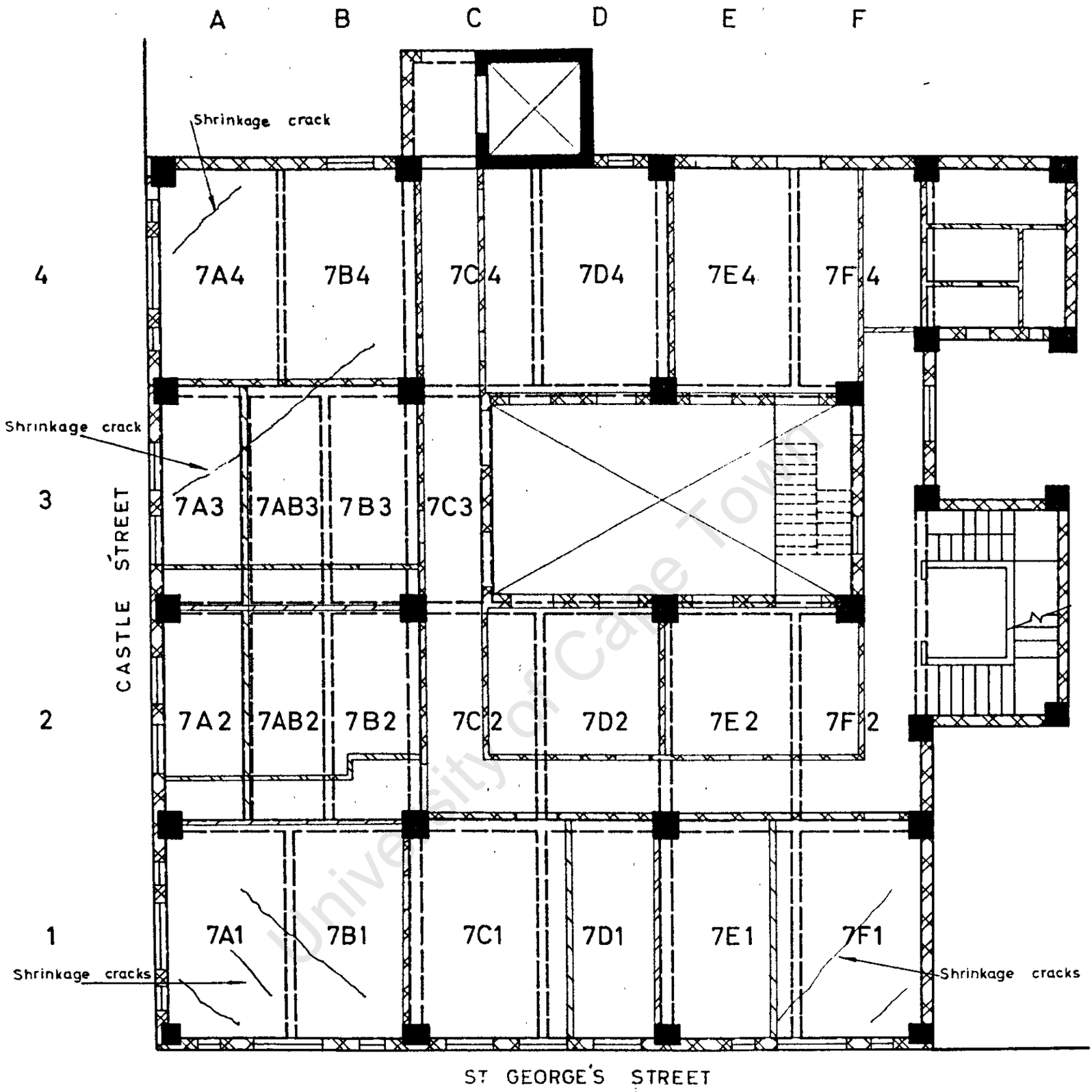

OLD ALLIANCE HOUSE

PLAN OF 7TH FLOOR CONSTRUCTION

Showing positions of brick partition walls under & above

SCALE

0 5 10 15 20 Feet

PARTITIONS

Above

Under

Under & Above

FIG. 31.

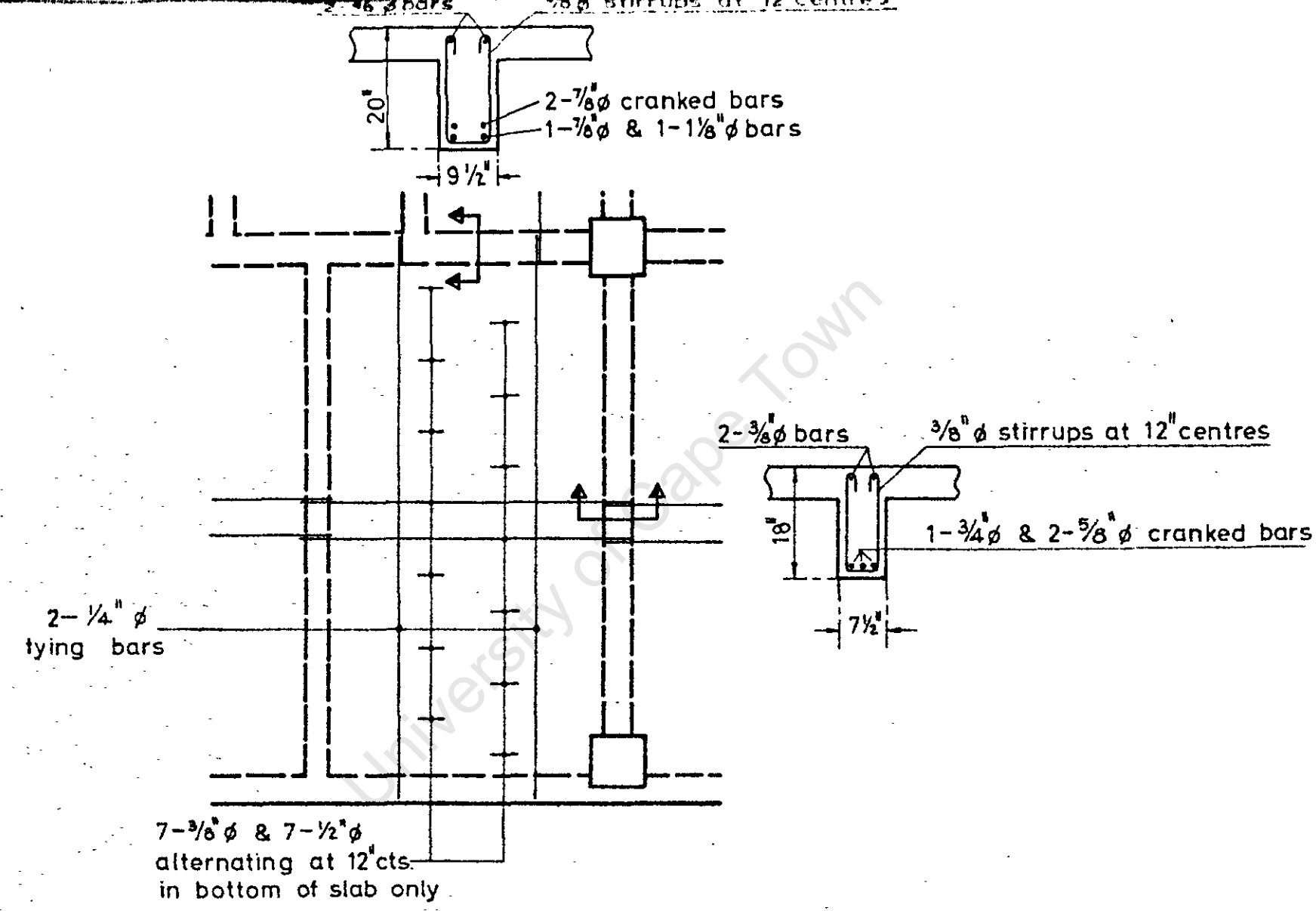

TYPICAL DETAIL OF PANEL REINFORCEMENT

FIG. 32.

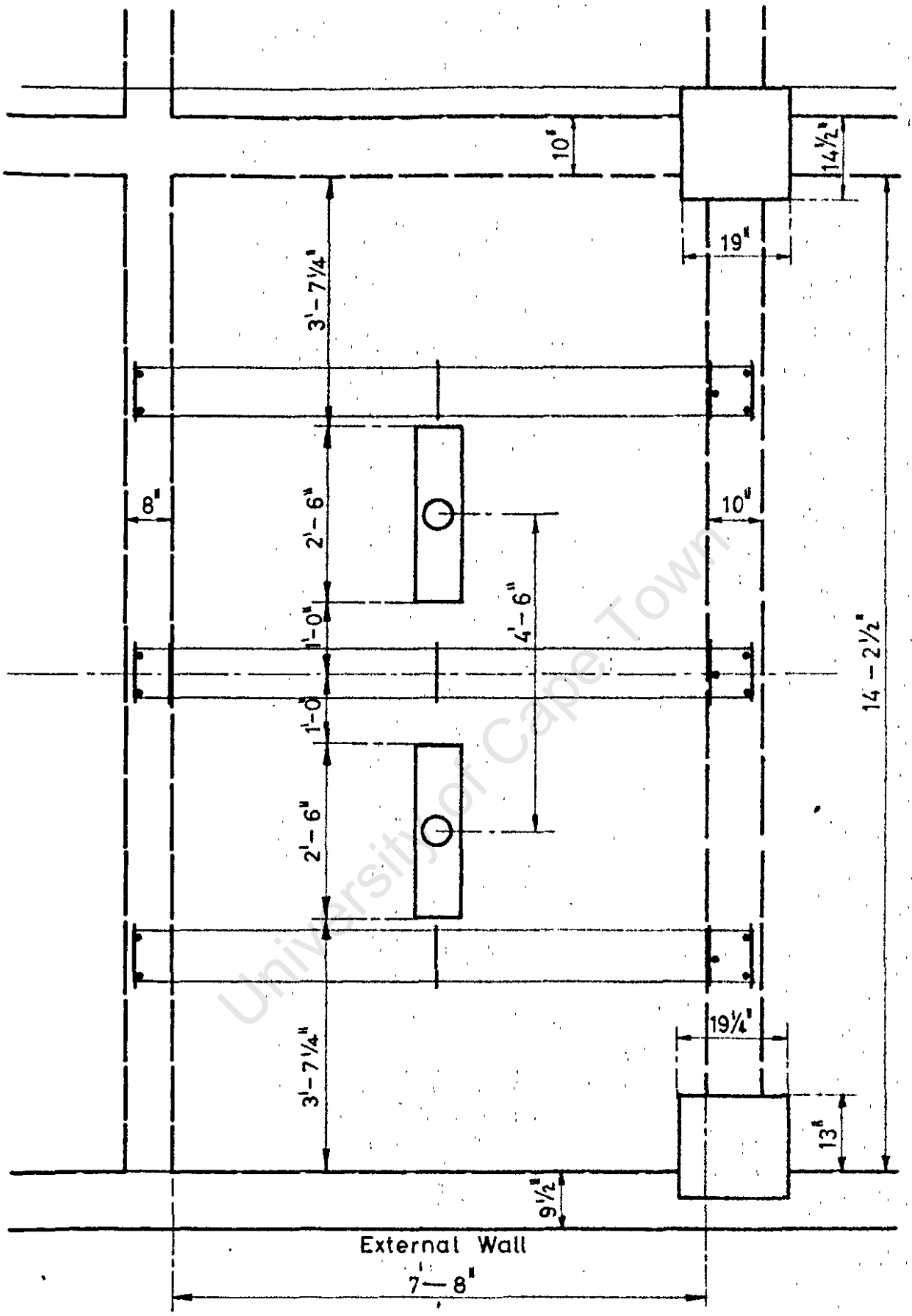

FIG. 33.

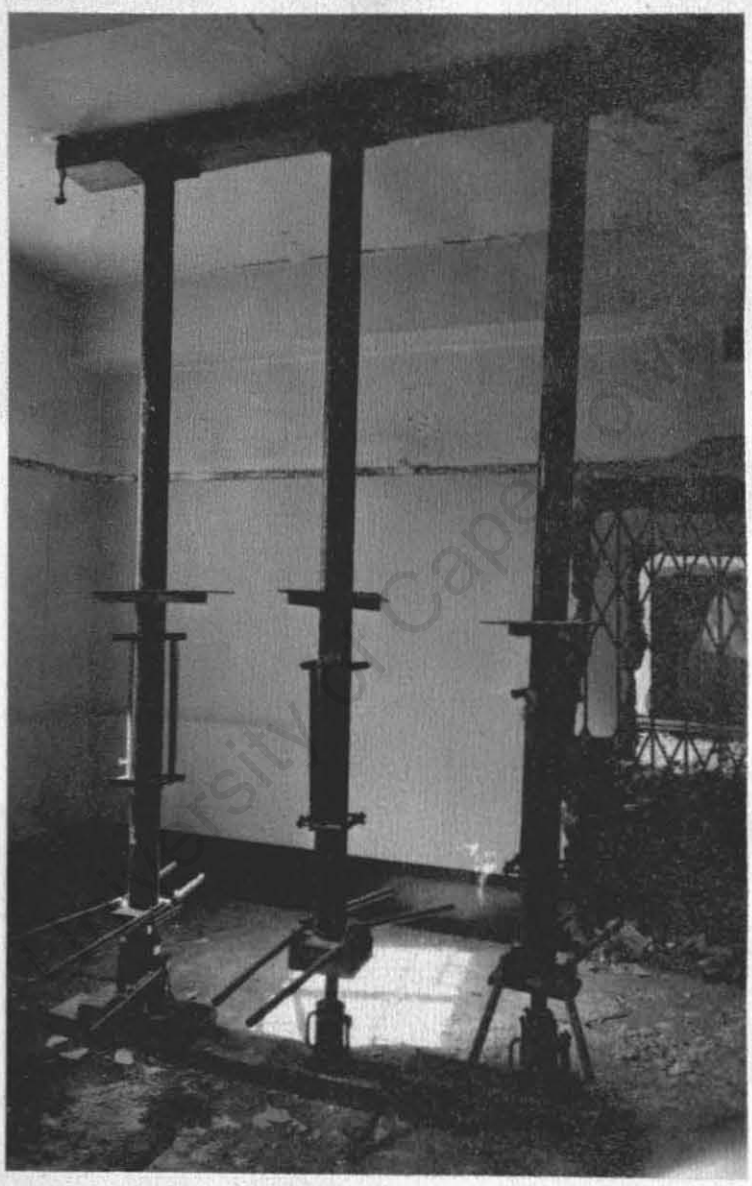

FIG. 34A.

TEST ON SLAB PANEL OF ALLIANCE HOUSE WITH 3 POINT LOADING

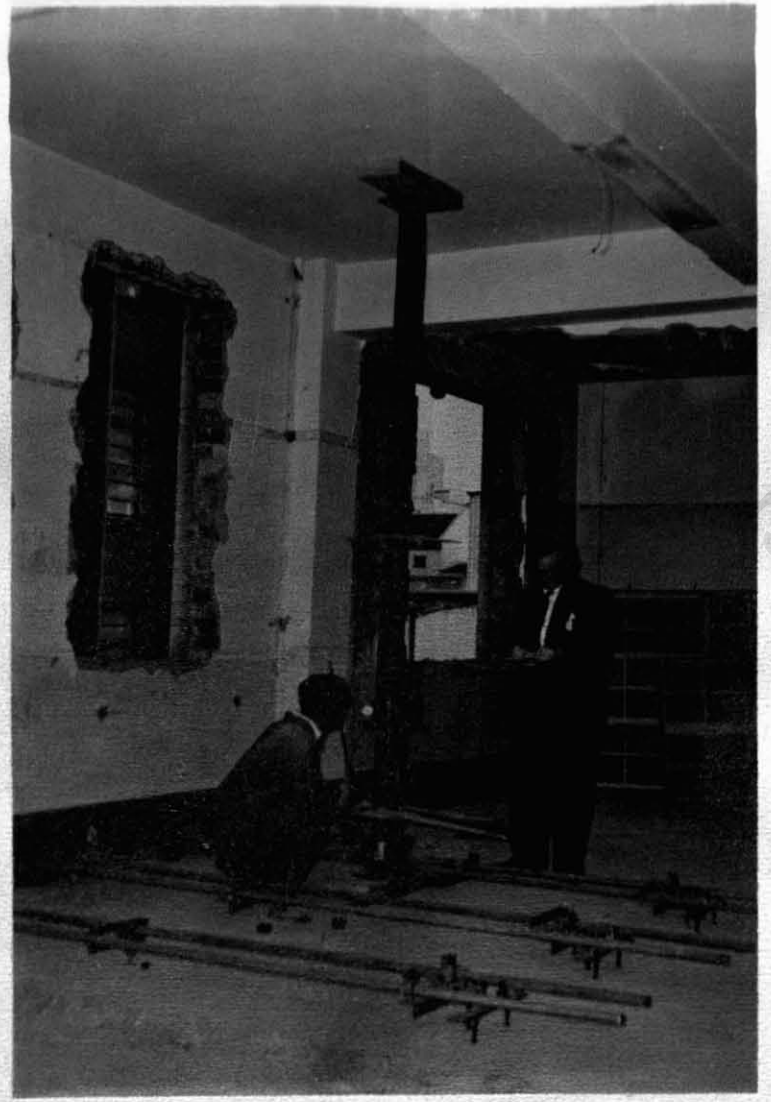

FIG. 35.

TEST ON SLAB PANEL OF ALLIANCE HOUSE
WITH SINGLE ECCENTRICALLY APPLIED LOAD

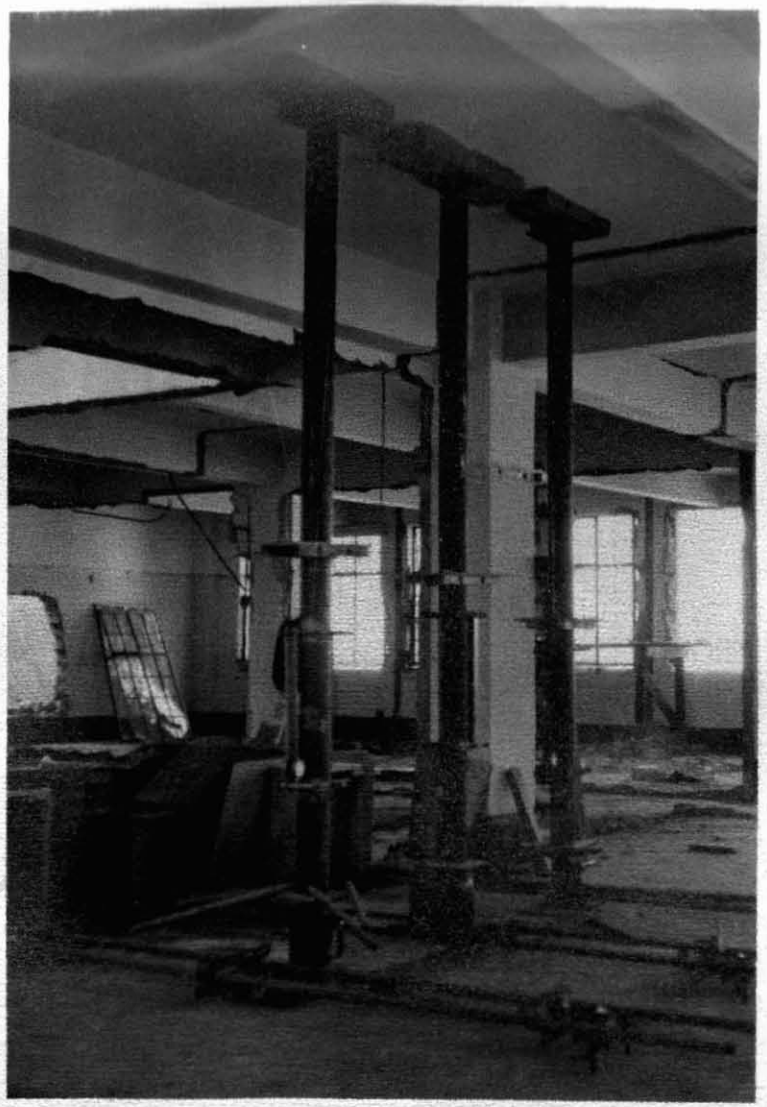

FIG. 34b.

TEST ON SLAB PANEL OF ALLIANCE HOUSE
WITH 3 POINT LOADING

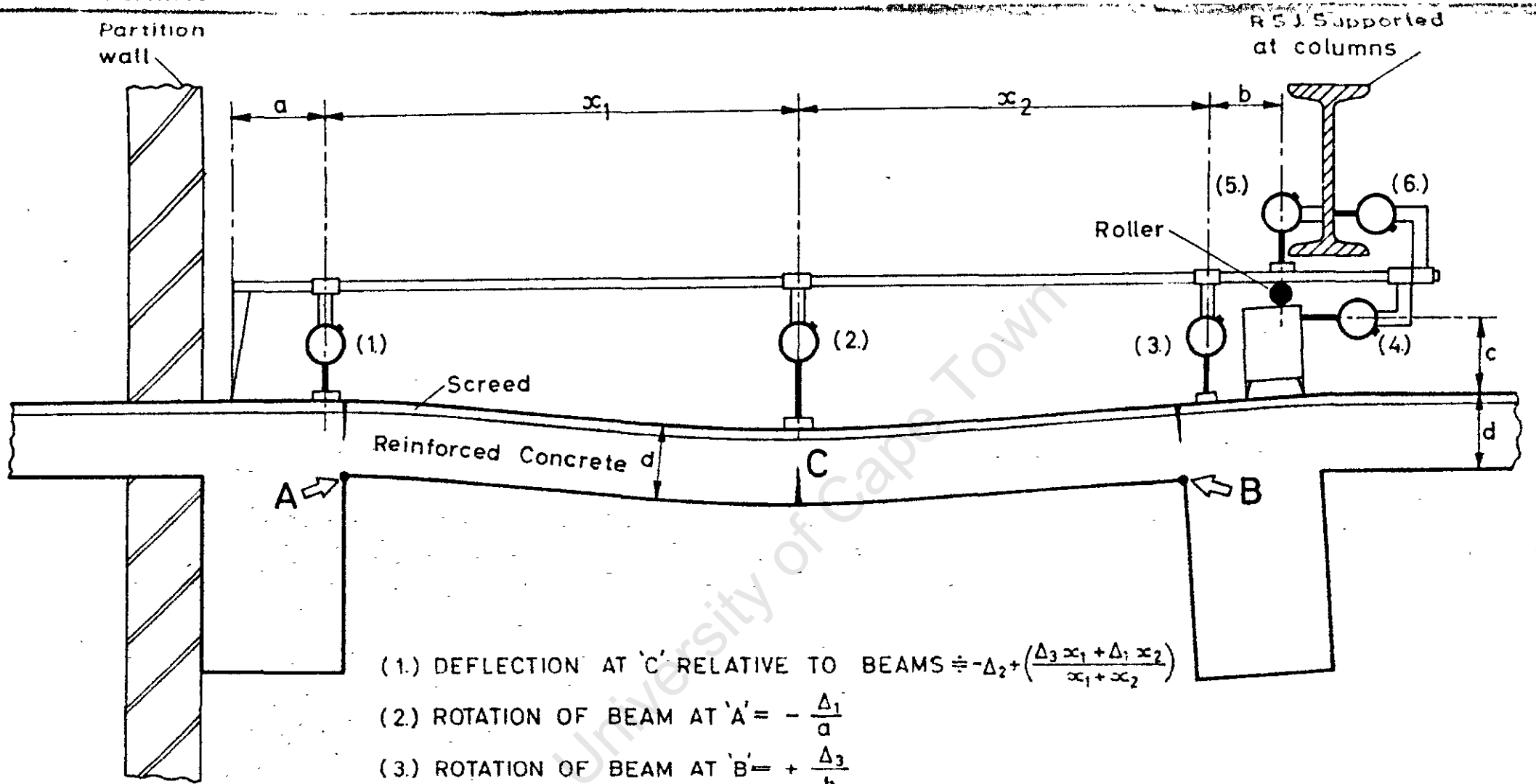

(1.) DEFLECTION AT 'C' RELATIVE TO BEAMS $\doteqdot -\Delta_2 + \left(\frac{\Delta_3 x_1 + \Delta_1 x_2}{x_1 + x_2}\right)$

(2.) ROTATION OF BEAM AT 'A' $= -\frac{\Delta_1}{a}$

(3.) ROTATION OF BEAM AT 'B' $= +\frac{\Delta_3}{b}$

(4.) HORIZONTAL DEFLECTION AT 'A' $= \Delta_A \doteqdot -\Delta_5 + \Delta_1\left(\frac{d}{a}\right)$

(5.) HORIZONTAL DEFLECTION AT 'B' $= \Delta_B \doteqdot +\Delta_4 - \Delta_6 - \Delta_3\left(\frac{c+d}{b}\right)$

(6.) EXPANSION OF A B' $= -\Delta_A + \Delta_B = \Delta_4 - \Delta_1\left(\frac{d}{a}\right) - \Delta_3\left(\frac{c+d}{b}\right)$

POSITIVE DISPLACEMENTS

POSITIVE DIAL GAUGE READING

FIG. 36.

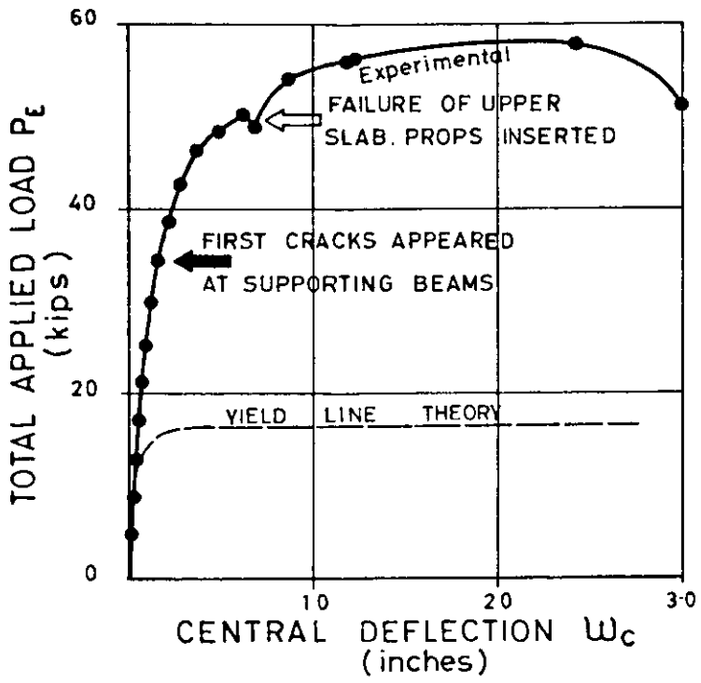

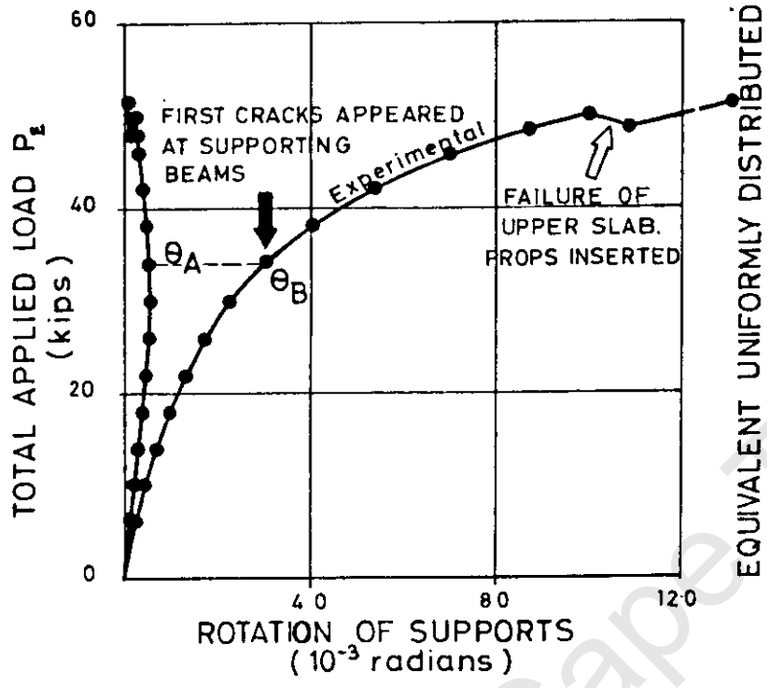

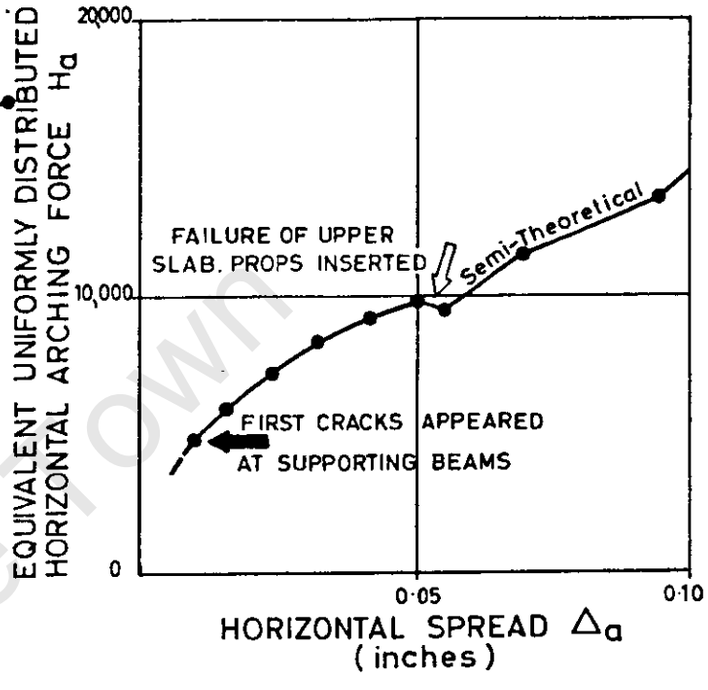

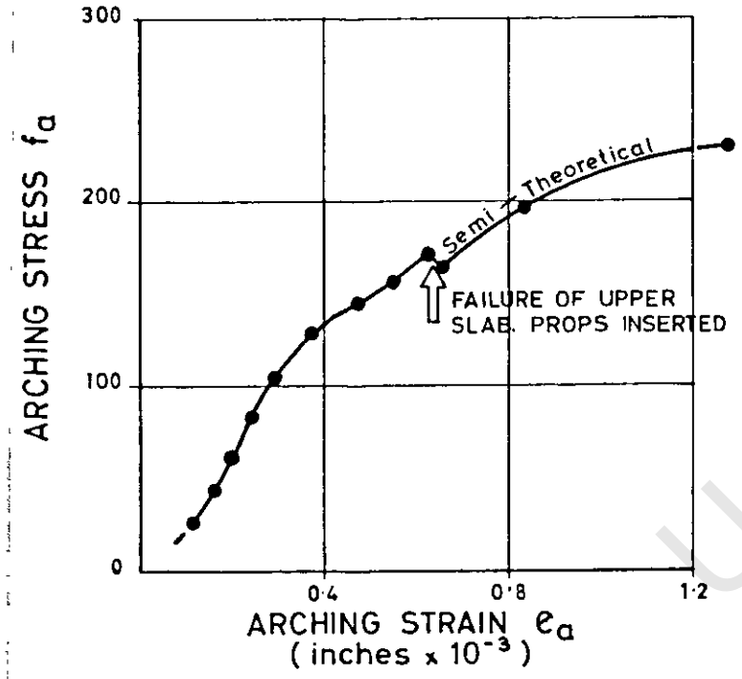

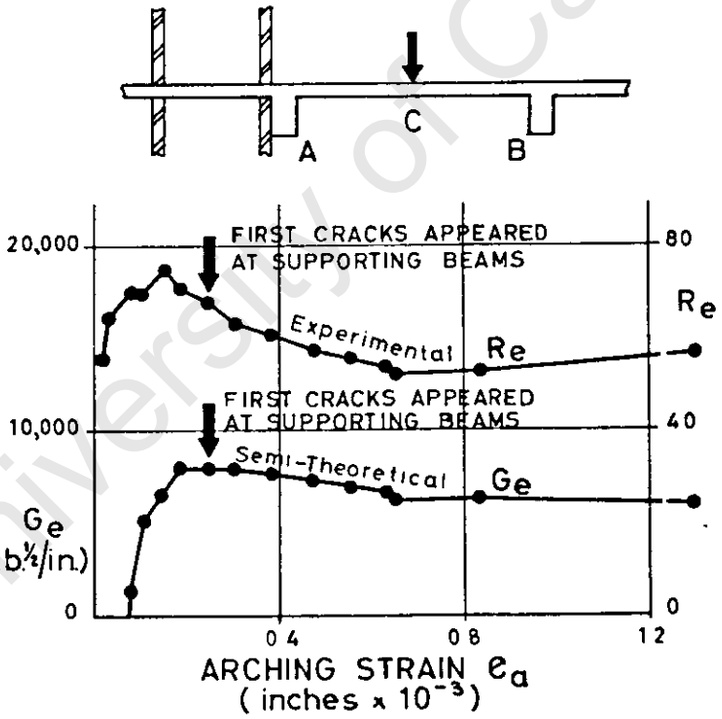

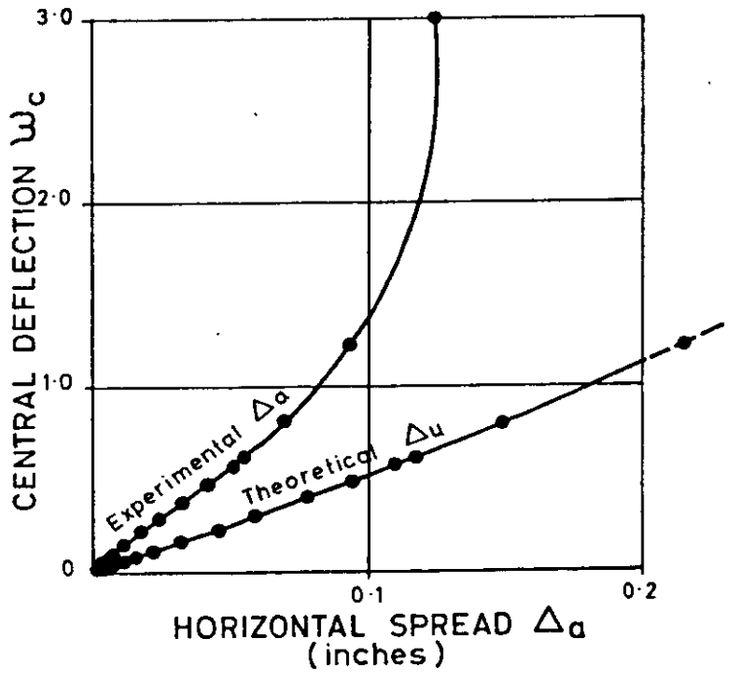

TYPICAL CURVES FOR TEST ON PANEL 6-B4 WITH 2 POINT DOWNWARDS LOADING

FIG.37.

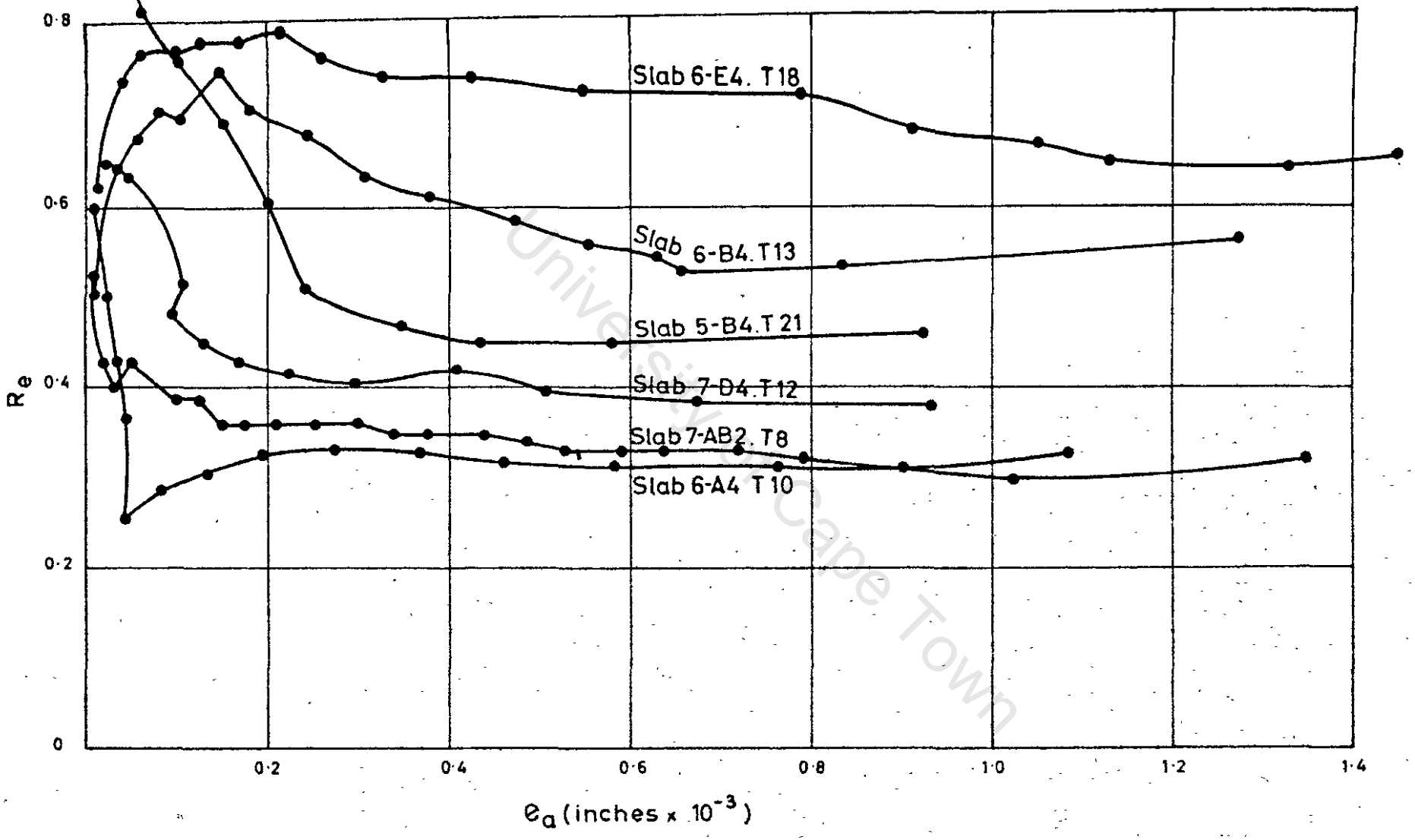

FIG. 38.

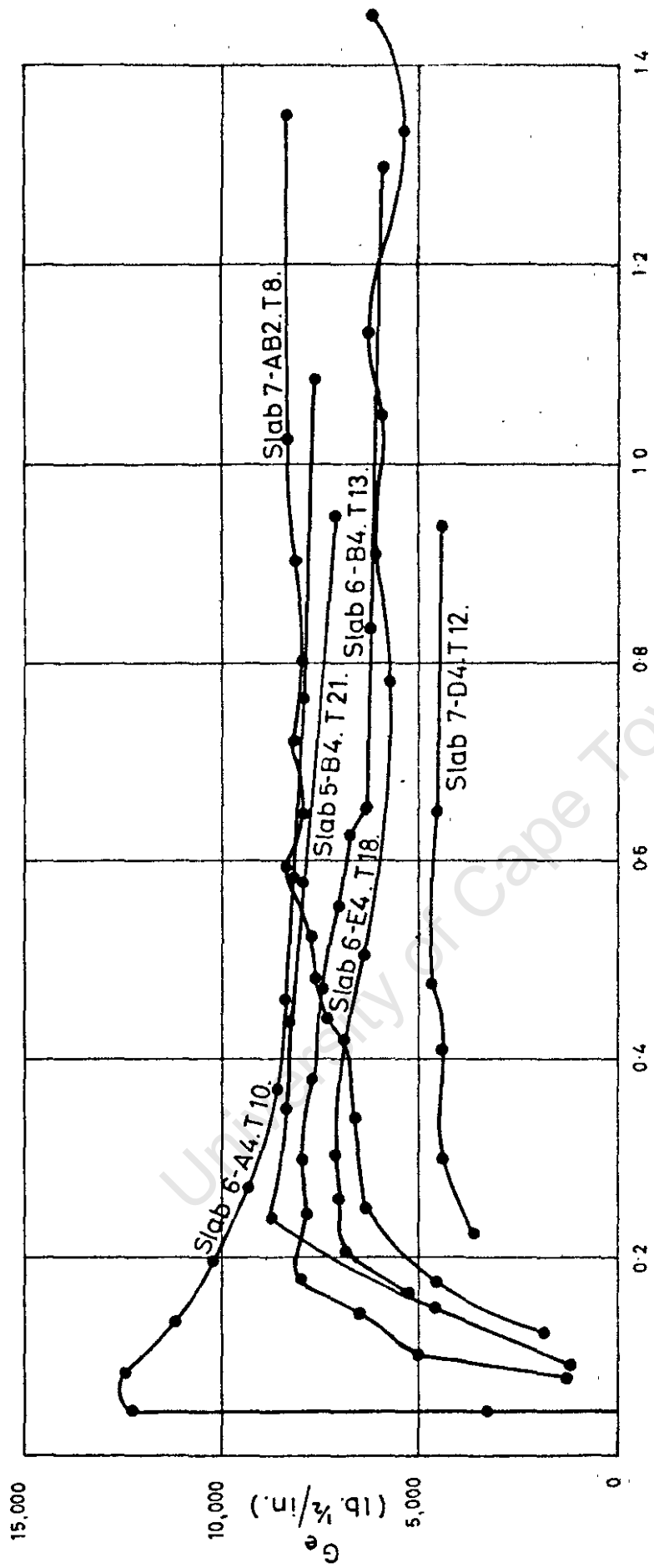

FIG. 39.

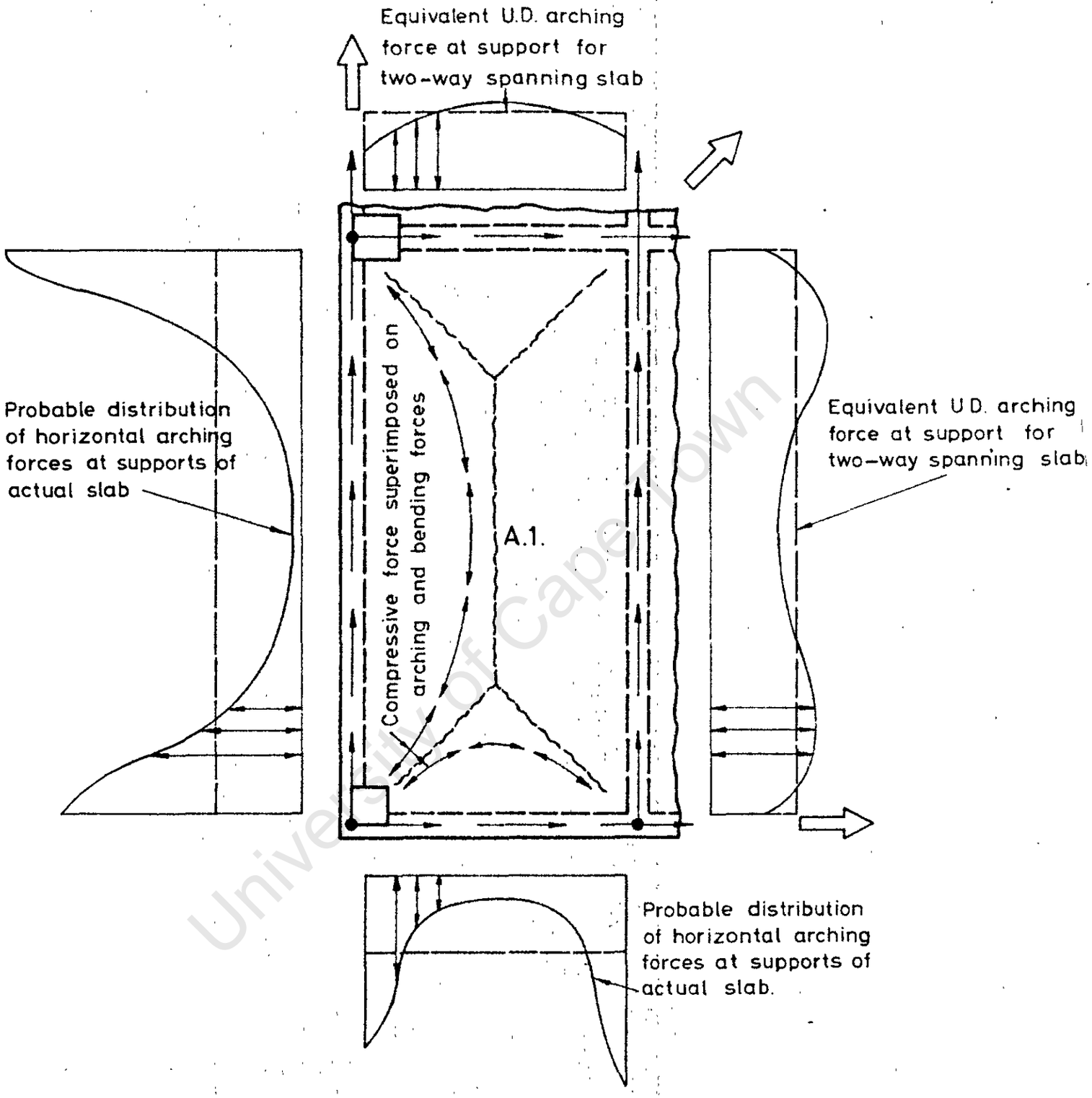

DISTRIBUTION OF ARCHING FORCES IN CORNER SLAB

FIG. 40.

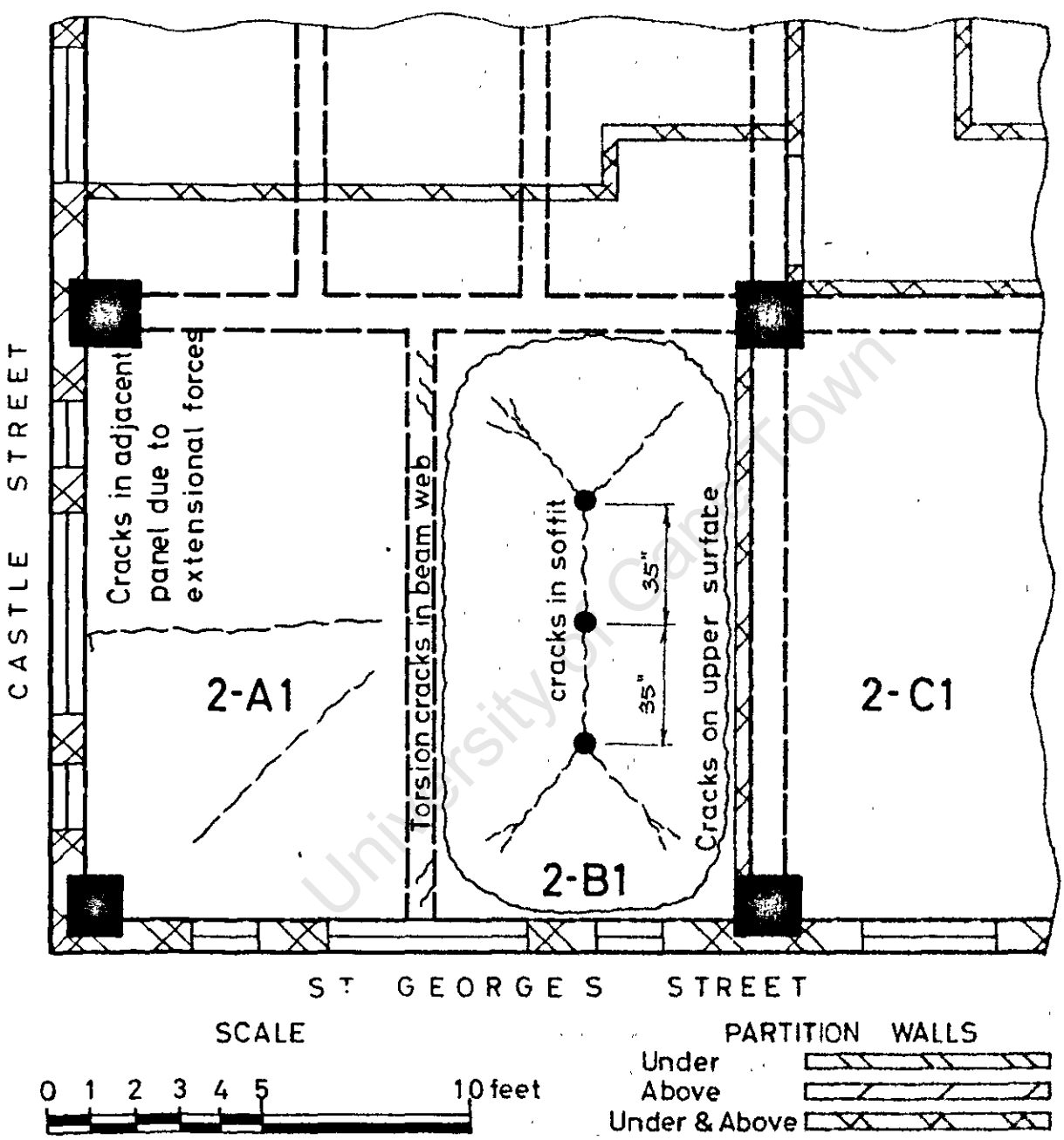

TEST T3 SHOWING MAJOR CRACKS

FIG. 41.

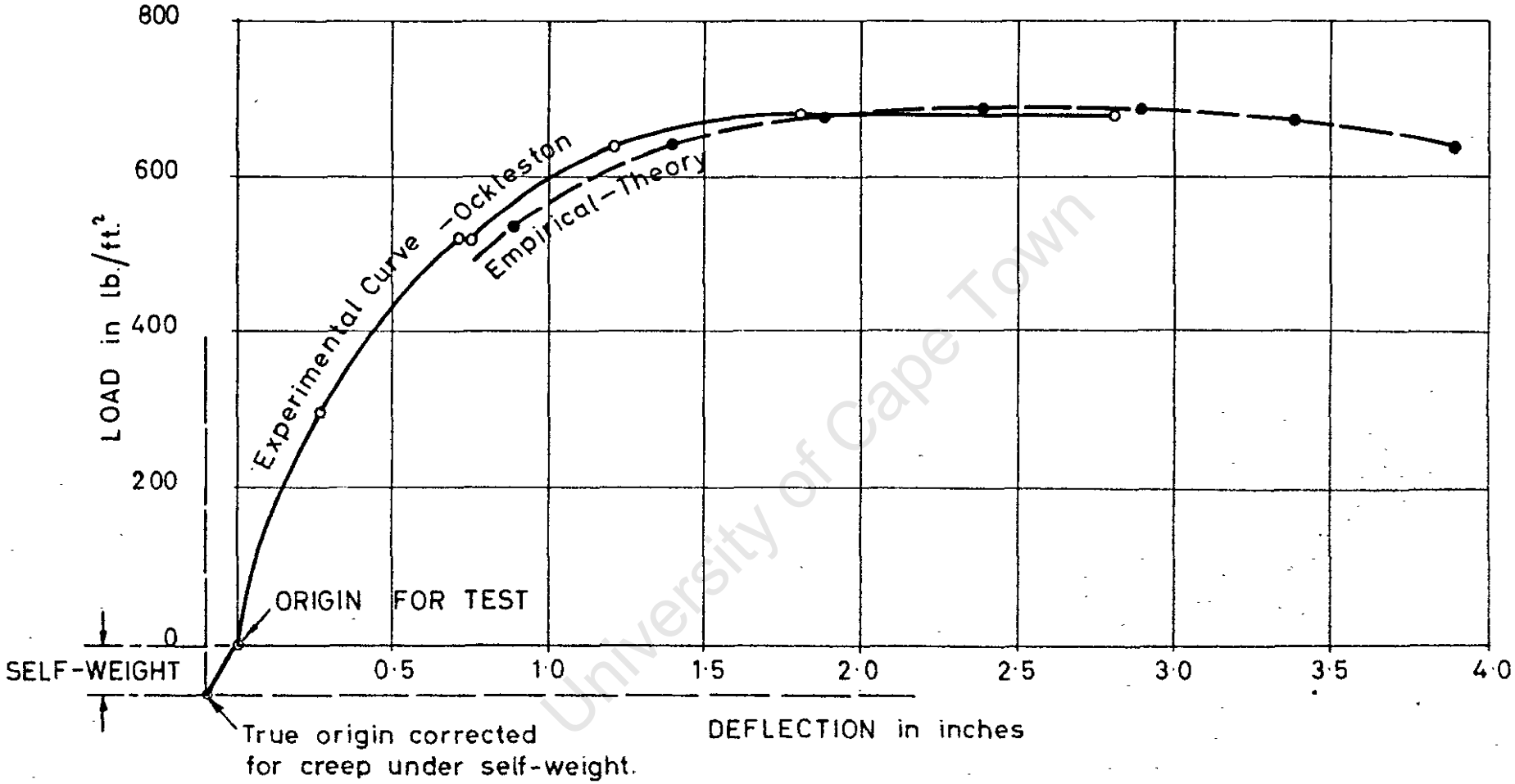

FIG.42.

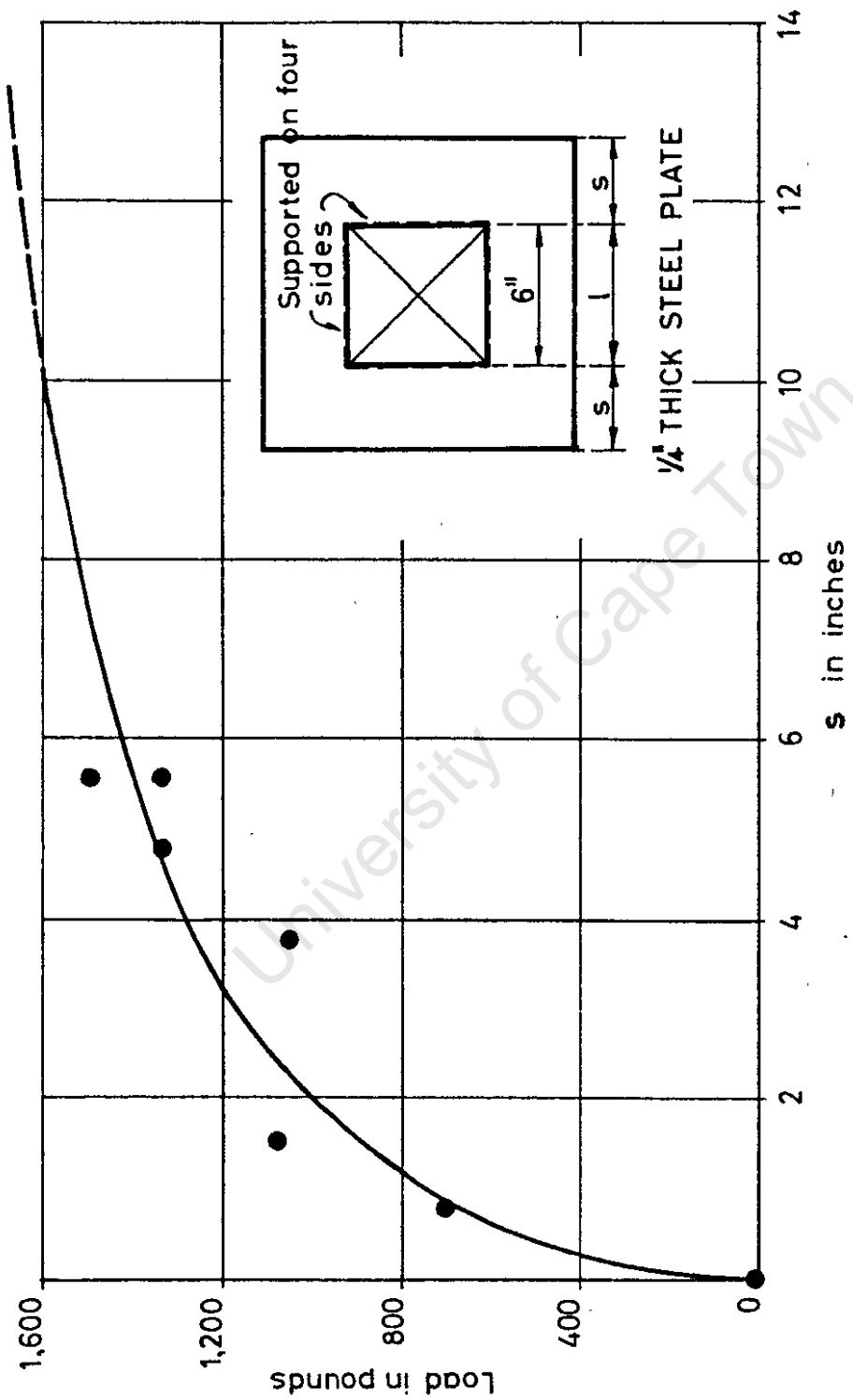

FIG.43.

A P P E N D I X III-8

EXTRACT FROM CONTRIBUTION

TO DISCUSSION OF PAPER

BY CHRISTIANSEN

PUBLISHED IN "THE STRUCTURAL ENGINEER"

JANUARY, 1964

NO. 1. VOL. 42.

$$r = R_2\,\sigma_\theta^{(1)} = 13{\cdot}56\cos\theta$$

$$\sigma_\theta^{(2)} = 59{\cdot}45 + 80{\cdot}20\cos\theta + 835{\cdot}80\cos 2\theta + 318{\cdot}33\cos 3\theta + 174{\cdot}10\cos 4\theta + 112{\cdot}97\cos 5\theta + \ldots$$

Table 1

r \ θ	0	$\frac{\pi}{4}$	$\frac{\pi}{2}$	$\frac{3\pi}{4}$	π	
R_1	−1697	+787	+955	−182	−817	kg/cm²
R_2	+1594	−353	−603	+124	+544	

Substituting the values of θ for the principal points, the stress σ_θ in kg/cm² can be determined. These are indicated in Table 1.

If it is necessary the stresses σ_r, $\tau_{r\theta}$ and the deformations $u + iv$ can be calculated by means of formulae 18 and 8.

References

1. Muskhelishvili, N. I., *Some Basic Problems of the Mathematical Theory of Elasticity*. Groningen, Noordhoff, 1953.
2. Sokolnikoff, I. S., *Mathematical Theory of Elasticity*. New York, McGraw Hill, 1956.
3. *Encyclopaedia of Physics*, Volume VI, 'Elasticity and Plasticity'. Berlin, Springer, 1958.
4. Girkmann, K., *Flächentragwerke*. Vienna, Springer, 1956.

Correspondence

'The Effect of Membrane Stresses on the Ultimate Strength of the Interior Panel in a Reinforced Concrete Slab' by K. P. Christiansen, published in *The Structural Engineer*, August 1963

Mr. R. Park, Lecturer in Civil Engineering at the University of Bristol, writes:—

'In Mr. Christiansen's paper an expression for the arching couple Ca is developed as a function of the central deflexion of the beam and the magnitude of the deflexion which makes Ca a maximum is determined. This maximum value of Ca is taken to be the arching couple at the ultimate (maximum) load of the beam. It appears that in some cases the central deflexion of the beam at the ultimate load so found is extremely small and Mr. Christiansen points out that in the tests conducted the ultimate load was reached at central deflexions which were larger than those predicted by the theory. This discrepancy in deflexions may result from the assumption that the plastic hinges of the beams are fully developed at all stages. When a beam is loaded to failure it will only develop full plasticity at the critical sections when the deflexion is large enough to cause the required strains. At small deflexions the stresses at the critical sections are less than the plastic values. Hence if the maximum arching couple given by the theory occurs at too small a deflexion it may be outside the range for which the theory is applicable. The theory should overestimate the ultimate load in this case since the beam will reach ultimate load at a higher deflexion and the arching couple will be reduced. It is evident that a method for determining the central deflexion at which full plasticity at the hinges has just developed is required, since only when this deflexion is reached does the theory become applicable. For laterally restrained beams the tension steel reaches yield stress before the concrete reaches its ultimate value. Hence the central plastic deflexion when the last plastic hinge fully develops could be written in terms of the ultimate strain at the compressed edge of the concrete, the length of the region of the hinge, the depth to neutral axis and the position of the hinge in the beam. It is evident, however, that some other features of the theory are conservative since the failing loads found by Mr. Christiansen's tests exceed the theoretical ultimates in spite of the difference in central deflexions.

'It is doubtful whether arching action can be utilized in the design of continuous one-way slabs since it would be difficult to provide for the large horizontal reactions at the end supports. For continuous slab and beam floors, however, there would appear to be no reason why the interior panels should not be designed to include membrane (arching) action since the stiffness of surrounding panels is large. It may be necessary to strengthen the supporting beams with additional reinforcement, however, in order to prevent the sagging moment yield lines which run into the corners of the panels from extending through the beams and allowing lateral movement.'

Mr. A. C. Liebenberg writes:—

'It is not clear why the author (in his justification of the idealized assumptions made in his analysis) considers that only the maximum value of the arching effect is of real interest. On the contrary, if arching effects are ever to be taken into consideration in the design of slabs, lower bound solutions will be essential.

'It is the writer's opinion that the first equation leading to the author's equation 1 is incorrect. The last term giving the plastic shortening should not be included at all as it is already included in the expression $a_1 2\delta\Delta/L$ which gives the lengthening due to rotation. Since a_1 is measured vertically between the stress blocks and decreases as the deflexion and depth of stress blocks increase, the "plastic" shortening is automatically included. It would have been a different matter had h been substituted for a_1, but then the expression would be an over-simplification. The expression for the elastic shortening should more correctly read $\alpha\delta CL/2E_c h$ where α would depend on the percentage of steel reinforcement and would vary as the load increased. α could initially exceed 2·0 for lightly reinforced slabs but could be less than unity for heavily reinforced slabs. The argument the author uses later to explain why the elastic shortening may be less than that assumed would appear to be incorrect as the neutral axis only coincides with the line of measurement at the crack. The neutral axis would rapidly diverge from this line beyond the crack where the section is uncracked. Although k would rarely be constant in practice there can be no argument against this approach for laboratory slabs tested in a steel frame.

The expression should accordingly read

$$\frac{k\delta CL}{2E_c h} = \frac{a_1 2\delta\Delta}{L} - \frac{\alpha\delta CL}{2E_c h}$$

giving $$\frac{(\alpha + k)L^2}{4E_c h}\frac{dC}{d\Delta} = a_1 \quad \cdots \quad (1a)$$

Using a more realistic stress block as shown in Fig 1,

$$a_1 = h - \Delta - \frac{(T_1 + T_2 + 2C)}{0{\cdot}85 f_c}$$

$$= k_1 h - \Delta_p - \frac{2C}{0{\cdot}85 f_c}$$

where $$k_1 h = h - \Delta_e - \frac{(T_1 + T_2)}{0{\cdot}85 f_c}.$$

If $\Delta_p = yh$; $C = 0{\cdot}85\,\lambda h f_c$; $\frac{(\alpha + k) f_c L^2}{8E_c h^2} = k_2$

equation 1a becomes $$1{\cdot}70\,k_2\frac{dx}{dy} + 2x = k_1 - y \quad \cdots \quad (2a)$$

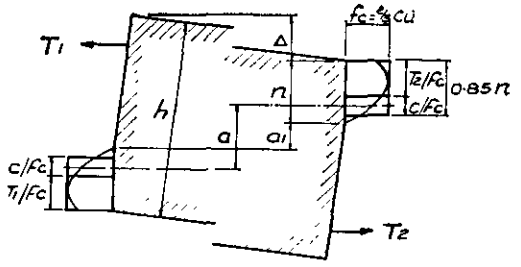

Fig 1

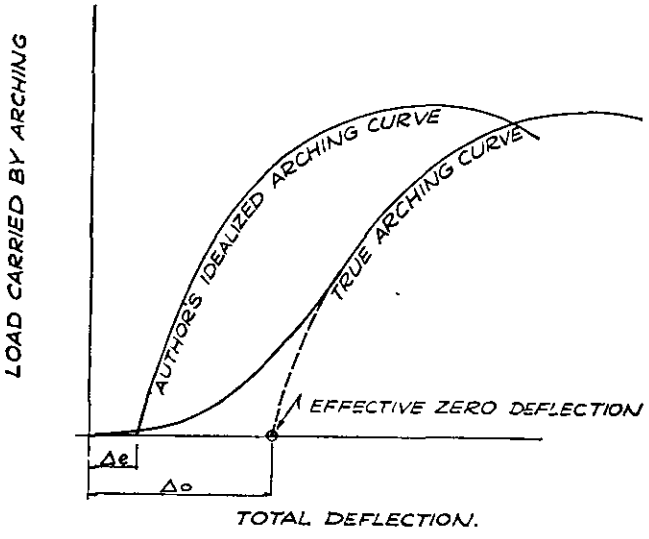

Fig 2

If we assume α, Δ_e and $(T_1 + T_2)$ to be constant we get, instead of the author's equation 3, the following solution:

$$x = \tfrac{1}{2}\left(k_1 + 0{\cdot}85\,k_2\right)\left(1 - e^{\frac{-y}{0{\cdot}85\,k_2}}\right) - \frac{y}{2} \quad \cdot \quad \text{(3a)}$$

If $k_3 = \dfrac{0{\cdot}15\,(T_1 + T_2)}{0{\cdot}85 f_c h}$ equation 4 becomes

$$Ca = 0{\cdot}85x\,(k_1 + k_3 - y - 0{\cdot}85x)h^2 f_c \quad \cdot \quad \cdot \quad \text{(4a)}$$

and equation 5 becomes

$$\frac{k_4 - 1{\cdot}425y - 0{\cdot}85\left(k_1 + 0{\cdot}85\,k_2\right)\left(1 - e^{\frac{-y}{0{\cdot}85\,k_2}}\right)}{k_4 - 2{\cdot}425y + 0{\cdot}15\left(k_1 + 0{\cdot}85\,k_2\right)\left(1 - e^{\frac{-y}{0{\cdot}85\,k_2}}\right)} = \frac{0{\cdot}85k_2}{(k_1 + 0{\cdot}85k_2)}\, e^{\frac{y}{0{\cdot}85\,k_2}} \quad \cdot \quad \cdot \quad \cdot \quad \cdot \quad \cdot \quad \text{(5a)}$$

'From these a different set of graphs can be prepared which differ somewhat from the author's and give higher values for $Ca/h^2 f_c$ but lower values for Δ_p/h.

'The author does not indicate how he calculated Δ_e, but this should not equal the elastic deflexion. It should include a correction for the non-linear behaviour of the slab so as to give an effective zero deflexion Δ_o from which arching action can be considered to be fully efficient. It is obvious that the arching action is only fully efficient near the ultimate load when the cracks and stress blocks are fully developed. This effect is illustrated in Fig 2. This is where the author has (in the writer's opinion) gone wrong and why he has underestimated the deflexions. The good agreement he gets for the experimental and theoretical loads appears to be coincidental in that he has used incorrect values for k_1 and k_2 and read the corresponding loads off incorrect curves. He is, however, quite correct in pointing out the flatness of the $Ca/f_c h^2$ curve, which makes an accurate assessment of these values unnecessary.

'In order to develop a more precise theory it would be necessary to assess the values of Δ_o and α which would depend on many factors such as the steel reinforcement, the mode of loading and the support restraints. In addition α is not a constant. In practice k would also vary so that the problem becomes extremely complex. Although initially attempting a similar approach the writer has, as a first step in analysing the results of full-scale tests carried out on 50 slab panels of a building prior to demolition, preferred to use an empirical-phenomenological approach to establish the behaviour pattern of the slabs. In the full-scale tests vertical deflexions of the panels and horizontal deflexions and rotations at the perimeters were recorded so that load-deflexion relationships could be established. By analysing a large number of laboratory tests carried out on model slab panels and elements in which the dimensions, crushing strength and reinforcement were varied, further relationships could be established. In these tests the horizontal restraints and rotations at the supports were controlled and measured by specially designed apparatus. From these results a useful theory has been formulated by developing an arching stress function similar to the function developed by the writer[1] for unrestrained concrete prisms subjected to uniaxial loading. The arching stress function is, however, expressed in terms of phenomenological concepts. A brief account of this work has been given by the writer in a paper[2].'

In reply Mr. Christiansen writes:—

'Mr. Park points out that equation 1 is correct only when full plasticity is developed at the hinges. It is, however, necessary to estimate the lateral movements that have taken place at earlier stages in order to evaluate the maximum arching effect. The author therefore assumed that the total elastic deformation between the hinges took place before the rotation at the hinges commenced and that the hinges behaved with full plasticity right from the start of this rotation. Although this tends to overestimate the initial values of a_1, it was not an attempt to find an upper bound solution but served to simplify the theory.

'Mr. Liebenberg is of the opinion that the plastic shortening should not be included in equation 1 as a_1 is already included in the term expressing the lengthening due to rotation. The term $4\Delta_p \delta C/Lf_c$ expressing the plastic shortening due to reduced crack depth, must, however, be included as this shortening is caused not by the rotation but purely by the increase in compression.

'The elastic deflexion Δ_e, calculated according to the idealized assumptions mentioned previously, is the central deflexion due to elastic bending of the member between the hinges with yield moments at the hinges. As the arching effect commences as soon as the first crack appears, the member was assumed to be uncracked at zero plastic deflexion. The plastic deflexion is then caused by the cracking, which was assumed to take place only near the hinges.

'The overestimate of arching effect caused by too large values of a_1 at the initial stages of the plastic deflexion may be compensated for by using a larger deflexion Δ_o for Δ_e, as suggested by Mr. Liebenberg. This and additional coefficients, as an empirical α for the elastic shortening and 1/0·85 for depth of compression, may tend to produce a more precise estimate of the arching (membrane) effect, but they do not prove the theory wrong.'

References

1. Liebenberg, A. C., 'A stress-strain function for concrete subjected to short-term loading', *Mag. Conc. Res.*, Vol. 14, No. 41, July 1962, pp. 85-90.

2. Liebenberg, A. C., 'Arching action in reinforced concrete slabs', *Proc. Diamond Jubilee Convention South African Inst. Civ. Engrs.*, 1963, pp. 99-102.

APPENDIX III-9

CONTRIBUTION TO THE DISCUSSION OF PAPER NO. 6705 BY R. PARK PUBLISHED IN THE PROCEEDINGS OF THE INSTITUTION OF CIVIL ENGINEERS, JUNE 1964. Vol. 28.

ULTIMATE STRENGTH OF RECTANGULAR CONCRETE SLABS UNDER SHORT-TERM UNIFORM LOADING WITH EDGES RESTRAINED AGAINST LATERAL MOVEMENT

The author is to be congratulated on his presentation of the paper. There can be little argument with the theory as presented on the basis of the assumptions made. These are however idealized and require careful consideration in terms of the true behaviour of slabs. The author's approach, which is basically similar to that of Wood, is an extension of yield-line theory based on idealized rigid-plastic assumptions and takes account of the membrane effect by considering the enhanced bending resistance. Although the slabs tested by the author, Wood and Powell cover a large range of dimensional and reinforcement ratios, the slabs were however all fully restrained against rotation and lateral displacement at the perimeter supports and in the case of some slabs tested by the author were completely unrestrained at one edge. The most important variable has accordingly been maintained at extreme values, a condition which will not always occur in practice. Full scale tests carried out on the old Alliance House, Cape Town, have in fact demonstrated the effective reduction in restraint caused by rotation.

In slabs where full restraint is not maintained the idealized portion BC of the load deflection curve (author's fig. 1) will accordingly not be attained and the AB portion becomes more important. For any accurate assessment of the peak load it is therefore essential to be able to predict the point B in terms of the true AB curve instead of in terms of the idealized portion BC of the curve.

It is only possible to do this in terms of an arch action analogy and the writer has preferred to extend the yield-line plate theory in this manner. A brief account of the basis of this theory was given in a paper read at the 1963 Diamond Jubilee of

/the South African ...

the South African Institution of Civil Engineers and a more detailed summary of the results of 50 full scale tests on slab panels and about 100 laboratory tests and the theory developed therefrom is given by the writer in a paper to be published shortly by the South African C.S.I.R. Admittedly the theory is more complex but it has produced encouragingly good results. No substantial details can be given within the space of this contribution, but for comparison the test results as obtained by Ockleston are given in fig. A with the author's theory and the writer's superimposed for comparison.

Admittedly the writer has worked backwards in terms of restraint parameters to get perfect agreement of peak load and deflection, but the important fact is the good agreement of the shapes of the experimental and theoretical curves and the fact that these parameters correspond exactly with the pattern established in the Alliance House tests. Close agreement would have been obtained by extrapolation of the restraint parameters established in these and the laboratory tests.

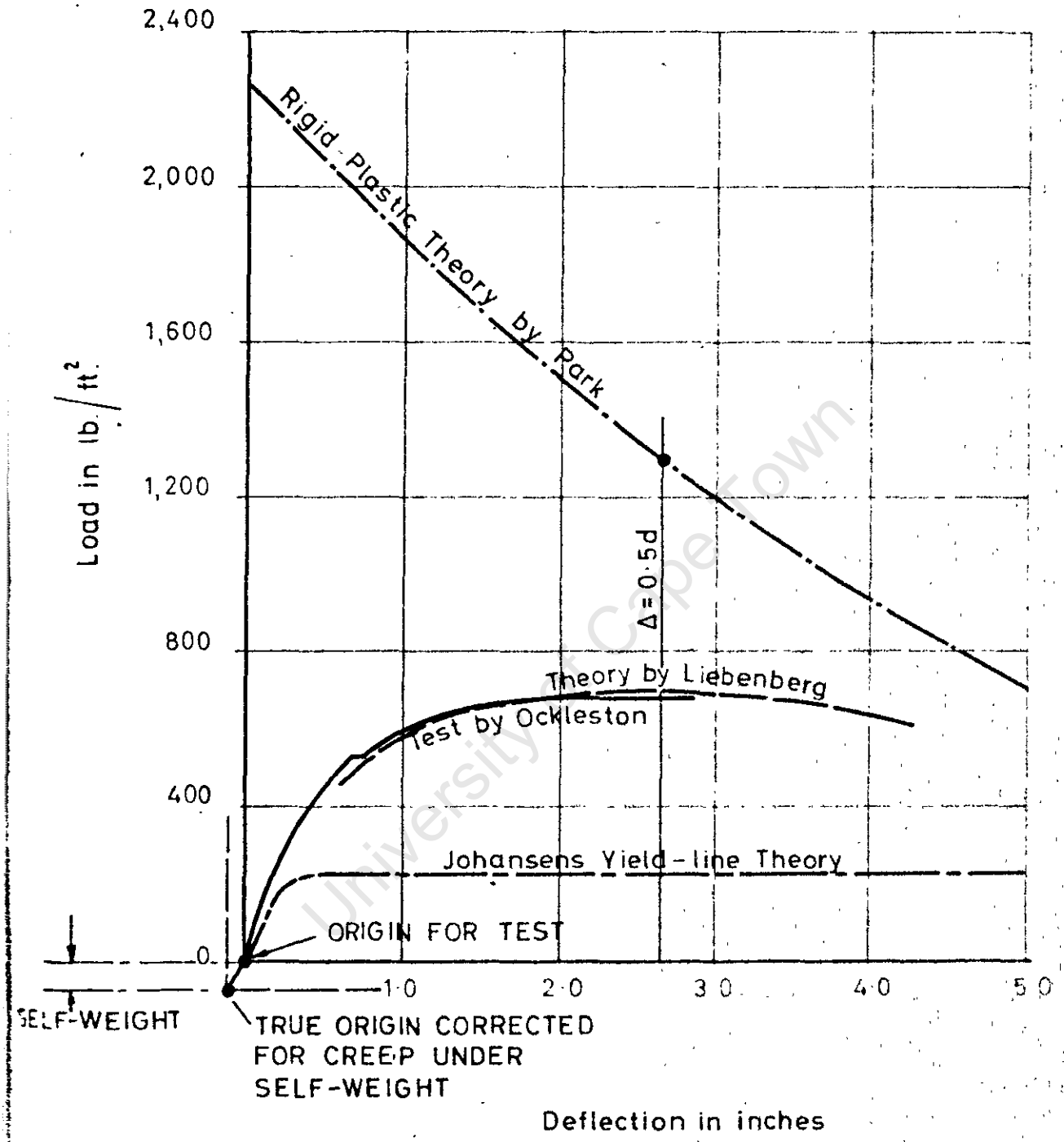

FIG. A.

APPENDIX III-10

CONTRIBUTION TO DISCUSSION OF PAPER "LOAD-CARRYING CAPACITY OF CONCRETE PAVEMENTS" BY G.G. MEYERHOF, PUBLISHED IN THE JOURNAL OF THE SOIL MECHANICS AND FOUNDATION DIVISION, JUNE 1962 (PAPER NO. 3174) AMERICAN SOCIETY OF CIVIL ENGINEERS

3378 December, 1962 SM 6

Journal of the
SOIL MECHANICS AND FOUNDATIONS DIVISION
Proceedings of the American Society of Civil Engineers

DISCUSSION

A. C. LIEBENBERG,[6] M. ASCE.—In the description of the mode of failure of plain and reinforced concrete pavements, the author refers to the collapse load that is reached "when a circumferential tension crack is formed on top of the slab," as distinct from the ultimate load when "complete failure occurs by punching through the slab at a greater load, provided the contact area is adequate."

The fact that punching shear failure had occurred at a greater load implies that a mode of resistance as a result of bending or extensional forces acting in conjunction with subgrade resistance had developed subsequent to cracking which was capable of carrying considerably greater loads than that indicated by the author's theory. As mentioned by Meyerhof, membrane action of the slab caused by tensile extensional forces is generally unimportant because the maximum deflection at collapse is only a small fraction of the slab thickness of plain concrete pavements. It can, however, be shown that loads of the magnitude indicated by the tests can be resisted by the so-called dome or arching action of the pavement slabs. Arching action in plane slabs under transverse loading can be defined as the resistance developed by a system of compressive forces distributed within the slab thickness in such a manner as to resemble the action of an arch or dome, as indicated in Fig. 14, and gen-

[6] Cons. Engr., Liebenberg & Stanter, Cape Town, South Africa.

erated in the slab after the development of some form of articulation, such as localized cracking, by geometric deformation of the slab elements bounded by these lines of articulation. These compressive forces, which are superimposed on the pure bending forces, are balanced either by external forces at the support boundaries that are induced by reaction against "abutments" or by peripheral tensile forces.

Arching action can occur in plain, normally reinforced and prestressed concrete slabs, whether suspended or supported on a subgrade and whether subjected to point loads or distributed loads, provided the necessary conditions of boundary restraint are present.

An extensive investigation of arching action in plain and reinforced concrete slabs has been completed by the writer in which the influence of parameters such as the slab dimensions, the reinforcement, the crushing strength of the concrete, and the boundary restraint of the slabs has been analyzed.

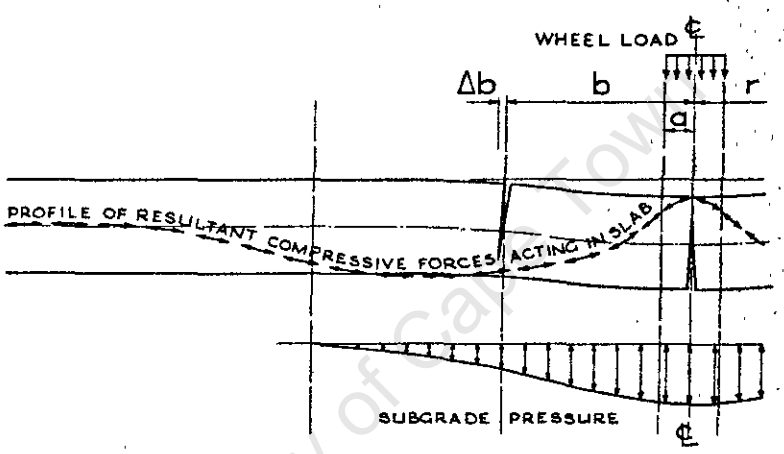

FIG. 14.—HALF SECTION THROUGH SLAB WITH EXAGGERATED VERTICAL SCALE

The program included tests to destruction on fifty slab panels of a building in Cape Town that were conducted in cooperation with R. G. Robertson and D. J. McGaw of the Civil Engineering Department of the University of Cape Town, prior to demolition in 1957. In these tests, vertical deflections as well as the "horizontal spread" of the slab boundaries were measured. The ultimate load consistently exceeded the theoretical failure load as predicted by yield line theory, in some cases by a factor of 3.0.

More than one hundred laboratory tests conducted subsequently have enabled the writer to develop a theory of arching that gives results in good agreement with the tests. This work has not yet been published but the results of tests on prestressed concrete slabs have been described in a paper by Y. Guyon[7] and also in a textbook on prestressed concrete by Guyon.[8]

In a paper[9] on prestressed concrete runways, A. J. Harris also refers to the tests conducted by Guyon, at Orly, and a brief account is given of the nature of the dome action. It does appear from the noted papers that these authors are of the opinion that arching action is significant only in prestressed concrete slabs. The writer has, however, found that this is not necessarily so and that, on the contrary, it is most likely to occur in plain or lightly reinforced concrete slabs with normal mild steel reinforcement, provided the required conditions of restraint exist. This contention is supported by the author's results.

7 "Essai sur des dalles continues précontraintes," by Y. Guyon, Supplement of "Annales de L'institut technique du batiment et des travaux publics," November, 1955.

8 "Prestressed Concrete," Vol. II, by Y. Guyon, John Wiley & Sons, Inc., New York, N. Y.

9 "Prestressed Concrete Runways: History, Practice and Theory," by A. J. Harris, Proceedings, Inst. of Civ. Engrs., London, Vol. 6, January 1957.

APPENDIX. III - 11.

Estimate of Ultimate load for square slab (Mark FS12) with 16-point loading as tested by R.H. Wood. (see reference 14 page 251.)

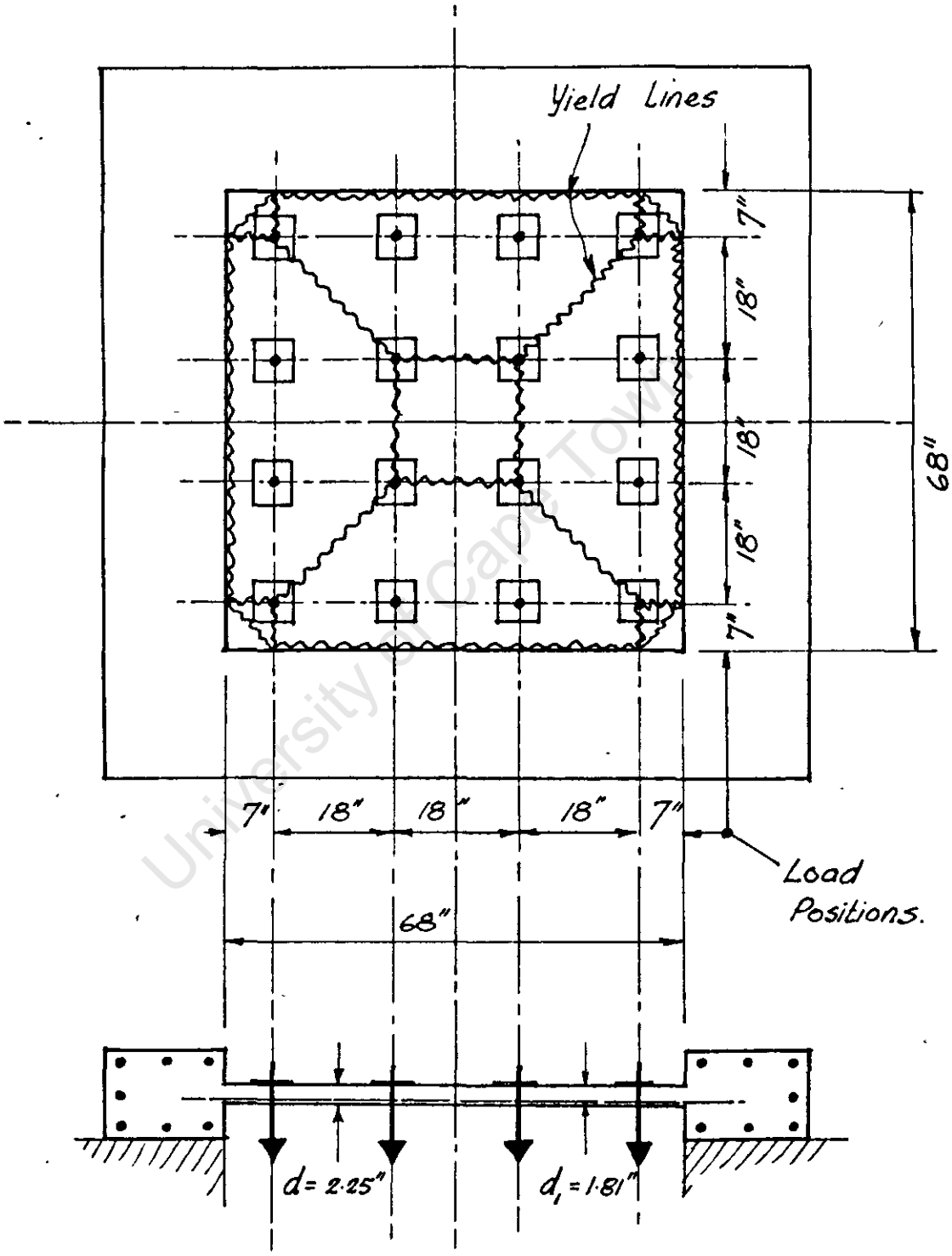

PLAN & SECTION OF TEST SLAB.

Steel reinforcement in slab : 3/16" ϕ @ 5 3/4" c/c both ways in bottom of slab only (f_y = 33,800 lb/in².)

Cube Strength u = 5,900 lb/in²

Yield Lines

The idealized pattern of yield lines shown on the previous page and based on plate VII of reference 14 will be assumed to develop at yielding of the steel.

Estimate of G_e (see page 187)

For a square slab panel with a well distributed loading G_e will probably exceed the value for G as determined for one-way spanning slab elements.

$$r_s = \frac{A_s d_1}{bd^2} \times 100 = \frac{0.5 \times 0.0278 \times 1.81 \times 100}{5.75 \times 2.25^2}$$

(Note: bottom steel only)

$$= 0.09\ \%$$

from fig. 22 $\quad \frac{M_{ai}}{fu} = \frac{G}{1+3.5r_s} \geqslant 20{,}000\ lb^2/in.$ for $\frac{l_s}{b} \to \infty$

Note: The values derived from the Alliance House tests were much lower but the loading was concentrated, the panels were rectangular, the concrete was old (see last paragraph on page 197).

Estimate of R_e.

In the Alliance House tests on internal panels, R_e varied between 0.30 and 0.60 (see page 197), the actual value apparently depending largely on the rotational restraint at the supports. For the slab tested by Ockleston (see page 235) the value appeared to approximate to 0.40. As the rotational restraint is comparitively great in the case under consideration it will be assumed that $R_e = 0.70$. (Note: For a fully rigid support $R_e = 1.0$)

Using the procedure described on pages 173 and 188. and considering a section along the centre-line :—

(i) The yield lines will be assumed as described above. P_B = Total load resisted by bending in accordance with yield-line theory = 7190 lb. (see page 251 of reference 14.)

(2) Assume $e_a = 0.0010$.

(3) $\therefore f_a = 20{,}000\sqrt{5{,}900}\left[1 - 6890(0.0010)^{1.5}\right]0.0010$

$= 1.535 \times 10^6 \times 0.00078$ (see fig. 24.)

$= 1{,}200$ lb/in².

(4) $\therefore H_a = 1200 \times 12 \times 2.25 = 32{,}300$ lb/ft.

(5) $\therefore d_a = 2.25 - \frac{(0.0578 \times 38{,}800) + 32{,}300}{\frac{2}{3} \times 5900 \times 12}$

$= 2.25 - 0.72 = 1.53$ in.

(6) $R_e = 0.70$ by assumption

$\therefore R_f = \frac{R_e}{1-R_e} = \frac{0.70}{0.30} = 2.33$

$\therefore \frac{R_s L}{n_a b d} = 2.33$

$\therefore n_a = \frac{f_a}{e_a} = \frac{1200}{0.0010}$

$= 1.2 \times 10^6$ lb/in² at $e_a = 0.0010$.

Note :- $H_a = \psi(\Delta_a)$, a non-linear function, where $\frac{\psi(\Delta_a)}{\Delta_a} = R_s$, a variable in this case, for any particular Δ_a.

$\therefore R_s = \frac{2.33 \times 1.2 \times 10^6 \times 12 \times 2.25}{68}$

$= 1.11 \times 10^6$ lb per in. per ft. width at this particular loading.

$\therefore \Delta_a = \frac{H_a}{R_s} = \frac{32300}{1.11 \times 10^6} = 0.0292$ in.

(7)

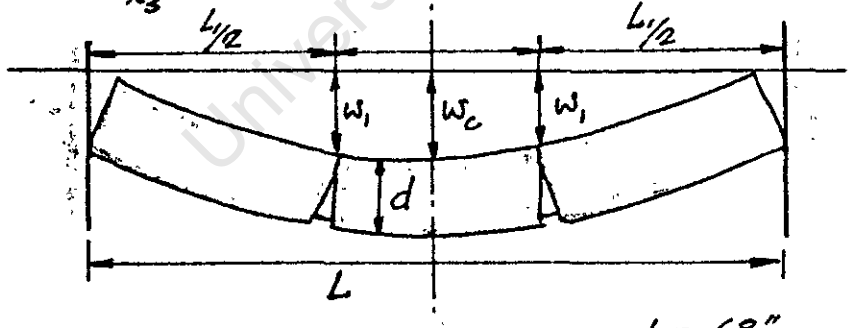

$L = 68''$ $L_1 = 50''$

$\Delta_u = \frac{4 W_1 (d - \frac{W_1}{2})}{L_1}$

$e_a = \frac{\Delta_u - \Delta_a}{L}$

i.e. $0.0010 = \frac{\Delta_u - 0.0292}{68}$ $\therefore \Delta_u = 0.097''$

(8) $\therefore 0.097 = \frac{4 W_1 (2.25 - \frac{W_1}{2})}{50}$

$\therefore 2 W_1^2 - 9.0 W_1 + 4.85 = 0$

$\therefore W_1 = 3.9$ or 0.63 in.

The additional deflection $(w_c - w_1)$

The additional deflection due to bending of the central element can be determined by considering the bending due to the reinforcing and the arch thrust. For the forces calculated above and assuming an equivalent modulus of say $\frac{1}{3} \times 60{,}000\sqrt{u}$ = 1,530,000 lb/in² the additional deflection $(w_c - w_1)$ is ≒ 0.065 in.

$\therefore \quad w_c = 0.63 + 0.07 \fallingdotseq 0.70$ in.

(9) Calculation of P_A.

Consider the equilibrium of one trapezium formed by the yield lines.

It will be assumed that the corner loads do not induce any vertical shear forces onto this trapezium. This appears to be amply substantiated by plate VII of reference 14.

If P_A = Total load resisted by arching then by taking moments about the support:

$$\left(\frac{P_A}{16} \times 15''\right) + \left(\frac{P_A}{8} \times 7''\right) = \left[\frac{H_a}{12} \times 18''\left(d_a - w_1\right)\right] + \left[\frac{H_a}{12} \times 36''\left(d_a - \frac{w_1}{2}\right)\right]$$

$$\therefore \quad 2.44\, P_A = 32{,}300\left[1.5(1.53 - 0.63) + 3.0(1.53 - 0.31)\right]$$

$$= 67{,}800 \text{ lb.}$$

$$\therefore \quad P = P_A + P_B = 67800 + 7190 = 75000 \text{ lb.}$$

$$\therefore \quad \frac{P}{P_B} = \frac{75000}{7190} = 10.4 \qquad \frac{w_c}{d} = \frac{0.70}{2.25} = 0.31$$

By repeating the procedure for various values of e_a the following relationships were determined.

e_a	$\frac{P}{P_B}$	$\frac{w_c}{d}$
0.0006	9.7	0.18
0.0010	10.4	0.31
0.0012	9.6	0.40
0.0015	8.0	0.50

TEST ON SQUARE SLAB BY R.H. WOOD. (fig 90 of ref. 14)

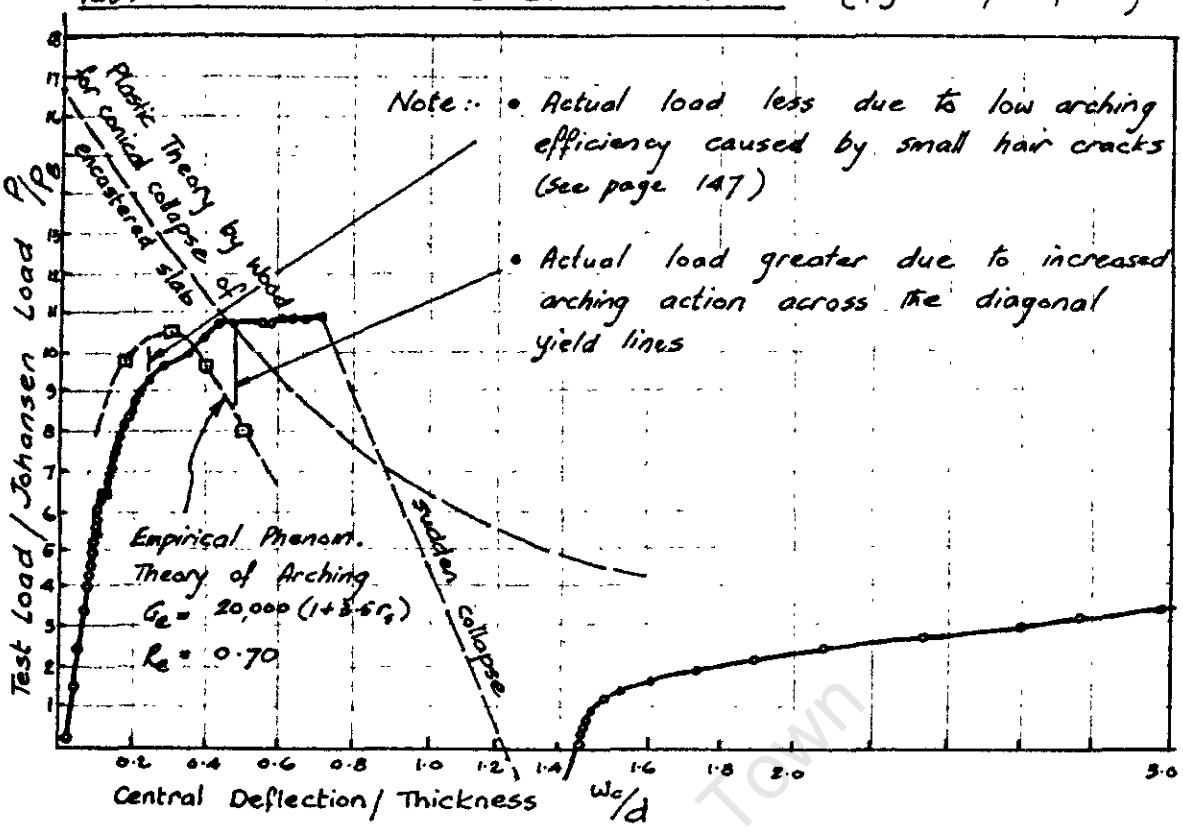

• If the procedure adopted in 3.3.9 on page 198 had been applied G_e would have been found to be less than $20.000\,(1+3.5r_s)$ for deflections less than $0.37d$ and vice versa. G_e would not therefore be a constant value but would increase with deflection. This is due to the fact that the arching function is expressed in terms of the central deflection and consequently underestimates the corner effect in square panels. The method will therefore be conservative except for certain cases of concentrated loading which may result in shear failure or in the case of a large longspan to shortspan ratio in which the yield lines may develop as shown in fig. 28.

• The distribution of the arching forces along the yield lines needs further investigation as well shear failure in conjunction with arching.

B O O K IV

THE EXTENSION OF THE COLUMNS OF STIFF FRAMES IN TALL BUILDINGS SUBJECTED TO HORIZONTAL FORCES

*

FOOTNOTE TO PAGE 299

The author was already familiar with a direct method based on the assumption that the bracing action of the frame could be expressed as a continuous function which had been developed in the form of a differential equation and solved for a very tall frame-shear wall combination of constant dimensions for the full height by the late J.H. van Wyk. (Unpublished). Similar methods have since been proposed by others (see references). For the problem referred to this method could not however be applied with accuracy due to the variation in storey heights and member sizes and the fact that the structure, being only 18 storeys, could not be classified as very tall. Although the sample calculation based on the special method given in Appendix IV-2 is applied to a frame with constant dimensions for simplicity, it would not require much additional work if every member had different dimensions. A direct solution as described above would not be accurate for a frame-shear wall combination of this height.

BOOK IV

THE EXTENSION OF THE COLUMNS OF STIFF FRAMES IN TALL BUILDINGS SUBJECTED TO HORIZONTAL FORCES.

INTRODUCTION

The author was faced during 1961 with the problem of designing an eighteen storey reinforced concrete structure which relied almost entirely on the lift shaft complex for lateral stability. This involved analysing the behaviour of shear walls and stiff frames inter-connected by beams and floor slabs. Being positioned eccentrically relative to the building structure, the lift shaft complex was subjected to torsional forces as well as shear and bending forces. The lift shaft complex was itself of unsymmetrical proportions, thus further complicating the analysis. It was also evident that it would be essential to take the extension of the columns of the stiff frames into account in the analysis.

The problem was accordingly one of great complexity and could not be solved by direct methods.* The method evolved is a combination of relaxation and iteration with the application of special procedures to accelerate the convergence of the compatibility equations at the various stages of relaxation. Initially it was sought to obtain convergence to total compatibility by automatic procedures but this proved to be impossible.

When this work was undertaken no publication describing a suitable method was available and papers dealing with similar problems have only recently appeared.(1) (2) (3) (4) (5) In all except two (3) (4) of these papers column extension is neglected and neither of these could readily cope with a problem of the complexity described above.

The procedures of relaxation and iteration used by the author are common knowledge except for the convergence techniques which he has evolved. On account of the difficulty of presentation when dealing with problems of this length and complexity only the original aspects will be dealt with and will be applied to

/ a simple ...

a simple problem for the purpose of explanation. Without the above-mentioned convergence techniques the method would have been extremely tedious, if not impossible.

THE NATURE OF THE PROBLEM

As briefly indicated above, the actual problem encountered in practice was far more complex but for the purpose of explanation it will be simplified to the case of a shear wall and stiff frame combination subjected to co-planar horizontal forces as illustrated in fig. 4.1. The foundations are assumed to be rigid, but it would be relatively simple to allow for the deformation of the foundations.

The central wall if allowed to deflect on its own would attain a profile similar to that of a cantilever beam which obviously differs radically from the deflection behaviour of a frame. When interconnected as shown, there will consequently be interaction between the wall and the frame elements, resulting in a peculiar distribution of forces. For frames of the type shown in fig. 4.1 the wall resists more than the total shear force at the lower levels, whereas the frames are subjected to negative shear forces. The extensional forces in the columns, in conjunction with the bracing beams, do however resist a large proportion of the overturning moment.

It is normal practice in the analysis of frames subjected to horizontal forces to consider sway deformations only and to neglect the effect of column extensions. When, however, the depth of the frame members (i.e. the cross-sectional dimension measured in the plane of the frame) is of the same order as the length of the members then the above approximation cannot be made. This applies particularly to tall multi-storey frames acting in conjunction with shear walls with members of similar proportions to those of the reduced frame illustrated in fig. 4.1.

BASIC ASSUMPTIONS

(1) It is assumed that the Bernoulli-Euler theory of bending applies to all members. This will only be sufficiently accurate for frame members that have a depth to span ratio of

3/ < less than ..

less than unity. This is a definite limitation of the theory developed below. It consequently cannot be applied to walls with relatively small door openings.

(2) The effective lengths of all frame members are taken as the distance between the points of intersection of the centroidal lines and these members are assumed to be connected rigidly at all joints. Where bracing beams are connected directly to shear walls as in the case of fig. 4.1, the assumption is made that such connection is rigid at the face of the shear wall, the localized non-linear distortion within the shear wall being neglected. This amounts to the equivalent assumption that the Bernoulli-Euler theory applies to the shear walls as in (1) above. This is obviously not quite correct but the error involved will in most cases be of secondary order.

(3) Axial extension of horizontal beams or braces is assumed to be negligible.

(4) All interconnecting floor slabs are assumed to be rigid in their own plane but to have negligible bending stiffness normal to this plane.

(5) Shear deformation of all members is neglected. In cases involving very stiff shear walls this assumption may lead to inaccuracies. The theory could however be extended to allow for this effect.

ANALYTICAL PROCEDURE

It is a relatively simple matter to determine shear forces, bending moments, and axial forces in a frame subjected to a particular deformation profile and from these internal forces to calculate the externally applied forces causing such deformation. This is due to the fact that we are dealing with discrete members of finite dimensions and deformations. The same is however not true of continous systems such as shear walls where the process of differentiating the deflection profile to the fourth degree to determine the applied load leads to small differences of relatively large quantities and consequential inaccuracy. Hence in the method developed below the principle

4/ adopted ...

adopted is that forces are applied to the shear wall to determine its deflected profile and this profile is then used to calculate the forces in the frames necessary to "force-fit" them to identical profiles. The calculations can therefore be done with sufficient accuracy by slide-rule.

For solving the particular problem in practice referred to in the introduction a method applicable only to that type of shear wall and frame combination was evolved and shall be referred to as the special method as it has various advantages over the more laborious general method applicable to all kinds of combinations.

The procedures for both methods and the relevant theory are given below and an example in which the frame illustrated in fig. 4.1 is analysed by the special method is given in Appendix IV-2.

THE SPECIAL METHOD

This method is applicable only to shear walls acting in conjunction with and connected by brace beams to frames consisting of not more than one column each side as illustrated in fig. 4.1. The method is however applicable to the case of a shear wall acting in conjunction with one frame and column only.

The method can be summarized as follows :-

Step (1) :

The total external load is applied to the shear wall element which in this first stage is considered to act independently as a free wall. The resultant slopes at brace beam levels are calculated.

Step (2) :

The frames are next subjected to deformation in such a manner that the resultant translations and rotations of the frame joints and of the brace beams where they adjoin the shear walls assume definite values which are determined as described below. The frame joints are however restrained against vertical translation.

S/ Step (3) ...

Step (3) : The internal forces acting in the frames as a result of the above deformations are calculated by slope deflection theory and the restraining moments applied in Step (2) at the column joints are relaxed by the Hardy Cross moment distribution method.

Step (4) : The vertical restraints acting at the frame joints are next relaxed by a special procedure so as to achieve compatibility of column stresses and strains. The other extremities of the brace beams where they would adjoin the shear wall are restrained at the original slopes and translations during these operations.

Step (5) :

The internal forces are recalculated after the completion of Step (4) and the resultant restraining forces in the form of couples, shear forces and axial forces acting at the junction with the shear wall are determined. The term "junction" must here be interpreted as referring to the actual structure. Until compatibility has been achieved the frame and shear wall are acting separately.

Step (6) : These restraining forces are next applied in reverse to the shear wall and the resultant reversal of rotations at the various levels calculated. The use of influence coefficients simplifies this work.

Step (7) : If the final slopes at brace beam levels of the shear wall do not correspond with the slopes assumed for the frame then the procedures described in steps (2) to (6) are repeated until a sufficient degree of compatibility has been achieved.

THEORY OF SPECIAL METHOD

In this special method deformations are expressed in terms of slopes or rotations for the reason that they are more readily calculated and provide the basis for a rapid convergence method. This method can unfortunately not be applied in general.

Step (1) :

The slope of the shear wall at level n relative

to the vertical due to the external forces P_E can be equated to

$$ {}_E\theta_n = \int_{H_n}^{\circ} \frac{M_E . dH}{E I_w} \qquad \text{... E4.1} $$

where M_E is the bending moment at any level H due to the forces P_E.

E is Young's modulus for the material or if of composite construction, the effective value.

I_w is the moment of inertia of the shear wall at level H.

H_n is the height of level n above the base.

Step (2) :

For the first cycle the rotations are assumed at arbitrary values less than ${}_E\theta_n$. For subsequent cycles the values are determined as follows

$$ {}_A\theta_{n,s+1} = \frac{{}_E\theta_n - {}_A\theta_{n,s}}{{}_R\theta_{n,s}} \cdot {}_A\theta_{n,s} \qquad \text{... E4.2} $$

where ${}_A\theta_{n,s+1}$ the assumed rotation of the frame joints at level n in cycle $s+1$.

${}_A\theta_{n,s}$ is the assumed rotation of the frame joints at level n in the previous cycle (s).

${}_E\theta_n$ the rotation of the shear wall at level n due to the external forces as applied in Step (1)

${}_R\theta_{n,s}$ is the reversal of rotation of the shear wall at level n due to the unbalanced restraining forces applied in Step (6) of Cycle s.

The application of equation E4.2 in successive cycles leads to rapid convergence. In adjusting the slope values after each cycle the formula applied at any particular level reduces the previous error and accordingly all force values throughout the structure are adjusted. The derivation of equation E4.2 is based on the approximate assumption that the ratio of the correct rotation to be applied to the brace beams of the frame at any level to the rotation assumed

7/ initially ...

initially or in the previous cycle is equal to the ratio of the required reversal of rotation of the shear wall to the actual reversal of rotation at that level. The convergence can be improved by an adjustment of these ratios based on experience.

Step (3):

With reference to fig. 4.2 the fixed end moments resulting from the rotations ${}_A\theta_{n,s}$ are determined by slope deflection theory. The F.E.M. in the brace beams are

$$ {}_bM_{An} = {}_bM_{wn} = \frac{6EI_{bn}}{\ell} \cdot {}_A\theta_{n,s}\left(1+\frac{b}{2\ell}\right) \qquad \text{..... E4.3} $$

where ${}_bM_{An}$ is the bending moment in the brace beam at level n where it adjoins column A.

${}_bM_{wn}$ is the bending moment in the brace beam at level n where it adjoins the shear wall.

I_{bn} is the moment of inertia of the brace beam at level n.

ℓ is the effective span of the brace beam

b is the width of the shear wall.

For a column deformed as in fig. 4.3 by the moments shown

$$ M_A = -\frac{2EI}{h}\left(-2\theta_A + \theta_B\right) $$

$$ M_B = \frac{2EI}{h}\left(-\theta_A + 2\theta_B\right) $$

$$ \therefore M_A + M_B = \frac{2EI}{h}\left(\theta_A + \theta_B\right) $$

$$ = \frac{2EI}{h}\theta_c $$

8/ Now ...

Now if $\frac{M_A}{M_B} = \beta$

$\therefore \quad M_A + M_B = M_A(1 + \frac{1}{\beta})$

or $\quad \frac{2EI}{h} \cdot \theta_c = M_A(\frac{1+\beta}{\beta})$

$\therefore \quad M_A = \frac{2EI}{h} \cdot \frac{\beta}{1+\beta} \cdot \theta_c$

... E4.4

For the case under consideration the column deformation subject to end rotations θ_A and θ_B will be of similar shape to that of the shear wall so that provided both are prismatic β will also approximate to the ratio of bending moments acting at the two levels in the shear wall. For the first cycle these moments are not known and it can be assumed that $\beta = 1.0$. Thereafter the moment ratio resulting from the previous cycle is used. In the initial cycles when the profiles do not coincide this formula will be approximate but it will become precise as they converge. The column fixed end moments due to the above deformations are usually small so that the initial inaccuracy is not important. For the case under consideration we accordingly have

$$ {}_A M_{n-1,n} = \frac{2EI_{An}}{h_n} \cdot \frac{\beta}{1+\beta} \cdot \theta_{n,n-1} \qquad \text{... E4.5} $$

where ${}_A M_{n-1,n}$ is the fixed end moment in the column A between levels $n-1$ and n acting at level $n-1$.

I_{An} is the moment of inertia of the column A between levels $n-1$ and n.

h_n is the height of the column between levels $n-1$ and n.

$\theta_{n,n-1}$ is the difference between the slopes at levels n and $n-1$.

β is the ratio of the moment acting in the shear wall at level $n-1$ to the moment acting at level n.

Similarly

$$ {}_{A}M_{n,n-1} = \frac{2EI_{An}}{h_n}\left[\frac{1}{1+\beta}\right]\cdot\theta_{n,n-1} \qquad \ldots [4.6 $$

where ${}_{A}M_{n,n-1}$ is the fixed end moment in the column A between levels $n-1$ and n acting at level n .

Step (4) :

Procedure for the relaxation of vertical restraints to columns

The shear forces in the brace beams after completion of Step 3 can be calculated from the internal bending moments. These shear foces will tend to extend or shorten the columns if the restraints are relaxed. Relaxation of these artificial restraints will result in deformation of the brace beams causing a reduction in the shear forces and bending moments until compatibility is achieved with the column forces which increase as the relaxation is carried out.

Let $\sum_{o}^{n} R_A$ = total vertical shortening or extension at level n of column A which for any particular shear wall profile would reduce the shear force and bending moments in the brace at level n to zero. It is obvious that only one condition can satisfy this requirement, viz. an undeformed brace beam. We therefore have

$$ \sum_{o}^{n} R_A = {}_{A}\theta_n\left(\frac{b}{2}+l\right) \qquad \ldots [4.7 $$

If the actual relaxation which is applied in the form of a vertical translation of column A at level n is $\sum_{o}^{n} r_A$ then it can be shown that the residual shear force acting in the brace after relaxation approximates to

$$ {}_{A}S'_{bn} \doteq {}_{A}S_{bn}\frac{\sum_{o}^{n} R_A - \sum_{o}^{n} r_A}{\sum_{o}^{n} R_A} $$

$$ = {}_{A}S_{bn}\left[1 - \frac{\sum_{o}^{n} r_A}{{}_{A}\theta_n\left(\frac{b}{2}+l\right)}\right] \qquad \ldots [4.8 $$

By equating the residual shear force ${}_{A}S'_{bn}$ in the brace to

/10 the ...

the increment of force acting in the column A we get

$$ {}_{A}S_{bn}\left[1-\frac{\sum_{o}^{n} r_A}{{}_{A}\theta_n\left(\frac{b}{2}+\ell\right)}\right] = \frac{A_n \cdot E}{h_n}\left[\sum_{o}^{n} r_A - \sum_{o}^{n-1} r_A\right] - \frac{A_{n+1} \cdot E}{h_{n+1}}\left[\sum_{o}^{n+1} r_A - \sum_{o}^{n} r_A\right] $$

... E4.9

where A_n = cross-sectional area of column A between levels $n-1$ and n.

h_n = storey height between levels $n-1$ and n.

For the topmost brace of the frame we have

$$ {}_{A}S_{bt} \neq \left[1-\frac{\sum_{o}^{t} r_A}{{}_{A}\theta_t\left[\frac{b}{2}+\ell\right]}\right] = \frac{A_t \cdot E}{h_t}\left[\sum_{o}^{t} r_A - \sum_{o}^{t-1} r_A\right] $$

... E4.10

For the lowest brace at level 1 we have

$$ {}_{A}S_{b1}\left[1-\frac{\sum_{o}^{1} r_A}{{}_{A}\theta_1\left(\frac{b}{2}+\ell\right)}\right] = \frac{A_1 \cdot E}{h_1}\left[\sum_{o}^{1} r_A\right] - \frac{A_2 \cdot E}{h_2}\left[\sum_{o}^{2} r_A - \sum_{o}^{1} r_A\right] $$

... E4.11

If a value for $\sum_{o_2}^{1} r_A$, the relaxation of the lowest column, is assumed then $\sum_{o}^{2} r_A$ the relaxation required at the second brace level for compatibility of stress and strain in the column below level 2 can be calculated from equation E4.11. By repetition of this procedure but using equation E4.9, the necessary relaxation at each level can be calculated in turn.

The values $\sum_{o}^{t} r_A$ and $\sum_{o}^{t-1} r_A$ at the uppermost two levels must however satisfy equation E4.10 and if they do not the procedure must be repeated by assuming a different value for $\sum_{o}^{1} r_A$ until compatibility at the top is achieved. Usually about four repetitions are sufficient as the convergence is rapid. The method is illustrated in the example in Appendix IV-2.

THE GENERAL METHOD

The general method described below is applicable to most types of combinations of shear walls and frames with any number of columns linked by brace beams or flexible ties (thin slabs) or both. The basic difference with the special method is that deflections are used to express deformation instead of rotations. The latter method although simpler cannot be applied in general.

When applied to a frame as illustrated in fig. 4.1 the general method can be summarized as follows :

Step (1) :

The total load (or a portion of the total load as indicated by intuitive judgement based on previous experience) is applied to the shear wall element which in this first stage is considered to act independently as a free wall. The resultant deflection profile and slopes are calculated.

Step (2) :

The frames are next "force-fitted" to attain the identical deflection profile with compatibility of slope and deflection at the junctions of the frames and shear wall. The other frame joints are however restrained against rotation and the columns against extension, only horizontal translation being applied.

Step (3) :

The rotational restraints at the frame joints are next removed by the Hardy-Cross moment distribution method The columns are however restrained against extension during this operation and the shear wall is restrained to maintain the profile determined in Step (1). The fixed end moments required for the moment distribution procedure are calculated by slope deflection theory from the relative translations and rotations applied.

Step (4) :

The shear forces acting in the bracing beams of the frames as a result of the forced profile and subsequent to the

12/ relaxation ...

relaxation of the restraining moments at the frame joints are then calculated.

Step (5) :

The column extensional restraints are next relaxed to attain compatibility of colum stresses and strains. A special procedure described later is used to accelerate this operation.

Steps (3), (4) and (5) can be repeated to attain complete compatibility for the frame subjected to this particular deflection profile but it is unnecessary to achieve great accuracy in the initial stages when the profile may still differ greatly from the correct profile.

Step (6) :

The unbalanced internal forces P_u (in the form of couples, shears, and axial forces), and consequently the external forces required to "force-fit" the frame, are next calculated.

Step (7) :

Calculated proportions of these unbalanced forces are next applied to the shear wall and the new deflections and slopes calculated. The method of determining the correct proportions of the forces P_u to give rapid convergence is described later.

Step (8) :

Steps (2) to (6) are repeated in terms of the new deformations and forces.

Step (9) :

The procedure is repeated until the unbalenced forces become negligible and a sufficient approximation to complete compatibility is attained.

THEORY :

Step 1

The horizontal deflection at any level n of the shear wall due to the external forces P_E can be equated to

$$_E\Delta_n = \int_{H_n}^{0} \frac{M_E.(H_n - H)dH}{EI_w}$$

... E4.12

where M_E is the bending moment at any level H due to the forces P_E.

E is Young's modulus for the material or, if of composite construction, the effective value.

I_W is the moment of inertia of the shear wall at level H.

H_n is the height of level n above the base.

The slope of the shear wall at level n relative to the vertical, due to the external forces P_E, can similarly be equated to

$$ {}_E\theta_n = \int_{H_n}^{0} \frac{M_E \, dH}{E I_W} \qquad \text{... E4.13} $$

Step 2

For the "force-fitting" described in Step 2 the ends of the bracing beams where they adjoin the shear wall are subjected to horizontal translations ${}_E\Delta_n$, vertical translations ${}_E\gamma_n = \frac{b}{2} \times {}_E\theta_n$ and rotations ${}_E\theta_n$ as illustrated in fig. 4.4. The other frame joints are subjected to horizontal translations ${}_E\Delta_n$ only.

The fixed end bending moments acting in the bracing beams of the frames as a result of the "force-fitting" are calculated from the slope deflection equations

$$ {}_bM_{An} = \frac{2EI_{bn}}{l} \cdot {}_E\theta_n \left[1 + \frac{3b}{l} \right] \qquad \text{.... E4.14} $$

$$ {}_bM_{wn} = \frac{2EI_{bn}}{l} \cdot {}_E\theta_n \left[2 + \frac{3b}{l} \right] \qquad \text{.... E4.15} $$

where ${}_bM_{An}$ is the fixed end bending moment in the brace at level n where it adjoins the column A.

${}_bM_{wn}$ is the fixed end bending moment in the brace at level n where it adjoins the shear wall.

I_{bn} is the moment of inertia of the brace beam at level n.

l is the effective span of the brace.

b is the width of the shear wall.

Step 3

After completion of Step 2 the bracing beams will be deformed as shown in fig. 4.4 The execution of Step 3 will result in rotation of the column joints.

Step 4 :

The shear forces in the bracing beams are calculated from the resultant bending moments after completion of Step 3.

Step 5 :

Procedure for the relaxation of vertical restraints to columns

This procedure is identical to that described in Step (4) of the special method except that $\sum_{o}^{n} R_A$ must be calculated for each joint in terms of the displacements of the adjoining joints.

This method does not result in immediate compatibility, as the shear forces change in the subsequent moment distribution operation when the rotational restraints are relaxed and must in the final cycles, when greater accuracy is required, be repeated. This is done by using only the unbalanced portions of the brace shear forces until they become negligible in magnitude. The total relaxation is then the sum of the relaxation increments at all joints.

Step 7

Method of determining the approximate proportions of the unbalanced forces P_u to be applied to get rapid convergence.

As mentioned previously the automatic execution of the analytical procedure described above with a repetitive application of the total unbalanced forces P_u resulting from the previous cycle does not readily produce a solution. It will be immediately obvious that the partical application of the unbalanced forces will achieve better results.

The method described below has been developed to ascertain the approximate proportions of the unbalanced forces that should be applied in the following cycle in order to

15 / accelerate ...

accelerate the reduction of these unbalanced forces. The horizontal deflection $_{E}\Delta_n$ and rotation $_{E}\theta_n$ at level n of the "free" shear wall due to the external forces P_E can be determined by equations E4.12 and E4.13. The reversal of deflection and rotation if the unbalanced forces P_u, resulting from the "force-fitting" of the frame, are applied to the "free" shear wall can likewise be calculated from

$$_{u}\Delta_n = \int_{H_n}^{\circ} \frac{M_u\,(H_n - H)\,dH}{E\,I_w} \qquad \text{.... E4.16}$$

$$_{u}\theta_n = \int_{H_n}^{\circ} \frac{M_u\,.\,dH}{E\,I_w} \qquad \text{.... E4.17}$$

where M_u is the bending moment at any level H due to the forces P_u.

The convergence method developed below is based on the assumption that the forces P_p (in the form of couples, shear forces and axial forces) which must be applied to the wall to get approximate compatibility can be expressed as a fraction of the forces P_u acting at any level n by the equation

$$P_{pn} = P_{un}\left[\frac{_{E}\Delta_n}{_{E}\Delta_n + {}_{u}\Delta_n}\right] \qquad \text{.... E4.18}$$

Equation E4.18 is derived as follows :

When compatibility of profile has been achieved between the shear wall and frame the forces P_{pn} applied in the final cycle to the shear wall at level n must equal the forces acting at the junction with the bracing beam.

If the assumption is made that a linear relationship exists between the forces P_{pn} acting at the above-mentioned junction and the resultant deflection $_{c}\Delta_n$ we have

$$P_{pn} \doteq P_{un}\,\frac{_{c}\Delta_n}{_{E}\Delta_n} \qquad \text{.... E.19}$$

This assumption is not accurate and will accordingly not directly give the desired result. The errors are however

16/ corrected ..

corrected in the process of relaxation and become negligible as the unbalanced forces P_u decrease.

The reversal of deflection $({}_E\Delta_n - {}_c\Delta_n)$ due to the application of a proportion of the unbalanced forces to the "free" shear wall is also directly related to P_{pn} as follows :-

$$P_{pn} \doteq P_{un}\left[\frac{{}_E\Delta_n - {}_c\Delta_n}{{}_u\Delta_n}\right] \qquad \ldots \text{E4.20}$$

From E4.19 and E4.20 we accordingly have

$$\frac{{}_c\Delta_n}{{}_E\Delta_n} = \frac{{}_E\Delta_n - {}_c\Delta_n}{{}_u\Delta_n}$$

$$\text{i.e. } {}_c\Delta_n = \frac{({}_E\Delta_n)^2 - ({}_c\Delta_n)({}_E\Delta_n)}{{}_u\Delta_n}$$

$$\therefore \frac{{}_c\Delta_n}{{}_E\Delta_n} = \frac{{}_E\Delta_n}{({}_E\Delta_n + {}_u\Delta_n)}$$

by substitution in equation E4.19

we can derive E4.18.

The procedure is therefore to start at the bottom of the frame and to calculate P_{P1} from the equation

$$P_{P1} = P_{u1}\frac{{}_E\Delta_1}{{}_E\Delta_1 + {}_u\Delta_1}$$

$$= P_{u1}\frac{\int_1^0 \frac{M_E(H_1-H)\,dH}{EI_w}}{\int_1^0 \frac{M_E(H_1-H)\,dH}{EI_w} + \int_1^0 \frac{M_u(H_1-H)\,dH}{EI_w}}$$

Similarly

$$P_{P2} = P_{u2}\frac{\int_2^0 \frac{M_E(H_2-H)\,dH}{EI_w}}{\int_2^0 \frac{M_E(H_2-H)\,dH}{EI_w} + \int_2^0 \frac{M_u(H_2-H)\,dH}{EI_w}}$$

The whole procedure is repeated in terms of the unbalanced external forces subsequent to each cycle until a sufficient degree of compatibility is achieved. The results of each cycle are then summated to give the final values of forces and deformations. With experience it is possible to further increase the rate of convergence by using a factor less than unity in equation E4.18. This factor however depends on the

17/ frame ...

frame proportions and no general rule for its assessment has yet been established.

Application of the Method

A worked example by the special method applied to the frame illustrated in fig. 4.1 is given in the Appendix IV-2.

The effect of assuming the columns to be inextensible is illustrated in figs. 4.5 and 4.6. Although the effect is not too serious in this case it becomes more important for taller frames and for cases where the relative stiffness of the bracing beams is increased.

In the case of the 18-storey building analysed by the author it was essential to take the column extension into account.

REFERENCES:

(1) FRISCHMANN, W.S., PRABHU, S.S. and TOPPLER, J.F., "Multi-storey Frames and interconnected shear-walls subjected to lateral loads" - Part 1. Concrete and Constructional Engineering, June 1963. Vol. LVIII. No. 6.

(2) FRISCHMANN, W.S. PRABHU, S.S., and TOPPLER, J.F., "Multi-storey Frames and interconnected shear-walls subjected to lateral loads" - Part 2. Concrete and Constructional Engineering. July 1963. Vol. LVIII. No. 7.

(3) ROSMAN, R., "Approximate analysis of shear walls subjected to lateral loads". Journal of the American Concrete Institute. June 1964. Proceedings V.61 No. 6. Part 1.

(4) CLOUGH, R.W., KING, I.P., and WILSON. E.L., "Structural analysis of Multi-storey Buildings". Journal of the Structural Division, Proceedings of the A.S.C.E. June 1964. Vol. 90. No. ST3. Part 1. Page 19.

(5) KHAN, F.R., and SBAROUNIS, J.A., "Interaction of shear walls and frames". Journal of the Structural Division, Proceedings of the A.S.C.E., June 1964. Vol. 90. No. ST3, Part 1. Page 285.

APPENDICES

TO BOOK IV

APPENDIX IV - 1

NOTATION OF BOOK IV

A_n = Cross-sectional area of column A between levels n-1 and n.

A_1, A_t = Cross-sectional area of the lowest and the topmost heights of column A.

b = Width of the shear wall.

E = Young's modulus for the material or if of composite construction, the effective value.

F.E.M. = Fixed end moment.

H = A variable dimension measured vertically from the base.

H_n = The height above the base of level n.

h = Length of column AB.

h_n = Storey height between levels n-1 and n.

h_1, h_t = The height of the lowest and topmost storeys, respectively.

I = Moment of inertia of a column AB.

I_{An} = The moment of inertia of the column A between levels n-1 and n.

I_{bn} = The moment of inertia of the brace beam at level n.

I_w = The moment of inertia of the shear wall at any level H where H is a variable measured vertically from the base.

l = The effective span of the brace beam.

M_A = Anti-clockwise bending moment at end A in a column AB.

M_B = Clockwise bending moment at end B in column AB.

M_E = The bending moment due to the forces at any level H where H is a variable measured vertically from the base.

bM_{An} = The fixed end bending moment in the brace beam at level n where it adjoins column A.

$_bM_{wn}$ = The fixed end bending moment in the brace beam at level n where it adjoins the shear wall.

$_AM_{n,n-1}$ = Fixed end moment in the column A between levels n-1 and n acting at level n.

M_u = The bending moment at any level H due to the forces P_u .

n = A number indicating a level above the base of the frame in terms of storey heights.

P_E = The external horizontal forces applied to the shear wall frame combination.

P_p = Proportion of P_u to be applied to the shear wall to get approximate compatibility.

P_{pn} = P_p at level n.

P_u = The unbalanced internal forces in the form of couples, shears and axial forces which are required to "forcefit" the frame to the shear wall profile in the general method.

P_{un} = P_u at level n.

$_AS_{bn}$ = Shear force in the brace beam at level n after completion of step 3 of the special method.

$_AS'_{bn}$ = Residual shear force in the brace beam at level n after relaxation of the column restraints.

$_AS_{b1}$, $_AS_{bt}$ = Shear force in the lowest and topmost brace beams respectively after completion of Step 3 of the special method.

s = An integer denoting the operational cycle number.

β = $\frac{M_A}{M_B}$

$_E\gamma_n$ = The vertical translation at end of shear wall at level n due to forces P_E .

$_E\Delta_n$ = The horizontal deflection at any level n of the shear wall due to the external forces P_E if the shear wall is considered to act independently as a "free" wall.

$_c\Delta_n$ = The horizontal deflection of the frame joint at level n due to P_{pn} .

$_{u}\Delta_{n}$ = The reversal of deflection at level n if the total unbalanced forces P_u resulting from the "force-fitting" of the frame are applied to the "free" shear wall.

θ_A = Anti-clockwise rotation of end A of column AB.

θ_B = Clockwise rotation of end B of column AB.

θ_C = $\theta_A + \theta_B$ = relative rotation of the ends A and B of column AB.

$\theta_{n,n-1}$ = The difference between the slopes of the column at levels n and n-1.

$_{A}\theta_{n}$ = The assumed rotation of the frame joints at level n.

$_{A}\theta_{1}$, $_{A}\theta_{t}$ = The assumed rotation of the lowest and top-most frame joints, respectively.

$_{A}\theta_{n,s}$ = The assumed rotation of the frame joints at level n in cycle s.

$_{E}\theta_{n}$ = The rotation or slope of the shear wall at level n relative to the vertical due to the application of the external forces P_E to the shear wall acting independently of the frame.

$_{R}\theta_{n,s}$ = The reversal of rotation of the shear wall at level n due to the application in reverse of the unbalanced restraining forces in cycle s of the special method.

$_{u}\theta_{n}$ = The reversal of rotation at level n if the total unbalanced forces P_u resulting from the "force-fitting" of the frame are applied to the "free" shear wall.

$\sum_{o}^{n} R_A$ = Total vertical shortening or extension at level n of column A which for any particular shear wall profile would reduce the shear force and bending moments in the brace at level n to zero.

$\sum_{o}^{n} r_A$ = Actual relaxation that is applied in the form of a vertical translation of the joint at level n in Coluan A.

$\sum_{o}^{1} r_A$, $\sum_{o}^{t} r_A$ = Actual relaxation that is applied in the form of a vertical translation of the lowest and topmost joints in column A, respectively.

APPENDIX IV-2

Analysis of Shear wall and frame combination by the Special Method.

The combination to be analysed is illustrated in fig. 4.1

Determination of Influence coefficients for the shear wall.

Unit Load.

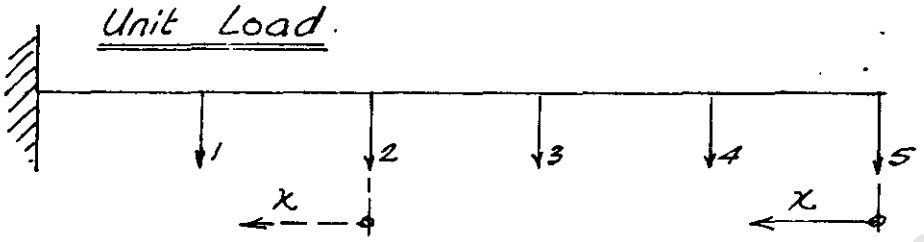

$$M = x = EI\frac{d^2y}{dx^2}$$

$$\therefore EI\frac{dy}{dx} = \frac{x^2}{2} + A$$

At $x = L$ $\quad \frac{dy}{dx} = 0 \quad \therefore A = -\frac{L^2}{2}$

$$\therefore EI\frac{dy}{dx} = \tfrac{1}{2}(x^2 - L^2) \longrightarrow$$

$$EIy = \tfrac{1}{2}\left[\frac{x^3}{3} - L^2x\right] + B$$

At $x = L$ $\quad y = 0$

$$\therefore B = -\tfrac{1}{2}\left[\frac{L^3}{3} - L^3\right] = \frac{L^3}{3}$$

$$\therefore EIy = \tfrac{1}{6}\left[x^3 - 3L^2x + 2L^3\right] \longrightarrow$$

$$\frac{1}{EI} = \frac{12}{3\times10^3 \times 144 \times 1 \times 8^3} = 0.543 \times 10^{-7} \text{ kips}^{-1}.\text{ft}^{-2}.$$

Unit load at position 1.

	L^2	x^2	$\frac{1}{2}(L^2-x^2)$	$\theta \times 10^6$
1	100	0	50	2.72
2				2.72
3				2.72
4				2.72
5				2.72

Unit Load at Position 1 (continued).

	x^3	$3L^2x$	$2L^3$	$\frac{1}{6}\Sigma$	$y \times 10^6$
1	0	0	2000	333	18·1
2					45·3
3					72·5
4					99·7
5					126·9

Unit Load at Position 2.

	L^2	x^2	$\frac{1}{2}(L^2-x^2)$	$\theta \times 10^6$
1	400	100	150	8·1
2	400	0	200	10·8
3				10·8
4				10·8
5				10·8

	x^3	$3L^2x$	$2L^3$	$\frac{1}{6}\Sigma$	$y \times 10^6$
1	1000	12000	16000	833	45·2
2	0	0	16000	2667	145·
3					253·
4					361·
5					469·

Unit Load at Position 3

	L^2	x^2	$\frac{1}{2}(L^2-x^2)$	$\theta \times 10^6$
1	900	400	250	13·6
2		100	400	21·8
3			450	24·4
4				24·4
5				24·4

Unit Load at Position 3 (continued)

	x^3	$3L^2x$	$2L^3$	$\frac{1}{6}\Sigma$	$y \times 10^6$
1	8000	54000	54000	1333	72
2	1000	27000		4333	235
3	0	0		9000	490
4					734
5					978

Unit Load at Position 4.

	L^2	x^2	$\frac{1}{2}(L^2-x^2)$	$\theta \times 10^6$
1	1600	900	350	19.0
2		400	600	32.6
3		100	750	40.7
4		0	800	43.5
5				43.5

	x^3	$3L^2x$	$2L^3$	$\frac{1}{6}\Sigma$	$y \times 10^6$
1	27000	144,000	128,000	1833	99.5
2	8000	96,000		6667	362.
3	1000	48,000		13,500	734.
4	0			21,333	1155.
5					1591

Unit Load at Position 5

	L^2	x^2	$\frac{1}{2}(L^2-x^2)$	$\theta \times 10^6$
1	2500	1600	450	24.4
2		900	800	43.5
3		400	1050	57.0
4		100	1200	65.0
5		0	1250	68.0

4.

Unit Load at Position 5 (continued)

	x^3	$3L^2x$	$2L^3$	$\frac{1}{6}\Sigma$	$y \times 10^6$
1	64000	300 000	250 000	2333	127
2	27000	225 000		8667	472
3	8000	150 000		18000	980
4	1000	75 000		29333	1590
5	0	0		41,667	2260

INFLUENCE COEFFICIENTS FOR COUPLES.

UNIT COUPLE.

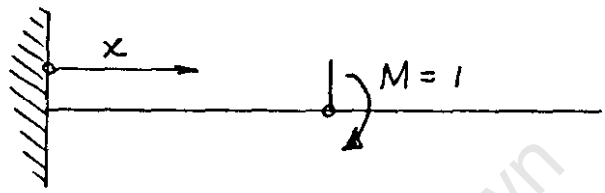

$$M = EI\frac{d^2y}{dx^2} = 1$$

$$\therefore EI\frac{dy}{dx} = x + A$$

At $x = 0$ $\frac{dy}{dx} = 0$ $\therefore A = 0$

$$EIy = \frac{x^2}{2} + B$$

At $x = 0$ $y = 0$ $\therefore B = 0$

$$\therefore \frac{dy}{dx} = \frac{x}{EI} \qquad y = \frac{x^2}{2EI}$$

Unit Couple at Position 1

	x	$\theta \times 10^6$	$y \times 10^6$
1	10	0·544	2·72
2		0·544	8·16
3		0·544	13·60
4		0·544	19·04
5		0·544	24·48

Unit couple at Position 2.

	x	$\theta \times 10^6$	$y \times 10^6$
1	10	0·544	2·72
2	20	1·088	10·88
3		1·088	21·76
4		1·088	32·64
5		1·088	43·52

Unit couple at Position 3.

	x	$\theta \times 10^6$	$y \times 10^6$
1	10	0·544	2·72
2	20	1·088	10·88
3	30	1·632	24·40
4		1·632	40·76
5		1·632	57·08

Unit couple at Position 4

	x	$\theta \times 10^6$	$y \times 10^6$
1	10	0·544	2·72
2	20	1·088	10·88
3	30	1·632	24·40
4	40	2·176	43·42
5		2·176	65·18

Unit couple at Position 5.

	x	$\theta \times 10^6$	$y \times 10^6$
1	10	0·544	2·72
2	20	1·088	10·88
3	30	1·632	24·40
4	40	2·176	43·42
5	50	2·720	68·60

6.

Frame Properties.

$I_{An} = \frac{1}{12} \times 1 \times 1^3 = 0.0834 \text{ ft}^4$. .... Frame of uniform

$I_{bn} = \frac{1}{12} \times 1 \times 2^3 = 0.667 \text{ ft}^4$. thickness = 1'-0"

$\frac{I_{An}}{h_n} = 0.00834 \text{ ft}^3$ $\frac{I_{bn}}{\ell} = 0.0785 \text{ ft}^3$

Distribution Factors (approximate)

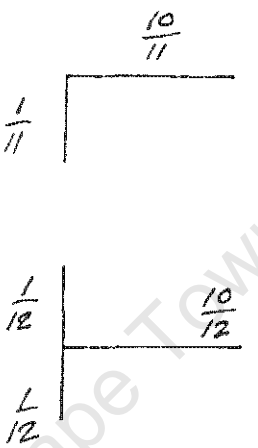

Fixed End Moments.

Brace beams ${}_bM_{An} = {}_bM_{wn} = \frac{6EI_{bn}}{\ell}\left(1 + \frac{b}{2\ell}\right)_A\theta_{n,s}$

$= 6 \times 3 \times 10^3 \times \frac{144}{8.5} \times 0.67 \times 1.47 \times {}_A\theta_{n,s}$

$= 300 \times 10^3 \times {}_A\theta_{n,s}$ kips-ft.

Columns. ${}_AM_{n-1,n} = \frac{EI_{An}}{h_n}\left(\frac{2\beta}{1+\beta}\right)\theta_{n,n-1}$

${}_AM_{n,n-1} = \frac{EI_{An}}{h_n}\left(\frac{2}{1+\beta}\right)\theta_{n,n-1}$

where $\beta = \frac{{}_AM_{n-1,n}}{{}_AM_{n,n-1}}$

$\frac{EI_{An}}{h_n} = \frac{3 \times 10^3 \times 144 \times 0.0834}{10} = 3.6 \times 10^3$.

for all n.

STEP (1).

Using Influence coefficients

$$_E\theta_1 = 678 \times 10^{-6} \text{ radians}$$
$$_E\theta_2 = 1114 \times 10^{-6} \text{ "}$$
$$_E\theta_3 = 1356 \times 10^{-6} \text{ "}$$
$$_E\theta_4 = 1464 \times 10^{-6} \text{ "}$$
$$_E\theta_5 = 1494 \times 10^{-6} \text{ "}$$

Using past experience a probable slope "profile" was drawn and the values recorded as the initial values $_A\theta_{n,1}$ to be used in the 1st cycle.
Almost perfect compatibility was achieved in six cycles. In practice less would be required.
For the purposes of example only the last cycle is given below:—

Cycle No. 6.

STEPS (2) AND (3)

	A	B	C	D	E	F	G	H
n	$_A\theta_{n,5}$	$_E\theta_n - {}_A\theta_{n,5}$	$_R\theta_{n,5}$	$_A\theta_{n,6}$	$_bM_{An}$	$\theta_{n,n-1}$	$_AM_{n-1,n}$	$_AM_{n,n-1}$
1	268	410	418	263	79.0	263	1.50	0.4
2	370	744	754	365	110.0	102	1.16	-0.43
3	378	978	989	374	112.5	9	—	-
4	351	1113	1125	348	104.2	-26	—	-
5	326	1168	1180	322	96.5	-26	—	—

Note: | All rotations and slopes in radians $\times 10^6$
| All bending moments in kips-ft.

$$| D = A \times \frac{B}{C}$$
$$| {}_bM_{An} = {}_bM_{Wn}.$$

| From previous cycle:
$\beta_{0,1} = 3.76 \quad \beta_{1,2} = -2.72$

STEP (3) CONTINUED

Note: ${}_A S_{bn} = \frac{6M_{An} + 6M_{Wn}}{8.5}$

$\sum_0^n R_A = {}_A\theta_{n,6} \times \frac{12.5 \times 12.}{10^3}$ ins $\times 10^3$

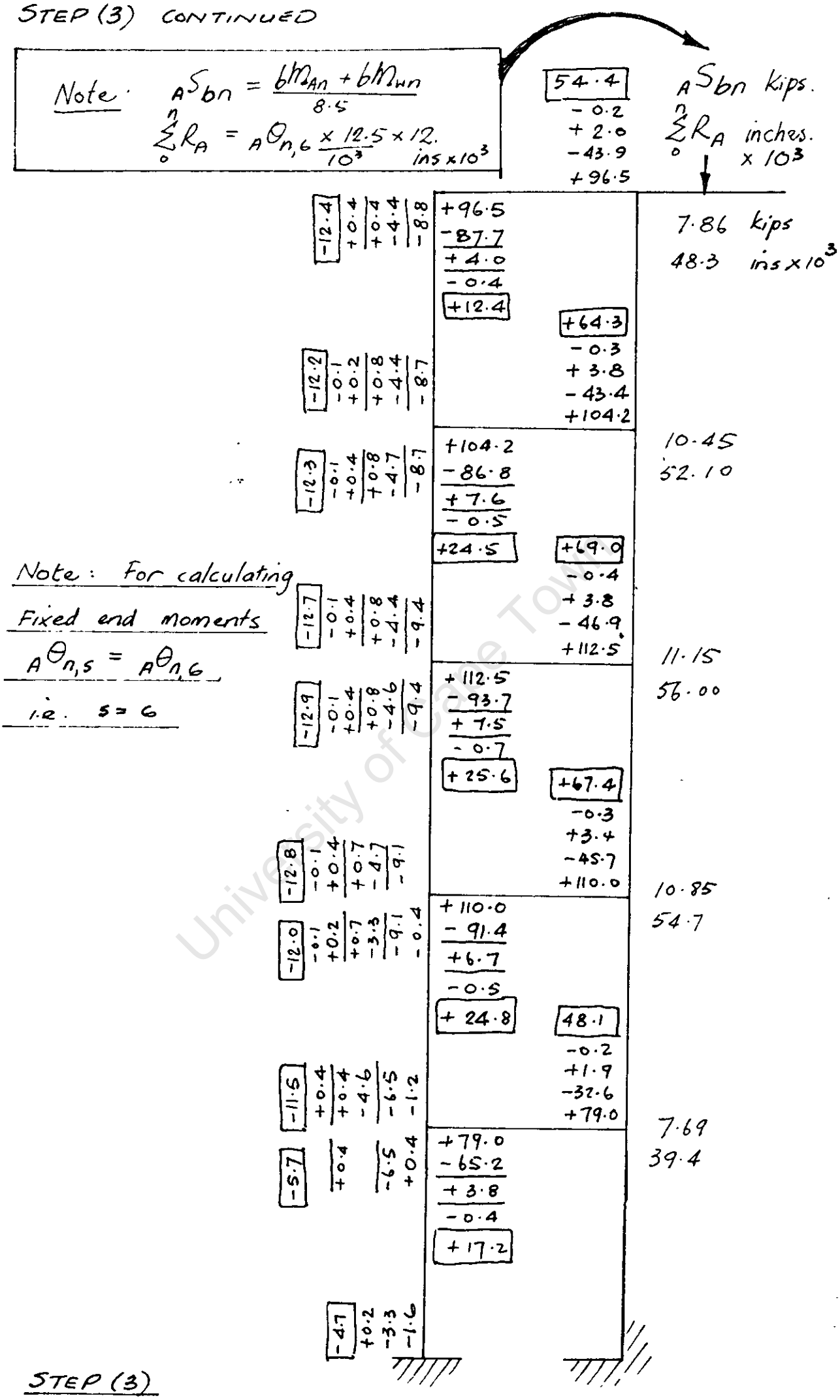

Note: For calculating Fixed end moments ${}_A\theta_{n,5} = {}_A\theta_{n,6}$ i.e. $5 = 6$

STEP (3)

Relaxation of frame joints by Mom. Distribn.

Columns restrained against vertical translation.

STEP (4)

RELAXATION OF COLUMNS

4th Trial

n	$\sum_0^n r_A$	$2\sum_0^n r_A$	$\sum_0^{n-1} r_A$	$\frac{h_n}{A_n E}\, {}_A S_{bn}\, \frac{\sum_0^n R_A - \sum_0^n r_A}{\sum_0^n R_A}$	$\sum_0^{n+1} r_A$
1	8·5	17·00	0	1·62	15·38
2	15·38	30·76	8·5	2·16	20·10
3	20·10	40·20	15·38	1·98	22·84
4	22·84	45·68	20·10	1·63	23·95
5	23·95				

Check.

$$\frac{h_t}{A_t E}\, {}_A S_{bt}\, \frac{\sum_0^t R_A - \sum_0^t r_A}{\sum_0^t R_A} = \left[\sum_0^t r_A - \sum_0^{t-1} r_A\right]$$

i.e. $\frac{10\times12\times7.86}{1\times3\times10^3\times144} \times \frac{48.3 - 23.95}{48.3} = 23.95 - 22.84$

i.e. $1.10 = 1.11$ ✓

Note: All relaxations in inches $\times 10^3$

$\frac{h_n}{A_n E} = 0.278 \frac{\text{inches}}{\text{kips}} \times 10^3$ for all n

For ${}_A S_{bn}$ and $\sum_0^n R_A$ see previous page.

STEP (4) (CONTINUED)

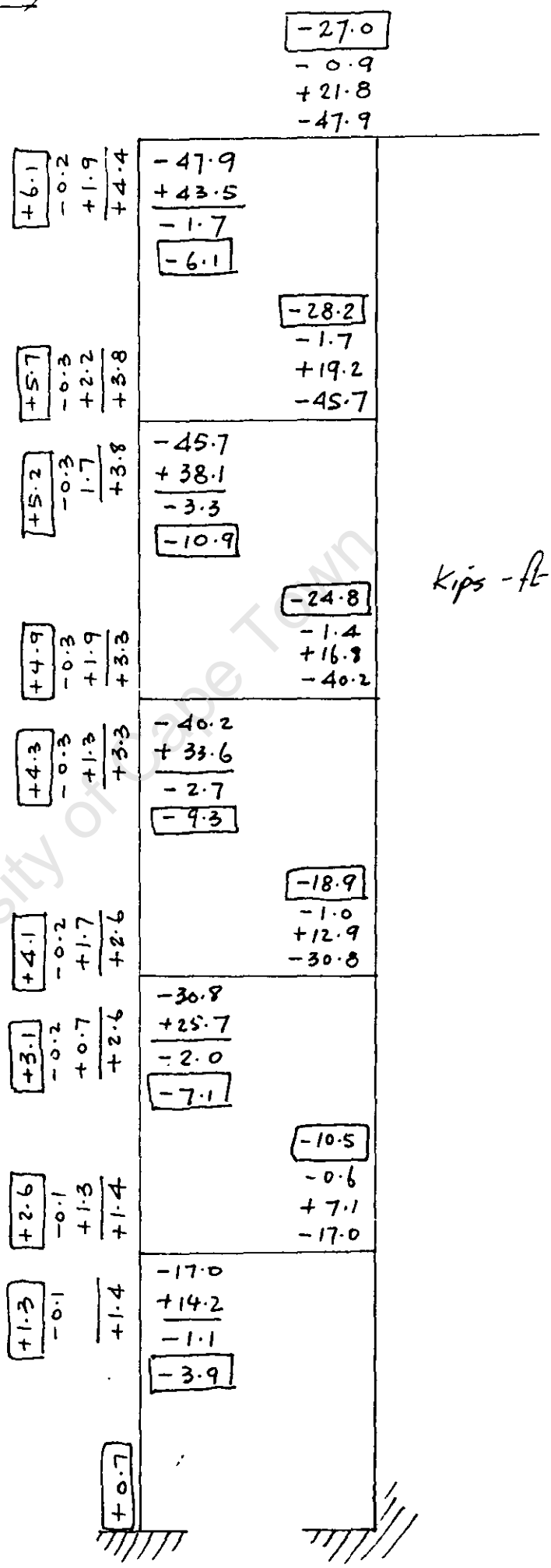

Fixed end moments in brace beams

$$= -\sum_{0}^{n} r_A \frac{6EI_{bn}}{l^2}$$

$$= -\sum_{0}^{n} r_A \frac{6 \times 3 \times 10^3 \times 144 \times 0.66}{(8.5)^2 \times 12 \times 10^3}$$

where $\sum_{0}^{n} r_A$ is in inches $\times 10^3$.

$$= -2.0 \sum_{0}^{n} r_A \text{ kips. ft.}$$

Step (4) (continued)

Relaxation of frame joints by Mom. Distribn. after relaxation of columns.

STEP (5)

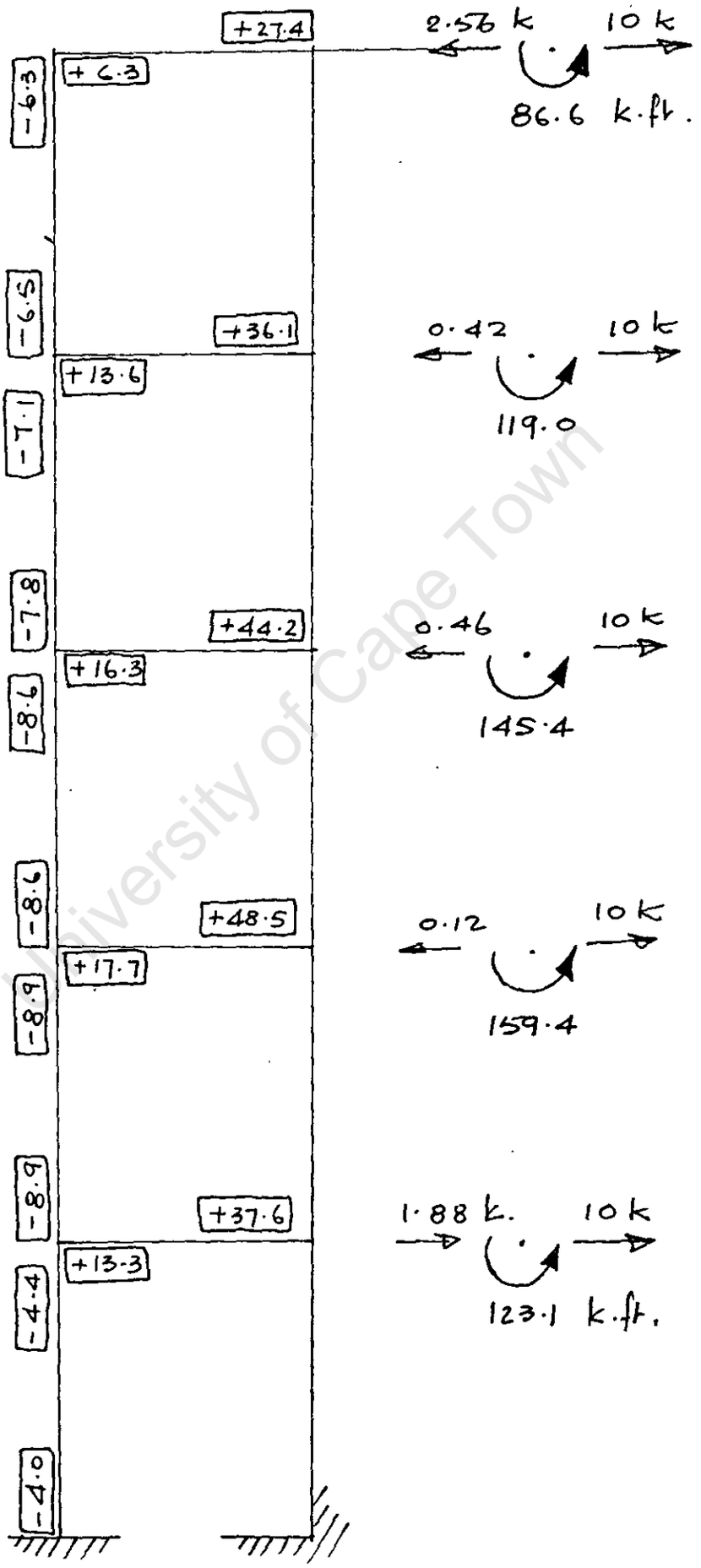

Final Bending moments in frame and couples and forces acting on shear wall.

STEP (6)

By Influence coefficients.

	P	1	2	3	4	5
1	-1.88	-5	-5	-5	-5	-5
2	0.12	1	1	1	1	1
3	0.46	6	10	11	11	11
4	0.42	8	14	17	18	18
5	2.56	63	111	146	166	174
Z_1		73	131	178	191	199
	M	1	2	3	4	5
1	123.1	67	67	67	67	67
2	159.4	86	173	173	173	173
3	145.4	79	158	237	237	237
4	119.0	65	129	194	258	258
5	86.6	47	94	142	189	236
Z_2		344	621	803	924	971
$Z_1 + Z_2 =$	${}_R\theta_n$	417	752	981	1115	1170
$E\theta_n - {}_R\theta_n =$	θ_n	261	362	375	349	324
c.f.	${}_A\theta_{n,6}$	263	365	374	348	322

High degree of compatibility

APPENDIX IV-3

D I A G R A M S

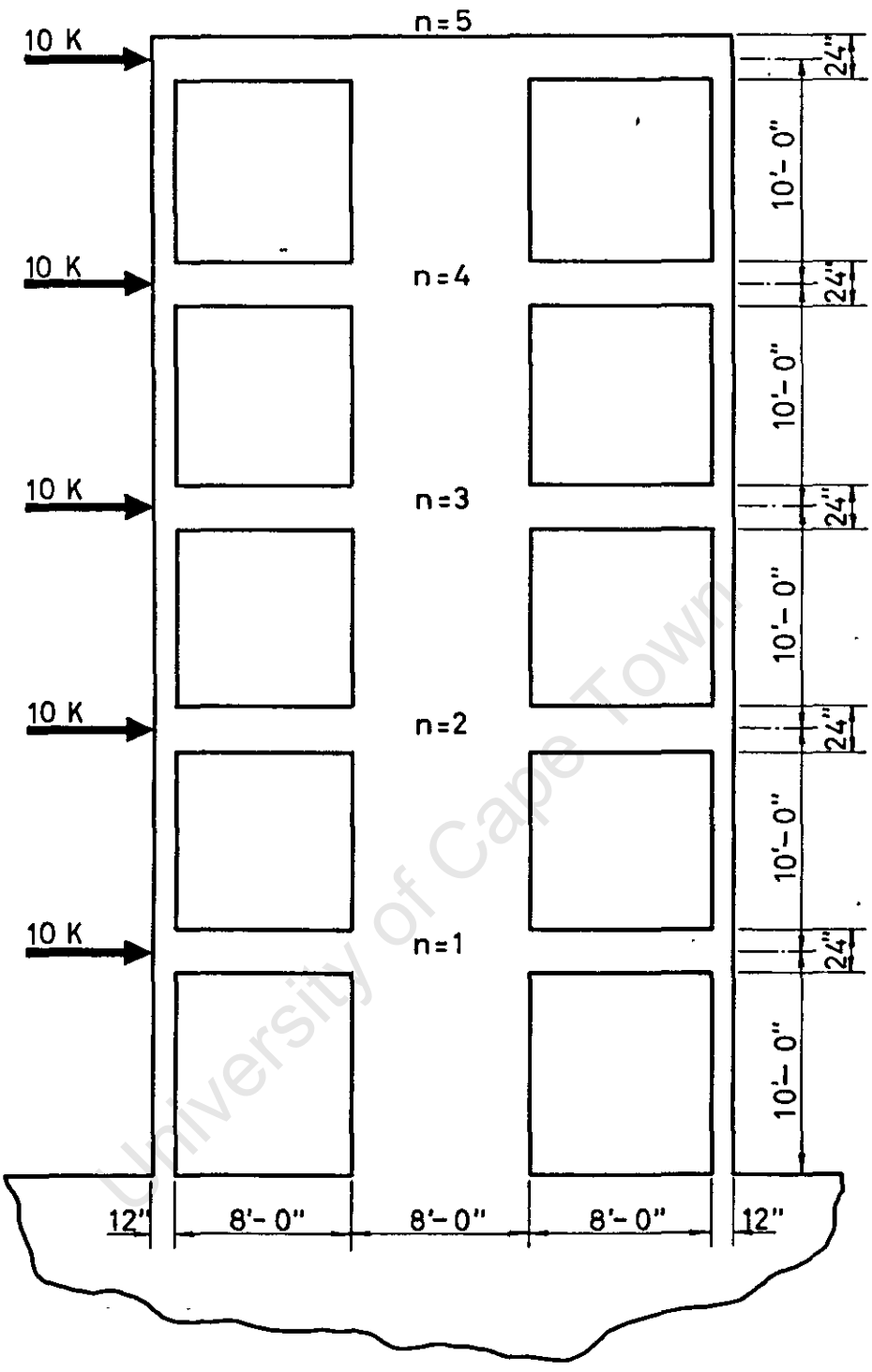

FIG. 4·1.

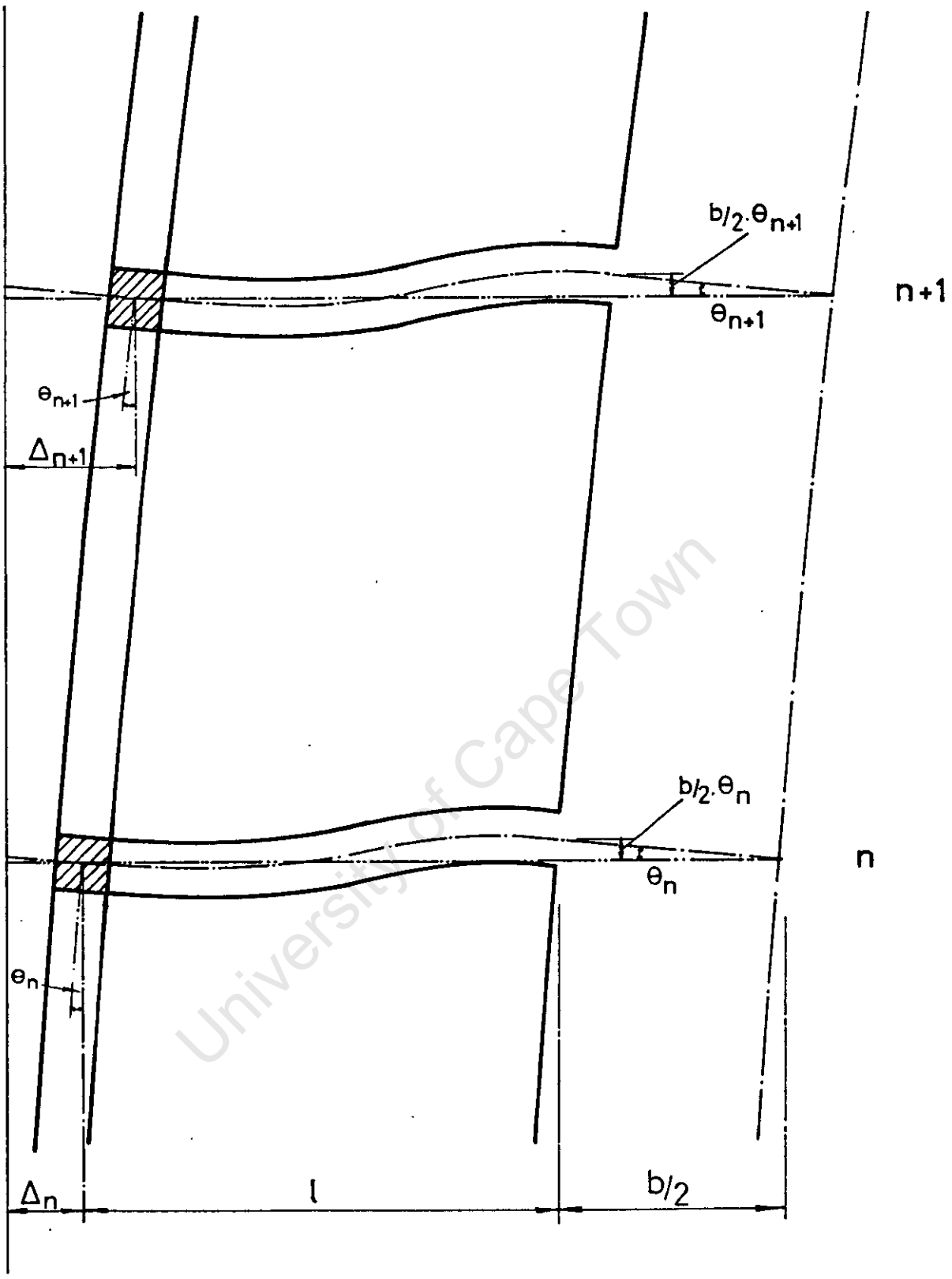

FIG. 4·2.

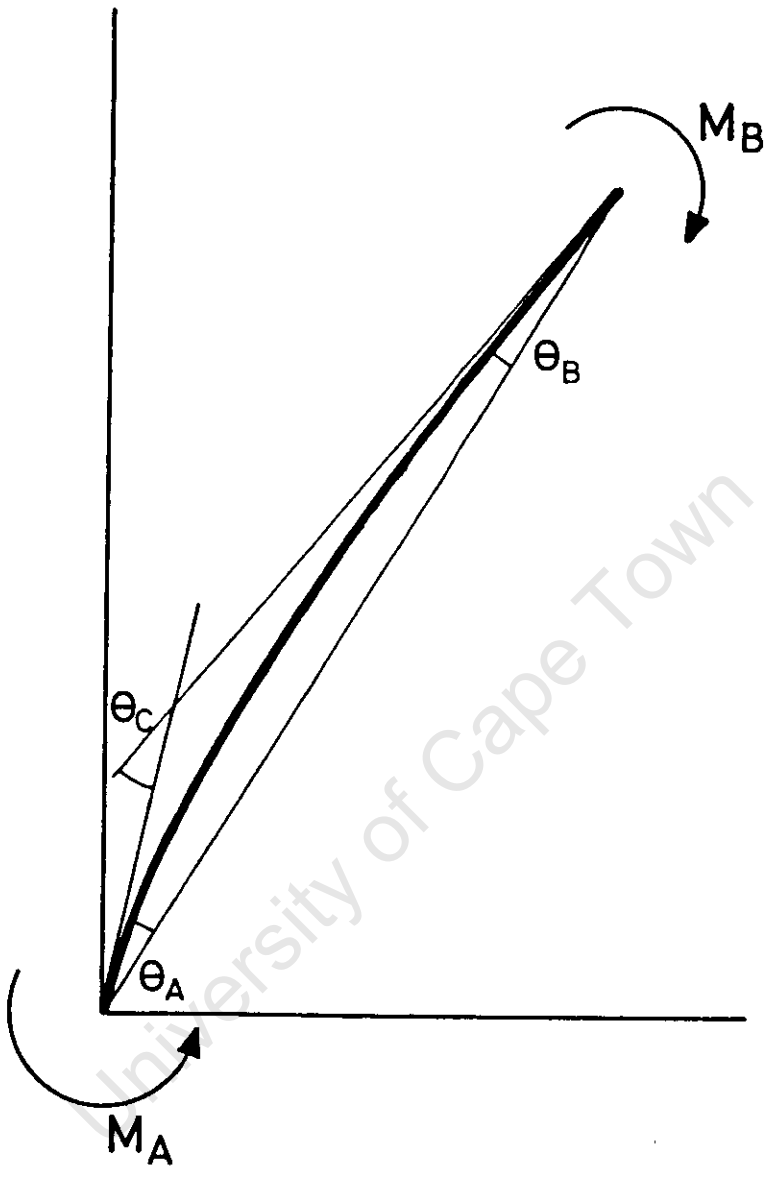

FIG. 4·3.

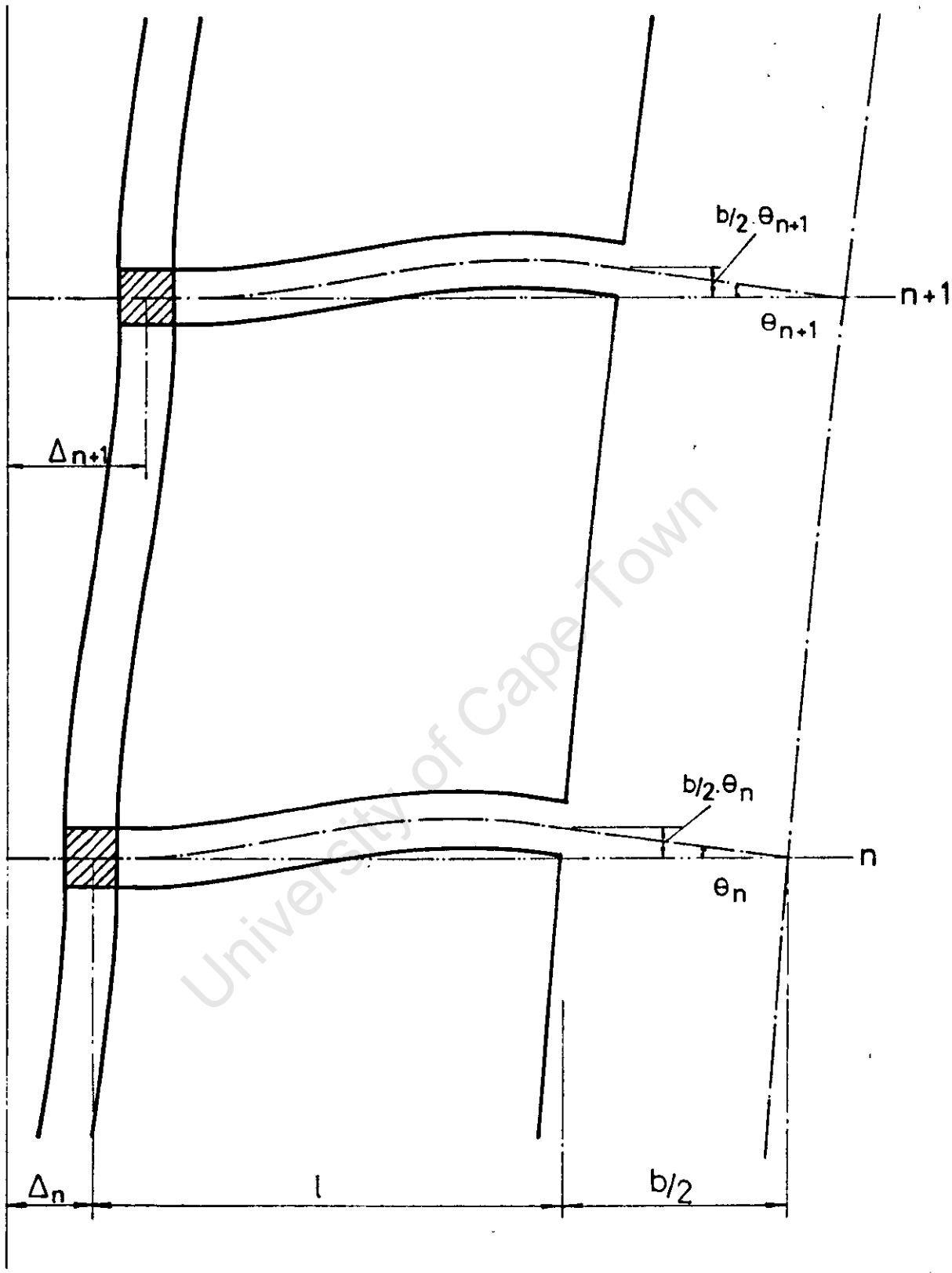

FIG. 4·4.

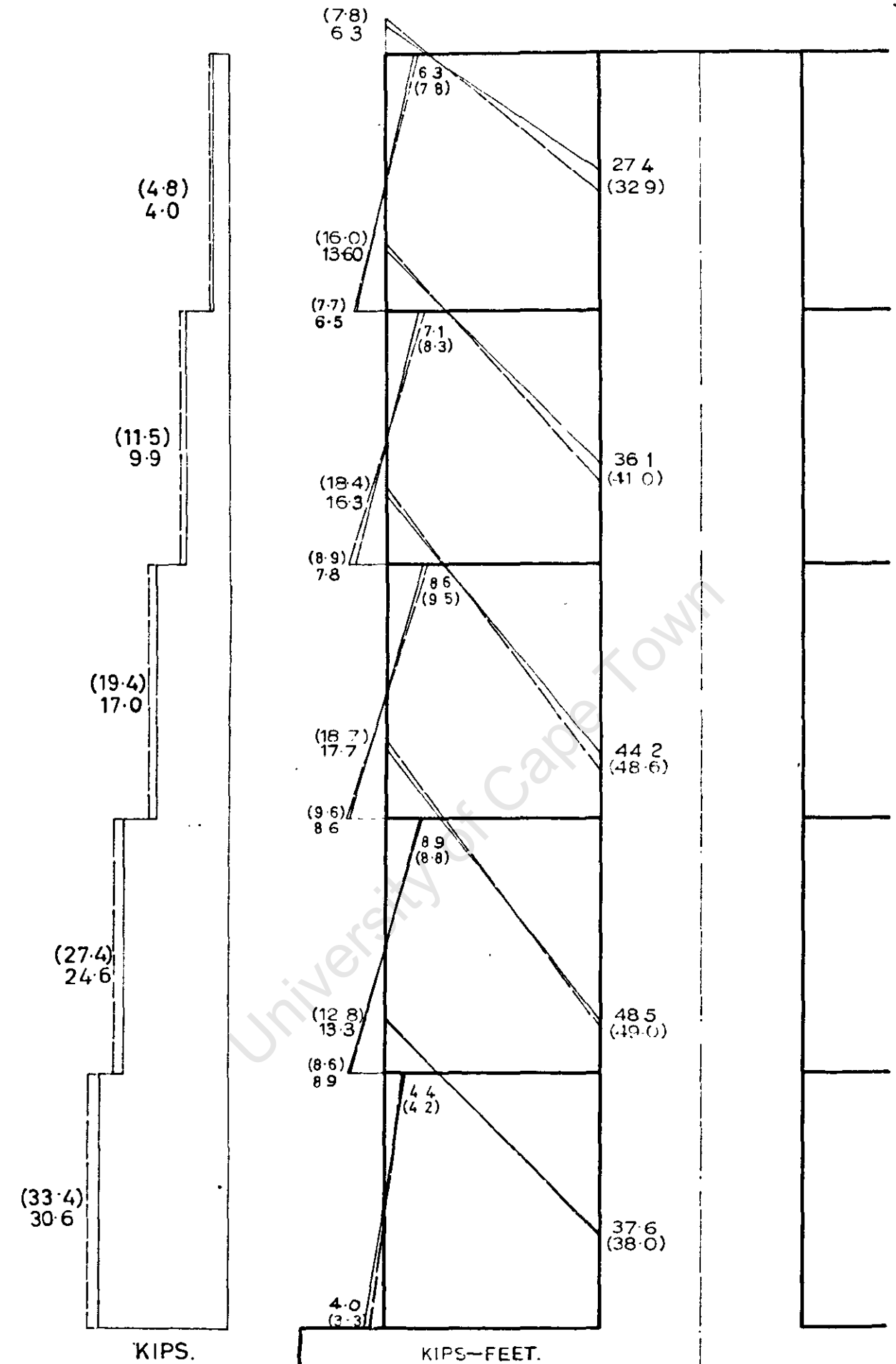

FIG. 4·5.

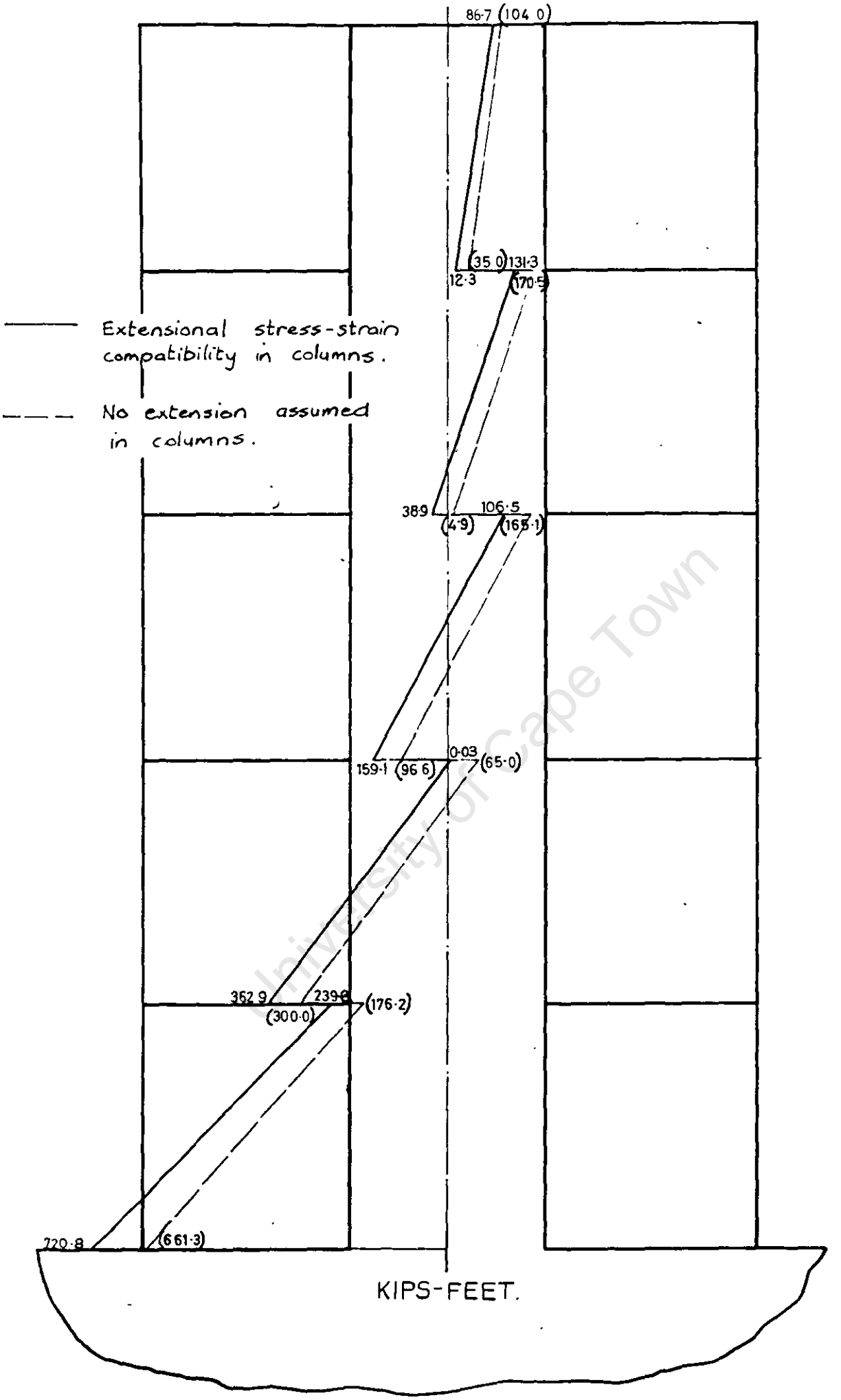

BENDING MOMENTS IN SHEAR WALL.

FIG. 4·6.